

Synthesis and Study of Molecules Based on Triangular Graphene Fragments

Inauguraldissertation

zur

Erlangung der Würde eines Doktors der Philosophie

vorgelegt der

Philosophisch-Naturwissenschaftlichen Fakultät

der Universität basel

von

Peter Ribar

aus Sered', Slowakei

Basel, 2020

Genehmigt von der Philosophisch-Naturwissenschaftlichen Fakultät

auf Antrag von

Prof. Dr. Marcel Mayor

Prof. Dr. Christof Sparr

Basel, den 26.03.2019

Prof. Dr. Martin Spiess

Dekan

“Wisdom comes from experience. Experience is often a result of lack of wisdom.”
— Terry Pratchett

*Dedicated to my family.
Venované rodine.*

ACKNOWLEDGEMENTS

I would like to express my deepest gratitude to Prof. Dr. Marcel Mayor and Prof. Dr. Michal Juríček for the opportunity to work in their groups, especially for the continuous support and almost limitless resources that they provided to me. Michal, you allowed me to work almost independently on my projects and allowed me to explore the beautiful chemistry of triangulene. Moreover, Michal, you were the best boss one could wish for, always helpful and appreciative.

Čo je možno ešte dôležitejšie, nikdy si sa ku mne nesprával ako k podriadenému, ale vždy ako ku rovnocennému. Za tých päť rokov si sa stal d'aleko viac ako len supervisor, bol si a si priateľ, na ktorého sa dá spoľahnúť aj v tých najťažších chvíľach.

I would like to extend my thanks to Prof. Dr. Christof Sparr for agreeing to co-referring my thesis and to Prof. Dr. Olivier Baudoin for chairing my PhD viva.

My deepest thank you goes to the members of Juríček group, namely, to Dr. Prince Ravat, Dr. Tomáš Šolomek and to Laurent Jucker, for the stimulating discussions and the nice environment that they provided. My special thanks goes to Dr. Tomáš Šolomek, for all the help with the triangulene projects.

Šolo, bol si tu pre mňa, keď mi bolo najhoršie, nikdy na to nezabudnem. Dúfam, že sa také nič nestane, ale ak ma bude treba, budem tu pre teba, aj keď to znamená ovracať matrac.

I am greatly appreciative to all the collaborators in course of this thesis. I want to give a special thanks to Dr. Daniel Häussinger for the discussions concerning the NMR spectroscopy and for the spectral analysis. Furthermore, I thank to Dr. Loïc Lepleux for the the measurements of electrochemistry and to Markus Neuburger and Alessandro Prescimone for collection and analysis of the crystallographic data.

I am very appreciative of Dr. Heinz Nadig and Sylvie Mittelheiser for all the HR MS measurements.

I would like to thank to the “Werkstatt” team for their continuous support in maintaining our department. In addition, I am thankful to Beatrice Erismann, Marina Mambelli, and Brigitte Howald for keeping this department running. I also would like to thank to Markus Hauri, Roy Lips, and Oliver Ilg from the “Materialausgabe” for their support.

My special thanks goes to the Lab 4, namely, to Yves, Sylvie, Lucas, Henrik, Prince, Laurent, Šolo and Michal, you guys were the reason for returning day by day after another reaction went to the trash. Special thanks goes to Yves for all the fun we had. And Henrik, you tortured me with your terrible taste in music for more than two years, I hope that you will be punished for that.

I would like to thank to the entire Mayor group for the stimulating discussions and the friendly environment they provided. Especially to Kevin for all the fun we had.

I am wholeheartedly grateful for my family, my mother Miroslava, my father Ján, my sister Mirka, my brother Ľuboš, my grandparents Blanka and Milan and my little niece and nephew Karolínka and Ľuboško. Vždy ste ma vo všetkom podporovali, či už to boli rozhodnutia dobré alebo hlúpe. Vďaka Vám som, kto som, nikdy Vám to nezabudnem!

And lastly my deepest thank you goes to the love of my life, Martina. Žabka, posledných pár mesiacov nebolo ľahkých, no vedz, že nech už to dopadne akokoľvek, si a vždy budeš láska môjho života. Som ti veľmi vďačný za všetku podporu, ktorú si mi dala. Vždy ťa budem ľúbiť. S láskou tvoj Zajko!

PREFACE

The present PhD dissertation summarizes my research findings in the research group of Prof. Dr. Michal Juriček from the period of February 2014 to January 2018.

The main goal of our group is development and synthesis of new functional organic materials based on hydrocarbon molecules that contain one or more unpaired electrons for application in spin electronics.

The present work aims at different strategies of synthesis of persistent Kekulé and non-Kekulé hydrocarbons and their application in molecular electronics.

Apart from a general introduction section (Chapter I), this dissertation is divided into four chapters. Each chapter represents research performed in the context of several projects, which were published or will be submitted to peer-reviewed journals. These chapters contain a brief introduction into the topic, followed by the corresponding experimental findings. The electronic supplementary information for Chapter IV can be found in the Appendices chapter.

The second chapter describes our efforts in the synthesis of triangulene precursors and subsequent generation and stabilization of the “naked” triangulene in a supramolecular complex with a cyclophane host.

The third chapter illustrates our efforts in the stabilization of the triangulene core by introducing bulky substituents. Our findings in this chapter encouraged us to explore the addition pattern on other extended π -aromatic systems.

In the fourth chapter, we designed and synthesised novel donor–acceptor molecules with a triangular shape and we studied their optoelectronic properties.

The fifth chapter describes our efforts in the design and synthesis of novel chiroptical and magnetic switch, featuring a [7]helicene backbone, operated solely by light.

LIST OF PUBLICATIONS

Excerpts from this thesis have been published in the following journals:

- Ravat, P.; Šolomek, T.; Ribar, P.; Juríček, M. “*Biradicaloid with a Twist: Lowering the Singlet–Triplet Gap*” *Synlett* **2016**, 27, 1613–1617.
- Ravat, P.; Ribar, P.; Rickhaus, M.; Häussinger, D.; Neuburger, M.; Juríček, M. “*Spin-Delocalization in Helical Open-Shell Hydrocarbon*” *J. Org. Chem.* **2016**, 81, 12303–12317.
- Ribar, P.; Šolomek, T.; Le Pleux, L.; Häussinger, D.; Prescimone, A.; Neuburger, M.; Juríček, M. “*Donor–Acceptor Molecular Triangles*” *Synthesis* **2017**, 49, 899–909.

CONTENTS

ACKNOWLEDGEMENTS	I
PREFACE	III
LIST OF PUBLICATIONS	IV
TABLE OF CONTENTS	V
LIST OF ABBREVIATIONS	VII
1. INTRODUCTION	1
1.1. FROM STONE TO CARBON	1
1.2. CARBON-BASED MATERIALS	1
1.3. CLAR'S SEXTET	6
1.4. SPIN-DELOCALIZED HYDROCARBON SYSTEMS	9
1.4.1. KEKULÉ AND NON- KEKULÉ HYDROCARBONS	11
1.4.2. DETERMINATION OF THE GROUND STATE WITH "STAR" RULE.....	12
1.5. HYDROCARBON BASED ORGANIC RADICALS.....	13
1.5.1. TRIPHENYLMETHYL RADICAL.....	13
1.5.2. PHENALENYL RADICALS.....	16
1.5.3. TRIANGULENE-BASED RADICALS.....	18
1.6. GOAL OF THE THESIS.....	23
2. TRIANGULENE PRECURSORS	24
2.1. INTRODUCTION.....	24
2.1.1. SYNTHESIS OF TRIANGULENE PRECURSORS	26
2.2. RESULTS AND DISCUSSION.....	31
2.2.1. STABILIZATION OF TRIANGULENE	42
2.3. CONCLUSION & OUTLOOK	47
2.4. EXPERIMENTAL SECTION	49
2.4.1. GENERALREMARKS	49
2.4.2. EXPERIMENTAL PROCEDURES	50
3. STERICALLY PROTECTED TRIANGULENE	65
3.1. INTRODUCTION.....	65
3.2. RESULTS & DISCUSSION.....	67
3.2.1. NUCLEOPHILIC ADDITIONS ON TRIANGULENE CORE	67
3.2.2. NUCLEOPHILIC ADDITIONS ON HEPTAATHRENE CORE.....	84
3.2.3. NUCLEOPHILIC ADDITIONS ON ANTHANTHRENE CORE.....	90
3.3. CONCLUSION & OUTLOOK	100
3.4. EXPERIMENTAL SECTION	101
3.4.1. GENERAL REMARKS	101

3.4.2. EXPERIMENTAL PROCEDURES	103
4. DONOR-ACCEPTOR TRIANGLES	136
4.1. IMPACT OF THE WORK.....	137
4.2. ABSTRACT	138
4.3. INTRODUCTION.....	138
4.4. RESULTS & DISCUSION	142
4.5. CONCLUSION & OUTLOOK.....	152
4.6. EXPERIMENTAL SECTION	153
4.6.1. GENERAL REMARKS.....	153
4.6.2. EXPERIMENTAL PROCEDURES	156
4.7. ACKNOWLEDGEMENT	166
4.8. SUPPORTING INFORMATION	166
5. SYNTHESIS OF DIBENZO[7_s]CETHRENE.....	167
5.1. INTRODUCTION.....	167
5.2. RESULTS & DISCUSION	174
5.3. CONCLUSION & OUTLOOK.....	187
5.4. EXPERIMENTAL SECTION	188
5.4.1. GENERAL REMARKS.....	188
5.4.2. EXPERIMENTAL PROCEDURES	189
REFERENCES	203
APPENDICES.....	A1

LIST OF ABBREVIATIONS

Å	Ångström
AFM	atomic force microscopy
BD	1,3-butadiene
BF ₃ ·Et ₂ O	boron trifluoride etherate
BPO	benzoyl peroxide
C ₁₀ H ₁₀	naphthalene
C ₆₀	buckminsterfullerene
C ₆ H ₃ Cl	1,3,5-trichlorobenzene
C ₆ H ₅ NO	nitrobenzene
CAS	Chemical Abstracts Service
°Hex	cyclohexane
°Hex ₃ P	tricyclohexylphosphine
cond.	conditions
COSY	correlation spectroscopy
CsOAc	cesium acetate
CT	charge transfer
CV	cyclic voltametry
DART MS	direct analysis in real time mass spectrometry
DDQ	2,3-dichloro-5,6-dicyano-1,4-benzoquinone
DFT	density functional theory
DMF	dimethylformamide
DMP	Dess–Martin periodinane
DMSO	dimethyl sulfoxide
DPV	differential puls voltametry
EPR	electron paramagnetic resonance
ESI	electrospray ionization
ESR	electron spin resonance
Et ₂ O	diethyl ether
EtOAc	ethyl acetate
EtOH	ethanol
(EtO) ₂ CO	diethyl carbonate
eV	electronvolt

GC-MS	gas chromatography mass spectrometry
HMBC	heteronuclear multiple-bond correlation spectroscopy
HMO	Hückel molecular orbital
HMQC	heteronuclear multiple-quantum correlation spectroscopy
HOMO	highest occupied molecular orbital
HR-MS	high-resolution mass spectrometry
$h\nu$	irradiation
$i\text{Pr}_2\text{O}$	diisopropyl ether
$i\text{PrMgBr}$	isopropylmagnesium bromide
K_a	association constant
LC-MS	liquid chromatography mass spectrometry
LUMO	lowest unoccupied molecular orbital
Me_2CO	acetone
Me_2SiCl_2	dichlorodimethylsilane
MeCN	acetonitrile
MeI	methyl iodide
MeMgBr	methylmagnesium bromide
MeOH	methanol
MO	molecular orbital
<i>m</i> -QDM	meta quinodimethane
MW	microwave irradiation
MWNT	multi-walled nanotube
Mz	megahertz
NBS	<i>N</i> -bromosuccinimide
$n\text{BuLi}$	<i>n</i> -butyllithium
NMR	nuclear magnetic resonance
NOESY	nuclear Overhauser effect spectroscopy
<i>o</i> -QDM	ortho-quinodimethane
PAH	polycyclic aromatic hydrocarbon
PCM	polarizable continuum model
Pd	palladium
Pd / C	palladium on activated charcoal
$\text{Pd}(\text{dppf})\text{Cl}_2$	1,1'-bis(diphenylphosphino)ferrocene]dichloropalladium
$\text{Pd}(\text{OAc})_2$	palladium acetate

PDI	perylene diimide
PhMe	toluene
ppm	parts per million
<i>p</i> -QDM	<i>para</i> -quinodimethane
<i>p</i> -TSA	<i>para</i> -toluenesulfonic acid
Py	pyridine
RT	room temperature
SiO ₂	silica gel
SOMO	singly occupied molecular orbital
STM	scanning tunnelling spectroscopy
SWNT	single-walled carbon nanotube
Tf ₂ O	trifluoromethanesulfonic anhydride
THF	tetrahydrofuran
TLC	thin-layer chromatography
TME	tetramethylenemethane
TMM	trimethylenemethane
UV/VIS	ultraviolet–visible spectroscopy
XRD	X-ray diffraction
Φ	photoluminescence quantum yield

CHAPTER I:

INTRODUCTION

1.1 FROM STONE TO CARBON

The use of materials has shaped the history of human civilization and changed the way we live, work, construct our buildings, eat or communicate. As one era replaces another (e.g., bronze age replaced stone age), newly discovered materials with better and more advanced properties are taking place of materials of the preceding times. Each new era brought numerous innovations that significantly shaped the landscape of our world and human civilization from both economic and sociological point of view. The so-called “silicon age” dominated the second half of the 20th century and transformed our society from isolated communities to one large globalized civilization. Since the beginning of the 21th century, the spotlight has shifted from silicon-based materials to new carbon-based materials, which are about to dominate the industry in near future and start the beginning of a new “carbon era”.^[1]

1.2 CARBON-BASED MATERIALS

Our ancestors have been using carbon and carbon-based materials including diamond, graphite, and charcoal since the prehistoric era. For instance, the very first art piece was created by using carbon-based ink in a cave painting around year 28000 BC.^[2] Although these materials consist solely of carbon atoms, they cover a broad range of properties and exhibit different functions. Diamond, one of the hardest known materials, is transparent and comes in different colours, while graphite is an opaque black material soft enough to create a drawing on a piece of paper.

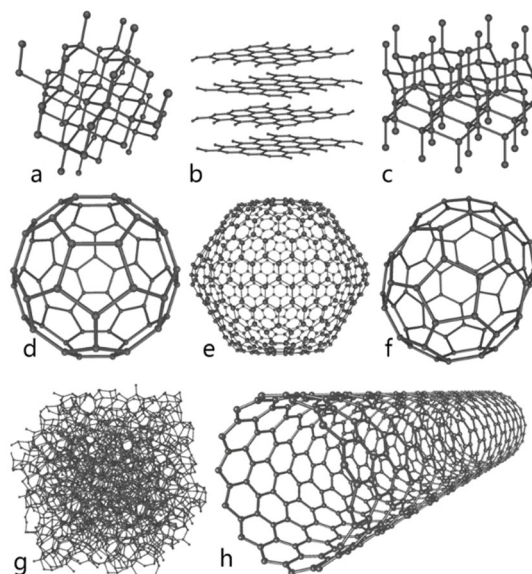


Figure 1.1: Allotropes of carbon: (a) diamond, (b) graphite and graphene, (c) lonsdaleite, (d) C_{60} – buckminsterfullerene, (e) C_{540} , (f) C_{70} , (g) amorphous carbon, (h) single-walled carbon nanotube (SWNT).^[4]

Accompanying the evolution of our society and modern science, a great progress in synthesis of new well-defined carbon-based materials has been made.^[3] Over the past four decades, the previously empty space between artificial organic molecules and naturally occurring carbon materials has been partly filled by discovery of new carbon allotropes.^[4] These new materials exhibit several unique and remarkable properties, which make them potential candidates for applications in technology.^[5]

The first discovered nanostructure was a 0D C_{60} molecule, commonly known as buckminsterfullerene, fullerene C_{60} , or buckyball (Figure 1.1. d).^[4] This molecule was first reported in 1985 by Kroto *et al.*^[6] during an experiment that was supposed to explain the formation of long-chain carbon molecules in interstellar space. Since then, many other fullerenes have been discovered, such as C_{540} or C_{70} (Figure 1.1. e, and f, respectively).^[4] Nevertheless, C_{60} represents the hitherto most studied fullerene.^[3, 6] Pure C_{60} lacks many of the typical properties characteristic for other carbon nanostructures, such as high conductivity or extreme mechanical strength. Unlike formally “infinite” graphene or diamond carbon networks, bulk C_{60} is an assembly of molecules with a limited well-defined

size. Because of the spherical structure and electron-deficient character, fullerene C₆₀ reacts readily with all types of free radicals. Due to this radical scavenger ability (also known as a radical sponge), fullerene C₆₀ has been widely studied as a potential material for protection of polymers from harmful radicals [3, 7-9], as well as an antioxidant in cosmetics and biological systems. [3, 7, 10-12] Another important feature of fullerenes is their ability to act as an electron acceptor in various donor–acceptor systems thanks to their high electron affinity and low reorganization energy of electron transfer. A large number of donor–acceptor systems containing fullerene as an acceptor have been prepared, usually featuring standard donors such as porphyrins, phthalocyanines and tetrathiafulvalenes. [13-15] Fullerenes with excellent electron-accepting properties are widely studied components for organic photovoltaics. [16-19]

Carbon nanotubes (Figure 1.1. h) [4] represent another significant achievement in the development of carbon nanomaterials. [3] They were first prepared by Iijima in 1991. [20] Because of their cylindrical shape, the properties of carbon nanotubes are significantly different from those of fullerenes. [3, 7] As a consequence, their potential application is also different. [3] The term “carbon nanotube” refers to a wide range of tubular nanostructures with similar structures and shapes. Depending on the number of layers, we can distinguish between single-walled carbon nanotubes (SWNT) consisting only from single graphenic wall, or multi-walled carbon nanotubes (MWNT), which have two or more layers. The single graphene layer can be wrapped in multiple ways (armchair, zig-zag or chiral). [21] Another common feature of carbon nanotubes is that they are not dispersible in water or organic solvents and are therefore usually held strongly in a bundle due the van der Waals interactions. [22-24] Due to the high strength of the covalent carbon–carbon double bond, the carbon nanotubes are among the strongest materials with high flexibility and plasticity. The conducting properties of carbon nanotubes are strongly dependent on the wrapping mode. [22] The armchair nanotubes are expected to exhibit metallic behaviour and possess excellent

conductivity.^[3, 25-26] On the other hand, zig-zag and chiral nanotubes are semiconductors.^[3, 27] Carbon nanotubes also possess interesting optical properties and are sometimes regarded as “practical black bodies” (theoretical body that absorbs all electromagnetic radiation).^[3, 28]

The existence of graphene (Figure 1.1 b) was predicted more than seven decades ago.^[29] Even though it was experimentally identified already in 1960’s^[30], graphene has been isolated only relatively recently—in 2004 by Geim and Novoselov by exfoliation of graphite.^[31] Since then, graphene has become one of the hottest topics in science. This two-dimensional, one-atom-thick transparent semiconductor with a tuneable zero band gap is comprised of sp^2 -hybridized carbon atoms arranged in a hexagonal manner, creating a robust honeycomb-like lattice.^[31-32] Graphene can be considered as a parent of all graphemic forms (Figure 1.1, d–h).^[4, 7] It displays remarkable electron mobility similar to mobility of photons. Moreover, the charge carriers obey a linear dispersion relation, and therefore mimic massless relativistic particles. Graphene also exhibits a high thermal conductivity and optical transmittance. It is currently the lightest, thinnest and strongest material in the universe with an outstanding elasticity.^[3, 7, 31-32] All these properties make graphene an ideal candidate for application in highly efficient sensors, fuel cells, renewable energy sources, transparent electrodes, and nanocomposite materials.^[32-38]

The importance of these new allotropes can be easily demonstrated not only by the vast interest of the scientific community, but also by the recognition they received. Both discovery of fullerenes and the isolation of graphene were awarded with a Nobel prize. In the case of fullerenes, the 1996 Nobel prize in Chemistry was awarded to Robert F. Curl, Sir Harold Kroto and Richard E. Smalley for “*their discovery of fullerenes*”. In the case of graphene, the 2010 Nobel Prize in Physics was awarded to Andre Geim and Konstantin Novoselov “*for ground-breaking experiments regarding the two-dimensional material graphene*”.^[39]

Organic chemists, encouraged by the developments and extraordinary properties of these nanostructures, worked in parallel on the design and synthesis of carbon allotropes in a more controlled manner. The total synthesis of fullerene C_{60} ^[40] has been established a long time ago and, similarly, a great progress has been made towards the controlled synthesis of carbon nanotubes, where belt-like molecules (nanobelts)^[41] have been synthesized as model compounds for armchair^[42-43], zig-zag^[44-46] as well as chiral carbon nanotubes. Well defined cut-outs of graphene could serve as models for studying the properties of graphene (Figure 1.2)^[46], but they often represent a synthetic challenge for scientists. They come in a variety of shapes and sizes, which affect their properties. For example, very stable fully benzenoid compounds (Figure:1.3 d) have a large HOMO–LUMO gap, while highly reactive compounds such as heptacene (Figure 1.2, top left), have a narrow HOMO–LUMO gap.^[46] The latter are of particular interest of the scientific community as they are expected, due to the presence of unpaired electrons in the low-lying excited states, to exhibit magnetic properties. These properties make graphene fragments an interesting material for the development of molecular spintronics and molecular memory devices.

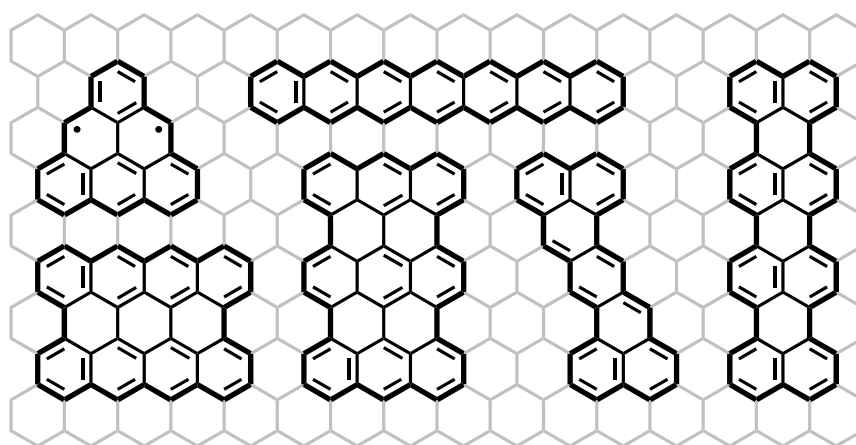


Figure 1.2: Structure of open-shell graphene fragment triangulene and low-band cut-outs of graphene.^[46]

1.3 CLAR'S SEXTET

Since the introduction of the concept by Kekulé in 1865^[47], aromaticity plays a critical role in organic chemistry, thanks to the possibility to rationalize the chemical structure, stability and reactivity of organic molecules.^[48-50] The Hückel $4n + 2$ rule^[51-55] represents an extremely important step towards definition of aromaticity, although it does not provide any explanation for polycyclic systems, as it is strictly valid for monocyclic conjugated system. Various attempts have been made towards postulating a rule for polycyclic aromatics. In 1972, based on the seminal work of Armit and Robinson,^[56] Clar came up with the model of extra stability of $6n$ π -electron benzenoid species, generally known as Clar's sextet rule.^[57-58] The Clar's rule states that the Kekulé resonance structure with the largest number of disjoint aromatic π -sextets (benzene-like moieties), is the most important for characterizing polycyclic aromatic hydrocarbons.^[57, 59-60] Additionally, the aromatic π -sextets are defined as six π -electrons localized in a single benzene-like ring separated from adjacent rings by formal C–C single bonds.

If we consider phenanthrene, we find that two Clar's resonance structures are possible, one with one fully isolated Clar's sextet in the central ring and one with two fully isolated Clar's sextets in the outer rings (Figure 1.3 a). The application of the Clar's rule indicates that the latter one is a more likely resonance in terms of stability. The outer rings are expected to have a larger local aromaticity (they are more aromatic) than the one central ring, which is expected to behave more like an olefin.^[58-60] This observation was experimentally proven by using different measures of local aromaticity,^[61-63] which is also the reason why bromine adds on the central ring of phenanthrene without the use of any catalyst.^[64]

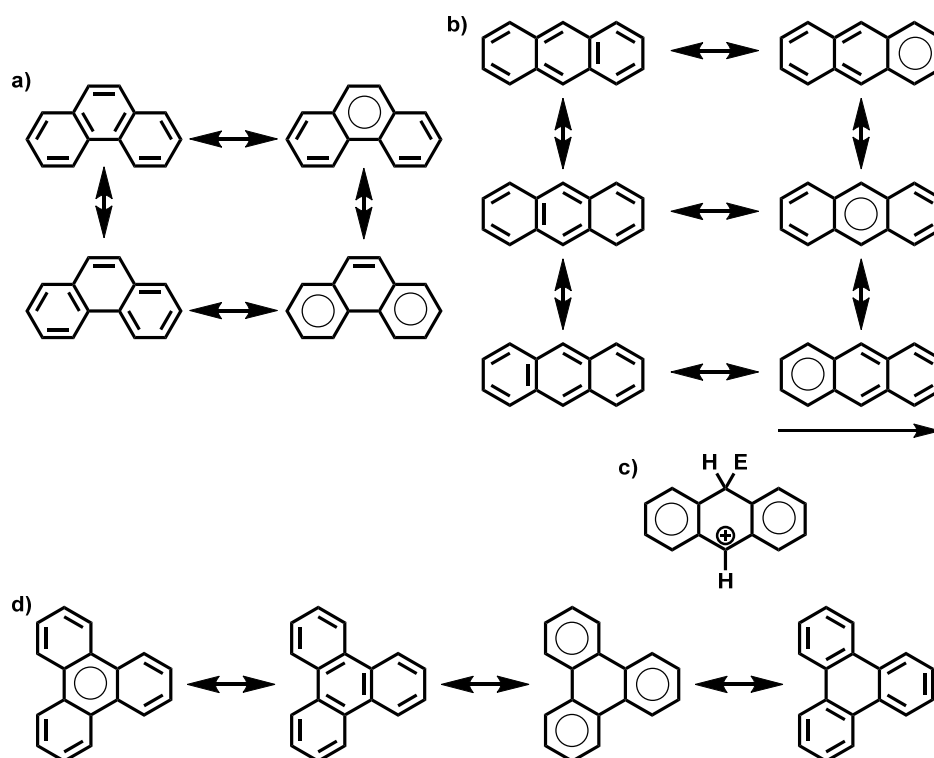


Figure 1.3: The representation of Clar's structures of a) phenanthrene; b) anthracene; d) triphenylene. c) The intermediate of addition reaction on anthracene stabilized by two Clar's sextets.

In anthracene, the situation is quite different. In total, three structures that have one Clar's sextet localized in one of the three rings (Figure 1.3 b) can be drawn. These structures are equivalent in Clar's rule and the Clar's structure is better described as superposition of all these three structures. This is usually described by an arrow below the structure (Figure 1.3 b, bottom) indicating the existence of the so-called "migrating sextet". Therefore, one can expect similar aromaticity for all three aromatic rings of anthracene. This prediction was also confirmed using different measures of local aromaticity.^[49, 60, 64] The existence of two Clar's sextets in phenanthrene compared to only one migrating sextet in anthracene suggests that phenanthrene is much more stable. Both theoretical and experimental studies have proven that phenanthrene indeed is more stable, as it has 4–8 kcal mol⁻¹ greater aromatic stabilization energy than anthracene.^[57, 65-67] Because of this, anthracene reacts faster than phenanthrene, especially on the central ring. The reason for this is the formation of

intermediate (Figure 1.3 c) which possesses two Clar's sextets, rather than just one migrating sextet. The existence of such intermediate provides larger stability and lowers the activation energy.^[68-70] The last example of Clar's structure is triphenylene (Figure 1.3. d), which has three fully separated Clar's sextets, which makes it more stable than phenanthrene and anthracene.

In Clar's rule, we can classify four types of six-membered rings: a) aromatic sextets (like phenanthrene's external rings); b) rings with localized double bonds (like phenanthrene's central ring); c) migrating sextets (like anthracene's rings); d) empty rings (like triphenylene's central ring). Similarly, we can differentiate three types of benzenoid molecules: a) those that contain Clar's sextet(s) and double bond(s) (phenanthrene, Figure 1.3 a); b) those that contain a single Clar sextet and rings with two double bonds, known as "migrating sextets" for which more than one Clar's structure can be drawn (anthracene, Figure 1.3 b); c) those that contain Clar's sextets and empty rings, known as fully benzenoid (triphenylene, Figure 1.3 d).^[57, 59]

The most stable are "fully benzenoid" structures, which only have 6π electron-rings and empty rings, for example, triphenylene (Figure 1.3 d). These molecules are known to have extra stability.^[57, 71] To support this statement, triphenylene was compared to a series of its isomers ($C_{18}H_{12}$), where each isomer contains maximum of two Clar's sextets. Out of all isomers, triphenylene has the largest resonance energy, is chemically least reactive, has the highest ionization potential and the largest HOMO-LUMO gap.^[57, 59, 68]

In general, fully benzenoid molecules have a large HOMO-LUMO gap and are very stable. On the other hand, the "migrating sextet" molecules have a small HOMO-LUMO gap and are less stable. This can be demonstrated by analyzing the UV/VIS spectra of different kinked isomers of heptacene (Figure 1.4). By a stepwise addition of one kink (and so one Clar's sextet), one observes a shift of the absorption maximum to shorter wavelengths

(from 840 to 328 nm). Unstable heptacene (one Clar's sextet) is green, but its isomer tetrabenzanthracene (five Clar's sextets) is colourless and stable.^[59-60, 71]

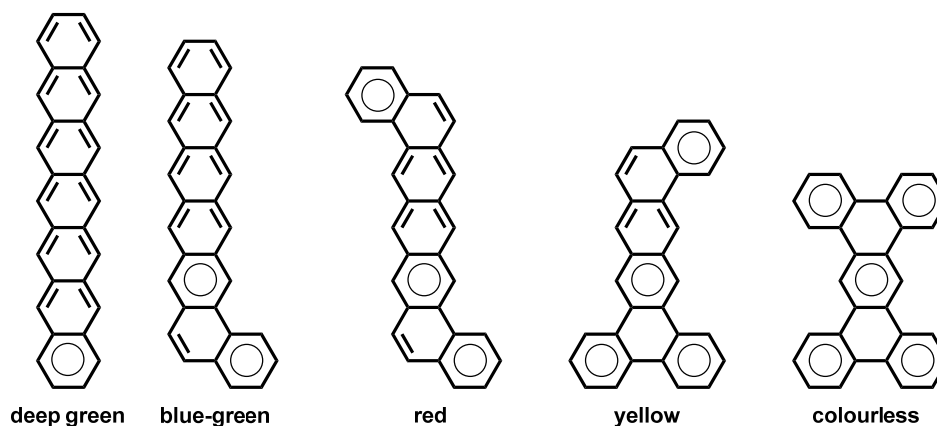


Figure 1.4: The change of colour of kinked heptacene derivatives depending on the number of Clar's sextets.

1.4 SPIN-DELOCALIZED HYDROCARBON SYSTEMS

If we cut single sheet of graphene with imaginary scissors, we can get different fragments, starting from single double bond through polyenes up to complex structures. The more complex cut-outs of graphene can be divided into two large groups with significantly different properties, namely, Kekulé and non-Kekulé fragments. In this chapter, we will have a closer look at both of them.

An allyl radical (Figure 1.5) represents the simplest case of a spin-delocalized system. In this molecule, one unpaired electron is delocalized between two possible positions, the terminal carbon atoms (1 and 3).^[72]



Figure 1.5: Spin-delocalization in allyl radical.

If we attach one additional sp^2 -carbon atom to the allyl radical moiety (Figure 1.6 a), depending on the position of the connection, two possible C_4H_6 isomers can be formed: 1,3-

butadiene (BD, connection at 1-position) and trimethylenemethane (TMM, connection at 2-position).^[73]

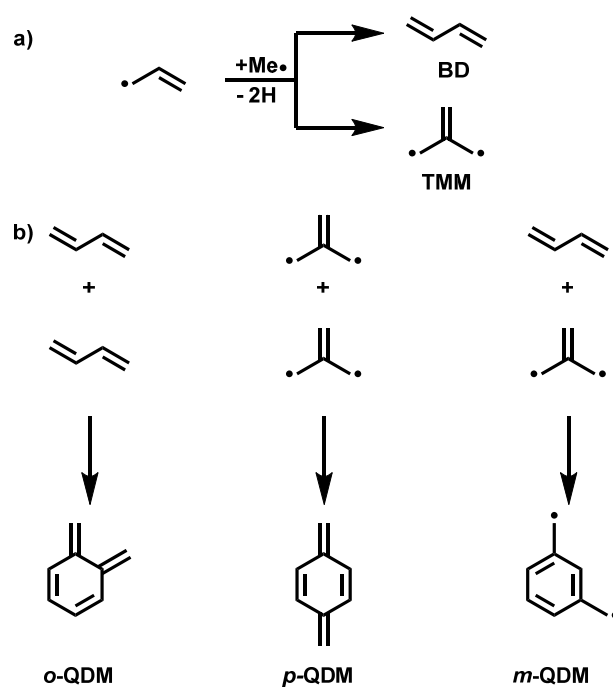


Figure 1.6: a) The formation of 1,3-butadiene (BD, top) and trimethylenemethane (TMM, bottom) by addition of one sp^2 -carbon atom to allyl radical. b) Possible ways to combine two TMM, two BD, or one TMM and one BD unit.

The simple alteration in mode of connection produces two electronically very different compounds. TMM has a non-Kekulé diradical structure containing two unpaired electrons and one double bond. On the other hand, BD has a Kekulé structure with two conjugated double bonds and no unpaired electrons. This example nicely illustrates the effect of topology of an sp^2 -carbon atom backbone on the electronic structure, which can be either open-shell (TMM) or closed-shell (BD). If we combine TMM and BD together (Figure 1.6 b), three different structures can be produced depending on the mode of connection, namely, *ortho*- (oQDM), *para*- (pQDM) and *meta*- (mQDM) xylylenes or quinodimethanes. In this case, the combination of two TMM or two BD unit gives Kekulé quinoidal structures (pQDM or oQDM) and only the combination of one TMM and one BD unit gives a non-Kekulé diradical structure (mQDM).^[74-78]

1.4.1 KEKULÉ AND NON-KEKULÉ HYDROCARBONS

The difference between the Kekulé and non-Kekulé structures can be easily demonstrated by the so-called “star” rule. All hydrocarbons previously mentioned in section 1.4 (allyl radical, BD, TMM, *o*QDM, *p*QDM, *m*QDM), belong to the group of alternant hydrocarbons. A π -conjugated hydrocarbon is alternant when a star can be placed on alternate sp^2 -carbon atoms in such a way that no two stars are in direct neighbourhood (they are adjacent).^[73, 75, 79] Alternant hydrocarbons can be further classified as a) even-alternant and b) odd-alternant hydrocarbons (Figure 1.7 b). In the case of even-alternant hydrocarbons, for example, *o*QDM or *p*QDM, the number of starred (n_s) and unstarred (n_u) carbon atoms is equal ($n_s = n_u$). This means that they have fully occupied bonding and empty antibonding orbitals, which are symmetrically distributed, and no non-bonding orbitals. Each molecule can be therefore represented by at least one Kekulé resonance structure, in which all electrons are paired in form of conjugated double bonds (Figure 1.7 a). The even-alternant or Kekulé hydrocarbon can be defined as molecules containing enough atoms and bonds to satisfy the standard rules of valence.^[80]

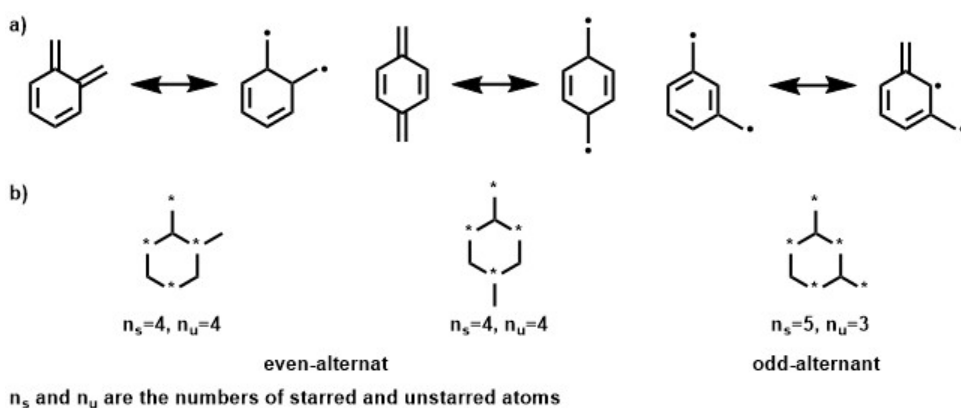


Figure 1.7: a) Quinoidal and radical structures of *o*-, *p*- *m*-xylylenes. b) Demonstration of the “star” rule on *o*-, *p*- *m*-xylylenes.

In the case of b) odd-alternant hydrocarbons, for example, TMM or *m*QDM, these molecules also have equal number of fully occupied bonding and empty antibonding orbitals,

but they also possess a set of non-bonding orbitals. The number of non-bonding orbitals equals to $n_s - n_u$ and each non-bonding orbital is occupied by one unpaired electron. Therefore, the number $n_s - n_u$ is also equal to number of unpaired electrons. In the case of these molecules, it is not possible to draw a Kekulé resonance structure, where all electrons are paired and only non-Kekulé structures are possible.^[74-78] Therefore, the non-Kekulé hydrocarbons can be defined as molecules containing enough atoms, but not enough bonds to satisfy the standard rule of valence.^[77]

1.4.2 DETERMINATION OF THE GROUND STATE WITH “STAR” RULE

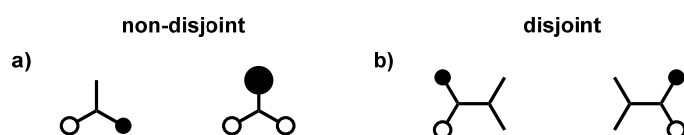


Figure 1.8: Examples of non-disjoint (TMM) and disjoint (tetramethyleneethane, TME) non-bonding molecular orbitals.

The “star” rule can be also applied for determination of the ground state of π -conjugated hydrocarbons.^[77, 80-81] When $n_s > n_u$, the non-bonding molecular orbitals of molecules have atoms in common (electron density is localized on the same atoms) and they are called non-disjoint (Figure 1.8 a). According to the Hund’s rule, each orbital is filled with one electron and all unpaired electrons have parallel spins in order to minimize the Coulomb repulsion. Therefore, diradical molecules with non-disjoint non-bonding molecular orbitals are expected to favour a triplet ground state (for example, TMM).^[77, 82] In contrast, when $n_s = n_u$, the ground state is typically singlet. Here, the non-bonding molecular orbitals do not have atoms in common (electron density is not localized at the same atoms), and they are called disjoint (Figure 1.8 b). With such molecular orbitals, the destabilization factor by the Coulomb repulsion becomes much smaller than for non-disjoint-type molecules. The relative stability of the singlet versus triplet ground state will therefore be nearly equal in the first approximation (for example, in tetramethyleneethane, TME).^[77, 83]

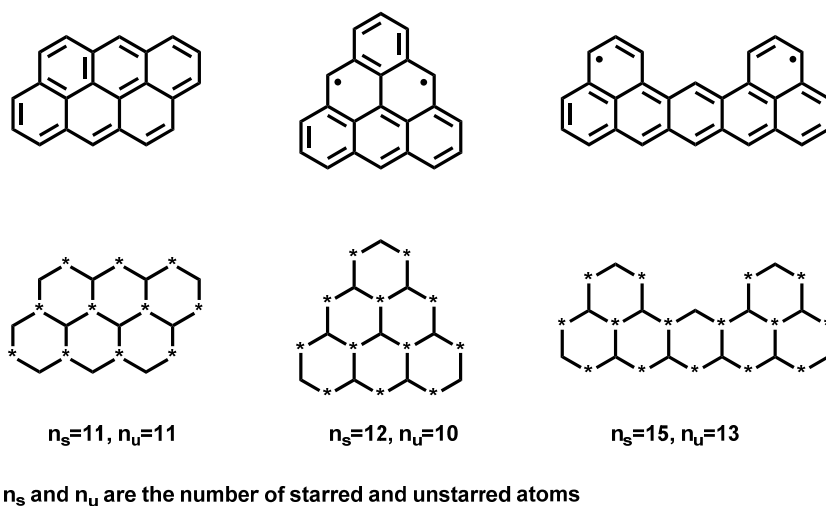


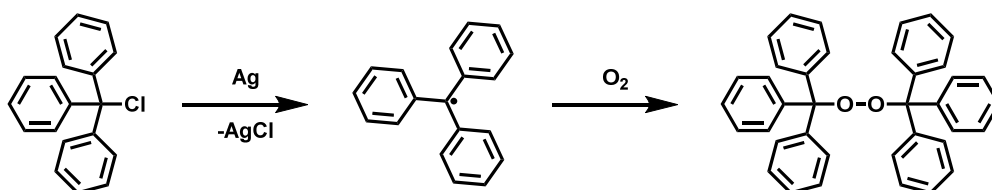
Figure 1.9: Application of the “star” rule on larger hydrocarbons.

The “star” rule can be also applied on the larger polyaromatic hydrocarbons (Figure 1.9), for example, anthanthrene ($n_s - n_u = 0$), which is a Kekulé structure, triangulene ($n_s - n_u = 2$), which is a non-Kekulé diradical structure and uthrene ($n_s - n_u = 2$), also a non-Kekulé structure. The synthesis and properties of these hydrocarbons will be further discussed in Chapters II and III.

1.5 HYDROCARBON-BASED ORGANIC RADICALS

1.5.1 TRIPHENYLMETHYL RADICAL

The beginning of radical chemistry can be dated back to 1900, when Moses Gomberg announced the formation of persistent triphenylmethyl radical (Scheme 1.1). Gomberg treated triphenylmethyl chloride with silver and obtained a coloured solution, which upon treatment with oxygen yielded peroxide (Scheme 1.1).^[84-85]



Scheme 1.1: Gomberg’s synthesis of trimethylmethyl radical and its subsequent oxidation.

In diluted and deoxygenated solution, the trimethylmethyl radical (or Gomberg's radical, later named after his discovery) exists in equilibrium with its σ -dimer. Initially, three possible structures for the σ -dimer were proposed: a head-to-head (Figure 1.10 a, left), head-to-tail^[86] (Figure 1.10 a, middle), and tail-to-tail σ -dimer^[87-88] (Figure 1.10 a, right). For more than fifty years, the wrong head-to-head structure was widely accepted as the correct structure for the σ -dimer. Only later it was corrected to the unsymmetrical head-to-tail structure of σ -dimer, based on the experimental data and structural analysis.^[89-90] Due to the sterical hindrance of three phenyl groups attached to the central carbon atom, the σ -dimer is not formed by linkage of the central carbon atoms of the two monomers, but rather by the linkage of one central carbon atom and one carbon atom at the *para*-position of one of the phenyl rings of the monomer. This type of linkage is possible due the partial delocalization of the radical, where the spin is not only localized at the central carbon atom, but also partially delocalized at the *ortho*- and *para*- carbon atoms of the phenyl rings (Figure 1.10 b, right).

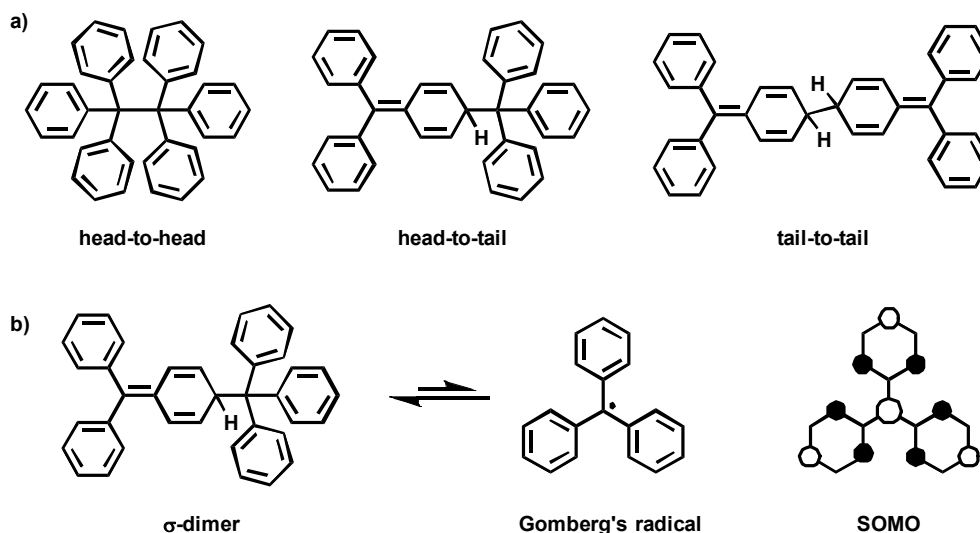


Figure 1.10: a) Three originally proposed structures for σ -dimer of triphenylmethyl radical, head-to-head dimer, connected via central carbon atoms (left); head-to-tail dimer, connected via one central carbon atom and one carbon atom at *para*-position of the phenyl ring (middle); tail-to-tail, connected via two *para*-position of the phenyl ring (right). b) Triphenylmethyl radical in an equilibrium with its σ -dimer (left); Partial delocalization of the electron (spin) in triphenylmethyl radical (right).

In order to explore the effect of substituents on stabilization of triphenylmethyl radical, Neumann *et al.* synthesised various *ortho*- and *para*-substituted derivatives of triaryls.^[91-92] The effect of substituents in stabilizing radicals was measured by EPR spectroscopy, which allowed determination of the equilibrium constants for dissociation of the dimers. This study concluded that the captodative radicals (radicals bearing donor- and acceptor-substituents at the same time) are slightly more stable than the symmetrically disubstituted triaryls.^[91]

Perchlorinated triphenylmethyl radicals represent an important subclass of derivatives based on the Gomberg's radical. First synthesized in 1971 by deprotonation of corresponding tris(pentachlorophenyl)methane, followed by subsequent oxidation of an anion by iodine (Scheme 1.11),^[93] these compounds are remarkably stable, with lifetime of several decades. Due to their extreme stability, they are characterized as inert carbon free radicals.

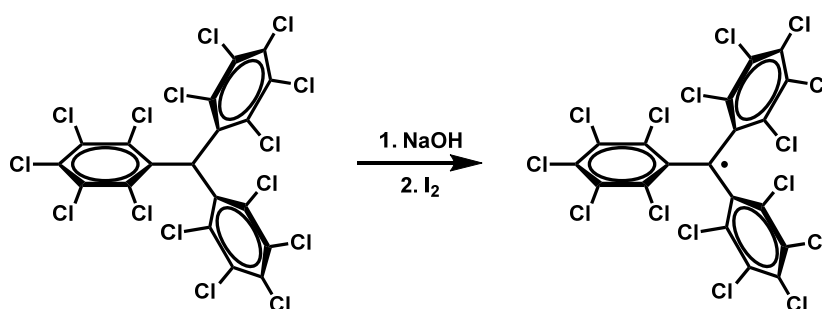


Figure 1.11: Preparation of perchlorotriphenyl methyl radical.

The stability of these compounds is caused by the presence of *ortho*-chlorine atoms in the aryl rings, which can effectively shield the central radical sides and therefore prevent reaction of perchlorinated radicals, with both oxygen and other molecules. Due to steric hindrance caused mostly by bulky chlorine atoms, the aromatic rings are slightly twisted around the bonds linking the central carbon atom with *ipso*-carbon atoms. As a result, the molecules have a propeller-like conformation.^[93-94] Because of the great stability, several derivatives of perchlorinated triphenylmethyl radical/biradical were synthesized and their electronic, magnetic and optical properties have been extensively investigated.^[95-97]

1.5.2 PHENALENYL RADICALS

Phenalenyl is the smallest polybenzoic odd-alternant hydrocarbon radical with high symmetry (D_{3h}), as well as the smallest open-shell graphene fragment. The phenalenyl radical has a triangular topology and is composed of three peri-fused benzene rings, containing only 13 carbon atoms and 13 π -electrons (odd-electron hydrocarbon).^[98] The phenalenyl radical was first generated in 1957 by air oxidation of phenalene^[99] (Figure 1.12 a, left) and later by oxidation of phenalenyl anion^[100] (Figure 1.12 a, right). The radical is extremely sensitive to air, however, it is stable in the deaerated solution where it exists in equilibrium with its σ -dimer.^[100-102] In contrast to Gomberg's radical, the unpaired electron in phenalenyl is delocalized uniformly throughout the periphery of the molecule at the six α -positions, which display the highest positive spin density (Figure 1.12 b, right). The carbon-carbon bond of the σ -dimer is formed between two α -carbon atoms, one from each phenalenyl subunit (Figure 1.12 b, left). In this way, the aromaticity in the C_{10} portion (naphthalene units) of each phenalenyl subunit is preserved. This scenario is preferred to the case when the central carbon atom would be involved in the σ -bond formation, which would lead to the loss of aromaticity.^[103]

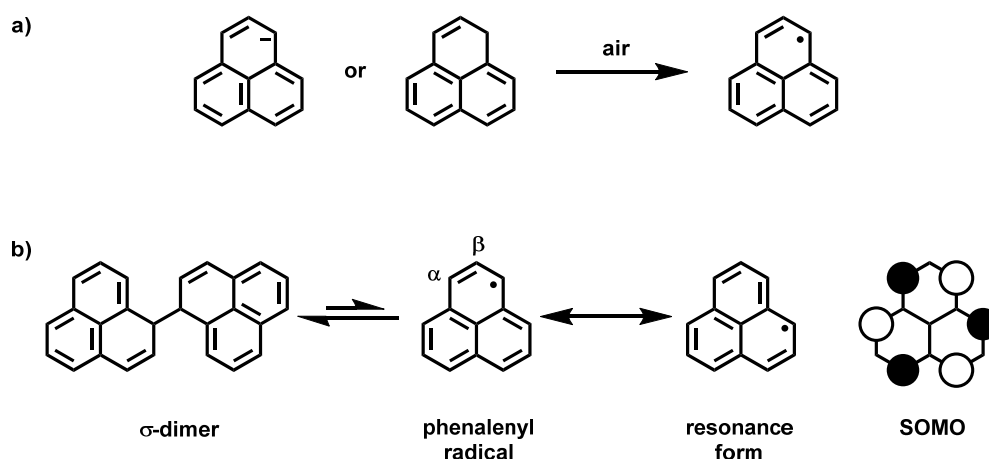


Figure 1.12: a) Preparation of a phenalenyl radical by air oxidation of phenalenyl anion (left) or phenalene (right). b) Phenalenyl radical in equilibrium with its σ -dimer (left); resonance structures and the SOMO of phenalenyl radical (right).

The chemical reactivity^[100-101, 104-106] and physical properties^[99, 102, 107] of phenalenyl radical in solution have been extensively studied for more than 60 years, but the solid-state properties were unknown for a long time due to the instability of the phenalenyl radical under air. To prevent the formation of the σ -dimer, Nakasuji *et al.* introduced bulky *tert*-butyl substituents at the β -positions to protect the reactive α -carbon atoms (Figure 1.13).^[108, 98] The crystallographic analysis showed that the introduction of bulky substituents indeed prevents the formation of the σ -dimer, however, a formation of a face-to-face π -dimer with two phenalenyl units stacked on top of each other in a staggered way, such that the steric repulsion of the *tert*-butyl groups is minimized, was observed (Figure 1.13). The interplanar distances in the π -dimer are significantly shorter (~ 3.25 Å) than the sum of the van der Waals radii of the carbon atoms (standard π - π stacking, ~ 3.4 Å).^[109-111]

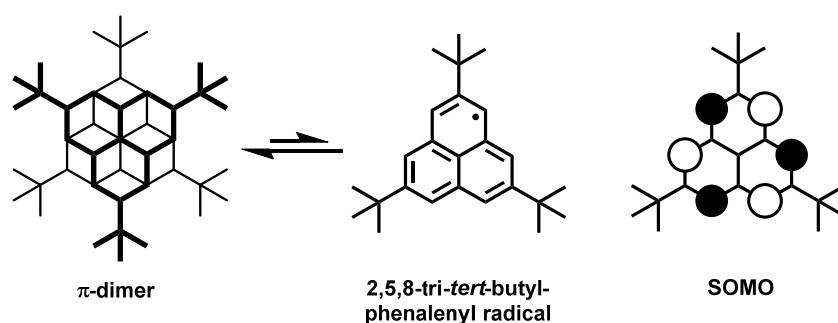


Figure 1.13: The 2,5,8-tri-*tert*-butyl-phenalenyl radical and its corresponding π -dimer (left). Singly occupied molecular orbital (SOMO; on the very right).

This phenomenon can be explained by the formation of the so-called “pancake bond”,^[103, 112-114] which is a multi-centred two-electron bonding interaction between two phenalenyl units. It is governed by attractive interactions derived from a covalent bonding interaction between two unpaired electrons. The observed orientation of one of the molecules with respect to the other one is related to the maximum overlap between two involved SOMOs (Figure 1.13) and minimum overlap between all carbons atoms. The π -dimers formed via a pancake bond usually display a small HOMO–LUMO gap and low-lying triplet

excited states that can be populated thermally, therefore, magnetic properties can be expected.^[103, 115-117] The short-contact distance between the dimers improves electron transport, thereby, the spin-delocalized molecules are promising candidates for self-assembled materials possessing both conducting and magnetic properties, a characteristic otherwise typical for metals.

1.5.3 TRIANGULENE BASED RADICALS

Extension of the π -conjugated electronic network of the phenalenyl radical leads to the series of triangular-shaped non-Kekulé polynuclear benzenoid hydrocarbons (open-shell graphene fragments), with phenalenyl as the smallest member (Figure 1.14). Due to the triangular topology, these systems possess multiple unpaired electrons, which are uniformly delocalized over the structure.^[85, 118, 119-121] Moreover, these systems are expected to have a ground state of highest possible multiplicity, due to the topological degeneracy of their non-bonding molecular orbitals, which have a non-disjoint character. This feature makes them potential candidates for use in molecular electronics,^[122-124] organic spintronics,^[125-129] and energy-storage devices^[118].

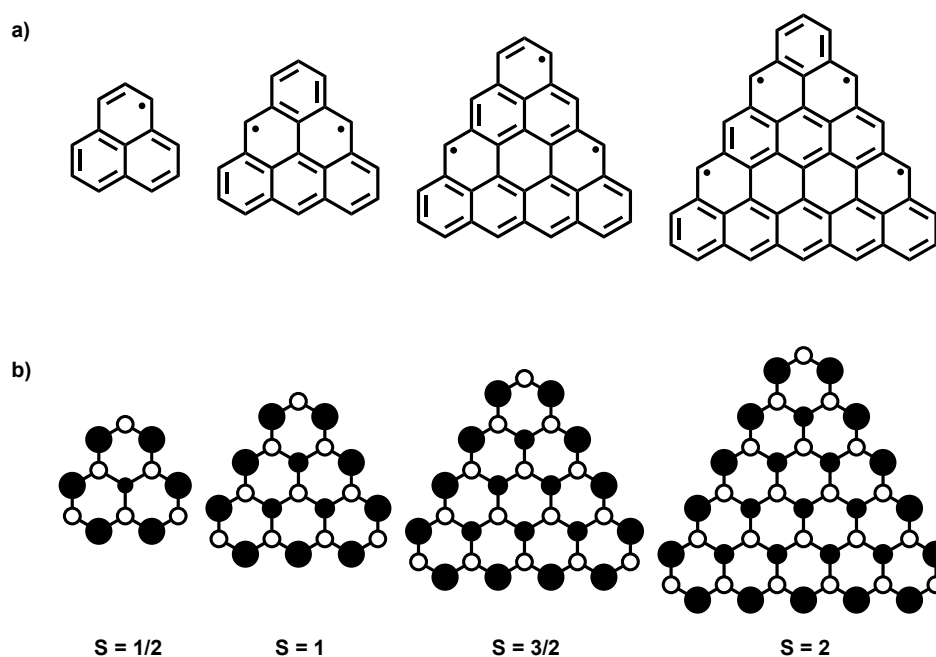


Figure 1.14: a) Structures of non-Kekulé polynuclear benzenoid hydrocarbons (open-shell graphene), phenalenyl (far left), triangulene (left) and supertriangulene. b) Spin-density distribution in the open-shell graphene fragments.

Triangulene is the smallest non-Kekulé polybenzoid with a triplet ground state.^[131] Its existence was first proposed in 1941 by a German chemist Erich Clar (the Godfather of hydrocarbon chemistry; triangulene is hence commonly known as Clar's hydrocarbon).^[132] Triangulene's open-shell triplet ground state originates from its two singly occupied molecular orbitals (SOMOs).^[131, 133, 144] As we discussed for the case of TMM (Chapter 1.4.2), triangulene possesses a pair of non-disjoint singly occupied molecular orbitals, which have atoms in common. The triangulene's triplet ground state is estimated to be about 20 kcal mol⁻¹ lower in energy than its singlet state.^[133-134] Similarly to the phenalenyl, the spin density is mostly localized at the periphery of the molecule (Figure 1.14 b, left), which makes triangulene highly reactive towards oxygen and polymerization.^[131, 133, 135-136]

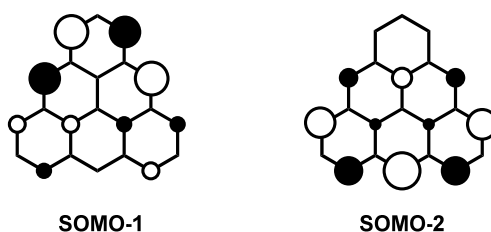


Figure 1.15: Singly occupied molecular orbitals (SOMOs) of triangulene diradical.

The first attempts to prepare triangulene can be dated back to 1950s, when Clar was investigating various methods for its preparation. (One of the synthetic routes will be discussed in detail in Chapter II). Clar have prepared numerous precursors, from which triangulene could be generated. However, the isolation of the final molecule was always unsuccessful. Clar concluded that triangulene was most probably generated, but because of its high instability and extreme reactivity, the molecule could not be isolated as it immediately polymerized. However, he proceeded to work in this area further, focusing

mostly on the preparation of different derivatives of triangulene in order to understand the properties of these compounds.^[137-140]

The first example of the radical based on a triangulene structure was prepared by Bushby *et al.* in 1990s, when they were investigating the potential of non-Kekulé hydrocarbons with heteroatomic modification for usage as molecular magnets.^[131, 135, 141-142] The trioxotriangulene diradical trianion was generated by chemical reduction of the corresponding diketone (Figure 1.16 a), which proceeded via two one-electron additions. The authors claimed that both the dianion radical and trianion diradical are stable in deaerated solution even at room temperature; however, they are extremely sensitive towards oxygen.^[142]

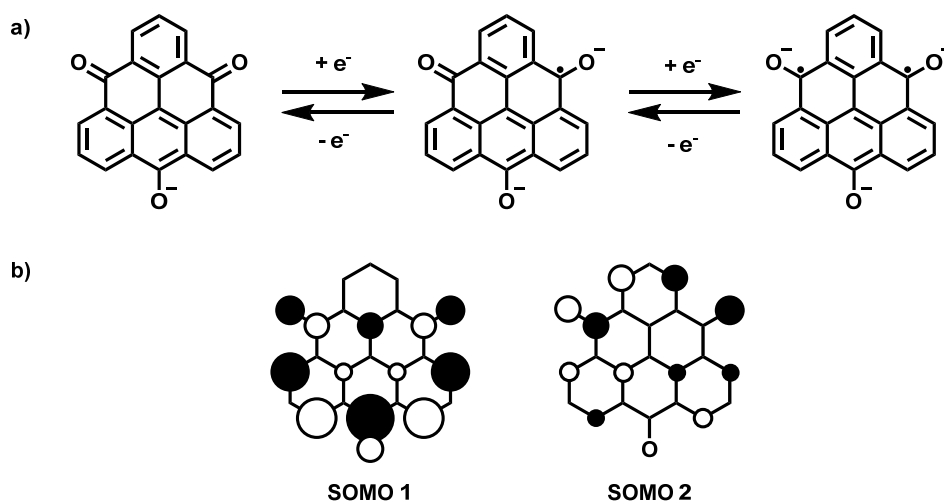


Figure 1.16: a) Generation of the trioxotriangulene trianion diradical via two one-electron reduction of the corresponding diketone. b) Singly occupied molecular orbitals of trioxotriangulene trianion diradical.

The EPR spectroscopy of the frozen solution confirmed that the ground-state multiplicity of the trianion diradical is a triplet.^[142-143] The introduction of the heteroatoms on the parent triangulene skeleton lifts the degeneracy of the non-bonding molecular orbitals, causing a kinetic exchange interaction to dominate over spin polarization in the parent π -system, which leads to the stabilization of the system (Figure 1.16 b).^[85, 133]

Another example of a triangulene derivative was synthesized by Inoue *et al.* in 2001, by introducing bulky tri-*tert*-butyl substituents on the carbon sites with nodes in the non-bonding molecular orbitals (in the corners of the triangulene structure), to protect the reactive carbon sites (Figure 1.17, left). These groups were chosen, as they would provide the least prominent effect on the structure in terms of electronics, [133, 85] when compared to heteroatoms used by Bushby *et al.* [131, 142-143] The tri-*tert*-butyl triangulene is prepared by *p*-chloranil oxidation of the corresponding dehydroprecursor. [133] The triplet ground-state of the tri-*tert*-butyl triangulene was validated by EPR spectroscopy of the frozen solution. The diradical exists only at low temperatures in a deaerated solution and once the sample is warmed it immediately oligomerizes at the carbon sites with large spin densities. [85, 133, 143]

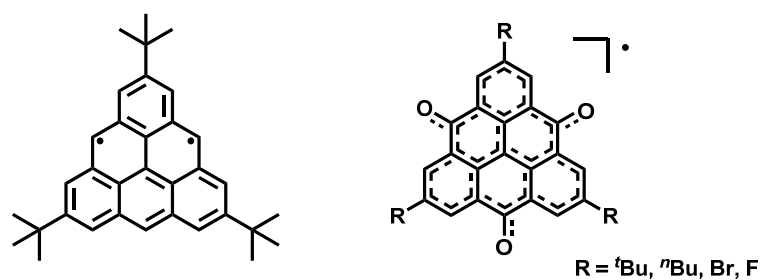


Figure 1.17: Structure of the tri-*tert*-butyl triangulene, left.; Monoradical derivatives of trioxotriangulene, right.

Later, Morita *et al.* synthesized a series of neutral monoradicals based on a trioxotriangulene radical to explore the possibility of their use as cathode-active materials for the development of molecular crystalline secondary batteries. (Figure 1.17, right) [85, 145-146] These radicals are extremely stable (decomposition point over 250 °C). The stability comes from the spin delocalization of the system, which is distributed over the whole structure with the highest density located on the central atom. [147-149] All these molecules possess multi-step redox ability (4 stages), that originates from extremely narrow energy gap between SOMO and doubly degenerate LUMO and forms a face-to-face π -dimers in the

solid state with central C–C distances significantly shorter ($\sim 3 \text{ \AA}$) than the standard π – π stacking. The π -dimers are further stacked to form one-dimensional column along the C–C axis. All these derivatives showed high battery capacity, exceeding those of Li-batteries, and are therefore promising candidates to replace the Li metal in the batteries in the near future.^[147, 148-151]

In the most recent work, Pavliček *et al.*^[152] explored the possibility to form triangulene on a surface by terms of atomic manipulation.^[153-155]

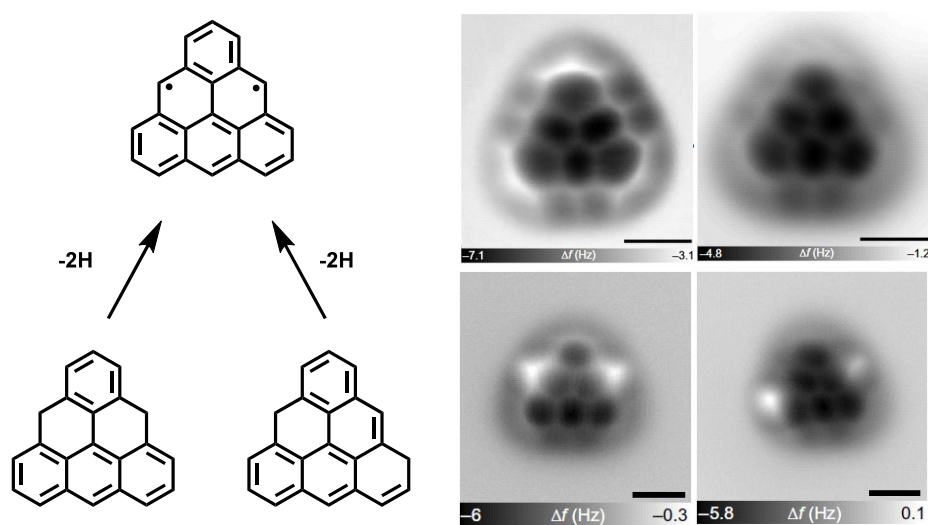


Figure 1.18: Dehydrogenation of the two dihydrotriangulene precursors present in the sample, left; AFM images of dihydroprecursors deposited on a NaCl surface, bottom right; AFM images of triangulene diradical on Cu (111) (top right) and Xe (111) (top far right) surface, respectively.^[152]

The dihydrotriangulene precursors (Figure 1.18, bottom left, synthesis will be discussed in Chapter II) were placed in an AFM/STM vacuum chamber. As can be seen in the AFM image of the precursors (Figure 1.18, bottom left), the bright areas show the sp^3 -carbon atoms with excess of hydrogen atoms. The triangulene was produced on Xe (111) surface by placing the CO STM tip over dihydrate region by pulsing a current of specific energy (hydrogen atoms were removed). The bright areas of the AFM images after the dehydrogenation (Figure 1.18, top right), correspond to the higher spin density localization than the dark areas.^[152]

1.6 GOAL OF THE THESIS

Silicon-based materials have dominated the world of computer science and industry for over 50 years. With the miniaturization of the devices, the silicon-based technology almost reached its limit, therefore, scientists are extensively looking in the ways how this vital part of modern world can be replaced in the near future.

Carbon-based materials caught the attention of the scientific community in recent years due to their intriguing properties that can be tuned by the chemical synthesis, cost of these materials as well as their broad application.

Since the discovery of graphene, this material found a wide range of application, from molecular electronics up to medicine. A specific group of graphene fragments is represented by spin-delocalized π -conjugated molecules. As these molecules contain one or more unpaired electrons, they exhibit magnetic and conducting properties, that are usually associated with metals. The magnetism in these systems emerges from the presence of unpaired electrons, either in the ground state or low-lying excited states. On the other hand, the conductivity in these arises on account of the short intermolecular distance between the molecules. Due to their challenging synthesis, only a handful of such systems are known to this day. The goals of the thesis are:

- 1) Synthesis of triangulene precursors.
- 2) Stabilization of the triangulene core by terms of encapsulation of the triangulene in the supramolecular complex with cyclophane and by building a protective shield around triangulene core.
- 3) Synthesis of donor–acceptor molecules based on the triangular motif and study of their properties.
- 4) Synthesis of molecular switch, featuring a [7]helicene backbone, that can be operated solely by light.

CHAPTER II:

TRIANGULENE PRECURSORS

2.1 INTRODUCTION

In the previous Chapter I, it was noted that the unsubstituted or “naked” triangulene has never been isolated, because it undergoes fast dimerization/polymerization, even when handled at temperatures below ambient. The reason for this is the presence of two unpaired electrons, which are delocalized mainly on the peripheral carbon atoms, making triangulene extremely reactive when these positions are not sterically hindered (Chapter 1.5.3)^[131, 133, 134, 136]. To overcome the problem of dimerization/polymerization, we proposed to encapsulate and therefore stabilize the “naked” triangulene in a supramolecular complex. The encapsulation should allow us to characterize triangulene in solution as well as in the solid state for the first time.

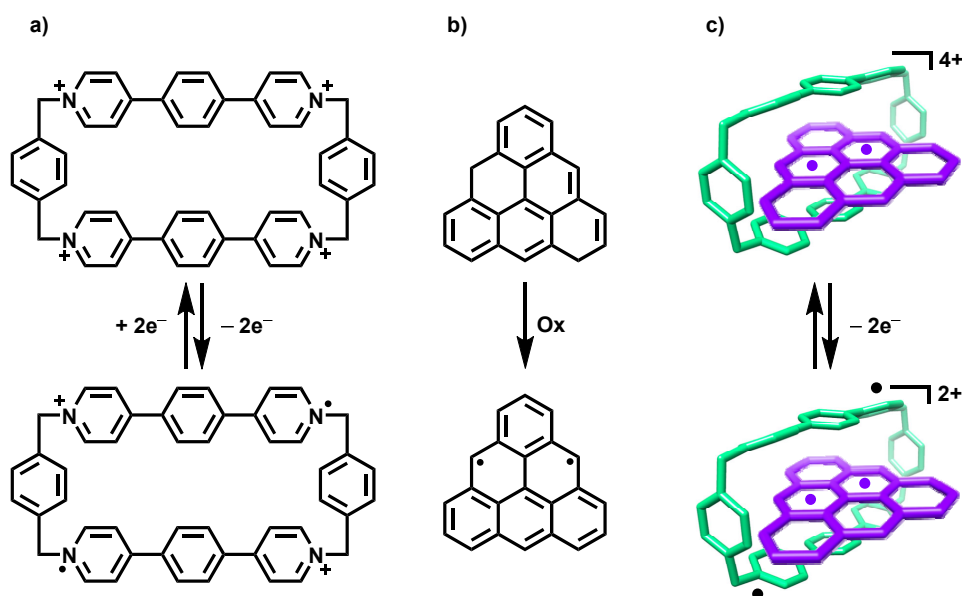


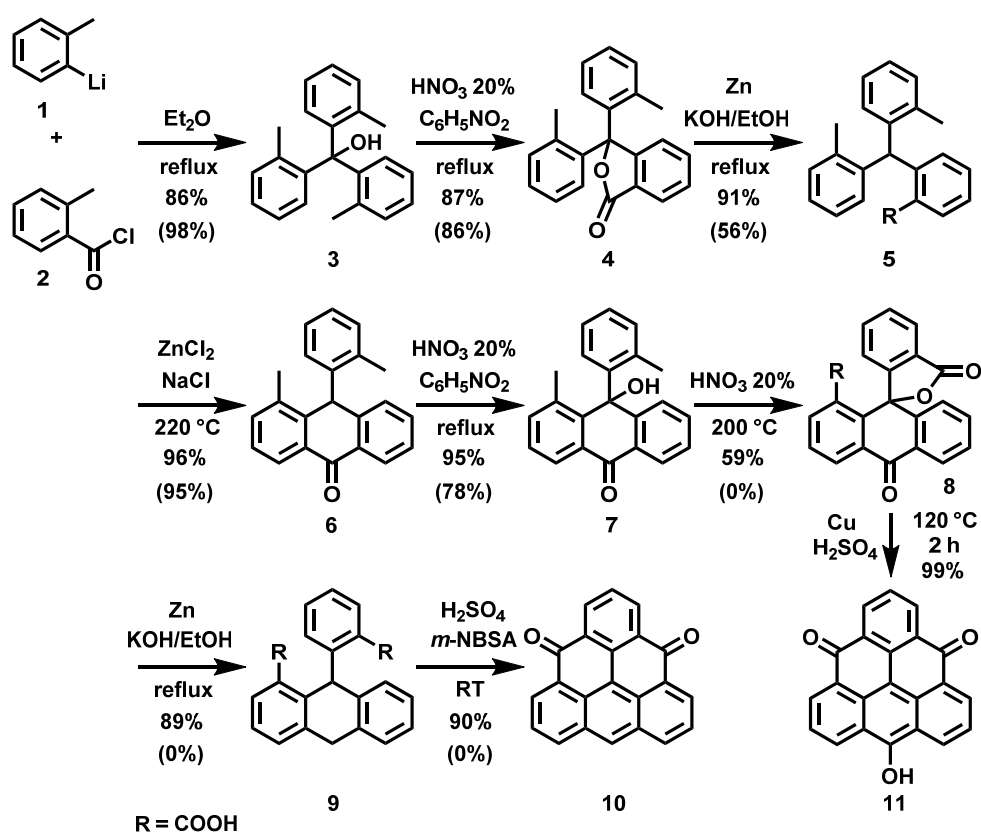
Figure 2.1: a) Structure of ExBox⁴⁺ and its reversible two-electron reduction to ExBox^{2(•+)}. b) Structure of dihydrotriangulene and its oxidation to triangulene. c) Illustration of supramolecular complex ExBox⁴⁺ ⊃ triangulene and its two-electron reduction.

A promising candidate that could serve as a host molecule to bind triangulene is ExBox⁴⁺ (Figure 2.1 a, top). This box-like tetracationic cyclophane that was reported in 2013 by Stoddart *et al.*^[156] is composed of eight aromatic rings and has a high affinity towards polycyclic aromatic hydrocarbons (PAH) of varying size, starting from naphalene up to coronene. The high affinity towards PAHs comes from the charge-transfer interactions between the ExBox⁴⁺ and PAH, with binding constants of about 10⁴ M⁻¹ for guests comprised of five or more fused rings. ExBox⁴⁺ is predicted to increase significantly the stability of triangulene, which is sterically suited to fit into the cavity of ExBox⁴⁺ in a 1:1 host-guest complex (Figure 2.1), as the binding constant of about 10⁵ M⁻¹ is expected for six benzene fused rings. In addition, the ExBox⁴⁺ can undergo a two-electron reduction (Figure 2.1 a) providing doubly charged diradical species ExBox²⁽⁺⁾, that can spin-pair with diradical triangulene (Figure 2.1 c) and can further increase their affinity towards each other.^[156]

The initial plan was to oxidize the triangulene precursor (Figure 2.1 b, top) in the presence of ExBox⁴⁺ at low temperatures in the oxygen-free environment to form the supramolecular complex ExBox⁴⁺ ⊂ triangulene in order to investigate its properties both in solution and, after obtaining single crystals, in the solid state. Subsequently, the two-electron reduction of the supramolecular complex of ExBox⁴⁺ ⊂ triangulene with the triplet ground state to ExBox²⁽⁺⁾ ⊂ triangulene with the singlet ground state would be investigated, as this system could potentially act as bistable redox-active switch, in which switching between the triplet and singlet states could be mediated by applying a voltage (Figure 2.1 c).

2.1.1 SYNTHESIS OF TRIANGULENE PRECURSORS

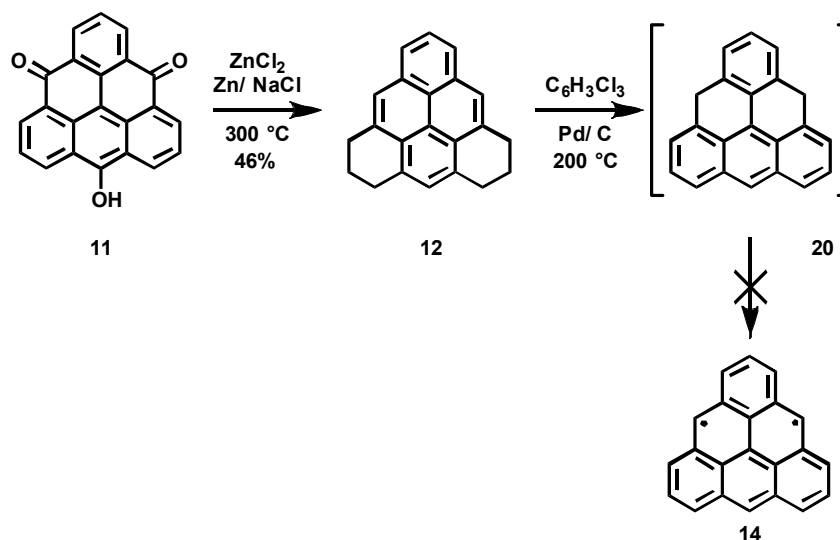
As mentioned in the previous chapter, several groups attempted to synthesise triangulene, however, its isolation in pristine form still remains a challenge. In 1950, Erich Clar investigated several possible routes towards triangulene, one of its shorter strategies is summarized in Scheme 2.1 (the yields in the brackets correspond to the yields that we obtained during our attempts to reproduce the Clar's procedures, and the synthesis will be discussed in the results and discussion section) [137-139]



Scheme 2.1: One of Clar's synthetic approaches towards triangulene. [137-139]

Clar started his synthesis by lithium-halogen exchange of *o*-tolyl chloride, followed by double-fold nucleophilic addition of lithiated species **1** on acetyl chloride **2**. The formed tritolyl carbinol **3** was subsequently oxidized with diluted HNO_3 producing lactone **4** that was reductively opened with zinc powder in ethanolic solution of KOH to form acid **5**. Friedel-Crafts acylation of **5** in the melt of $\text{ZnCl}_2/\text{NaCl}$ yielded anthrone **6** that was subsequently oxidized to hydroxyanthrone **7**, which was further oxidized with diluted HNO_3

to the lactone **8**. The lactone **8** can be directly cyclized by Friedel–Craft acylation in H_2SO_4 in the presence of copper to diketohydroxy triangulene **11**, or the keto-group of the anthrone can be reduced with zinc powder and the formed diacid **9** can be closed by Friedel–Crafts acylation to diketotriangulene **10**.^[137-139]

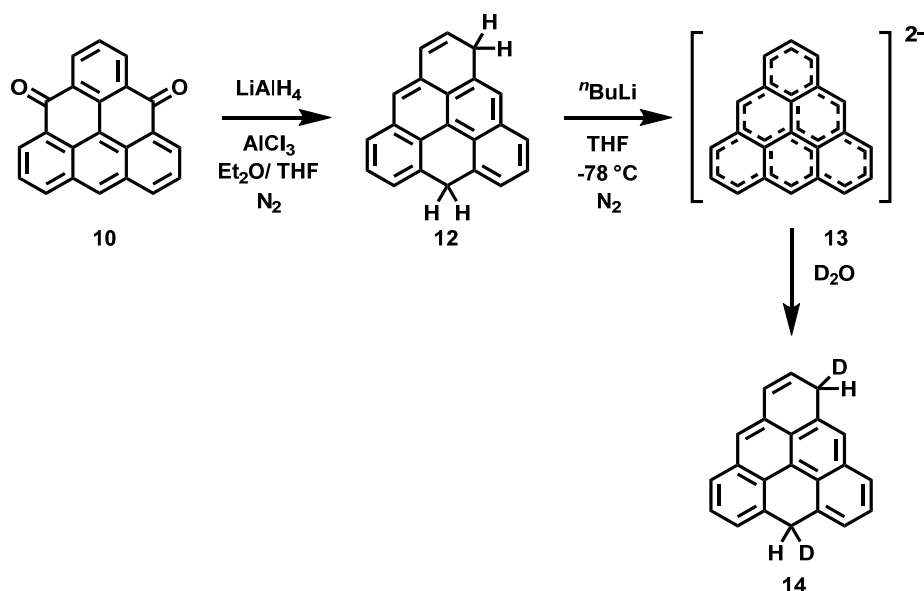


Scheme 2.2: Clar's unsuccessful synthesis of triangulene.^[137-139]

Clar attempted to prepare triangulene (**14**) by dehydrogenation of compound **12**, which was prepared by reduction of diketohydroxy triangulene **11** with zinc powder under extremely harsh conditions. Clar reported that during the course of the dehydrogenation, dihydrotriangulene **20** was observed by means of UV spectroscopy. However, by the end of the reaction, only brown solid of unknown nature and small amounts of unreacted starting material were isolated. Following this result, Clar concluded that triangulene was most probably formed, however, due its high reactivity and instability, it immediately polymerized and the isolation was therefore not possible.^[137-139]

Another significant step towards the synthesis of triangulene was achieved by Murata *et al.* in 1977, who were able to successfully prepare the dianion **13** (Scheme 2.3). The reduction of diketotriangulene **10** with AlH_3 (formed in situ from AlCl_3 and LiAlH_4) first yielded the dihydrotriangulene **12**, subsequent treatment of this compound with $n\text{BuLi}$ at -78

°C yielded the dianion **13**. The formation of the dianion **13** was established by NMR spectroscopy at $-50\text{ }^{\circ}\text{C}$ and a subsequent treatment of the dianion species with D_2O , which added two deuterium atoms, one at each dihydro site, producing compound **14**. Its formation was confirmed by mass spectroscopy.^[157]

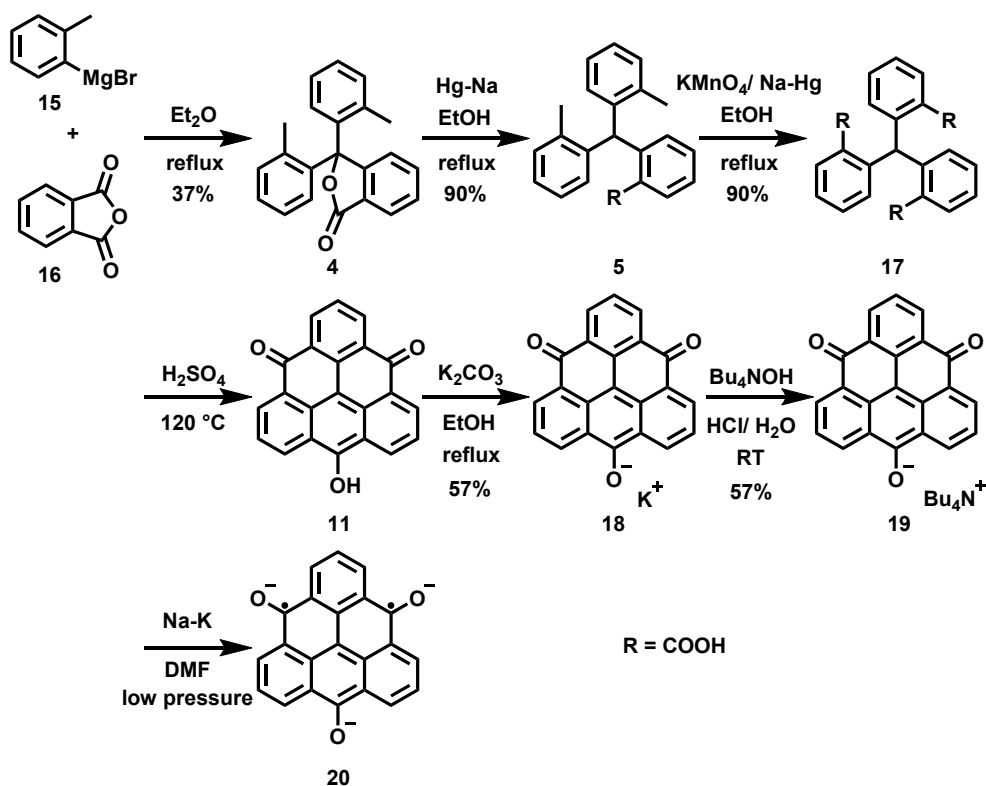


Scheme 2.3: Synthesis of triangulene dianion.^[157]

The synthesis of trioxo triangulene diradical trianion **20** achieved by Bushby *et al.*^[134, 141-142] in 1993 was very similar to the Clar's original approach, but it was simplified and the hazardous reagents were replaced for more secure ones.

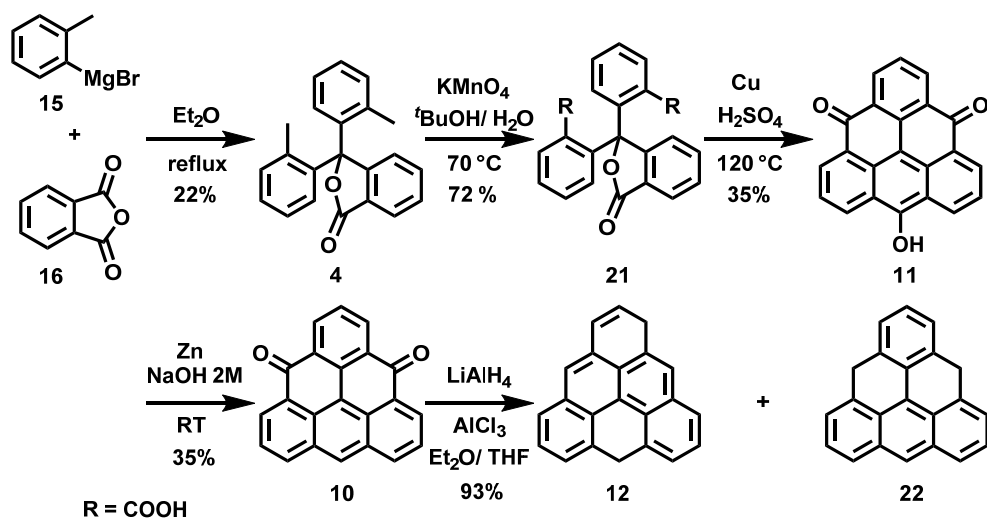
Similarly to Clar, Bushby's synthesis (Scheme 2.4) started with double-fold nucleophilic addition of *o*-tolylmagnesium bromide **15** on phthalic anhydride **16**. The formed lactone **4** was then opened reductively with sodium amalgam to the corresponding acid **5**. Oxidation of acid **5** with potassium permanganate yielded triacid **17**, which was cyclised by means of intramolecular Friedel–Crafts acylation to diketohydroxy triangulene **11**. Treatment of compound **11** with potassium carbonate produced the potassium salt **18**. The subsequent ion exchange with *tert*-butyl ammonium hydroxide, yielded the final precursor **19**. The trioxo triangulene diradical trianion **20** was generated by Na–K reduction of the

precursor **19** in DMF at low pressure and the triplet ground state was validated by ESR spectroscopy.^[134, 141-142]



Scheme 2.5: Synthesis of trioxo triangulene diradical trianion **20** by Bushby *et al.*^[134, 141-142]

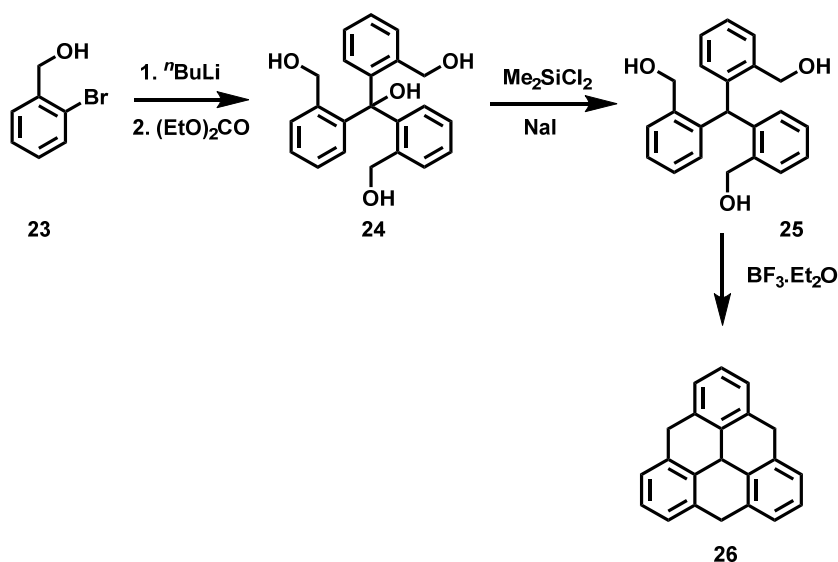
In the most recent work of Pavliček *et al.*^[152] were able to generate the triangulene species on the ASM/AFM surface by means of chemical manipulation. Their synthetic approach (Scheme 2.6) have a common first step with Bushby *et al.*,^[134, 141-142] but the formed lactone **4** is not reductively opened, but rather oxidized directly to the diacid lactone **21** to avoid the use of toxic sodium amalgam. The diacid lactone was then cyclized by Friedel–Craft acylation in the presence of copper to form diketohydroxy triangulene **11**. This intermediate was then reduced with zinc powder to yield diketotriangulene **10**, which was subsequently reduced by AlH₃ method developed by Murata *et al.*^[157] to the corresponding dihydroprecursors **12** and **22**.



Scheme 2.6: Synthesis of dihydrotriangulene precursors by Pavliček *et al.*^[152]

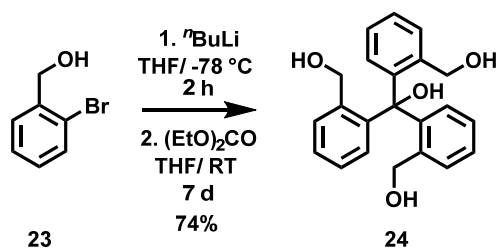
2.2 RESULTS & DISCUSSION

Our original proposal for the construction of the triangulene skeleton was significantly shorter and simpler than previously reported synthetic routes (Scheme 2.7). The proposed sequence started from commercially available bromoalcohol **23** that undergoes a lithium–halogen exchange with n BuLi, followed by triple-fold nucleophilic addition to diethylcarbamate, to form tetrahydroxy compound **24**. The middle hydroxy group would be then reduced by a literature procedure using dichloro dimethylsilane and NaI.^[158] The formed triol **25** should undergo a three-fold Friedel–Crafts alkylation to form the triangular compound **26**.



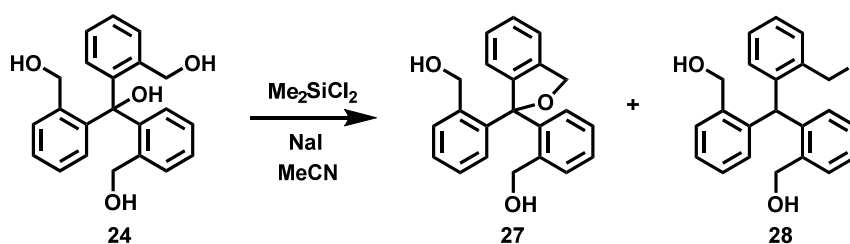
Scheme 2.7: Our original proposal for the formation of the triangulene skeleton.

The first step of the sequence proved to be working extremely well (Scheme 2.8). The reaction was quenched by the addition of water, upon which the product crashed out and was simply collected by filtration. No additional purification was required. Moreover, the reaction could be performed on a multi-gram scale (largest run for us was 35 g of starting material).



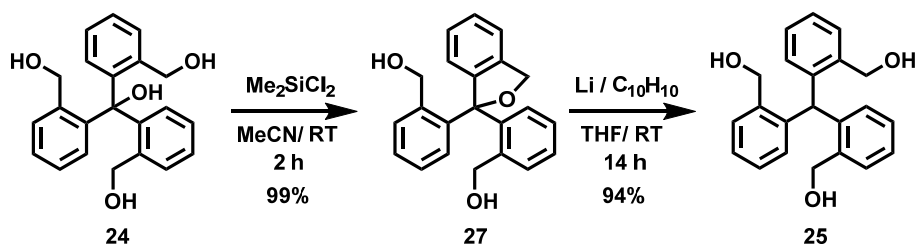
Scheme 2.8: The three-fold nucleophilic addition of bromoalcohol **23** to diethyl carbonate (left); the experimental setup for large-scale reaction (right).

With the tetrahydroxy compound in our hands, we attempted to remove the central hydroxy group by following a literature procedure,^[158] using dichlorodimethyl silane and NaI. These reaction conditions, however, failed to produce the desired trialcohol **25**. Instead, compound **27** and traces of **28** were observed (Scheme 2.9).



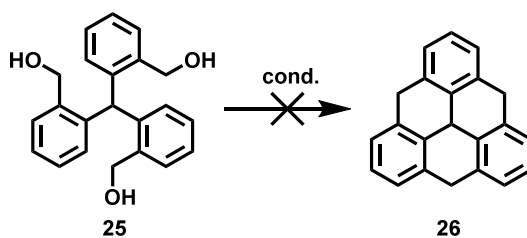
Scheme 2.9: The attempted removal of the central hydroxy group of **24** and two observed products: major **27** and minor **28**.

Although our attempt for optimization of the reaction conditions failed to produce the desired product **25** directly, the absence of NaI in the reaction produced solely compound **27** in a quantitative yield. Moreover, compound **27** could be treated with lithium naphthalenide,^[159] to produce the desired alcohol **25** in excellent yield (Scheme 2.10, far right).



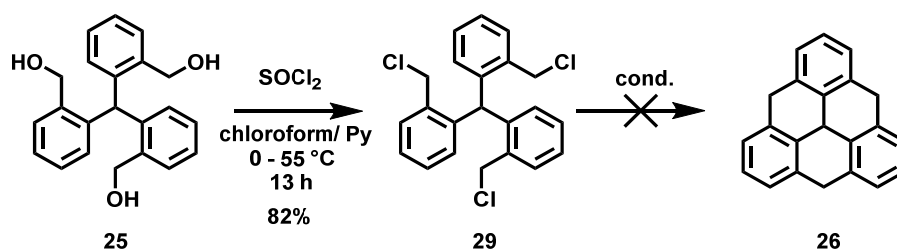
Scheme 2.10: Optimized reaction conditions for the synthesis of trialcohol **25**.

With the reliable synthetic method for the preparation of **25** in our hands, we tried to perform the Friedel–Crafts alkylation to form the triangular compound **26** (Scheme 2.11). We tested two different reaction conditions: first, compound **25** was heated under reflux in toluene in the presence of a catalytic amount of *p*-TSA and, second, trialcohol **25** was treated with $\text{BF}_3 \cdot \text{Et}_2\text{O}$ in CH_2Cl_2 upon cooling. In both cases, the starting material was fully consumed, but only complex mixtures of products were formed.



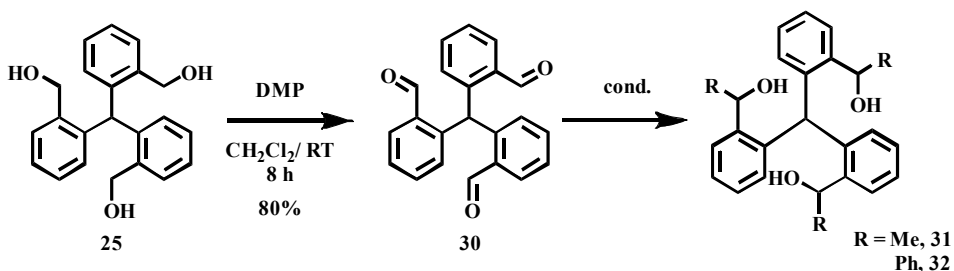
Scheme 2.11: The unsuccessful cyclization of trialcohol **25**.

We propose two possible explanations as to why this reaction failed. One possibility is that the starting material is not stable under the reaction conditions and is decomposing, forming complex mixtures of products, or the formed product is not stable. To investigate the second option, we decided to prepare trichloroderivative **29** to test the standard conditions for Friedel–Crafts alkylation. The trichloroderivative was prepared in one step from trialcohol **25** by chlorination using thionyl chloride in chloroform and pyridine in a very good yield (Scheme 2.12).



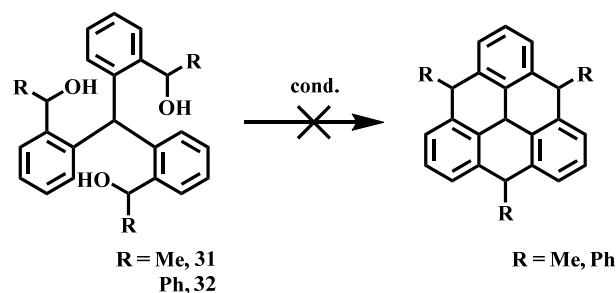
Scheme 2.12: Preparation of trichloroderivative **29** and the failed attempt to prepare the triangular compound **26**.

Cyclization of trichloro compound **29** to the corresponding triangular compound **26** was tested by using two Lewis acids, namely, AlCl_3 and FeCl_3 in CH_2Cl_2 . In both cases, formation of complex mixtures was observed. Such a formation can be explained by formation of the product that is not stable and decompose. However, as we have not enough evidence for such conclusion, a simple formation of oligomeric or polymeric products would lead to the same result. Subsequently, we decided to introduce substituents at the central positions, which could provide additional stability for isolation of the triangulene precursor as well as should help to stabilize the positive charge of the intermediate. Therefore, we synthesised a trialdehyde derivative **30** as it can be easily functionalized by Grignard additions. Aldehyde **30** was prepared in one step by Dess–Martin oxidation of trialcohol **25** in a very good yield.



Scheme 2.13: Synthesis of trialdehyde **30** and subsequent Grignard reactions to form compounds **31** and **32**.

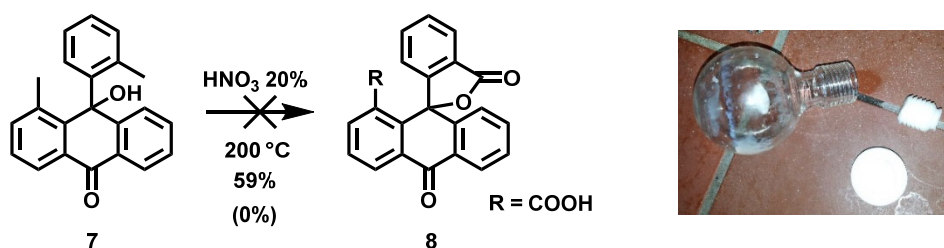
Two substituents were introduced by terms of Grignard additions, namely, methyl and phenyl. Both derivatives were prepared in good yields (90 % for Me and 82% for Ph).



Scheme 2.14: Failed attempts for the preparation of the triangular compounds **33** and **34**.

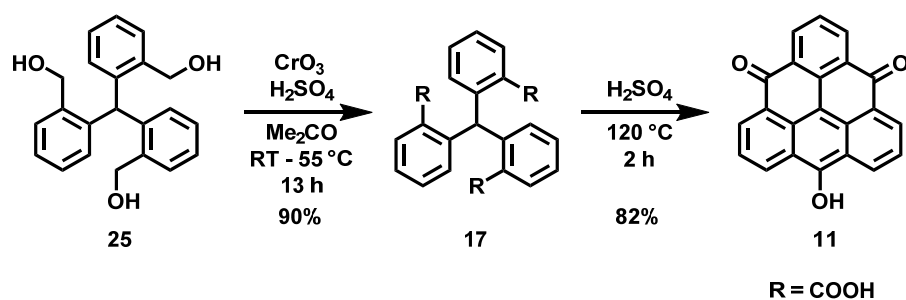
Next, both alcohols **31** and **32** were treated with $\text{BF}_3 \cdot \text{Et}_2\text{O}$ in CH_2Cl_2 upon cooling. In both cases, the formation of the desired product was observed by MALDI MS. Unfortunately, after the work-up of both reactions, a complex mixture of products was observed with several spots on TLC. Our attempts for purification did not lead to any significant improvement. After this result, we decided to abandon this strategy and we focused on different methods for preparation of the triangulene precursor.

As we mentioned previously, we attempted to reproduce the original Clar's synthesis of the triangulene precursors (Scheme 2.1).^[137-139] The synthesis worked well, and we were able to obtain similar yields for all reaction steps with some exceptions. However, the transformation of hydroxyanthrone **7** to lactone **8** by oxidation in diluted HNO_3 proved to be irreproducible (Scheme 2.15). The original conditions required heating of the reaction mixture in a pressure tube at $200\text{ }^\circ\text{C}$. We attempted to reproduce this reaction twice. In both cases, the reaction vessel exploded, causing severe damage to the protective shield, especially in the second case. After the second explosion, we decided that these conditions are too dangerous and therefore not suitable for our purposes.



Scheme 2.15: Our attempt to reproduce the oxidation of anthrone **7** (right); the reaction vessel after explosion (right).

In the synthetic approach of Bushby *et al.*^[134, 141-142], it was possible to prepare the diketo hydroxytriangulene **11** from triacid **17** by Friedel–Crafts acylation (Scheme 2.5). As we had large quantities of easily obtainable trianol **25**, we decided to prepare triacid **17** and then follow the procedure of Bushby *et al.*^[134, 141-142] The acid was prepared in one step by Jones oxidation of the trianol **25** in a very good yield, without the necessity of purification (Scheme 2.16).



Scheme 2.16: Preparation of triacid **17** and its subsequent Friedel–Crafts acylation to diketo hydroxytriangulene **11**.

Next, acid **17** was cyclized by means of Friedel–Crafts acylation by heating in sulphuric acid. After the work-up, a deep-blue solid (similarly to Bushby *et al.*)^[134, 141-142] was obtained, which was insoluble in almost all organic solvent, therefore, the characterization was challenging. However, as the compound was very well soluble in sulphuric acid, we decided to perform the NMR characterization in D₂SO₄. The analysis of the spectra revealed the presence of highly symmetrical compound with only two signals in the aromatic region (Figure 2.2, top). As the HR-MS fitted the desired diketo hydroxytriangulene, we concluded

that both keto groups in this molecule are protonated with D^+ and therefore all aromatic protons became equal.

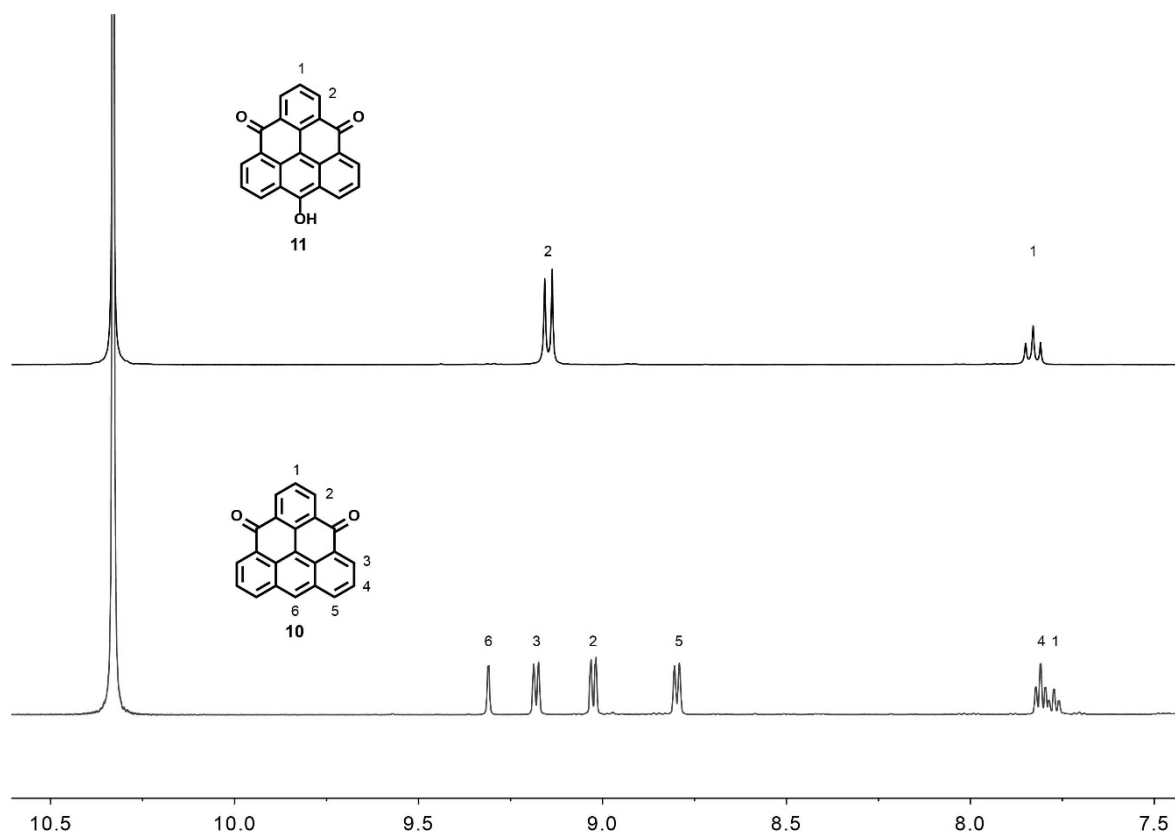
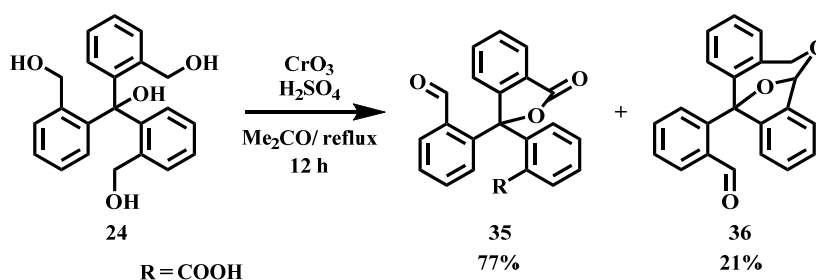


Figure 2.2: The ¹H NMR spectra of diketo hydroxytriangulene **11** (top) and diketotriangulene **10** (bottom) recorded in D_2SO_4 .

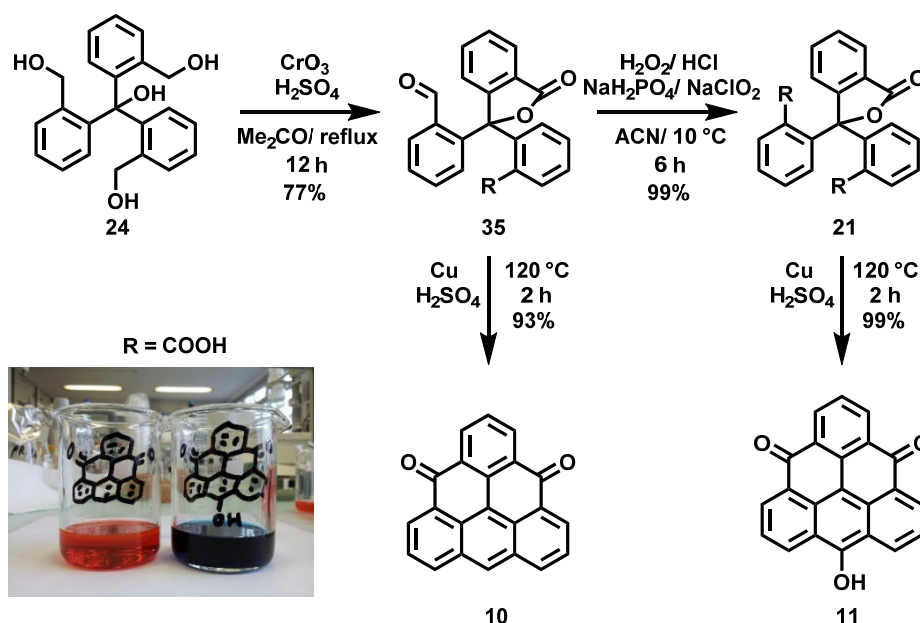
Encouraged by the positive result of this reaction, we decided to apply the Jones conditions to the tetrahydroxy compound **24** in order to explore the possibility to shorten the reaction pathway towards compound **11**. We assumed that under these conditions, compound **21** will be formed and, therefore, we would be able employ the copper-mediated Friedel–Crafts acylation (Scheme 2.6).



Scheme 2.17: Jones oxidation of tetrahydroxy compound **24**.

To our surprise, the monitoring of the reaction by LC-MS showed that the reaction did not proceed all the way to the desired lactone **21**. Formation of compounds **35** and **36** was observed. Our attempts for optimization of the reaction conditions, by changing the reaction temperature and rate of addition of the Jones reagent, in order to prepare the desired compound **21** failed. However, we were able to maximize the efficiency of the formation of aldehyde **35** and minimize the formation of compound **36**. These two compounds can be easily separated by column chromatography.

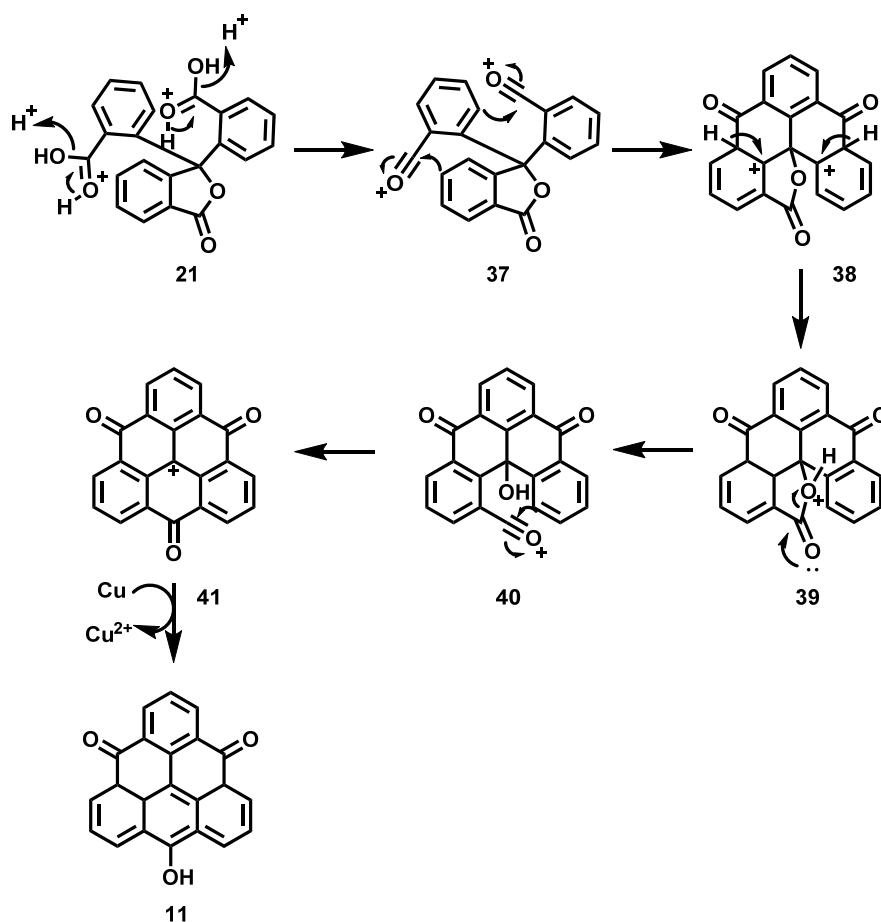
Aldehyde **35** was subjected to the copper-mediated Friedel–Craft conditions in sulphuric acid. Once the reaction reached the desired temperature (120 °C), the colourless thick solution immediately changed colour to deep-red, as reported by Bushby *et al.*^[134] The reaction mixture was cooled to room temperature and water was added, and the red precipitate was filtered. Even though Bushby *et al.*^[134] reported the ¹H NMR spectra of the diketotriangulene **10** in CDCl₃, we were not able to record the NMR spectra in any organic solvent, because of the extremely poor solubility. This problem was overcome, similarly as in case of the diketo hydroxy triangulene **11**, by recording the spectra in deuterated sulphuric acid (Figure 2.2, bottom).



Scheme 2.17: Optimized reaction conditions for the synthesis of diketortriangulene **10** and diketo hydroxytriangulene **11**.

The possibility of oxidation of the aldehyde **35** was explored in order to utilize the synthetic strategy towards both triangulene precursors **10** and **11**. As it was mentioned previously, the Jones conditions did not lead to **11**, therefore, we decided to use a more powerful oxidant such as hydrogen peroxide and sodium chlorite. Using these conditions, aldehyde **35** was smoothly converted to the desired lactone **21** in excellent yield. Moreover, after aqueous work-up, the compound was pure, therefore, no additional purification was required. Lactone **21** was subsequently converted to the diketo hydroxytriangulene **11** using copper-mediated Friedel–Crafts acylation and the desired product was obtained in excellent yield (Scheme 2.17). Again, no further purification was required. The proposed mechanism for copper-mediated Friedel–Crafts acylation is shown in Scheme 2.18. First, a Friedel–Crafts acylation occurred on both carboxylic acids, a molecule of water being formed (water as leaving group) under the acidic conditions. This leads to the formation of symmetrical structure **41** with a tertiary carbocation in the middle of the structure. The carbocation is then

reduced by copper and a further tautomerization leads to the formation of the stable diketo hydroxytriangulene **11**.



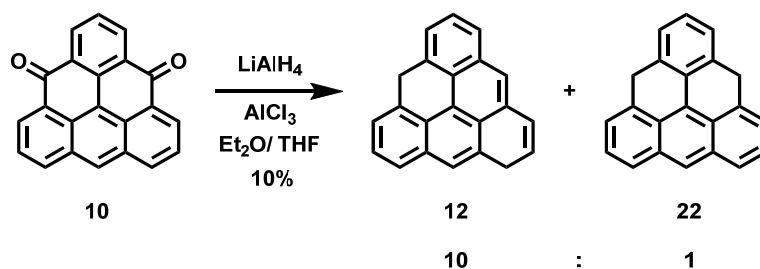
Scheme 2.18: Proposed mechanism for cyclization of lactone **35** to triangulene precursor **11**.

Overall, we succeeded to significantly shorten the previously reported synthetic pathways to triangulene precursors **10** and **11**, as they can be prepared in three and four steps, respectively (Scheme 2.17). Both compounds can be prepared using the same methodology and can be prepared on a multi-gram scale. Moreover, only one column chromatography is required in both cases.

With both triangulene precursors **10** and **11** in our hands, we moved forward towards stabilization of the sensitive triangulene core. The diketo hydroxytriangulene **11** represents

the starting material for kinetically stabilized triangulene by use of bulky substituents and its use is discussed in Chapter III.

The diketo triangulene **10** was subjected to the reductive conditions developed by Murata *et al.*^[157] AlH₃ was prepared in situ from LiAlH₄ and AlCl₃ in THF/ Et₂O solvent mixture and was added dropwise to the suspension of diketo triangulene **10** in THF.



Scheme 2.19: Reduction of diketo triangulene **10**

This reduction step has proved to be troublesome due to the low solubility of the starting material. After the work-up and column chromatography, only low amounts (1–2%) of yellow cotton-like reduced product and formation of pink, low soluble by-products were observed. The low solubility side products were not identified, however, if these were subjected to the same reductive conditions, the formation of desired product in higher yields was observed. Therefore, we concluded that the low solubility by-products are most probably monoreduced species. After several cycles of reduction (4–5) of the by-products, we were able to collect sufficient amount of the desired product **12** (10%). The dihydrotriangulene **12** is not stable under ambient conditions and it undergoes oxidation back to diketo triangulene **10** within several hours. To minimize the oxidation during the work-up, the crude product was purified by deaerated column chromatography in darkness under an argon atmosphere. Under these purification conditions, the oxidation was almost completely suppressed and once the product is pure it can be stored under an argon atmosphere in freezer for several weeks or in the glove box under ambient conditions for months.

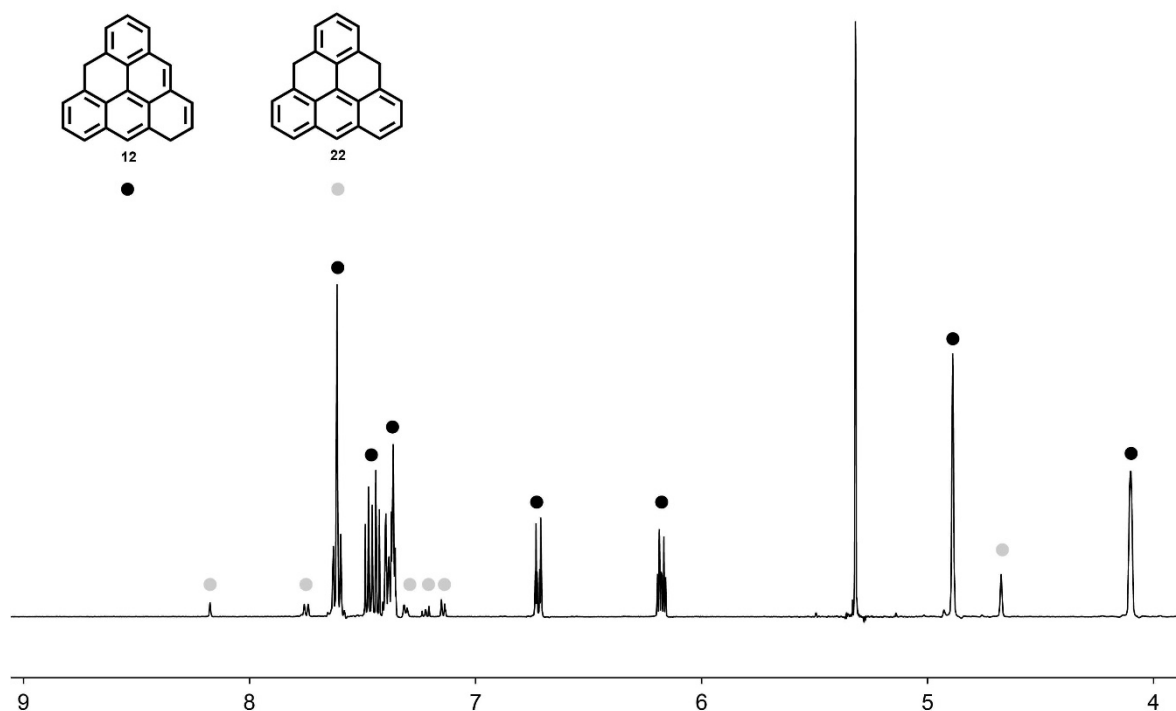


Figure 2.3: ^1H NMR spectrum of dihydrotriangulene **12** in deaerated CD_2Cl_2 . The protons of **12** are highlighted with black dots and the protons of **22** are highlighted with grey dots.

The analysis of the ^1H NMR (Figure 2.3) spectrum of dihydrotriangulene **12** revealed that it contains approximately 10% of species containing an anthracene moiety. As both MALDI-TOF and DART MS analysis revealed only single mass corresponding to the dihydrotriangulene, we concluded that the impurity is the different isomer of dihydrotriangulene, we concluded that the impurity is the different isomer of dihydrotriangulene **22** (Figure 2.3, protons are highlighted by grey dots). This observation is in agreement with observations previously reported by Pavliček *et al.* [152] and was supported by 2D NMR spectroscopy.

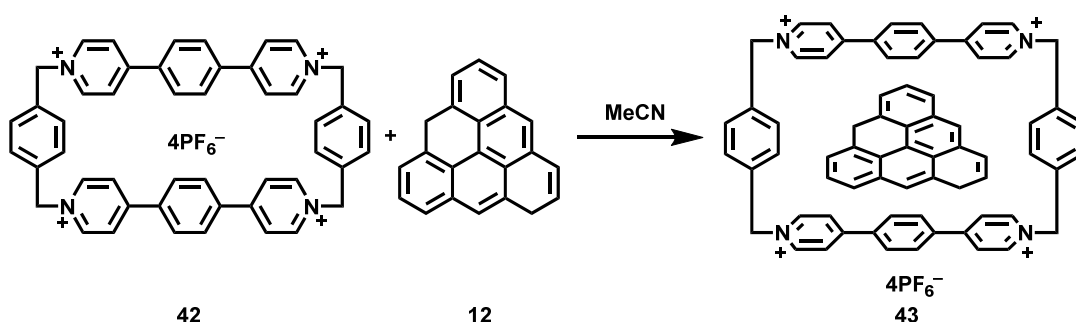
2.2.1 STABILIZATION OF TRIANGULENE

Once we successfully prepared the dehydrotriangulene **12** we draw our attention to its stabilization in a supramolecular complex. In the recent years, Stoddart *et al.* [156] demonstrated the ability of cyclophanes, such as ExBox⁴⁺ to successfully bind PAHs of

varying size in supramolecular complex, due to charge-transfer interactions between ExBox⁴⁺ and PAH.

As the cavity of ExBox⁴⁺ is large enough to accommodate dihydrotriangulene **12**, we decided to form a 1:1 host-guest supramolecular complex of **12** ⊂ ExBox⁴⁺. Once such a complex is formed, we wanted to proceed with generation of complex of ExBox⁴⁺ with diradical triangulene. Such complex should be possible to generate by using strong oxidation agents such as DDQ. Once the formation of the complex is confirmed by terms of EPR spectroscopy, our next objective would be isolation of this complex in a crystalline form.

The ExBox⁴⁺ was prepared in three steps according to literature procedure.^[156] With both components, dihydrotriangulene **12** and ExBox⁴⁺ in our hands, we first investigated the formation of the supramolecular complex **43** (Scheme 2.20).



Scheme 2.20: Generation of the supramolecular complex **43**.

ExBox⁴⁺ was dissolved in CD₃CN and the solution was degassed by three freeze-pump-thaw technique in three cycles before the equimolar amount of dihydrotriangulene **12** was added in the glove box. The suspension was vigorously shaken until it was completely dissolved (ca. 30 sec). It is important to note that dihydrotriangulene **12** is practically insoluble in CD₃CN. The complete dissolution of dihydrotriangulene **12** represents a strong evidence for the formation of supramolecular complex **43**.

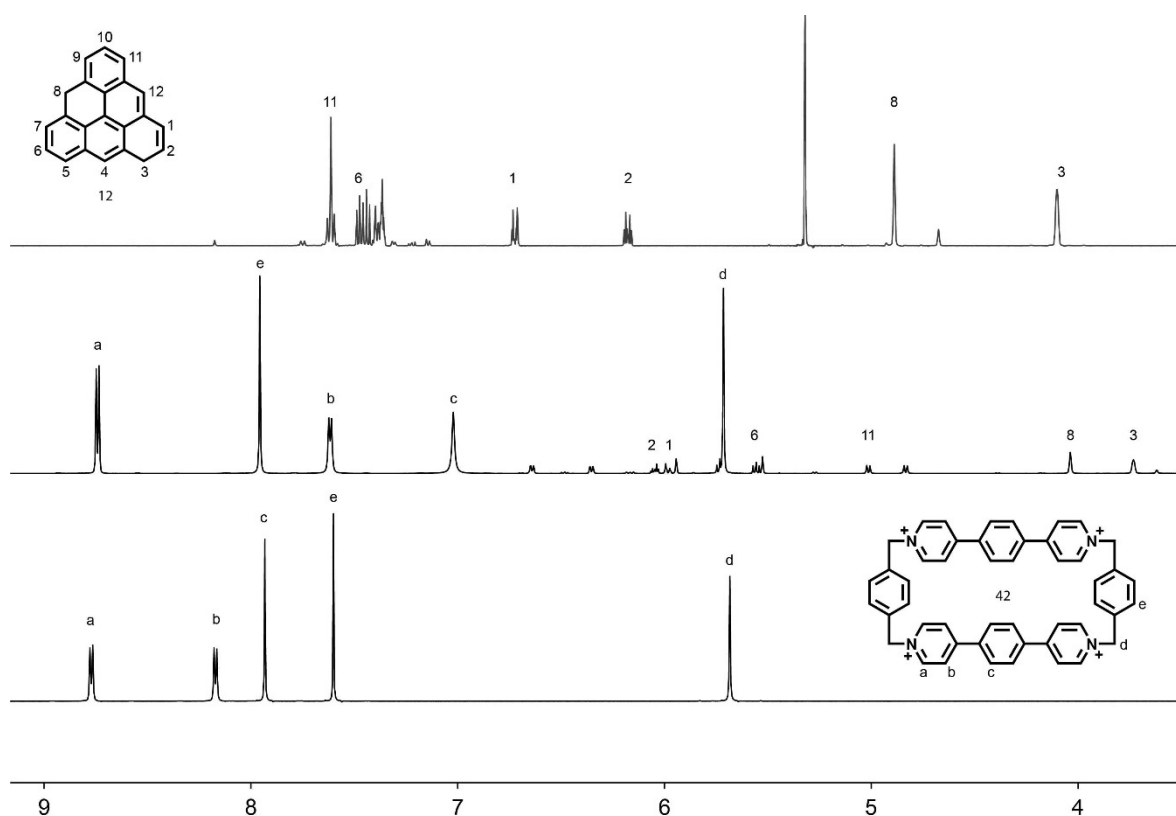


Figure 2.4: ^1H NMR spectrum of dihydrotriangulene **12** (top) and ExBox^{4+} (bottom). ^1H NMR spectrum of the 1:1 supramolecular complex **43** (middle).

The ^1H NMR spectrum (Figure 2.4, middle) of the 1:1 **12** \subset ExBox^{4+} complex **43** displays significant upfield shifts for signals corresponding to *b* and *c* protons of ExBox^{4+} and all signals for the protons of dihydrotriangulene **12** as well as a downfield shift of the phenylene protons *e* of ExBox^{4+} . This pattern is caused by π -electron shielding of the face-to-face oriented aromatic rings, which occurs upon complexation. The *a* and *d* protons of ExBox^{4+} display only very small shift in the ^1H NMR spectra. This can be explained by the location of these protons in the “corners” of the ExBox^{4+} , where are not affected by the shielding effect of the guest. This behaviour is in a very good agreement with the inclusion of other guests inside of ExBox^{4+} in solution state.^[156] Once the formation of the supramolecular complex **43** was verified, we were able to obtain the association constant $K_a \sim 0.8 \times 10^4 \text{ M}^{-1}$. The association constant was obtained by ^1H NMR titration.

The formation of the supramolecular complex **43** was additionally verified upon obtaining single-crystal structure (Figure 2.5). Single crystals of the supramolecular complex

12-CExBox^{4+} **43** were grown by slow vapour diffusion of ${}^i\text{Pr}_2\text{O}$ into the solution of $\text{ExBox}\cdot 4\text{PF}_6$ and dihydrotriangulene **12** (1:1.1) in MeCN over the course of one week. The presence of the dihydrotriangulene **22** caused a disorder in the crystal structure.

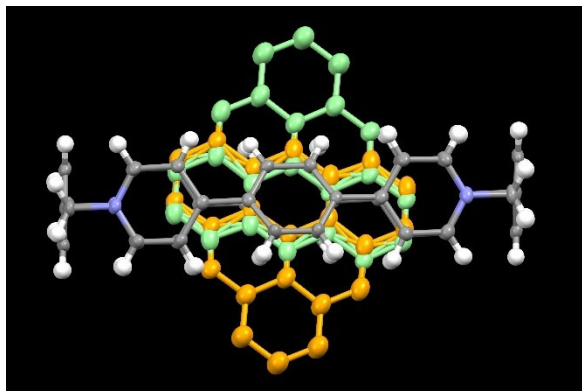
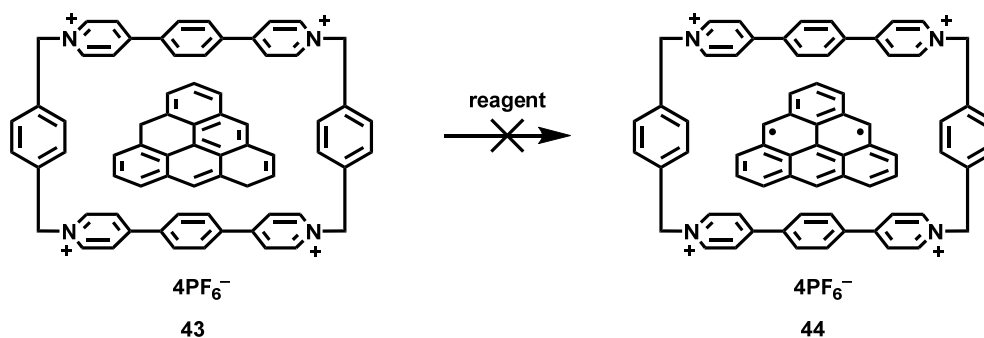


Figure 2.5: Crystal structure of the supramolecular complex **43**.

With the proof that the complex **43** is indeed formed, we moved to the final objective, the generation of the supramolecular complex **44**. We attempted to generate complex **44** with several strong oxidating agents such as *p*-chloranil and DDQ, however, no visible change occurred and the ${}^1\text{H}$ NMR spectra also showed no change.



Scheme 2.21: Unsuccessful generation of the supramolecular complex **44**

Upon addition of NaH, the colour of the sample changed from yellow to blue. The ${}^1\text{H}$ NMR spectra showed disappearance of the signals, however, the EPR analysis did not prove the existence of the formation of the complex **44**, as no signal was recorded, therefore, no paramagnetic species are present in the sample. With this result, we can speculate that these

methods are either not suitable for the formation of the complex **44**, or that the complex is formed, but the protection of the triangulene core is not sufficient enough in ExBox⁴⁺ and dimerization/polymerization can still occur. Because of time constraints, further analysis could not be carried out and further investigation is therefore necessary.

2.3 CONCLUSION & OUTLOOK

In summary, we developed a novel synthetic strategy for dihydrotriangulene **12** employing copper-mediated Friedel–Crafts acylation as a crucial synthetic step. The desired dihydrotriangulene **12** was prepared in four steps, out of which two do not require purification by column chromatography. Moreover, the synthesis of diketotriangulene **10** can be achieved on the multigram scale in a short time. Compared to the known synthetic methodologies for diketotriangulene **10**, our method is significantly shorter, does not require intensive purification and produces the desired material in high purity. Dihydrotriangulene **12** forms a supramolecular complex with ExBox⁴⁺ with association constant $K_a = 0.8 \times 10^4 \text{ M}^{-1}$, which was obtained by ¹H NMR titration. The formation of the final supramolecular complex **44** was not observed, most probably due to insufficient protection provided by ExBox⁴⁺, or by the fact that the chosen conditions were not suitable for the formation of the complex **44**. Further investigation on this matter is ongoing in the research group of Prof. Dr. Juriček.

In the case of the failure of the generation of the supramolecular complex **44**, due to insufficient protection provided by ExBox⁴⁺, we propose to change ExBox⁴⁺ for a different cyclophane, for example, ExCage⁶⁺ (Figure 2.5)^[161] that was recently developed by Stoddart *et al.* ExCage⁶⁺ exhibits similar properties in terms of binding of polyaromatic hydrocarbons to ExBox⁴⁺, however, due its triangular shape it can provide better steric protection in comparison with ExBox⁴⁺. The investigation on this matter is already ongoing in the research group of Prof. Dr. Juriček.

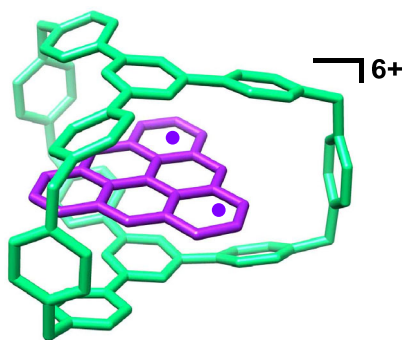


Figure 2.5: Encapsulation of triangulene in a supramolecular complex with ExCage⁶⁺.

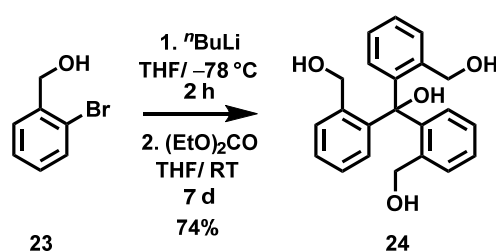
2.4 EXPERIMENTAL SECTION

2.4.1 GENERAL REMARKS

All chemicals and solvents were purchased from commercial sources and used without further purification unless stated otherwise. The reactions and experiments that are sensitive to oxygen were performed using Schlenk techniques and argon-saturated solvents. The solvents were saturated with argon by either passing argon gas through the solvent or using the freeze-pump-thaw technique in three cycles. All reactions were monitored by either thin-layer chromatography, GC-MS, LC-MS or MALDI-TOF MS. Yields refer to purified and spectroscopically pure (^1H NMR) compounds unless the crude product was used in the next step. For column chromatography, either silica gel Silicaflash[®] p60 (40 – 60 μm) from Silicycle or Alumina, activated (basic Brockmann Activity I) or neutral was used in dot was purchased from Fluka. The thin-layer chromatography was performed using silica-gel plates Silica Gel 60 F254 (0.2 mm thickness), purchased from Merck and visualized under a UV lamp (254 or 365). The NMR experiments were performed on Bruker Avance III NMR spectrometers operating at 400, 500, or 600 MHz proton frequencies. The instruments were equipped with a direct-observe 5 mm BBFO smart probe (400 and 600 MHz), an indirect-detection 5 mm BBI probe (500 MHz), or a five-channel cryogenic 5 mm QCI probe (600 MHz). All probes were equipped with actively shielded z -gradients (10 A). The experiments were performed at 295 or 298 K unless indicated otherwise and the temperatures were calibrated using a methanol standard showing accuracy within ± 0.2 K. Standard Bruker pulse sequences were used, and the data was processed on Topspin 3.2 (Bruker) using two-fold zero-filling in the indirect dimension for all 2D experiments. Chemical shifts (δ) are reported in parts per million (ppm) relative to the solvent residual peak. ^1H NMR titrations were performed by adding small amounts of dihydro triangulene **12** to a solution ExBox⁴⁺ in CD_3CN . Significant upfield shifts of ^1H resonances for c protons were observed to

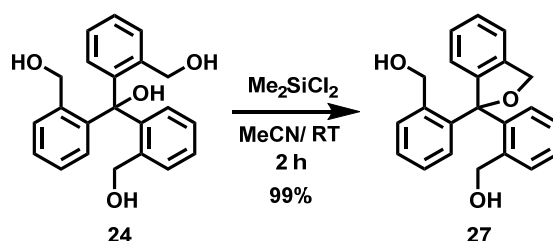
determine the association constant (K_a). The K_a values were calculated using Dynafit,^[P] a program which employs nonlinear least-squares regression on ligand–receptor binding data. The low-resolution mass spectra were recorded either on Bruker amaZon™ X for Electro Spray Ionization (ESI), on a Shimadzu GSMS-QP2010 SE gas chromatography system with ZB-5HT inferno column (30 mm x 0.25 mm x 0.25 mm) at 1 ml/ min He-flow rate (split = 20:1) with a Shimadzu electron ionization (EI 70 eV) mass detector, or Bruker microflex system for MALDI-TOF. High-resolution mass spectra (HRMS) were measured as HR-ESI-ToF-MS with a Maxis 4G instrument from Bruker with the addition of NaOAc. Data collections for the crystal structures were performed at low temperatures (123 K) using CuK α radiation on a Bruker APEX II diffractometer. Integration of the frames and data reduction was carried out using the APEX2 software. The structures were solved by the charge-flipping method using Superflip. All non-hydrogen atoms were refined anisotropically by full-matrix least-squares on F using CRYSTALS. Both structures were analyzed using Mercury.

2.4.2 EXPERIMENTAL PROCEDURES



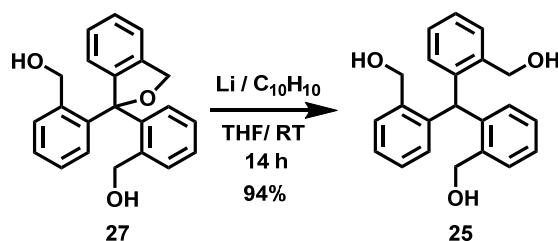
((Hydroxymethanetriyl)tris(benzene-2,1-diyl))trimethanol (24): A cold ($-78\text{ }^\circ\text{C}$) solution of *n*-butyllithium (300 mL, 479 mmol, 1.6 M solution in hexane) was added dropwise via cannula to a cooled ($-78\text{ }^\circ\text{C}$) solution of (2-bromophenyl)methanol (23, 45.3 g, 240 mmol) in dry THF (1.0 L) under an argon atmosphere. The reaction mixture was stirred at $-78\text{ }^\circ\text{C}$ for 2 h before diethyl carbonate (9.41 mL, 76.1 mmol) was added dropwise at $-78\text{ }^\circ\text{C}$. The reaction mixture was then allowed to warm to room temperature overnight and it

was stirred at room temperature for additional 10 days before water (500 mL) was added to quench the reaction. The white precipitate of the product was filtered off using suction, washed with ethyl acetate and the filtrate was extracted with CH₂Cl₂ (3 × 150 mL). The combined organic layers were washed with brine, dried over anhydrous Na₂SO₄, and filtered. After evaporation of the solvents, the residue was purified by crystallization from ethyl acetate. The precipitates were combined to afford the desired product (**24**; 19.7 g, 74%) as a white solid. ¹H NMR (400 MHz, CDCl₃, ppm): δ 8.18 (s, 1 H), 7.44 (dd, *J* = 7.5, 1.3 Hz, 3H), 7.33 (td, *J* = 7.4, 1.1 Hz, 3H), 7.09 (td, *J* = 7.8, 1.3 Hz, 3H), 6.47 (dd, *J* = 7.9, 0.9 Hz, 3H), 4.54 (d, *J* = 12.0 Hz, 3H), 4.27 (d, *J* = 12.0 Hz, 1H), 3.81 (s, 3H). ¹³C NMR (101 MHz, CDCl₃, ppm): δ 145.4, 140.0, 132.5, 129.7, 128.6, 127.7, 87.1, 65.1. HRMS (ESI): *m/z* [M + Na]⁺ calcd for C₂₂H₂₂O₄Na⁺: 373.1410; found 373.1412 (|Δ| = 0.5 ppm).



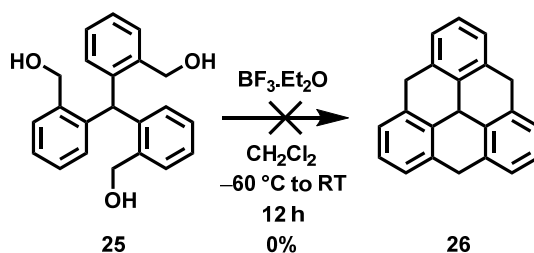
((1,3-Dihydroisobenzofuran-1,1-diyl)bis(2,1-phenylene))dimethanol (27): To a stirred solution of ((hydroxymethanetriyl)tris(benzene-2,1-diyl))trimethanol (**24**; 950 mg, 2.71 mmol) in dry MeCN (40 mL), dichlorodimethylsilane (329 μL, 2.71 mmol) was added dropwise at room temperature under an argon atmosphere and the resulting mixture was stirred at room temperature for 2 h. The reaction was then diluted with EtOAc (50 mL). The organic layer was washed with water (25 mL), sat. aq. Na₂CO₃ solution, dried over Na₂SO₄, and filtered. After evaporation of the solvents, the residue was purified by column chromatography over silica gel using ^cHex/EtOAc (1:1) as an eluent to afford the desired product (**27**; 900 mg, 99%) as a pale-brown solid. ¹H NMR (400 MHz, CDCl₃, ppm): δ 7.50

(d, $J = 7.2$ Hz, 2H), 7.38–7.22 (m, 6H), 7.14 (td, $J = 7.6, 1.2$ Hz, 2H), 6.89 (d, $J = 7.3$ Hz, 1H), 6.82 (d, $J = 7.6$ Hz, 2H), 5.09 (s, 2H), 4.37 (s, 4H). ^{13}C NMR (101 MHz, CDCl_3 , ppm): δ 142.7, 141.5, 140.3, 138.9, 131.7, 128.9, 128.4, 128.1, 127.7, 127.3, 125.0, 121.4, 96.3, 70.7, 63.9. HRMS (ESI): m/z $[\text{M} + \text{Na}]^+$ calcd for $\text{C}_{22}\text{H}_{21}\text{O}_3\text{Na}^+$: 333.1485; found 333.1486 ($|\Delta| = 0.2$ ppm).

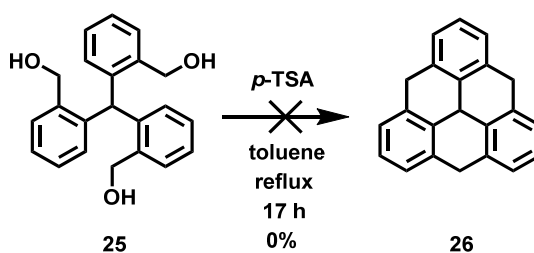


(Methanetriyltris(benzene-2,1-diyl))trimethanol (25): Solution of Li (254 mg, 36.2 mmol) and naphthalene (803 mg, 6.26 mmol) in dry THF (10 mL) was activated in the sonicator under an argon atmosphere for 15 min until deep-green solution was formed. Then, ((1,3-dihydroisobenzofuran-1,1-diyl)bis(2,1-phenylene))dimethanol (**27**; 1.72 g, 5.17 mmol) was added dropwise over a period of 1 h as a solution in dry THF (2 mL). The reaction mixture was then stirred at room temperature under an argon atmosphere for 14 h. Afterwards, the reaction mixture was filtered through a glass filter (porosity 3) and then poured onto ice. The organic layer was separated, and the aqueous layer was extracted with CH_2Cl_2 (3×10 mL). The combined organic layers were washed with water (10 mL), brine (20 mL), dried over Na_2SO_4 , and filtered. After evaporation of the solvents, the residue was purified by column chromatography over silica gel using $^{\circ}\text{Hex}/\text{EtOAc}$ (1:1) as an eluent to afford the desired product (**25**; 1.63 g, 94%) as a white solid. ^1H NMR (400 MHz, $\text{DMSO}-d_6$, ppm): δ 7.47 (dd, $J = 7.6, 1.1$ Hz, 3H), 7.25 (td, $J = 7.5, 1.1$ Hz, 3H), 7.13 (td, $J = 7.5, 1.0$ Hz, 3H), 6.60 (dd, $J = 7.5, 1.0$ Hz, 3H), 5.98 (s, 1H), 5.19 (t, $J = 5.4$ Hz, 3H, OH), 4.35 (d, $J = 5.3$ Hz, 6H). ^{13}C NMR (101 MHz, $\text{DMSO}-d_6$, ppm): δ 140.2, 139.40, 128.1, 126.7,

126.39, 126.35, 60.4, 42.6. HRMS (ESI): m/z $[M + Na]^+$ calcd for $C_{22}H_{22}O_3Na^+$: 357.1461; found 357.1465 ($|\Delta| = 1.2$ ppm).

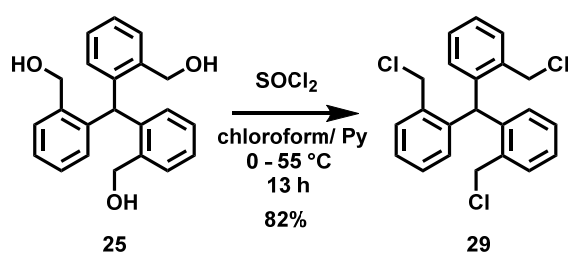


3a2,4,8,12-Tetrahydrodibenzo[cd,mn]pyrene (26): To a cooled (-60 °C) solution of (methanetriyltris(benzene-2,1-diyl))trimethanol (**31**, 50 mg, 0.15 mmol) in dry CH_2Cl_2 (50 mL), $BF_3 \cdot Et_2O$ (0.11 mL, 0.90 mmol) was added dropwise over a period of 6 h. The mixture was then allowed to warm to room temperature over a period of 4 h and it was stirred at room temperature for additional 2 h. Afterwards, the reaction was quenched by the addition of MeOH (5 mL), followed by water (10 mL). The organic layer was separated, and the aqueous layer was extracted with CH_2Cl_2 (3×15 mL). The combined organic layers were washed with water (25 mL), brine (25 mL), dried over Na_2SO_4 , and filtered. After evaporation of the solvents, the residue was purified by column chromatography over silica gel using o Hex. The 1H NMR spectrum of the residue after column chromatography showed a complex mixture of products, which could not be separated and identified.



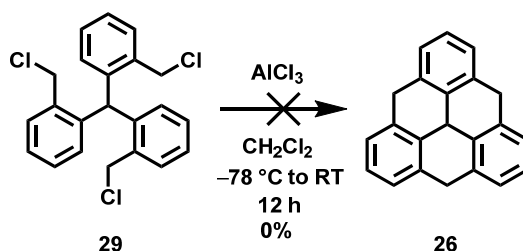
3a2,4,8,12-Tetrahydrodibenzo[cd,mn]pyrene (26): A mixture of (methanetriyltris(benzene-2,1-diyl))trimethanol (**25**; 100 mg, 0.30 mmol) and a catalytic amount of p -toluenesulfonic acid monohydrate in toluene (50 mL) was heated at reflux for

17 h by using the Dean–Stark apparatus to continuously remove water, which formed during the course of the reaction. After the reaction was completed, water (100 mL) was added and the organic layer was separated, washed with a saturated aqueous NaHCO₃ solution, dried over Na₂SO₄, and filtered. After evaporation of the solvents, the residue was purified by column chromatography over silica gel using ^oHex. The ¹H NMR spectrum of the residue after column showed a complex mixture of products, which could not be separated and identified.

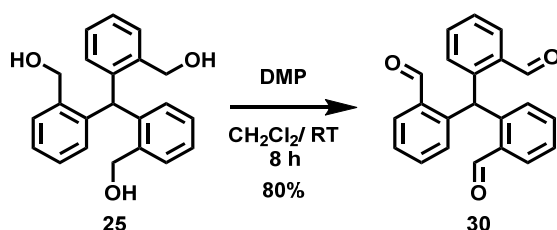


Tris(2-(chloromethyl)phenyl)methane (29): To a cooled (0 °C) solution of (methanetriyltris(benzene-2,1-diyl))trimethanol (**25**; 401 mg, 1.20 mmol) and pyridine (293 μ L, 3.59 mmol) in dry chloroform (40 mL), thionyl chloride (523 μ L, 7.18 mmol) was added dropwise at 0 °C under an argon atmosphere. The reaction mixture was stirred at 0 °C for 30 min, before it was allowed to warm to room temperature over 1 h. The reaction mixture was then heated at 55 °C under an argon atmosphere for 12 h, before it was quenched with careful addition of water (20 mL). The organic layer was separated, and the aqueous layer was extracted with CH₂Cl₂ (3 \times 10 mL). The combined organic layers were washed with sat. aq. NaHCO₃ solution (20 mL), brine (20 mL), dried over Na₂SO₄, and filtered. After evaporation of the solvents, the residue was purified by column chromatography over silica gel using ^oHex/EtOAc (5:1) as an eluent to afford the desired product (**29**, 383 mg, 82%) as a pale-brown solid. ¹H NMR (400 MHz, DMSO-*d*₆, ppm): δ 7.44 (dd, *J* = 7.5, 1.4 Hz, 3H), 7.30 (td, *J* = 7.5, 1.4 Hz, 3H), 7.21 (td, *J* = 7.6, 1.5 Hz, 3H), 6.65 (dd, *J* = 7.7, 1.4 Hz, 3H), 4.49

(s, 6H). ^{13}C NMR (101 MHz, CDCl_3 , ppm): δ 141.4, 136.4, 131.3, 130.2, 129.0, 127.7, 44.9, 44.2.

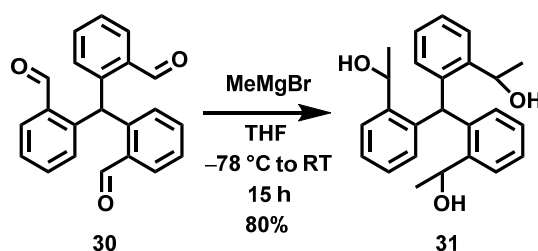


3a2,4,8,12-Tetrahydrodibenzo[cd,mn]pyrene (26): To a cooled ($-78\text{ }^\circ\text{C}$) solution of tris(2-(chloromethyl)phenyl)methane (**29**; 55 mg, 0.14 mmol) in dry CH_2Cl_2 (30 mL), AlCl_3 (23.4 mg, 0.42 mmol) was added in one portion at $-78\text{ }^\circ\text{C}$ and the mixture was stirred at $-78\text{ }^\circ\text{C}$ for 3 h under an argon atmosphere before it was allowed to warm to room temperature over a period of 5 h and it was stirred at room temperature for additional 4 h. Afterwards, the reaction was quenched by the addition of water (10 mL). The organic layer was separated and the aqueous layer was extracted with CH_2Cl_2 ($3 \times 15\text{ mL}$). The combined organic layers were washed with water (25 mL), brine (25 mL), dried over Na_2SO_4 , and filtered. After evaporation of the solvents, the residue was purified by column chromatography over silica gel using $^\circ\text{Hex}$. The ^1H NMR spectrum of the residue after column chromatography showed a complex mixture of products, which could not be separated and identified.



2,2',2''-Methanetriyltribenzaldehyde (30): To a stirred solution of (methanetriyltris(benzene-2,1-diyl))trimethanol (**25**; 502 mg, 1.50 mmol) in dry CH_2Cl_2 (40

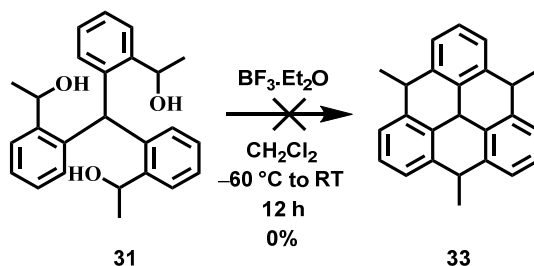
mL), DMP (2.55 g, 6.00 mmol) was added portion wise over 1 h at room temperature under an argon atmosphere. The reaction mixture was then stirred for 8 h at room temperature under an argon atmosphere, before it was quenched by the addition of sat. aq. Na₂CO₃ (20 mL). The organic layer was separated and the aqueous layer was extracted with CH₂Cl₂ (3 × 15 mL). The combined organic layers were washed with water (25 mL), brine (25 mL), dried over Na₂SO₄, and filtered. After evaporation of the solvents, the residue was purified by column chromatography over silica gel using ^cHex/EtOAc (1:1) as an eluent to afford the desired product (397 mg, 80%) as a white solid. ¹H NMR (400 MHz, CDCl₃, ppm): δ 10.17 (s, 3H), 8.51 (s, 1H), 7.94–7.85 (m, 3H), 7.50–7.39 (m, 6H), 6.88–6.77 (m, 3H). ¹³C NMR (101 MHz, CDCl₃, ppm): δ 192.2, 144.6, 133.9, 133.7, 133.6, 130.9, 127.5, 42.9.



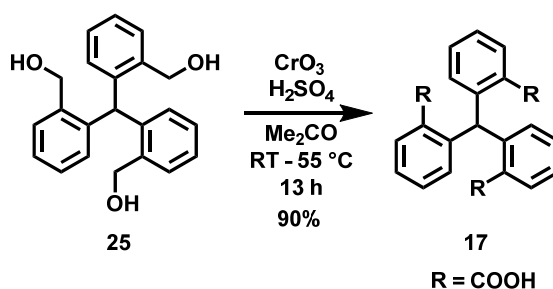
1,1'-(((2-(-1-hydroxyethyl)phenyl)methylene)bis(2,1-phenylene))bis(ethan-1-ol) (31):

To a cooled (−78 °C) solution of 2,2',2''-methanetriyltribenzaldehyde (**30**; 316 mg, 0.962 mmol) in dry THF (30 mL), MeMgBr (3.80 ml, 3.66 mmol, 1.00 M solution in Bu₂O) was added dropwise over a period of 40 min at −78 °C under an argon atmosphere. The reaction mixture was then stirred at −78 °C for 2 h under an argon atmosphere. Afterwards, the mixture was allowed to warm up to room temperature over 30 min before it was stirred at room temperature under an argon atmosphere overnight. The reaction was quenched by the addition of water (30 mL). The organic layer was separated and the aqueous layer was extracted with CH₂Cl₂ (3 × 15 mL). The combined organic layers were washed with water (25 mL), brine (25 mL), dried over Na₂SO₄, and filtered. After evaporation of the solvents, the residue was purified by column chromatography over silica gel using ^cHex/EtOAc (1:3)

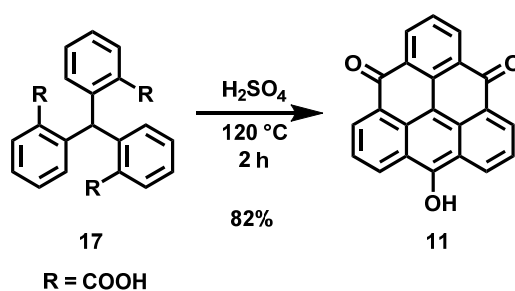
as an eluent to afford the desired product (**31**; 291 mg, 80%) as a white solid. $^1\text{H NMR}$ (400 MHz, CD_3OD , ppm): δ 7.67–7.53 (m, 3H), 7.33–7.24 (m, 3H), 7.16–7.05 (m, 3H), 6.80–6.58 (m, 3H), 5.04–4.94 (m, 3H), 1.58–0.83 (s, br. 9H).



4,8,12-Trimethyl-3a,4,8,12-tetrahydrodibenzo[cd,mn]pyrene (33): To a cooled ($-60\text{ }^\circ\text{C}$) solution of 1,1'-(((2-((R)-1-hydroxyethyl)phenyl)methylene)bis(2,1-phenylene))bis(ethan-1-ol) (**31**; 160 mg, 0.43 mol) in dry CH_2Cl_2 (70 mL), $\text{BF}_3 \cdot \text{Et}_2\text{O}$ (0.10 mL, 0.80 mmol) was added dropwise over a period of 6 h. The mixture was then allowed to warm to room temperature over a period of 4 h and it was stirred at room temperature for additional 2h. Afterwards, the reaction was quenched by the addition of MeOH (10 mL), followed by water (20 mL). The organic layer was separated, and the aqueous layer was extracted with CH_2Cl_2 (3×15 mL). The combined organic layers were washed with water (25 mL), brine (25 mL), dried over Na_2SO_4 , and filtered. The residue was purified by column chromatography over silica gel using $^o\text{Hex.}$ The $^1\text{H NMR}$ spectrum of the residue after column chromatography showed a complex mixture of products, which could not be separated and identified.

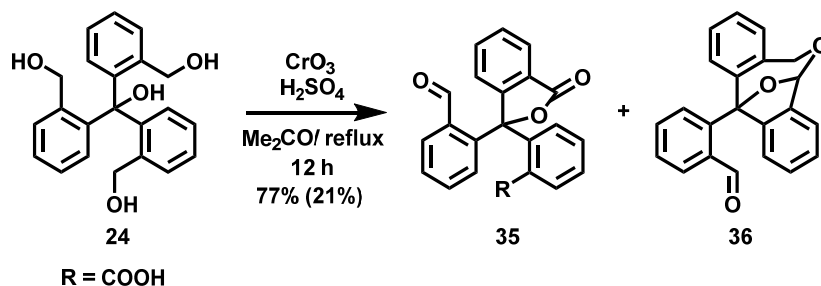


2,2',2''-Methanetriyltribenzoic acid (17): To a solution of (methanetriyltris(benzene-2,1-diyl))trimethanol (**25**; 401 mg, 1.10 mmol) in acetone (25 mL), Jones reagent (1.80 mL, 4.80 mmol, 2.67 M solution) was added dropwise over a period of 2 h at room temperature. The mixture was then heated under reflux for 1 h before another portion of Jones reagent (1.80 mL, 4.80 mmol, 2.67 M solution) was added. The mixture was then stirred under reflux for 12 h. Water (100 mL) was added to quench the reaction. The reaction mixture was extracted with ethyl acetate (3 × 80 mL). The combined organic layers were washed with brine, dried over anhydrous Na₂SO₄, and filtered. After evaporation of the solvents, the desired product (**17**; 430 mg, 90%) was obtained as a white solid, which was used in the next step without further purification. This compound was also prepared and characterized elsewhere.¹³⁷⁻¹³⁸ The recorded spectra are in agreement with those reported previously. ¹H NMR (400 MHz, DMSO-*d*₆, ppm): δ 12.42 (s, br, 3H), 8.02 (s, 1H), 7.82 (dd, *J* = 7.6, 1.4 Hz, 3H), 7.39 (td, *J* = 7.5, 1.4 Hz, 3H), 7.27 (td, *J* = 7.6, 1.2 Hz, 3H), 6.80 (dd, *J* = 7.6, 1.2 Hz, 2H). ¹³C NMR (101 MHz, DMSO-*d*₆, ppm): δ 168.0, 145.4, 131.2, 130.9, 130.6, 130.3, 125.8, 46.6. HRMS (ESI): *m/z* [M + Na]⁺ calcd for C₂₂H₁₆O₆Na⁺: 399.0839; found 399.0839 (|Δ| = 0.0 ppm).



12-Hydroxydibenzo[*cd,mn*]pyrene-4,8-dione (11): A solution of 2,2',2''-methanetriyltribenzoic acid (**17**; 400 g, 8.29 mmol) in conc. H₂SO₄ (20 mL) was heated at 120 °C for 2 h before it was allowed to cool to room temperature and ice-cold water was added. The precipitate that formed was filtered and washed with water, acetonitrile and Et₂O to afford the desired product (**11**; 282 mg, 82%) as a deep-blue solid. This compound was also prepared elsewhere.^[131, 133] ¹H NMR (400 MHz, D₂SO₄, ppm): δ 9.72 (d, *J* = 8.1 Hz,

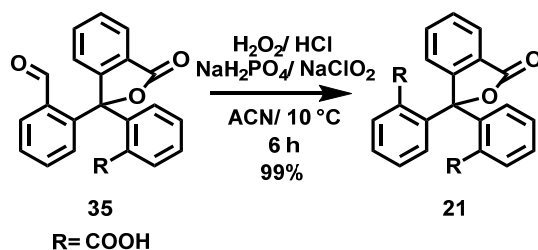
1H), 8.40 (t, $J = 8.1$ Hz, 1H). ^{13}C NMR (101 MHz, D_2SO_4 , ppm): δ 170.5, 139.5, 125.4, 124.0, 115.7, 102.7. HRMS (ESI): m/z $[\text{M} - \text{H}]^-$ calcd for $\text{C}_{22}\text{H}_9\text{O}_3^-$: 321.0561; found: 321.0561 ($|\Delta| = 1$ ppm).



2-(1-(2-Formylphenyl)-3-oxo-1,3-dihydroisobenzofuran-1-yl)benzoic acid (35): To a stirred solution of ((hydroxymethanetriyl)tris(benzene-2,1-diyl))trimethanol (**24**; 4.65 g, 13.1 mmol) in acetone (185 mL), Jones reagent (17.2 mL, 45.9 mmol, 2.67 M solution) was added dropwise over a period of 3 min at room temperature. The mixture was then heated under reflux for 1 h before another portion of Jones reagent (4.91 mL, 13.1 mmol, 2.67 M solution) was added. The mixture was then stirred under reflux for 12 h. Water (100 mL) was added to quench the reaction. The reaction mixture was extracted with ethyl acetate (3 \times 80 mL). The combined organic layers were washed with brine, dried over anhydrous Na_2SO_4 , and filtered. After evaporation of the solvents, the residue was purified by column chromatography over silica gel using $\text{CH}_2\text{Cl}_2/\text{MeOH}$ (30:1 to 10:1) as an eluent to afford the desired product (**35**, 3.70 g, 77%) as a white solid and a side product (**36**; 941 mg, 22%) as a white solid. ^1H NMR (400 MHz, CD_3COCD_3 , drop of TFA-*d* was used, ppm): δ 10.2 (s, 1H), 8.00–7.97 (m, 2H), 7.95 (dt, $J = 7.6, 1.0$ Hz, 1H), 7.87 (td, $J = 7.5, 1.2$ Hz, 1H), 7.72 (td, $J = 7.5, 0.9$ Hz, 1H), 7.62–7.43 (m, 5H), 7.34–7.26 (m, 2H). ^{13}C NMR (101 MHz, CD_3COCD_3 , drop of TFA-*d* was used, ppm): δ 191.3, 170.2, 169.0, 151.3, 143.0, 140.4, 135.9, 135.2, 133.8, 132.4, 131.4, 131.0, 130.6, 130.0 (two overlapped signals), 129.6,

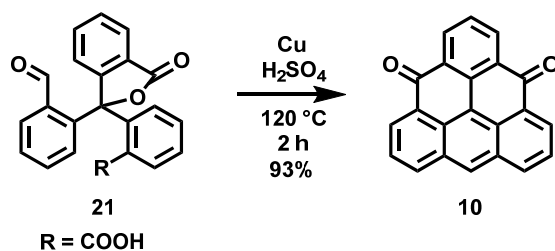
129.3, 128.7, 126.9, 126.8, 126.7, 91.6. HRMS (ESI): m/z $[M + Na]^+$ calcd for $C_{22}H_{14}O_5Na^+$: 381.0733; found 381.0735 ($|\Delta| = 0.4$ ppm).

Side product **36**: 1H NMR (400 MHz, $CDCl_3$, ppm): 10.39 (d, $J = 0.8$ Hz, 1H), 8.35 (dd, $J = 7.6, 1.6$ Hz, 1H), 8.09 (dd, $J = 7.7, 1.4$ Hz, 1H), 7.79–7.70 (m, 3H), 7.70–7.55 (m, 4H), 6.95 (dt, $J = 6.3, 1.7$ Hz, 1H), 6.83 (s, 1H), 5.01 (d, $J = 14.8$ Hz, 1H), 4.26 (d, $J = 14.8$ Hz, 1H). ^{13}C NMR (101 MHz, $CDCl_3$, ppm): 192.6, 148.0, 141.6, 141.3, 138.6, 137.9, 136.1, 132.9, 129.9, 129.5, 129.05, 129.04, 128.7, 127.8, 127.7, 127.1, 126.7, 124.6, 122.8, 103.3, 94.5, 68.2. HRMS (ESI): m/z $[M + Na]^+$ calcd for $C_{22}H_{16}O_3Na^+$: 351.0992; found 351.0994 ($|\Delta| = 0.8$ ppm).



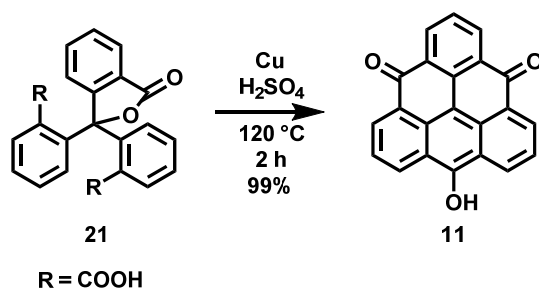
2,2'-(3-Oxo-1,3-dihydroisobenzofuran-1,1-diyl)dibenzoic acid (21): A mixture of hydrogen peroxide (3.92 mL, 41.4 mmol, 30% solution in water) and sodium phosphate (462 mg, 3.32 mmol) in water (10 mL) was acidified with conc. HCl (pH = 2) and was added into cold (<10 °C) solution of 2-(1-(2-formylphenyl)-3-oxo-1,3-dihydroisobenzofuran-1-yl)benzoic acid (**35**, 3.00 g, 8.29 mmol) in acetonitrile (80 mL). A solution of sodium chlorite (1.31 g, 11.6 mmol) in water (5 mL) was then added within 3 h and the mixture was stirred at 8 °C for additional 2 h. As the reaction was not complete, a solution of sodium chlorite (630 mg, 4.56 mmol) in water (5 mL) was added again within 1 h followed by the addition of conc. HCl (1 mL) and the reaction was stirred at 8 °C for additional 1 h before it was quenched by the addition of sat. Na_2SO_3 (10 mL). The reaction mixture was then extracted with ethyl acetate (3×10 mL). The combined organic layers were washed with brine, dried

over anhydrous Na₂SO₄, and filtered. After evaporation of the solvents, the desired product (**21**; 3.10g, 99%) was obtained as a white solid, which was used in the next step without further purification. This compound was also prepared and characterized elsewhere.^[136] The recorded spectra are in agreement with those reported previously. ¹H NMR (400 MHz, 400 MHz, CD₃COCD₃, drop of TFA-*d*, ppm): δ 7.88 (dt, *J* = 7.9, 0.9 Hz, 1H), 7.84 (dt, *J* = 7.5, 0.9 Hz, 1H), 7.77 (td, *J* = 7.8, 1.1 Hz, 1H), 7.63 (td, *J* = 7.5, 0.9 Hz, 1H), 7.60–7.54 (m, 2 H), 7.47–7.39 (m, 4H), 7.38–7.31 (m, 2H). ¹³C NMR (101 MHz, CD₃COCD₃, drop of TFA-*d*, ppm): δ 169.9, 169.56, 152.7, 139.9, 134.6, 133.6, 130.7, 130.6, 130.4, 129.2, 129.0, 127.3, 126.4, 126.2, 91.6. HRMS (ESI): *m/z* [M + Na]⁺ calcd for C₂₂H₁₄O₆Na⁺: 397.0683; found 397.0686 (|Δ| = 0.8 ppm).

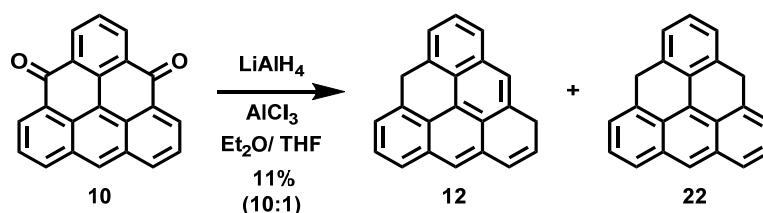


Dibenzo[*cd,mn*]pyrene-4,8-dione (10): A mixture of 2-(1-(2-Formylphenyl)-3-oxo-1,3-dihydroisobenzofuran-1-yl)benzoic acid (**21**, 2.50 g, 6.63 mmol) and copper powder (506 mg, 7.96 mmol) in conc. H₂SO₄ (40 mL) was heated at 120 °C for 2 h before the reaction mixture was filtered through a glass filter to remove the unreacted copper. The glass filter was washed with hot conc. H₂SO₄ (20 mL). Water was added, the precipitate that formed was filtered and washed with water, acetonitrile, and Et₂O to afford the desired product (**10**; 1.89 g, 93%) as a deep-red solid. This compound was also prepared and characterized elsewhere.^[131, 133] ¹H NMR (400 MHz, D₂SO₄, ppm): δ 9.31 (d, *J* = 1.6 Hz, 1H), 9.18 (dd, *J* = 7.6, 1.4 Hz, 2H), 9.02 (dd, *J* = 8.0, 1.7 Hz, 2H), 8.79 (dd, *J* = 8.0, 1.4 Hz, 2H), 7.81 (td, *J* = 7.8, 1.4 Hz, 2H), 7.77 (td, *J* = 8.0, 1.8 Hz, 1H). ¹³C NMR (101 MHz, D₂SO₄, ppm): δ

179.8, 153.7, 153.3, 148.8, 144.8, 135.1, 131.4, 131.1, 130.8, 123.3, 121.4, 114.3. HRMS (ESI): m/z $[M - H]^+$ calcd for $C_{22}H_{11}O_2^+$: 307.0754; found: 307.0750 ($|\Delta| = 1.1$ ppm).

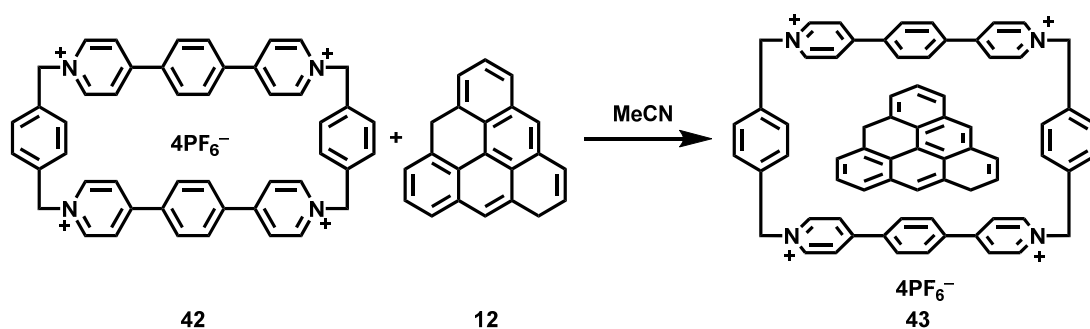


12-Hydroxydibenzo[*cd,mn*]pyrene-4,8-dione (11): A mixture of 2,2'-(3-oxo-1,3-dihydroisobenzofuran-1,1-diyl)dibenzoic acid (**21**; 3.10 g, 8.29 mmol) and copper powder (631 mg, 9.94 mmol) in conc. H_2SO_4 (20 mL) was heated at 120 °C for 2 h before the reaction mixture was filtered through a glass filter to remove the unreacted copper. The glass filter was washed with hot conc. H_2SO_4 (20 mL). Water was added, the precipitate that formed was filtered and washed with water, acetonitrile, and Et_2O to afford the desired product (2.61g, 98%) as a deep-blue solid. This compound was also prepared and characterized elsewhere.^[131, 133] 1H NMR (400 MHz, D_2SO_4 , ppm): δ 9.72 (d, $J = 8.1$ Hz, 1H), 8.40 (t, $J = 8.1$ Hz, 1H). ^{13}C NMR (101 MHz, D_2SO_4 , ppm): δ 170.5, 139.5, 125.4, 124.0, 115.7, 102.7. HRMS (ESI): m/z $[M - H]^-$ calcd for $C_{22}H_9O_3^-$: 321.0561; found: 321.0561 ($|\Delta| = 1$ ppm).



1,8-Dihydrodibenzo[*cd,mn*]pyrene (12): To a stirred suspension of $LiAlH_4$ (104 mg, 2.74 mmol) in dry Et_2O (25 mL), a solution of $AlCl_3$ (731 mg, 5.49 mmol) in dry Et_2O (25 mL) was added dropwise at room temperature under an argon atmosphere and the mixture was stirred for 5 min. To this mixture, suspension of dibenzo[*cd,mn*]pyrene-4,8-dione (**10**; 500 mg, 1.63 mmol) was added portionwise over 3.5 h at room temperature under an argon

atmosphere. The resulting mixture was then decanted in a clean 250 mL round-bottomed flask, the solution was bubbled with argon, cooled in an ice bath and quenched by the addition of water (3 mL, deaerated with a stream of argon for 10 min). To this solution, SiO₂ (10 g) and ^oHex (deaerated with a stream of argon for 15 min) were added and the mixture was concentrated in vacuum. The crude mixture was purified by column chromatography (SiO₂, ^oHex, deaerated with a stream of argon for 30 min) under an argon atmosphere in the dark. The desired product (**12**; 50 mg, 11%) was isolated as a cotton-like yellow solid and was stored in the freezer under an argon atmosphere. The desired product contained a small amount (ca. 10%) of isomer **22**. ¹H NMR (400 MHz, CD₂Cl₂, ppm): δ 7.65–7.60 (m, 3H), 7.48 (dd, *J* = 8.0, 7.1 Hz, 1H), 7.45 (t, *J* = 7.4 Hz, 1H), 7.42–7.39 (m, 1H), 7.39–7.36 (m, 2H), 6.73 (dt, *J* = 9.8, 2.0 Hz, 1H), 6.18 (dt, *J* = 9.8, 4.0 Hz, 1H), 4.91 (s, br., 2H), 4.11 (s, br., 2H). ¹³C NMR (101 MHz, CD₂Cl₂, ppm): δ 134.7, 134.7, 133.0, 132.6, 131.0, 128.7, 128.4, 127.9, 127.4, 127.3, 127.2, 126.3, 125.9, 125.7, 125.6, 125.2, 125.0, 124.9, 123.6, 34.6, 32.3. One signal is missing due to signal overlap.



Supramolecular complex dihydrotriangulene e^c ExBox⁴⁺ (43): To a degassed solution of ExBox⁴⁺ (**42**; 12.0 mg, 9.58 μmol) in dry CD₃CN, dihydrotriangulene (**12**; 0.27 mg, 9.58 μmol) was added in one portion as a solid in the glove box. The suspension was shaken for 30 sec until a homogenous solution formed. The NMR tube was sealed and the ¹H NMR spectra was measured. ¹H NMR (500 MHz, CD₃CN, ppm): δ 8.74 (d, *J* = 6.5 Hz, 8H), 7.96

(s, 8H), 7.62 (d, $J = 6.5$ Hz, 8H), 7.02 (s, 8H), 6.64 (dd, $J = 7.2, 1.4$ Hz, 1H), 6.35 (dd, $J = 7.1, 1.4$ Hz, 1H), 6.05 (dt, $J = 9.9, 3.8$ Hz, 1H), 5.98 (dt, $J = 9.8, 2.1$ Hz, 1H), 5.94 (d, $J = 1.9$ Hz, 1H), 5.74 (d, $J = 7.6$ Hz, 1H), 5.71 (s, 8H), 5.56 (t, $J = 7.5$ Hz, 1H), 5.53 (s, 1H), 5.01 (d, $J = 7.8$ Hz, 1H), 4.83 (d, $J = 7.8$ Hz, 1H), 4.04 (s, 2H), 3.73 (s, 2H).

CHAPTER III:

STERICALLY PROTECTED TRIANGULENE

3.1 INTRODUCTION

As it was mentioned in the previous Chapters I and II, pristine triangulene or any triangulene derivative has never been isolated in the solid form. Due to the presence of two unpaired electrons, which are mainly delocalized at the peripheral α -positions (Figure 3.1 a, far left, in black), triangulene can rapidly dimerize/polymerize or react with oxygen (Chapter 1.5.3).^[131, 133, 134, 136]

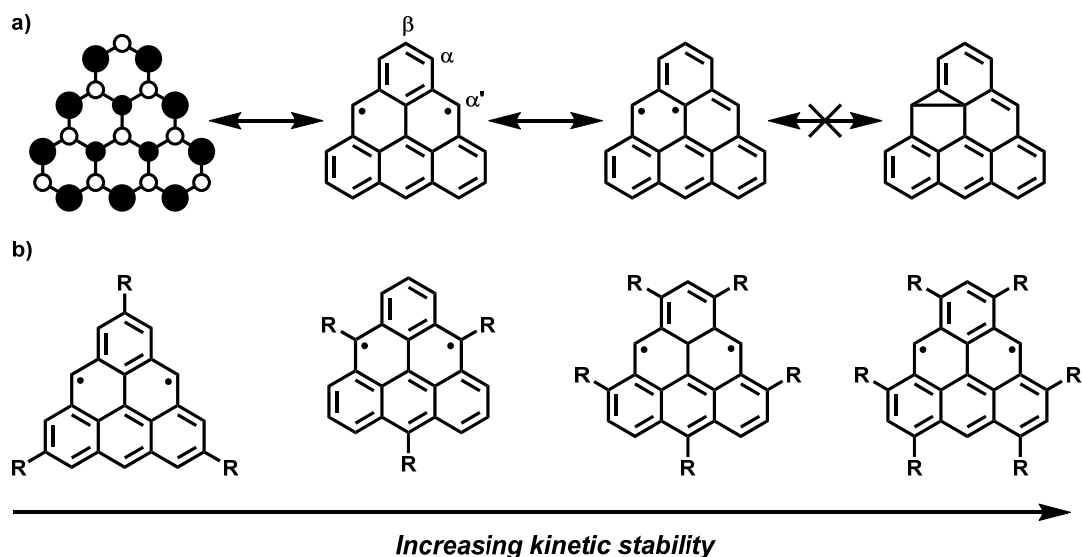
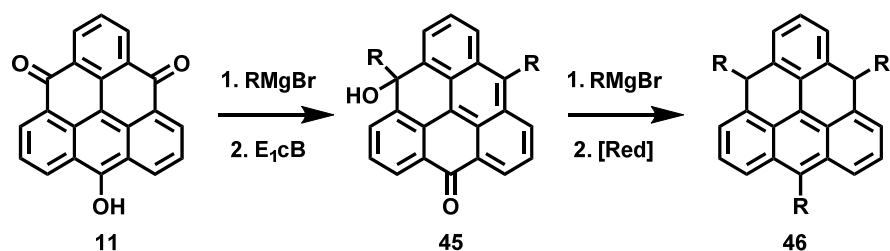


Figure 3.1: Electron spin density distribution in a diradical triangulene (Figure 3.1 a, far left) and its resonance structures and derivatives of diradical triangulene (Figure 3.1 b).

Several groups have previously attempted to stabilize the triangulene core by introduction of bulky substituents (Figure 3.1b, far left) at the β -positions or heteroatoms at the α' -positions, strategies that previously led to the successful stabilization and isolation of phenalenyl radical. However, in the case of triangulene analogues, these compounds could not be isolated in their solid forms, and their properties could only be investigated in oxygen-free solutions at low temperatures. Nevertheless, triangulene that is bearing three *tert*-butyl

groups at the β -positions (Figure 3.1b, far left) remains the only derivative of triangulene, comprised of only carbon and hydrogen atoms with a triplet ground state detectable by ESR spectroscopy, that was made to this day.

In the previous Chapter II, synthesis of the diketohydroxy triangulene precursor **11** was described (Scheme 3.1). Our goal in this chapter was to stabilize the triangulene core by introduction of bulky substituent at the α' -positions, by means of nucleophilic substitution using Grignard reagent as nucleophiles.



Scheme 3.1: Synthetic strategy towards trisubstituted triangulene **46**.

Such a functionalization should provide sufficient stability to the triangular core, that should allow us to isolate and study the properties of triangulene, both in solution and in the solid state for the first time. If this protection is not sufficient, strategies for higher substituted derivatives with larger protective shell (Figure 3.1, right) will be developed.

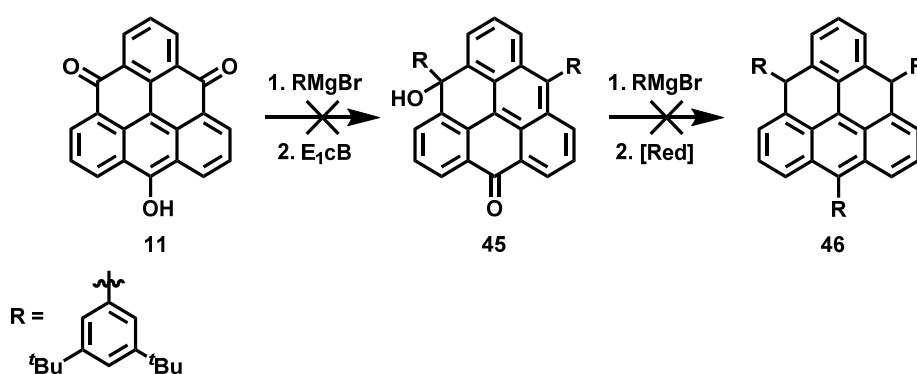
3.2 RESULTS & DISCUSSION

3.2.1 NUCLEOPHILIC ADDITIONS ON TRIANGULENE CORE

As mentioned previously, the objective of this chapter was to synthesize for the first time a persistent triangulene derivative and validate, both by experimental and theoretical means, its properties in solution and in the solid state. To achieve this challenging goal, we proposed to create a “protective shell” around the triangulene core by introduction of extremely bulky substituents that are expected to suppress self-recombination of the diradical species and allow for their isolation in the solid state.

In the previous Chapter II, we successfully established synthetic strategy towards diketohydroxytriangulene **11**, which can be prepared efficiently in four steps on a multigram scale. This beautiful deep-blue compound represents the basic starting material for all our proposed synthetic strategies towards sterically protected triangulene.

Our first strategy represents a direct introduction of substituents to diketotriangulene **10** and diketo hydroxytriangulene **11** (Scheme 3.2) by means of nucleophilic addition to the carbonyl groups, using Grignard reagents or lithium salts. The substituents will be introduced at the α' -positions, where the majority of the spin electron density is localized.



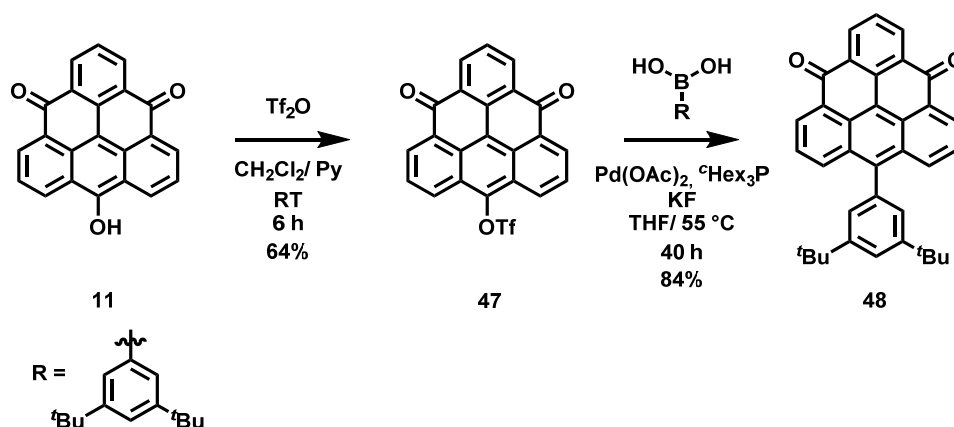
Scheme 3.2: Unsuccessful synthetic strategy towards trisubstituted triangulene **46**.

Di-*tert*-butylphenyl was chosen as a substituent of choice, as its sterical bulkiness should provide sufficient protection of the triangulene core as well as it should boost solubility of

the decorated triangulene. Moreover, its magnesium bromide can be prepared easily from di-*tert*-butylphenyl bromide and magnesium turnings.

Both diketotriangulene **10** and diketo hydroxytriangulene **11** were therefore treated with excess of the corresponding Grignard reagent in dry THF at low temperature. Unfortunately, these reactions led only to a very low conversion of the starting material and to a formation of the complex mixture of products. Our attempts for optimization of the reaction conditions by temperature elevation did not improve the conversion. We also tried to use lithium salts as source of the nucleophile, however, this also had no effect on the reaction. A possible explanation for very low conversion and a formation of the complex mixture of the product could be a very limited solubility of both diketotriangulene **10** and diketo hydroxytriangulene **11**.

To overcome the problem with solubility of the triangulene **11**, we decided to introduce a solubilizing group first. The presence of the phenolic hydroxy group in triangulene **11** suggests that it might be converted to a pseudo-halide, such as triflate, which might undergo a palladium-catalysed cross-coupling reaction.



Scheme 3.3: Transformation of diketo hydroxytriangulene **11** to the corresponding triflate derivative **47** and its subsequent Suzuki coupling with boronic acid to the monosubstituted diketo triangulene **48**.

Hydroxytriangulene **11** was therefore reacted with triflic anhydride (Tf₂O) in dichloromethane/pyridine mixture at room temperature (Scheme 3.3). After evaporation of

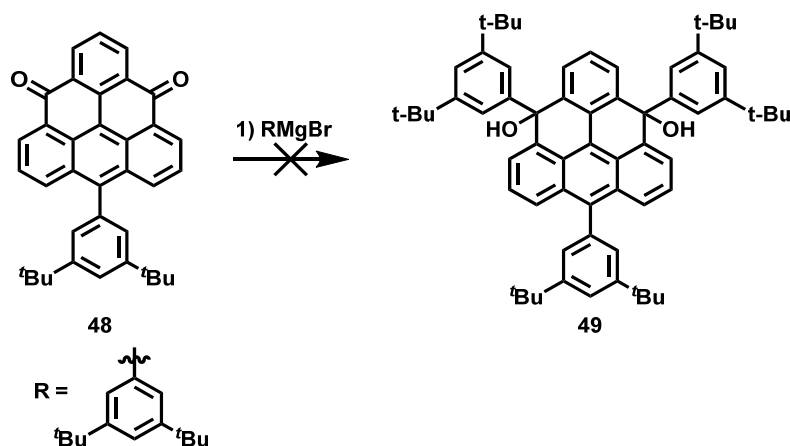
the solvents, the desired triflate derivative **47** was obtained after column chromatography using CH₂Cl₂ to CH₂Cl₂/MeOH (50:1) as an eluent as a red-metallic compound in a good yield. The triflate derivative **47** is relatively soluble in common organic solvents, however, it is sensitive towards moisture and both acidic and basic conditions. This makes the purification and identification challenging. Once the reaction is reproduced on a large scale (larger than 200 mg), the column chromatography must be performed extremely swiftly, to minimize the hydrolysis of the product to triangulene **11**, however, the hydrolysed starting material can be recovered. The ideal quantity of the starting material for this reaction is 500 mg. Once the reaction is performed on a larger scale, the overall yield drops significantly. Compound **47** aggregates strongly in common NMR solvents such as CDCl₃ and CD₂Cl₂. This aggregation in combination with moisture sensitivity did not allow us to measure unequivocal ¹³C NMR spectrum of monomeric **47**. The molecule **47** is therefore characterized only by its ¹H NMR, ¹⁹F NMR and HR MS. However, the presence of a single signal in ¹⁹F NMR spectrum typical for triflates (ca. -72 ppm) in combination with HR MS is a strong evidence that the triflate derivative **47** was indeed prepared.

Our attempts to perform a Suzuki cross-coupling reaction, utilizing standard catalytic conditions, with Pd(PPh₃)₄ and corresponding boronic acid in the presence of water and strong base (carbonates) under elevated temperatures lead to the full hydrolysis of triflate **47**. Since triflate **47** is not stable under aqueatic basic conditions, we performed this reaction also under strict anhydrous conditions, however, the final result was the same as in the previous case, full hydrolysis of the starting material was observed.

We therefore tested a more active palladium catalyst employing a different ligand. The palladium catalyst formed *in situ* from Pd(OAc)₂ and ^cHex₃P lead to approximately 50% conversion of the triflate **47** forming the desired monofunctionalized triangulene **48** in the presence of KF in dry THF at room temperature, and only a minor hydrolysis of the starting

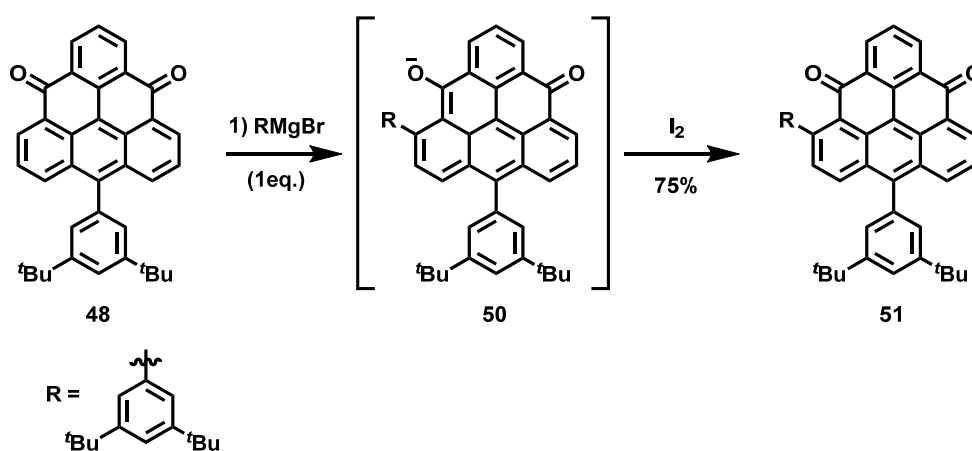
material **47** was observed. Further optimization of the reaction conditions, using absolutely dry components (catalyst, ligand and KF) and elevated temperature (55°C) formed desired monofunctionalized triangulene **48** in a very good 84% yield (Scheme 3.3). The introduction of the bulky di-*tert*-butylphenyl substituent prevented the π - π aggregation and significantly increased the solubility of the parent triangular system.

Once we overcame the problem with the solubility of parent triangulene system **11** by introduction of bulky substituent, we continued with our effort to introduce the substituents to the α' -positions of the system by terms of nucleophilic substitution. Two equivalents of the corresponding Grignard reagent were added to the triangulene **48** at -78 °C in dry THF. The mixture lost its characteristic deep-red colour suggesting that the extended π -conjugation in **48** was disrupted. It is important to note here that the di-*tert*-butylphenyl magnesium bromide was prepared freshly and its concentration was determined by titration of iodine in 0.5 M solution of LiCl in THF.^[163] However, the analysis of the reaction mixture after aqueous work-up again resulted in a formation of complex mixture of products (Scheme 3.4). Therefore, we concluded that our initial hypothesis, namely, the solubility of the diketo hydroxytriangulene **11**, was not the major obstacle in the introduction of the two remaining substituents to the α' -positions of triangulene.



Scheme 3.4: Unsuccessful addition of Grignard reagent on diketotriangulene **49**.

To understand what is happening in this system, we conducted more experiments. This time we added only single equivalent of the Grignard reagent to the THF solution of **48** at -78°C , the solution again lost its characteristic deep-red colour, suggesting again that the extended π -conjugation in **48** was disrupted. TLC analysis of the reaction mixture revealed that a single yellow compound was formed. Once this yellow compound was exposed to the air, the red colour re-appeared. The reaction mixture was, therefore, quenched by the addition of water and the resulting solution was exposed to ambient atmosphere for several hours. The newly formed compound was isolated and purified by column chromatography. We were able to determine the structure of the newly formed compound by means of 2D NMR spectroscopy and the compound was identified as a product of 1,4-addition **51** (Scheme 3.5) and not 1,2-addition. Once we knew what is happening in this reaction system, the oxidation step was speeded up by the addition of iodine (Scheme 3.5).



Scheme 3.5: Addition of one equivalent of Grignard reagent on diketotriangulene **48** and its subsequent oxidation with iodine to triangulene **51** bearing two di-*tert*-butylphenyl functionalities.

A Hückel molecular orbital (HMO) calculation (Figure 3.2, top) provided a simple explanation to such observation. The LUMO in diketotriangulenes is mostly localized at the anthracene core with only small contribution of the carbonyl antibonding π -molecular orbitals. Carbonyl's MOs have large contributions in the LUMO+1 (Figure 3.2, bottom) but

it is the LUMO, which dictates the regioselectivity in the nucleophilic additions. The large number of anthracene carbon atoms that contribute to the LUMO explains the formation of the complex mixtures of products observed when two and more equivalents of a Grignard reagent were added to the reaction mixture. The HMO calculations suggest that one equivalent of a Grignard reagent should add in a Michael 1,4-addition fashion to the *ortho*-position of **48** with respect to the carbonyl group to form intermediate **50**, disrupting thus the aromaticity of the anthracene subunit. This addition process also leads to the loss of the typical deep-red colour for the substituted diketotriangulenes. Oxidation of the intermediate **50** then restores the aromaticity, forming diketotriangulene **51** with two bulky substituents (as confirmed by 2D NMR).

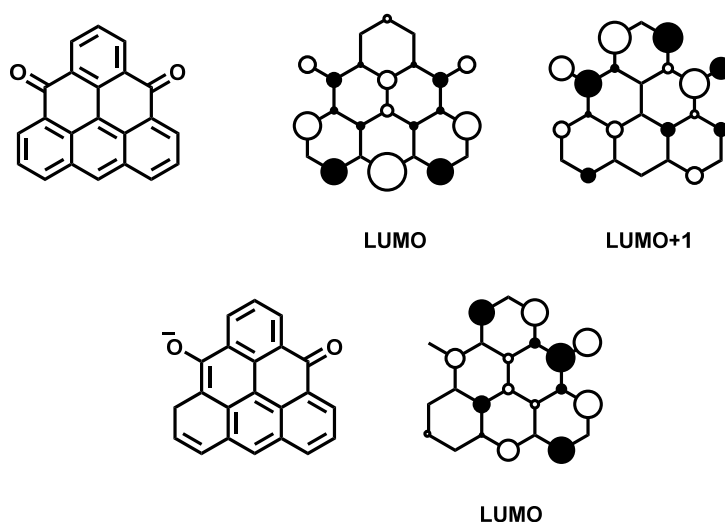
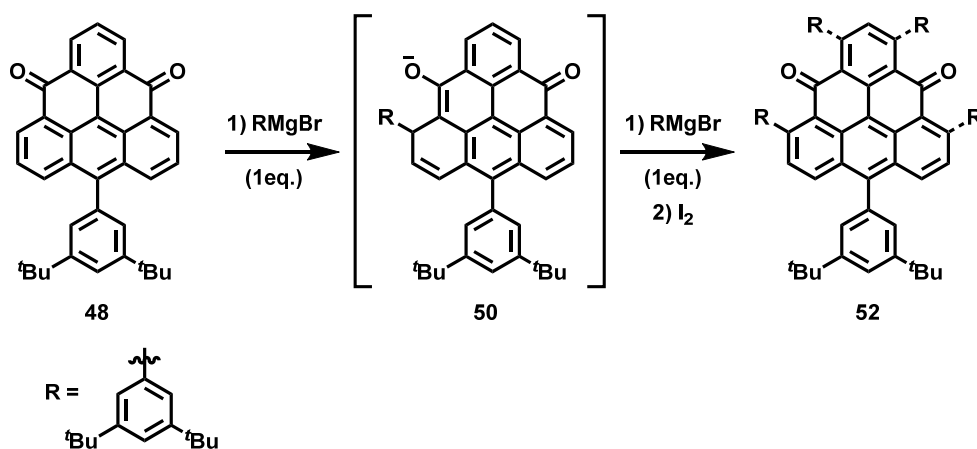


Figure 3.2: LUMO and LUMO+1 molecular orbitals of diketotriangulene (top) and LUMO of ketotriangulene enolate (bottom).

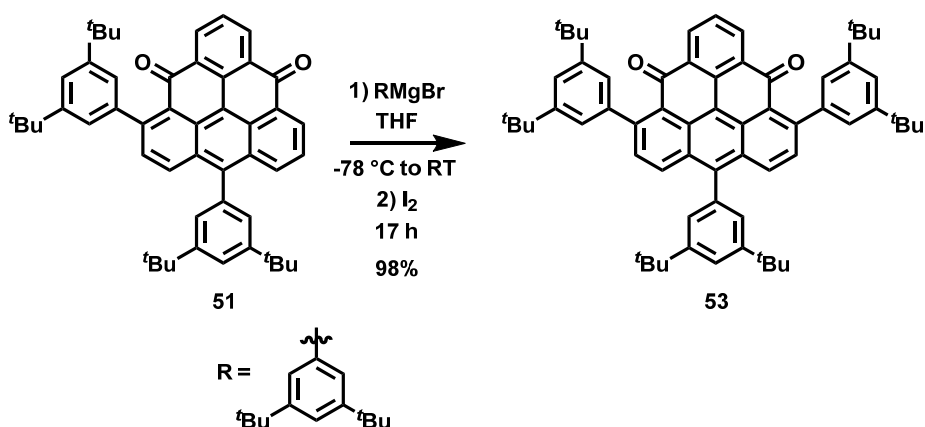
When more than two equivalents of Grignard reagent are used (Scheme 3.6), it is the intermediate **50** that is attacked by the excess nucleophile. Therefore, the regioselectivity of the reaction has to follow the pattern of its LUMO (Figure 3.2, bottom). Again, the contribution of the carbonyl antibonding MO is small and thus a Michael addition is expected. We analysed the mixture obtained from the addition of two equivalents of the Grignard reagent (Scheme 3.4) and we confirmed that an approximately statistical mixture

of three possible products was observed (Scheme 3.6, the three isomers are highlighted with dotted substituents).



Scheme 3.6: Addition of additional equivalent of the Grignard reagent to the intermediate **50**.

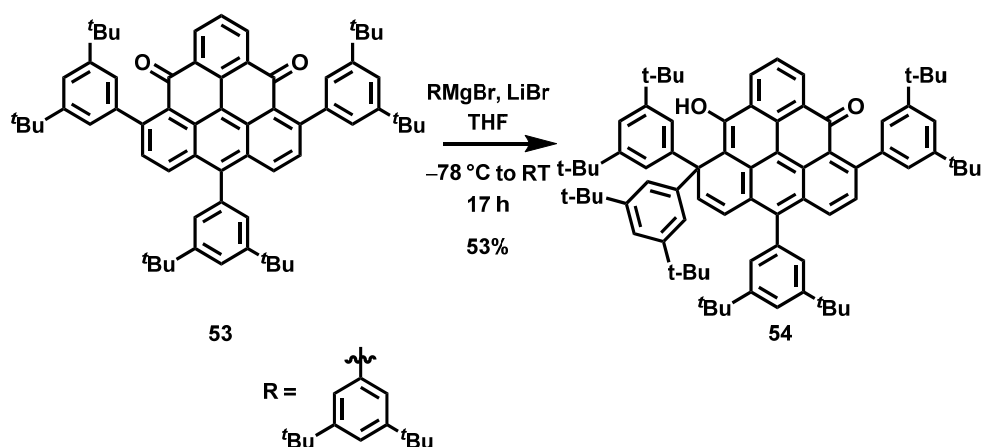
This understanding of the addition pattern allowed as to continue with introduction of additional substituents to the triangulene core. The third substituent was introduced in a similar fashion as the previous one. One equivalent of the Grignard reagent was added to the solution of disubstituted diketotriangulene **51** in dry THF at $-78\text{ }^\circ\text{C}$ (Scheme 3.7). Once the starting material was consumed, according to the TLC and MALDI-TOF MS analysis, the reaction was quenched by the addition of a small amount of water, followed by the addition of excess of iodine and the mixture was stirred for several more hours. After aqueous work-up and column chromatography, the desired trisubstituted diketotriangulene **53** was obtained as a red solid in an excellent yield. 2D NMR spectroscopy provided unequivocal evidence that triangulene **53** was indeed prepared.



Scheme 3.7: Addition of one equivalent of Grignard reagent to diketotriangulene **51** and its subsequent oxidation with iodine to form trisubstituted diketotriangulene **53**.

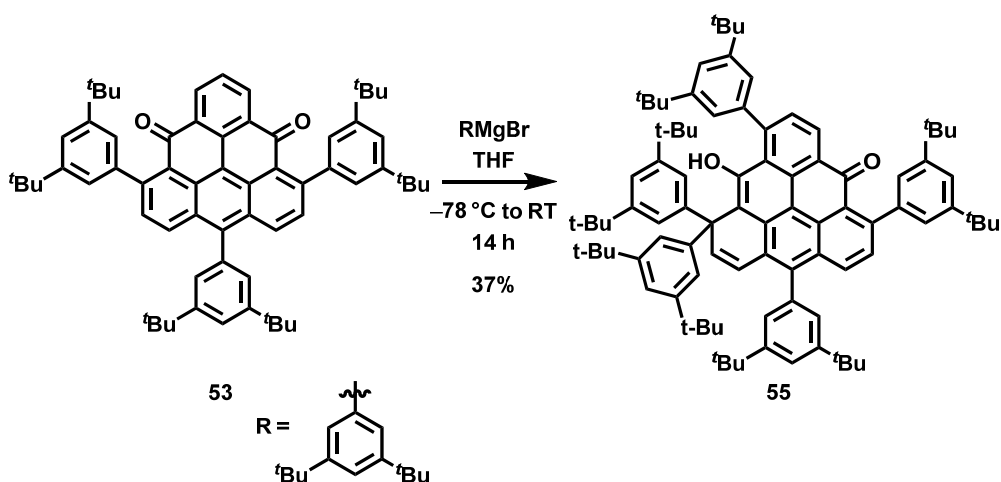
Introduction of the fourth substituent to the triangular core turned out unexpectedly, as upon the addition of one equivalent of Grignard reagent to **53**, compound **54** was isolated. The formation of this compound can be again rationalized by the shape of the LUMO, as the addition strictly follows the MO pattern in this orbital. Another rationalization for formation of such compound could be a disruption of the Clar sextet, compound **54** have two but the product of the desired addition would have only one. (Scheme 3.8). This molecule cannot be oxidised to a diketo derivative and therefore the colour of the derivative **54** remains yellow.

If more than just one equivalent of the Grignard reagent was added to the trisubstituted diketotriangulene **53**, we observed similar result as in the case of the addition of two equivalents to monosubstituted triangulene **51** (Scheme 3.6). The addition of the first equivalent followed the LUMO of the diketotriangulene and the nucleophilic attack occurred in the anthracene core of the triangulene. When the second equivalent is used, it is again the enolate intermediate that is attacked by the excess nucleophile, thus, the regioselectivity of the reaction has to follow the pattern of its LUMO (Figure 3.2, bottom). Therefore, the triangulene derivative bearing five substituents **55** is formed (Scheme 3.9). However, also this molecule cannot be oxidised to a diketo derivative, and it retains the yellow colour.



Scheme 3.8: Addition of one equivalent of Grignard reagent on to diketo triangulene **53**.

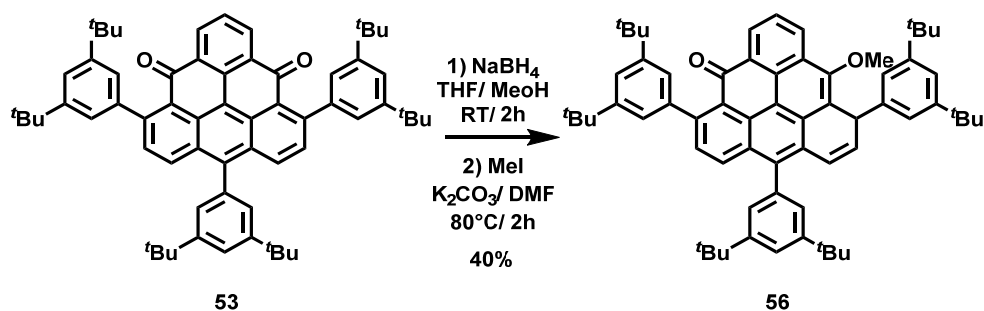
Our attempts to alter the energies of the LUMO and LUMO+1 in diketotriangulene **53** by the addition of strong Lewis acid (such as LiBr, up to 4M solution) to the THF solution prior to the addition of the Grignard reagent, proved to be unsuccessful (Scheme 3.8). We were not able to identify any Lewis acid that would be compatible with these reaction conditions. Therefore, this approach proved to be infeasible.



Scheme 3.9: Addition of an excess of Grignard reagent to diketo triangulene **55**.

The experiments with the intermediacy of the ketotriangulene enolate **50**, however, gave us an idea how the tetrasubstituted triangulene could be prepared. As the addition of the nucleophile to the enolate strictly follows its LUMO, we decided to “lock” the enolate by introduction of a methyl group. The methylated hydroxy ketotriangulene cannot be oxidized

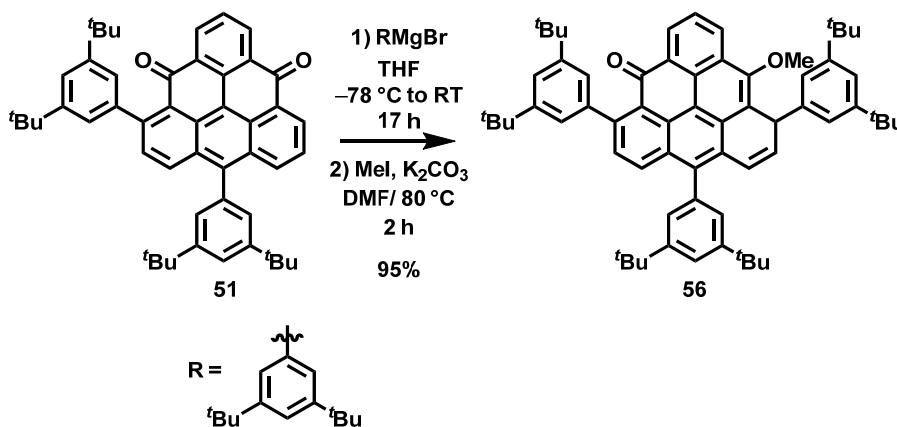
back and the attack of the nucleophile must occur at the carbon atom with the largest LUMO coefficient. To prove this theory, we attempted to prepare the triangulene with three substituents bearing one carbonyl and one methoxy group. Our first idea was to reduce one of the carbonyl groups with NaBH₄ and then react this compound with MeI in the presence of a base in DMF (Scheme 3.10). Even though this reaction worked, and we were able to detect the desired compound bearing one methoxy group, the yield of this reaction was rather low (ca. 40%). Even larger problem was the purification, as we were not able to prevent partial re-oxidation of the reduced triangulene. As both diketotriangulene **53** and monomethoxy ketotriangulene **56** have very similar *R_f* values, the separation of this compound was extremely challenging. Partial separation was achieved, however, the obtained monomethoxy ketotriangulene **56** was not pure. Therefore, this approach was not suitable for the preparation of larger quantities.



Scheme 3.10: Reduction of the trisubstituted diketotriangulene **53** with NaBH₄ and subsequent trapping of its anion with MeI.

To overcome the problem with the reduction, we decided to trap the enolate directly after introduction of the third substituent. From the previous experiment, we knew that the anion is present in the solution and it needs to be oxidized either with air or with iodine. Therefore, one equivalent of the Grignard reagent was added to the THF solution of disubstituted diketotriangulene **51** at -78 °C (Scheme 3.11) and, once the starting material was fully consumed (TLC analysis), the reaction mixture was quenched with a small amount of deaerated water (to quench any excess of the Grignard reagent). The solvent was then

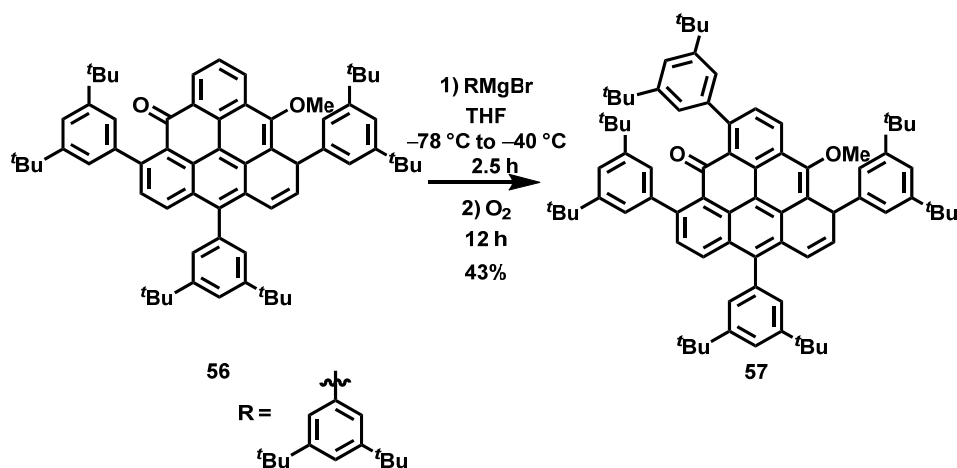
evaporated to dryness and dry K_2CO_3 was added followed by deaerated DMF and MeI. The reaction mixture was then heated at 80 °C for 2 h. After aqueous work-up followed by column chromatography, the desired trisubstituted monomethoxy ketotriangulene was obtained as a yellow solid in an excellent yield and high purity. The structure of the triangulene **56** was confirmed by 2D NMR spectroscopy.



Scheme 3.11: Addition of one equivalent of the Grignard reagent to triangulene **51** and subsequent trapping of the formed enolate intermediate with MeI.

With compound **56** in our hands, we continued with our efforts to prepare the tetrasubstituted triangulene **57**. The nucleophilic substitution in this case proved to be more challenging than in the previous cases. Our standard conditions, addition of one equivalent of the Grignard reagent, were unsuccessful. After extensive optimization of the reaction conditions, we found out that the reaction proceeds once the reaction mixture is concentrated enough (concentration higher than 0.1 M). Also, a higher amount of the Grignard reagent needs to be used (more than three equivalents). The monomethoxy triangulene **56** was dissolved in 2 mL of dry THF and the reaction mixture was cooled to -78 °C, then three equivalents of the Grignard reagent were added dropwise, and the reaction mixture was allowed to warm to -40 °C (Scheme 3.12). Once the starting material was fully consumed (according to TLC analysis, after ca. 2.5 h), the reaction mixture was quenched by the

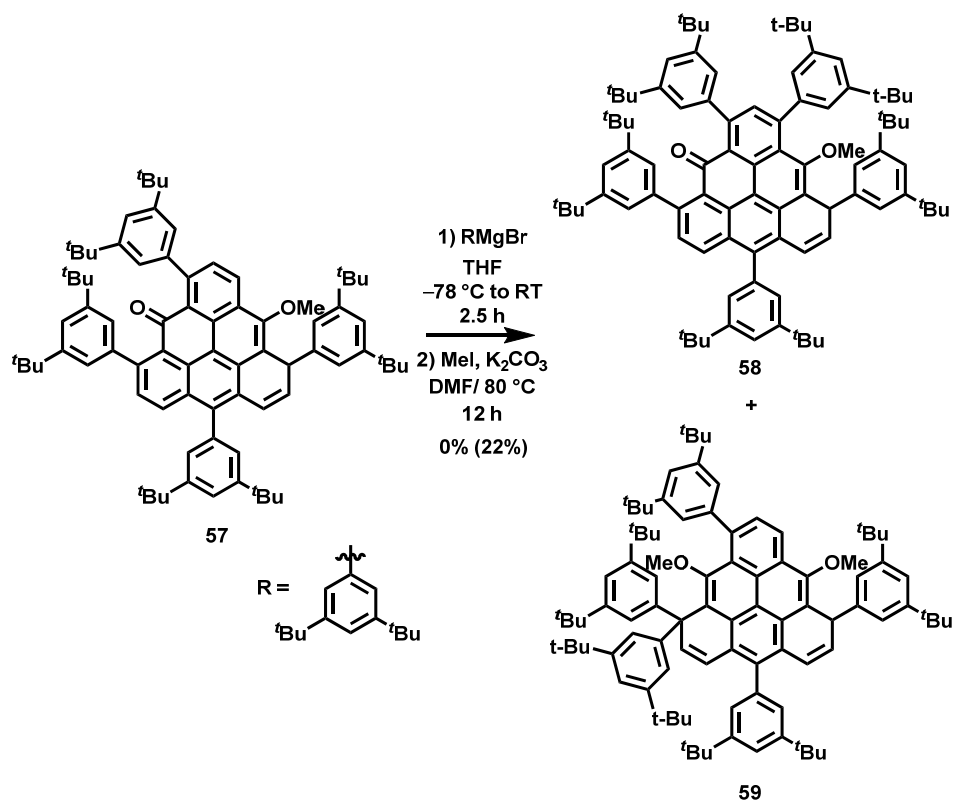
addition of water. In this case, the addition of iodine did not oxidize the resulted hydroxy compound. Therefore, the reaction mixture was purged with air supplied by air pump overnight. After aqueous work-up, the crude product was purified by column chromatography and the desired tetrasubstituted triangulene **57** was prepared as a yellow solid in a good (43%) yield. Our attempt for optimization of the reaction yield were unsuccessful. The rest of the crude reaction mixture was a highly polar compound, the structure of which we were not able to determine. The structure of the tetrasubstituted triangulene **57** was proved by 2D NMR spectral analysis.



Scheme 3.12: Preparation of the tetrasubstituted triangulene **57**.

With four substituents successfully installed around the triangulene core, our final attention turned to the installation of the fifth and last substituent. Utilizing all the previous experience with installation of the fourth substituent, we decided to use the same reaction conditions. Therefore, we directly used excess of the Grignard reagent (three equivalents) and we reduced the reaction volume to a minimum (1 mL). However, these conditions prove to be insufficient. The TLC analysis of the reaction mixture showed only a minimal conversion of the starting material **56**. Therefore, we were increasing the amount of the Grignard reagent and, in the end, we had to use 60 equivalents to observe full conversion of the starting material. TLC and MALDI-TOF MS analysis of the reaction mixture revealed formation of a single compound. For the simple characterization of the final compound, we

decided to trap the enolate with MeI. This was achieved similarly as in the case of trisubstituted triangulene **56**, by reaction of the enolate with MeI in dry DMF in the presence of the base. After work-up and column chromatography, the obtained compound was further spectroscopically analysed. The ^1H NMR spectroscopy revealed that the sample is not pure and at least one more compound with identical molecular mass was present (ca. 20%). As the separation on the standard column chromatography failed, we performed semi-preparative HPLC to purify the sample. The main compound was isolated, the quantities of the minor component were too low for characterization. Once the major sample was pure, we analysed it by means of NMR spectroscopy.



Scheme 3.13: Addition of the fifth substituent to the triangulene core.

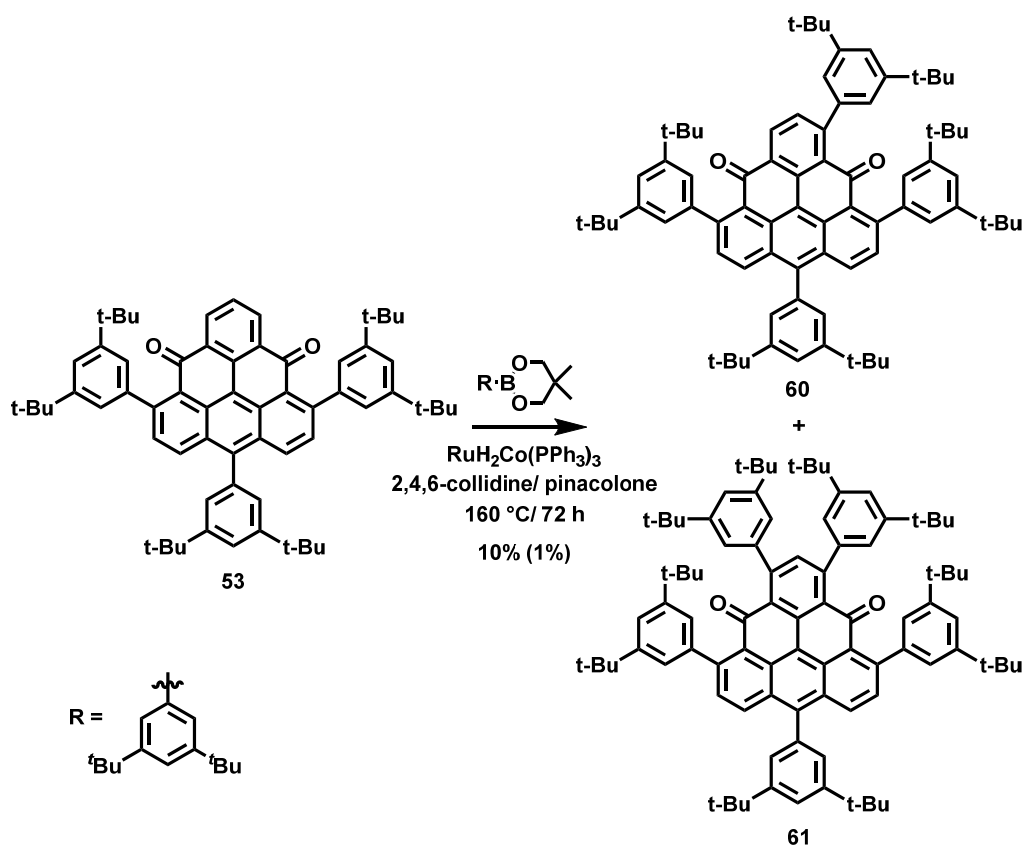
Unfortunately, we were not able to record all the necessary NMR spectra, due to loss of the sample during a holiday period. From the spectra, which we had, we concluded that the most probable structure of the triangulene after the addition is triangulene **59** (Scheme 3.13).

We have no explanation for the formation of such a structure. Most probably the LUMO coefficient in the last free position is not large enough and the final addition proceeds on the anthracene core of the triangulene, despite the steric bulk. Alternatively, the last addition proceeds in this fashion to preserve the aromaticity of the pyrene core within the triangulene. If the final addition would proceed in the last free position, the aromaticity of the pyrene core would be disrupted.

It is possible that the minor product of the addition is the desired triangulene **58**. However, due to low quantities, we were not able to characterize it.

These reactions demonstrate the unexpected beauty of diketotriangulene chemistry. Unfortunately, the introduction of five substituents around the diketotriangulene core using this chemistry proved to be tedious and unsuccessful.

After the addition method for preparation of the pentasubstituted triangulene failed, we were looking for alternative ways how to prepare this molecule. One of the most promising method represents direct C_{sp2}-H activation with a ruthenium catalyst (Scheme 3.14). This reaction produced two compounds, tetra- and penta-substituted triangulenes **60** and **61**, respectively. Both of these compounds were isolated after column chromatography and their structures were characterized by NMR spectroscopy. However, the yield for both compounds is very low, 10% for tetrasubstituted and less than 1% for pentasubstituted triangulene.

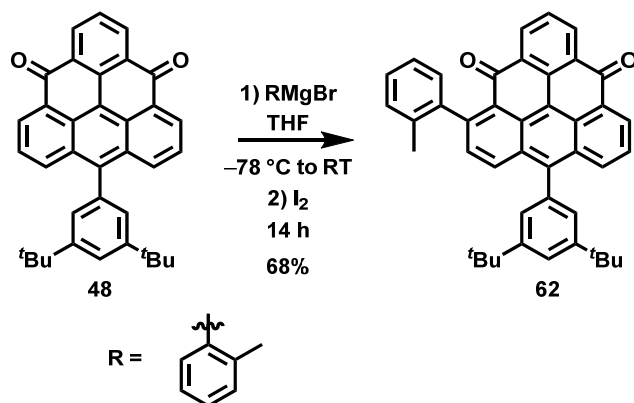


Scheme 3.14: Preparation of tetra- and pentasubstituted triangulenes by direct $\text{C}_{\text{sp}^2}\text{-H}$ activation.

Again, this chemistry demonstrates that the contribution of the remaining two carbon atoms to the LUMO of diketotriangulenes is negligible. Additional work to optimize the reaction conditions to improve the yield of **61**, producing it in sufficient amount for its further reduction is necessary. On the other hand, a DFT-optimized molecular structure of **61** suggests that the di-*tert*-butylphenyl substituents used are too bulky and will probably prevent a reducing reagent (AlH_3) to approach the two carbonyl groups. The proximity of the *tert*-butyl groups on different phenyl rings was also clearly observable in the NOESY experiment with a solution of **57**. We, therefore, put our efforts to replace these bulky di-*tert*-butylphenyl groups with less sterically demanding 2-methylphenyl (2-MePh) groups.

With our experience gained previously from the addition reactions of di-*tert*-butylphenyl substituents to the triangulene core, the installation of the 2-PhMe substituent was straightforward. One of the di-*tert*-butylphenyl substituents installed by Suzuki coupling

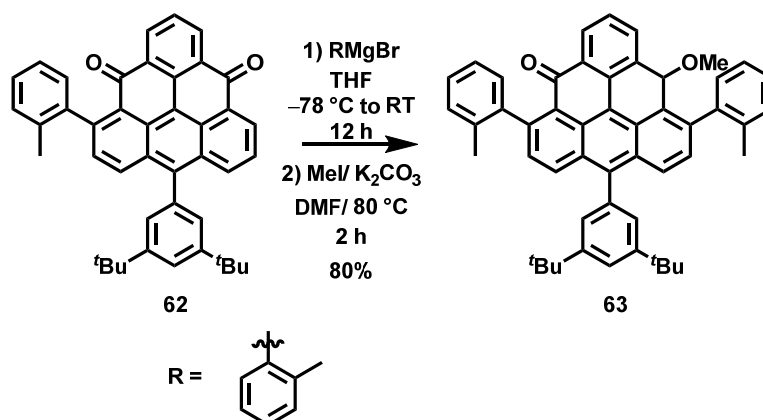
was kept on the triangulene core to provide solubility of the system. The first 2-MePh substituent was installed in similar fashion as the di-*tert*-butyl phenyl substituent. One equivalent of the Grignard reagent was added to the THF solution of triangulene **48** at -78 °C (Scheme 3.15). Once the starting material was fully consumed (TLC analysis), the reaction was quenched by the addition of water, followed by the addition of iodine and the mixture was heated at elevated temperature for 2 h. After aqueous work-up, the crude was purified by column chromatography and the desired monosubstituted product **62** was isolated as deep-red solid in a good yield. The 2D NMR spectroscopic analysis proved the structure of triangulene **62**.



Scheme 3.15: Addition of one equivalent of Grignard reagent to diketotriangulene **48**.

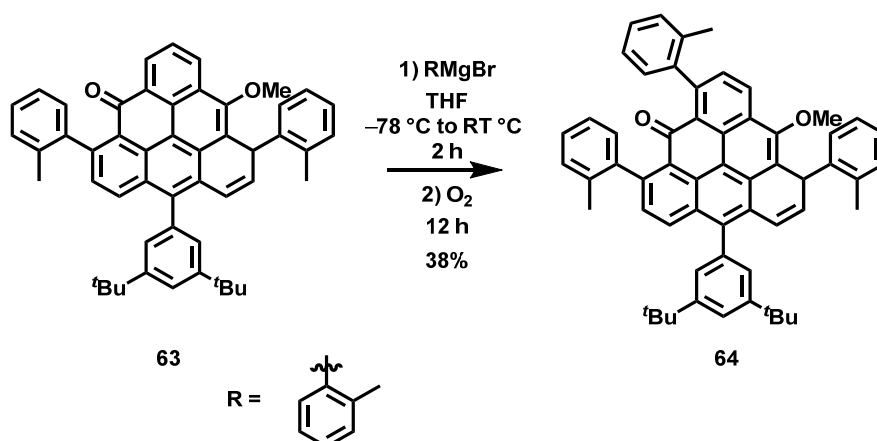
The second 2-MePh substituent was introduced in a similar fashion as the first one. However, this time the reaction mixture was quenched with a small amount of deaerated water, the solvents were evaporated to dryness and the crude mixture was treated with anhydrous K_2CO_3 in deaerated DMF followed by the addition of MeI (Scheme 3.16). The reaction mixture was heated at 80 °C for 2 h. After aqueous work-up, the crude mixture was purified by column chromatography and the desired trisubstituted triangulene **63** was isolated as a yellow solid in a very good yield. This molecule exists in two rotameric forms, the interconversion of which is slow relative to the NMR time scale. Due to heavy signal overlap, we were not able to resolve all signals in the ^{13}C NMR spectrum (out of 86 signals

only **67** could be resolved). However, ^1H NMR spectrum in combination with obtained HR MS gave us the confidence that the desired triangulene **63** was indeed prepared.



Scheme 3.16: Addition of one equivalent of the Grignard reagent to triangulene **62** and subsequent trapping of the formed enolate intermediate with MeI.

With the trisubstituted triangulene **63** in our hands, we turned our attention to introduction of the third 2-MePh substituent. In contrast to the di-*tert*-butyl phenyl substituent, where three equivalents of Grignard reagent had to be used, only one equivalent of 2-MePhMgBr was sufficient for the successful preparation of triangulene **64**. The reaction was carried out under our standard conditions and after full consumption of the starting material, the hydroxy intermediate was oxidized with air (Scheme 3.17). After aqueous work-up, the crude mixture was purified by column chromatography and the desired triangulene **64** was prepared as a yellow solid in moderate yield but high purity.



Scheme 3.17: Preparation of the tetrasubstituted triangulene **64**.

The identification of the structure, similarly as in the previous case, proved to be challenging. The tetrasubstituted triangulene **64** exists in three rotameric forms. Due to a heavy signal overlap, we were not able to resolve all signals in the ^{13}C NMR spectrum. With the aid of 2D NMR spectra as well as HR MS, we are confident that compound **64** was prepared.

Due to the lack of time, we could not introduce the last fifth substituent on the triangulene core. As we expected that the addition of the nucleophile would lead to the same result as in case of the di-*tert*-butyl phenyl Grignard reagent, the fifth substituent needs to be introduced by means of direct $\text{C}_{\text{sp}^2}\text{-H}$ activation. To successfully finish this project, a better catalytic system for the direct $\text{C}_{\text{sp}^2}\text{-H}$ activation needs to be found. Once the fifth substituent is installed, the methoxy group will be deprotected and the obtained triangulene would be reduced by standard conditions using AlH_3 as reducing agent. After successful preparation and purification, the properties, especially the triplet ground state, will be investigated both in solution and in solid state. The protective shell of five bulky substituents should be definitely large enough to suppress the polymerization of the triangulene core in deaerated solution, and possibly could also prevent reaction with oxygen.

3.2.2 NUCLEOPHILIC ADDITIONS ON HEPTAAUTHRENE CORE

Inspired by this beautiful and unexpected chemistry of triangulene, we decided to look deeper into the additions on extended π -aromatic systems. One compound that was of interest for us next was 1,14:11,12-dibenzopentacene (Figure 3.4, far right), commonly known as heptaauthrene. Similarly, to triangulene (Figure 3.3, middle), heptaauthrene is a non-Kekulé hydrocarbon and it can be regarded as a structure, where two phenalenyl radicals are fused together via spacer, with a predicted triplet ground state. The first attempt for the synthesis of heptaauthrene was by Clar in 1950's, however, the as-formed molecule quickly polymerized due to its open-shell character.^[140] Latest breakthrough was done by Wu *et*

al.^[163], who were able to synthesize and characterize kinetically persistent derivative of heptaauthrene **67** (Scheme 3.18), bearing two mesitylene groups. Wu *et al.*^[163] was able to measure a low temperature EPR spectrum and he proved that this compound has a triplet ground state.

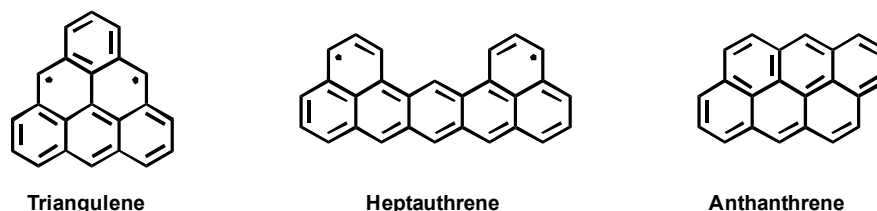
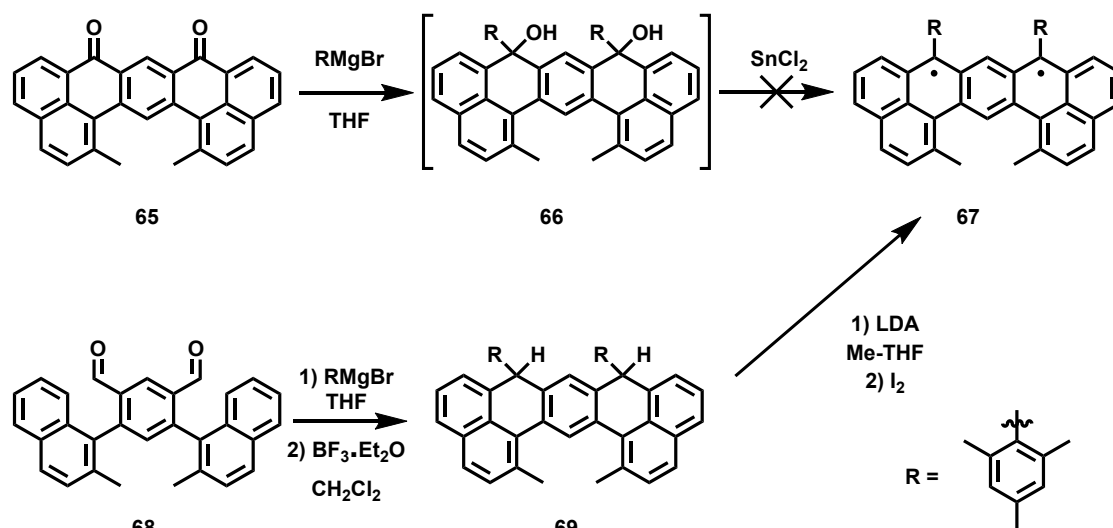


Figure 3.3: Extended π -aromatic systems discussed in this chapter.

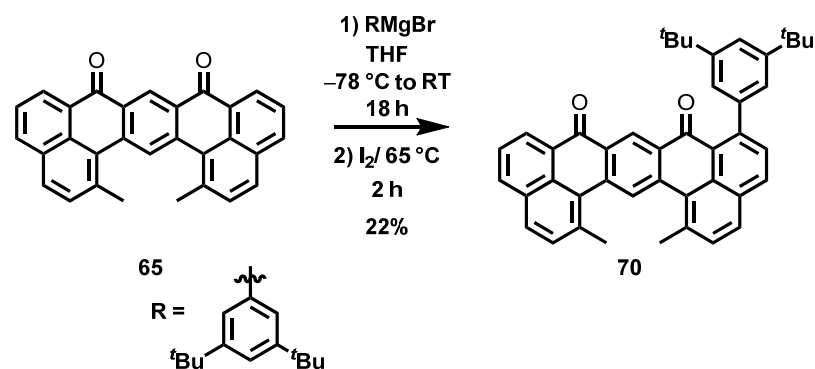
Synthesis of a persistent derivative of heptaauthrene is a significant breakthrough, but the reason this paper caught our attention was the synthetic approach for the preparation of this molecule. The original synthetic proposal of Wu *et al.*^[163] was based on nucleophilic additions of mesitylene magnesium bromide to the keto groups of diketohexaauthrene **65** (Scheme 3.18, top). Similarly to our synthetic attempt to introduce more than two equivalents of the Grignard reagent to diketotriangulene **48**, Wu *et al.*^[163] obtained a complicated mixture of high-polarity products and no desired product. They justified such an observation by the instability of the diradical at room temperature. However, we think that the reason for this is similar as in the case of diketotriangulene, namely, that the addition is not proceeding in a 1,2-fashion, but in a 1,4-fashion. In the end, Wu *et al.*^[163] was able to synthesize the heptaauthrene derivative **67** in a different way. The starting dialdehyde **68** was first substituted by a nucleophile and subsequently closed by the Friedel–Crafts acylation. The desired diradical was then prepared by deprotonation and subsequent oxidation (Scheme 3.18).



Scheme 3.18: Synthesis of the kinetically persistent heptaauthrene **67**.

To prove our theory, we decided to investigate in which fashion the nucleophilic addition proceeds on the diketoheptaauthrene **65**. The diketoheptaauthrene **65** was prepared in five steps according to the literature procedure.^[163] The solubility of this orange compound is very limited in organic solvents. As a nucleophile of choice, we again chose the di-*tert*-butylphenyl magnesium bromide, as it can be easily prepared, it improves solubility, and can be easily characterized.

One equivalent of the Grignard reagent was added to the THF solution of diketoheptaauthrene **65** at low temperature (Scheme 3.19). The progress of the reaction was monitored by TLC and MALDI-TOF MS. A formation of a new polar spot was observed, and the observed mass was corresponding to the product of monoaddition. Even though the starting material was not fully consumed, the reaction was quenched by a small amount of water, followed by iodine to oxidize the enolate intermediate. After aqueous work-up, the crude mixture was purified by column chromatography. To our delight, only single product was isolated, which was identified as a product of Michael 1,4-addition **70**. Even though the yield of the reaction was low, only 22%, the rest of the material corresponds to the unreacted starting material, which was recovered. The low yield was most probably caused by the poor solubility of the starting material.



Scheme 3.19: Addition of one equivalent of the Grignard reagent to the diketoheptaauthrene **65**.

To rationalize this observation, we draw our attention once again to the Hückel molecular orbital (HMO) calculations (Figure 3.4, bottom). The LUMO of the diketoheptaauthrene is mostly localized at the naphthalene cores and the contribution of the carbonyl antibonding π -molecular orbital is relatively small. The larger number of naphthalene carbon atoms that contribute to the LUMO explains the formation of the complex mixtures that were observed by Wu *et al.*^[163] Similarly, as in case of diketotriangulenes, the HMO suggests, that one equivalent of the Grignard reagent should add to diketoheptaauthrene in a Michael 1,4-addition fashion at the *ortho*-position with respect to the carbonyl group.

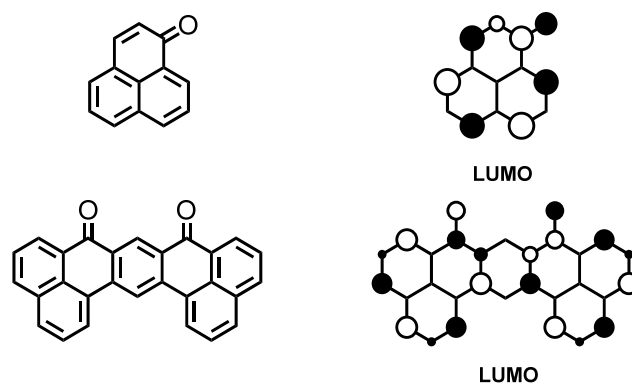
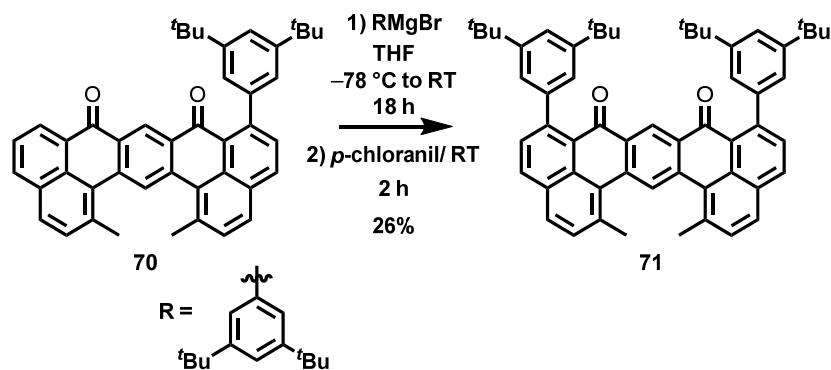


Figure 3.4: LUMO of phenalenone (top) and LUMO of diketoheptaauthrene (bottom).

Diketoheptaauthrene contains two phenalenyl (Figure 3.4, top) units fused together via spacer. Phenalenone is a keto derivative of phenalenyl and since its first discovery in 1940's,^[164] it plays a fundamental role in phenalenyl chemistry. In 1950's, Koelsch *et al.*^[165]

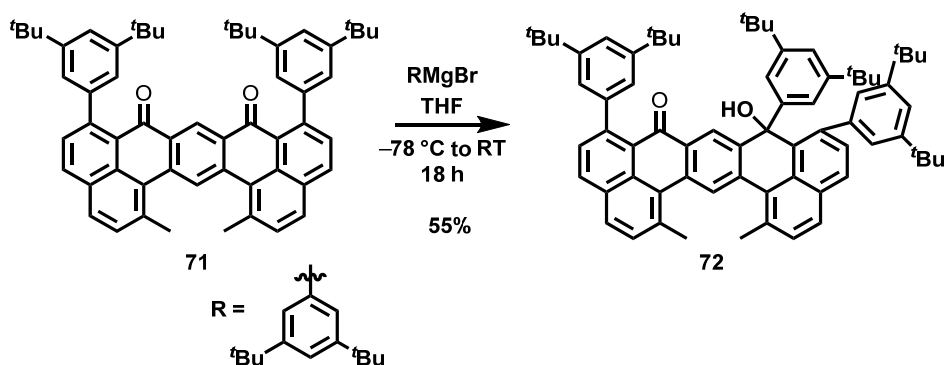
found out that phenalenone reacts with nucleophiles exclusively in Michael 1,4-fashion with respect to the carbonyl group. This observation is widely used in natural product synthesis. [166–168] If we have a look at the LUMO of phenalenone, the situation is very similar to the situation in diketoheptaauthrene. The LUMO of the phenalenone is mostly localized at the naphthalene core and the contribution of the carbonyl antibonding π -molecular orbital is small. Therefore, a Michael 1,4-addition is expected. As diketoheptaauthrene contains two phenalenone units, 1,4-addition is expected for both first and second addition.

Indeed, when one equivalent of the Grignard reagent was added to the monosubstituted diketoheptaauthrene **70** at low temperature, formation of one single product was observed. After work-up and column chromatography, the product of Michael 1,4-addition **71** was isolated as a yellow compound (Scheme 3.20). The yield of the reaction is not great, and again this can be explained by poor solubility of the starting material. All the unreacted starting material was recovered.



Scheme 3.20: Addition of one equivalent of the Grignard reagent to the diketoutherene **70**.

With two substituents successfully installed in predicted positions, we decided to add the third substituent. This time, however, we used a large excess of the Grignard reagent (Scheme 3.21).



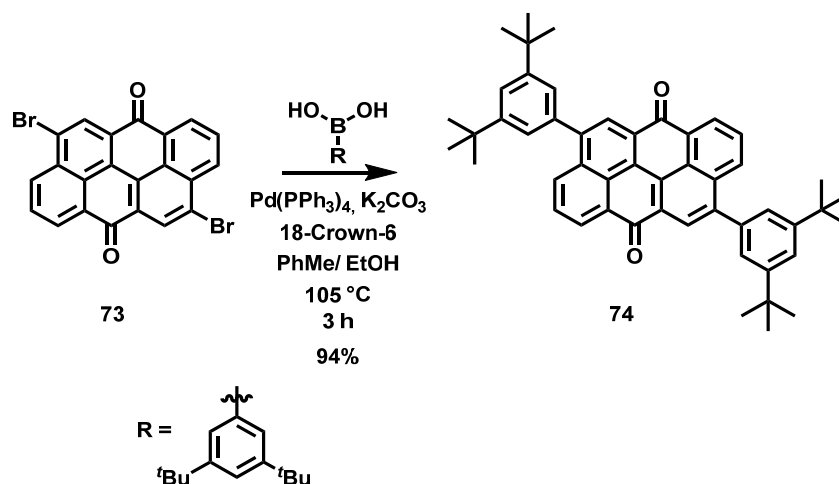
Scheme 3.21: Addition of the Grignard reagent to the diketoheptaauthrene **71**.

The TLC and MALDI-TOF MS analysis revealed formation of a single new compound. Once the starting material was fully consumed, the reaction was quenched. After aqueous work-up, the crude was purified by column chromatography. A single compound with mass of two extra protons to what would be expected was isolated in a good yield. The structure of the isolated compound was determined by 2D NMR spectroscopy and, to our surprise, it corresponded to the product of 1,2-addition. We have no explanation, why the addition of the third substituent followed the 1,2-addition pattern. From the LUMO of diketoheptaauthrene, we can only say that it is partially localized at the carbonyl group and the concentration of LUMO on keto groups is significantly larger compared to diketotriangulenes. A driving force for this 1,2-addition could be preservation of the aromaticity of the naphthalene ring, that would be otherwise lost in the case of Michael 1,4-addition. To fully understand what is happening in this system, further calculations are required.

3.2.3 NUCLEOPHILIC ADDITIONS ON ANTHANTHRENE CORE

Another compound in which we were interested in was anthanthrene (Figure 3.3, left) as it is an isomer of triangulene. Compared to heptauthrene and triangulene, which both belong to the group of non-Kekulé hydrocarbons, anthanthrene is a Kekulé hydrocarbon. For their semiconducting properties, the derivatives of anthanthrene are very attractive for specific applications such as light-emitting diodes^[169], solar cells^[170] and field-effect transistors^[171].

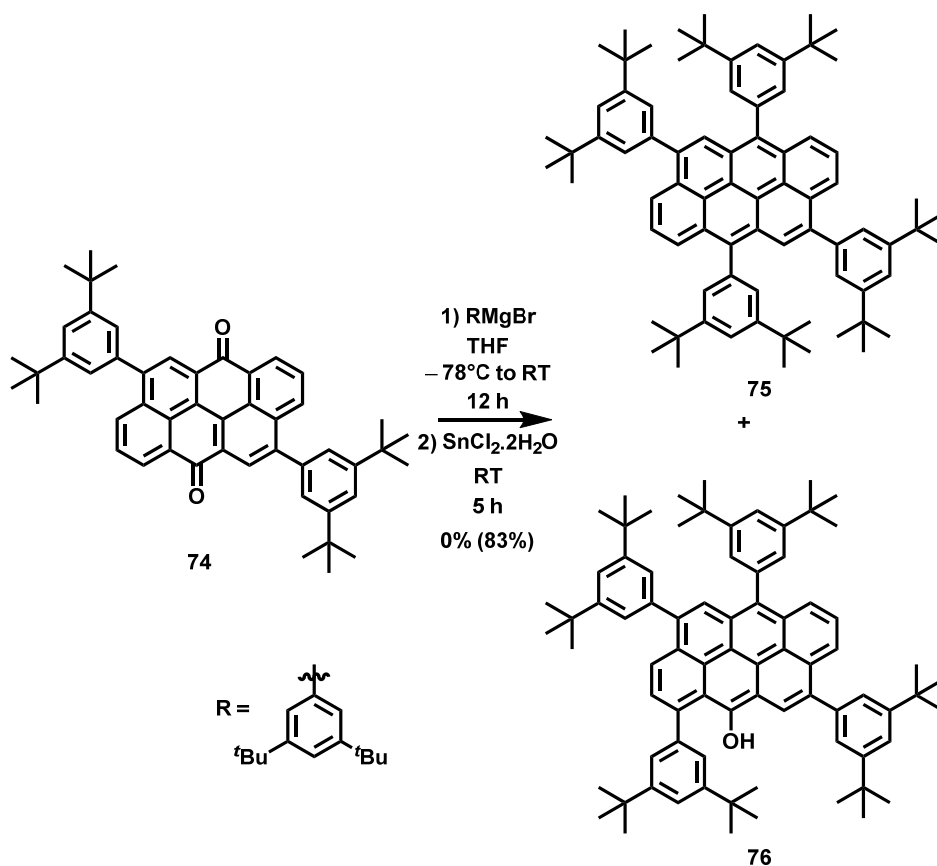
Anthanthrone (Figure 3.4), is a diketo derivative of anthanthrene. As anthanthrone is very poorly soluble in organic solvents, the compound needs to be functionalized to improve the solubility. As an ideal candidate for such functionalization is commercially available dibromo anthanthrone, commonly known as VAT Orange 3. The presence of the two bromines suggests that the solubilizing group could be introduced by means of Suzuki coupling.



Scheme 3.22: Introduction of solubilizing groups to dibromoanthanthrone 73.

Dibromoanthanthrone was therefore reacted with di-*tert*-butyl phenyl boronic acid in toluene/EtOH in the presence of Pd(PPh₃)₄ and base (Scheme 3.22). We decided to use the di-*tert*-butylphenyl solubilizing group as we knew it will significantly enhance the solubility and, moreover, the corresponding boronic acid is widely available in our group. Once the starting material was fully consumed, the reaction was quenched. After aqueous work-up,

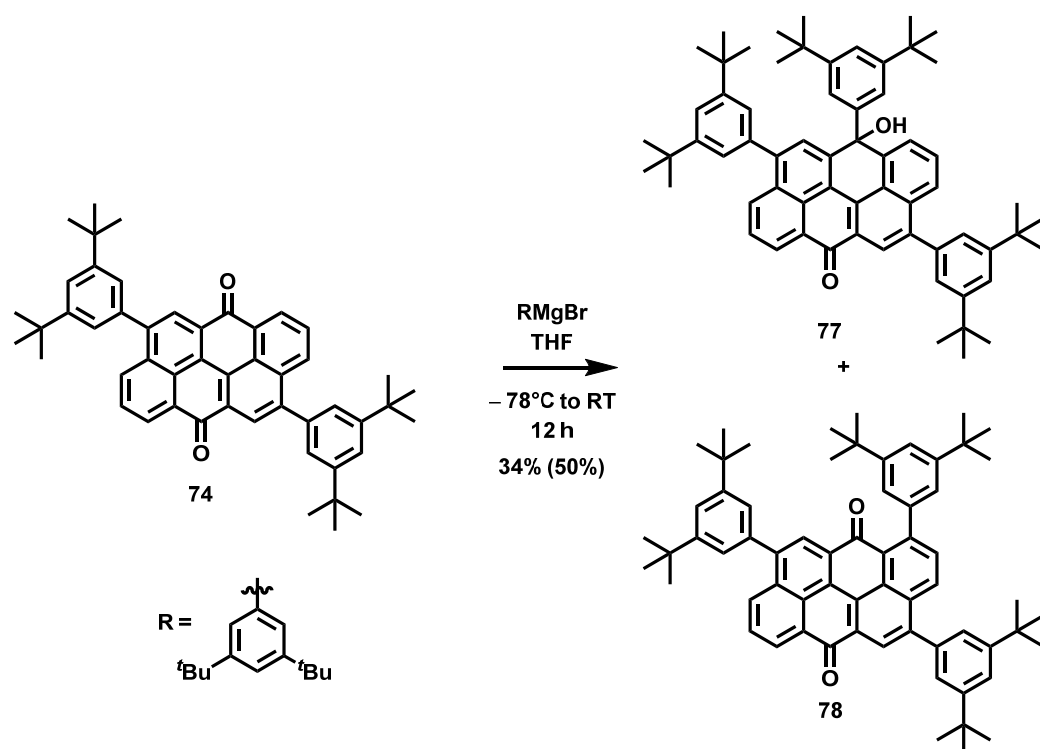
the crude was purified by column chromatography and the desired product **74** was isolated as a red solid. The introduction of the bulky groups significantly increased the solubility of the parent compound, and the functionalized compound **74** is reasonably soluble in most organic solvents.



Scheme 3.23: Addition of the excess of nucleophile to anthanthrone **74**.

As we were not expecting any surprise reactions, we decided to use directly an excess of the nucleophilic agent, in this case Grignard reagent. The starting material was consumed within several hours, and TLC revealed formation of one new spot. To remove the hydroxy groups from the intermediate, we added SnCl₂. After aqueous work-up, the crude mixture was purified by column chromatography. A single compound was isolated, however, the mass did not fit to the desired compound **75**, but the mass corresponded to M+16. 2D NMR analysis revealed that the isolated compound is **76** and not **75**.

To understand what is happening in this system, we once again tested the addition of single equivalent of Grignard reagent (Scheme 3.24).



Scheme 3.24: Addition of one equivalent of Grignard reagent to anthanthrone **74**.

Upon the addition of one equivalent of the Grignard reagent in THF at low temperature, we observed formation of two new spots with R_f values very close to each other. However, one of the spots changed colour to red upon exposure to the ambient atmosphere. This observation suggested that part of the Grignard reagent reacted in 1,2-addition (spot that remained yellow) fashion and that the other part reacted in Michael 1,4-addition fashion. After aqueous work-up and column chromatography, indeed two compounds corresponding to the 1,2-addition product **77** a product of 1,4-addition were isolated. The product of Michael addition was isolated in a higher yield.

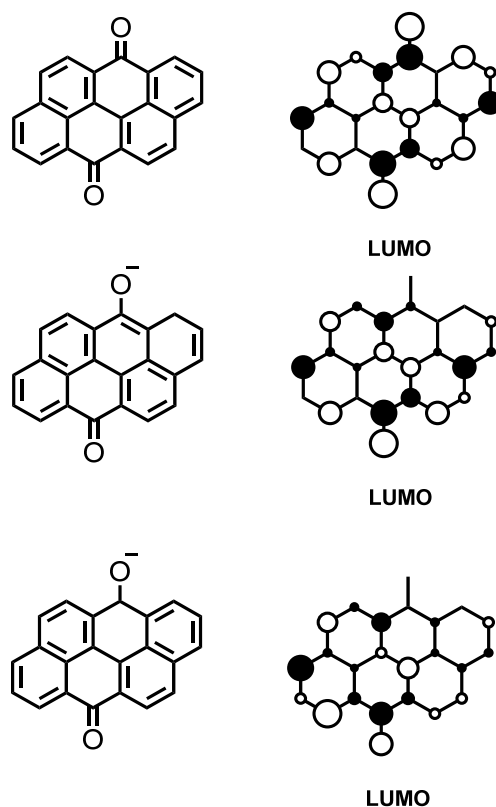
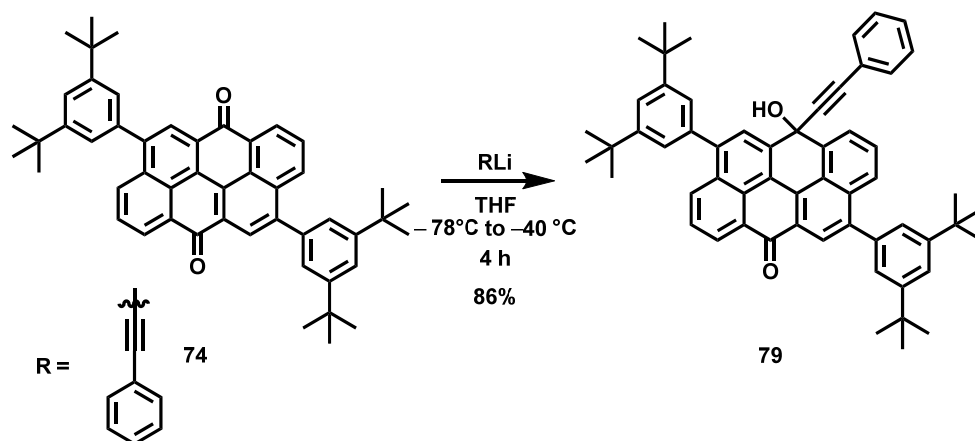


Figure 3.4: Anthanthrone and its LUMO and LUMO of its corresponding enolate and alkoxide.

In this case, the explanation by using LUMO is not so straightforward. According to the Hückel molecular orbital (HMO) calculations, the largest coefficient of LUMO in anthanthrone (Figure 3.4, top) is located at the carbonyl positions, however, the contribution of the naphthalene positions is also significant. Therefore, the addition of single equivalent of the Grignard reagent proceeds at both positions. By the addition of the second equivalent, the reaction follows the pattern of the LUMO of the corresponding anion. When the first equivalent is added in the Michael fashion, the second equivalent then follows LUMO of the enolate (Figure 3.4, middle). As the largest coefficient is located at the carbonyl group, the nucleophilic attack occurs at the carbonyl. When the first equivalent attacks the carbonyl first, then the reaction with second equivalent follows the LUMO of the alkoxide (Figure 3.4, bottom). In this case, the largest coefficient is located at the naphthalene core. This nicely explain the formation of the compound **76**, if an excess of the nucleophile is used. As

di-*tert*-butylphenyl is a large substituent, the sterical hindrance most probably also plays a significant role.

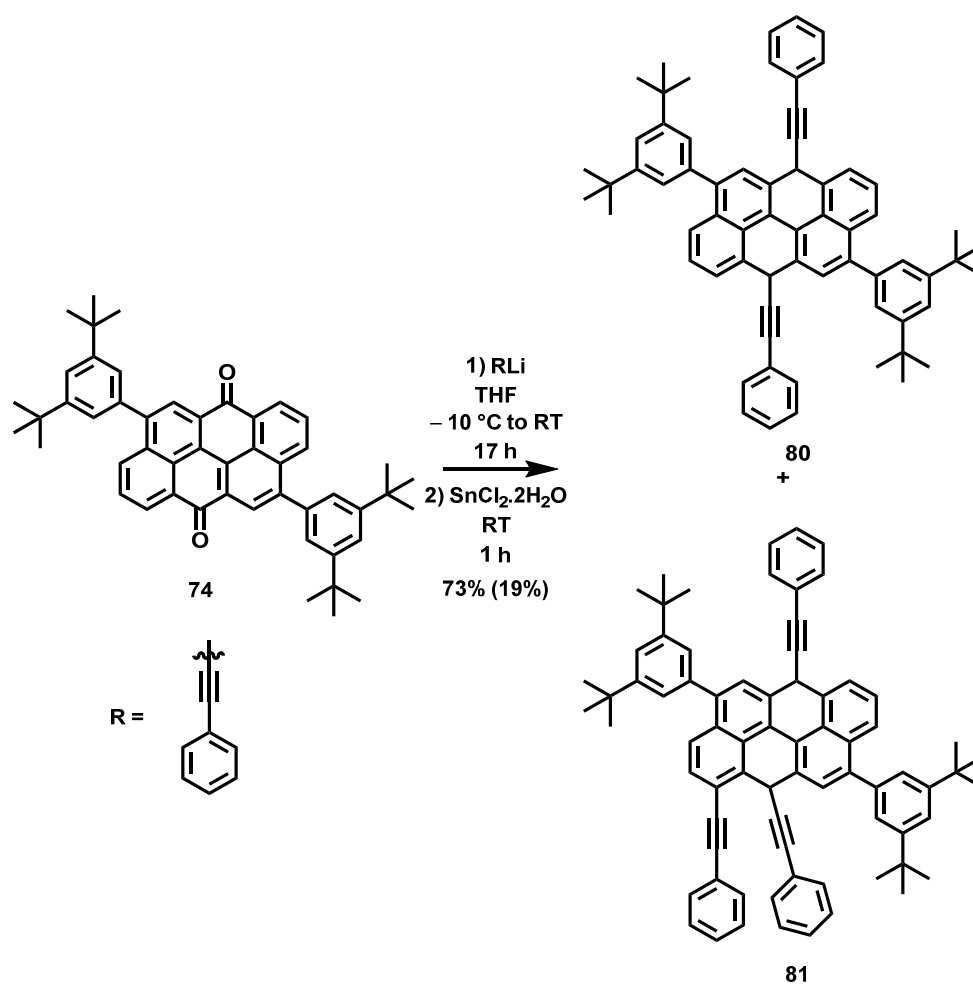
To understand which role plays the factor of sterical hindrance, we decided to add a substituent which is smaller and more compact, such as phenylethynyl. First, we added one equivalent of the lithium salt to the anthanthrone **74** at low temperature (Scheme 3.25). We observed a formation of single new yellow spot, that remained yellow even after exposure to the ambient atmosphere. From our previous experience, we were expecting the addition in 1,2-fashion. After work-up and column chromatography, a product of 1,2-addition was indeed isolated in a very good 86% yield (partial decomposition on the column).



Scheme 3.25: Addition of one equivalent of lithium salt to anthanthrone **74**.

With this result, we moved to addition of two equivalents of lithium salt to anthanthrone **74** (Scheme 3.26). In this case, TLC revealed formation of two new spots. From MALDI-TOF MS analysis, we found that the desired product of double-fold 1,2-addition was formed and the second spot corresponded to the trisubstituted derivative. After purification, we were able to isolate both compounds and, indeed, the 2D NMR structure analysis confirmed the formation of two products **80** and **81**. The formation of the trisubstituted derivative **81** can be explained simply by the fact that we used commercial lithium salt without titration, therefore, the lithium salt could have a higher concentration.

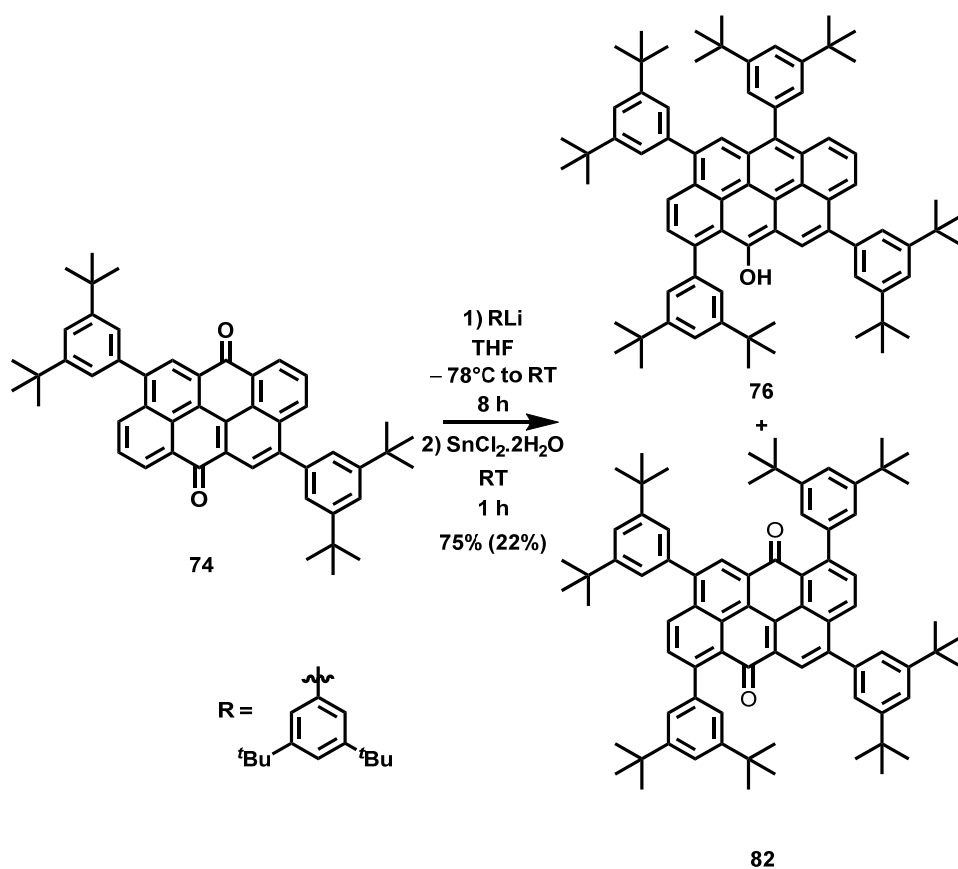
This experiment, however, represents a significant prove that steric hindrance plays an important role in additions to the anthanthrone. Another factor which we considered was the “hardness” of the nucleophile. Both Grignard reagent and lithium salt are considered as hard nucleophiles, phenylethynyl lithium is, however, a harder nucleophile compared to the *tert*-butylphenylmagnesium bromid, due to higher polarisation between C–Li bond, compared to C–Mg bond.



Scheme 3.26: Addition of two equivalents of lithium salt to anthanthrone 74.

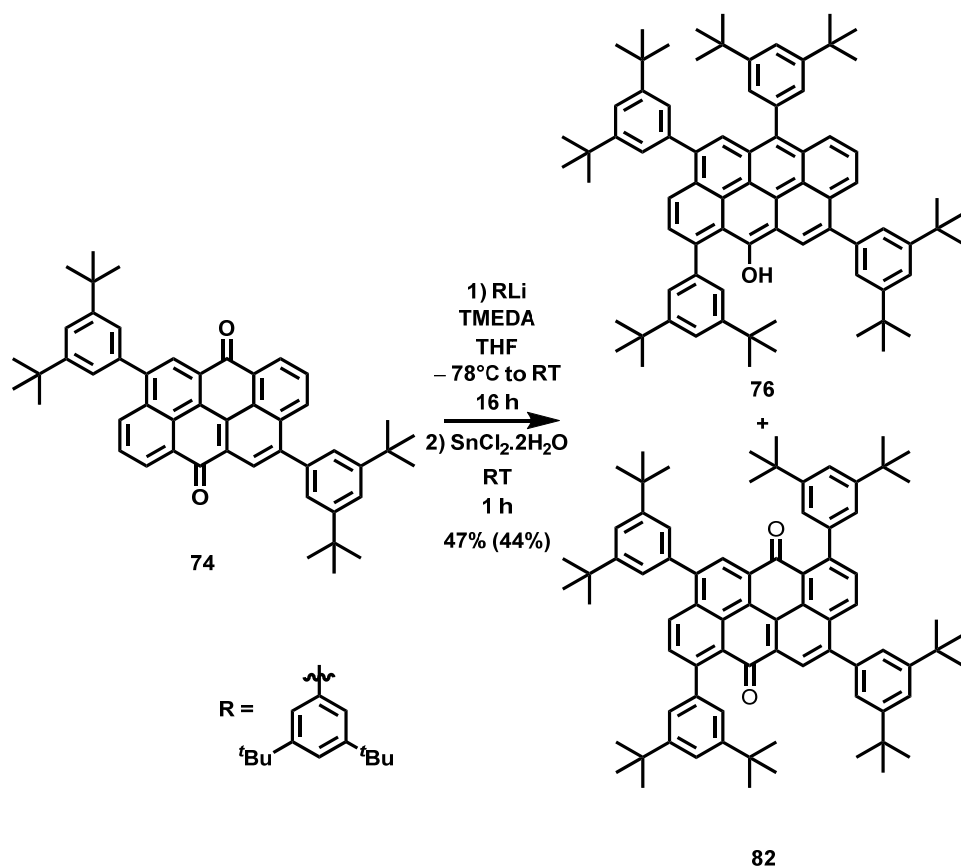
We performed two more experiments with harder nucleophiles, to gain more insight into the addition behaviour of anthanthrone 74. The first nucleophile was a lithium salt of di-*tert*-

butylphenyl, which was added at low temperature to anthanthrone **74**. TLC analysis revealed a formation of two spots, one that corresponds to anthanthrone **76** and one new one.



Scheme 3.27: Addition of lithium salt to anthanthrone **74**.

The new spot changed its colour, once it was exposed to the air atmosphere. This behaviour suggested formation of the Michael product. Once the reaction was completed, we isolated both compounds. The major product corresponded to anthanthrone **76** and the minor product indeed corresponded to the product of double-fold Michael addition **82** (Scheme 3.27). Such a result was completely unexpected. Here we can only speculate, why something like this happened. We think that, if the first addition occurs on the carbonyl, the second addition simply follows the LUMO of its anion. But when the first addition proceeds in a Michael fashion, the second addition follows its LUMO, where the coefficients are almost identical, and a simple statistical reaction is observed.



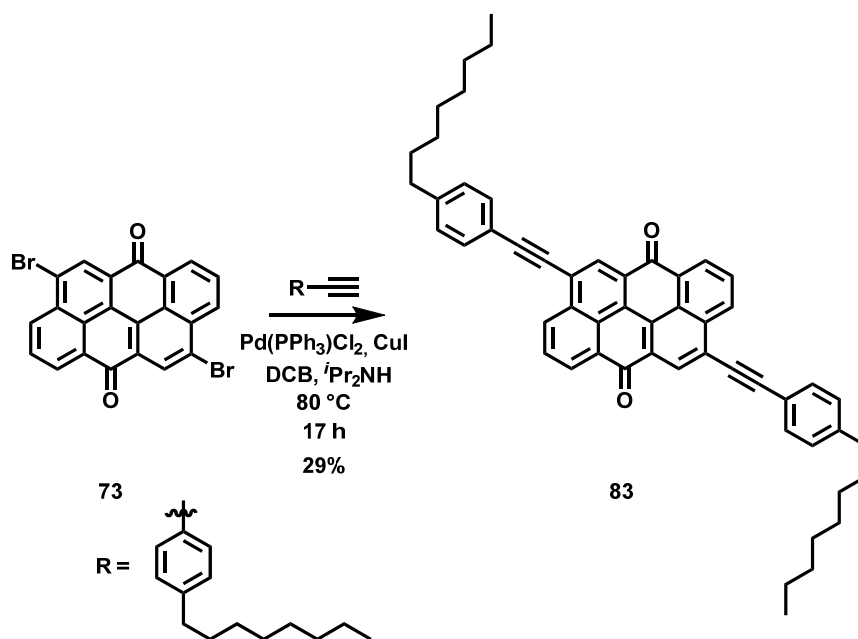
Scheme 3.28: Addition of lithium salt to anthanthrone **74** in the presence of TMEDA.

The next experiment also implemented an organolithium salt, however, this time TMEDA was used as an additive to coordinate to the monomeric phenyllithium salt and improve its nucleophilicity (Scheme 3.28).^[172]

In this case (Scheme 3.28), even larger amount of double-fold Michael product **82** was isolated and the ratio of the two products was almost 1:1. It is possible that the double-fold Michael product **82** is formed on account of lower steric hindrance in the molecule. However, for such a conclusion, we need more data and more advanced calculations.

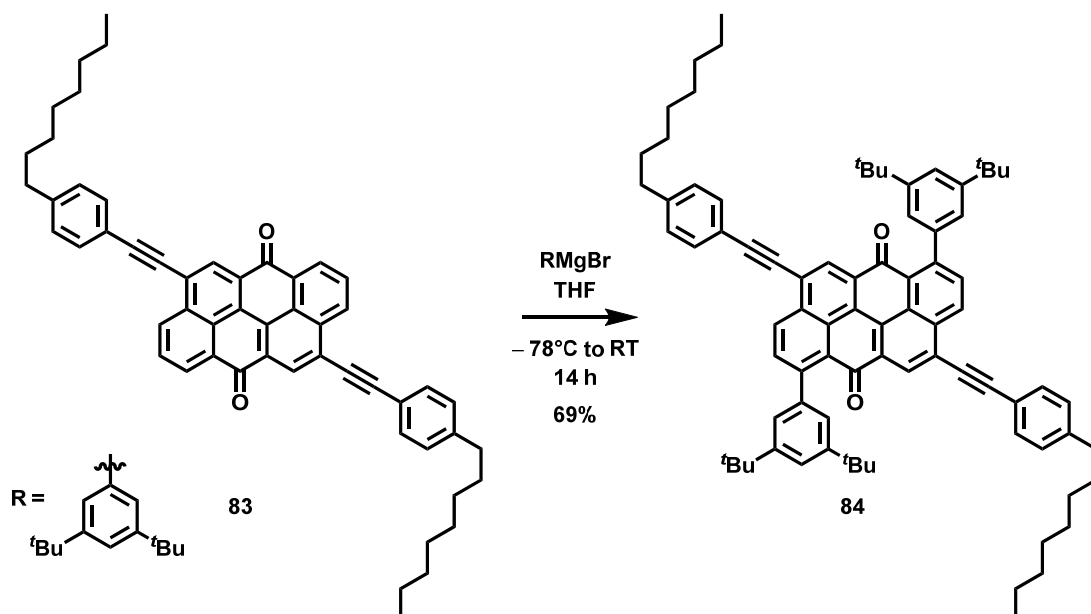
Last three experiments were conducted with the objective to verify our theory, that steric hindrance is the primary cause for such unpredictable behavior of anthanthrone. We, therefore, switched the solubilizing group for less sterically demanding one. For this purpose, we used a phenylethynyl group bearing a long aliphatic side chain. The solubilizing

group was introduced by terms of Sonogashira cross coupling (Scheme 3.29) on dibromoanthanthrone utilizing standard coupling conditions. The disubstituted compound was isolated in a relatively low yield, but high purity. The obtained yield is, however, comparable for similar Sonogashira couplings on this system.



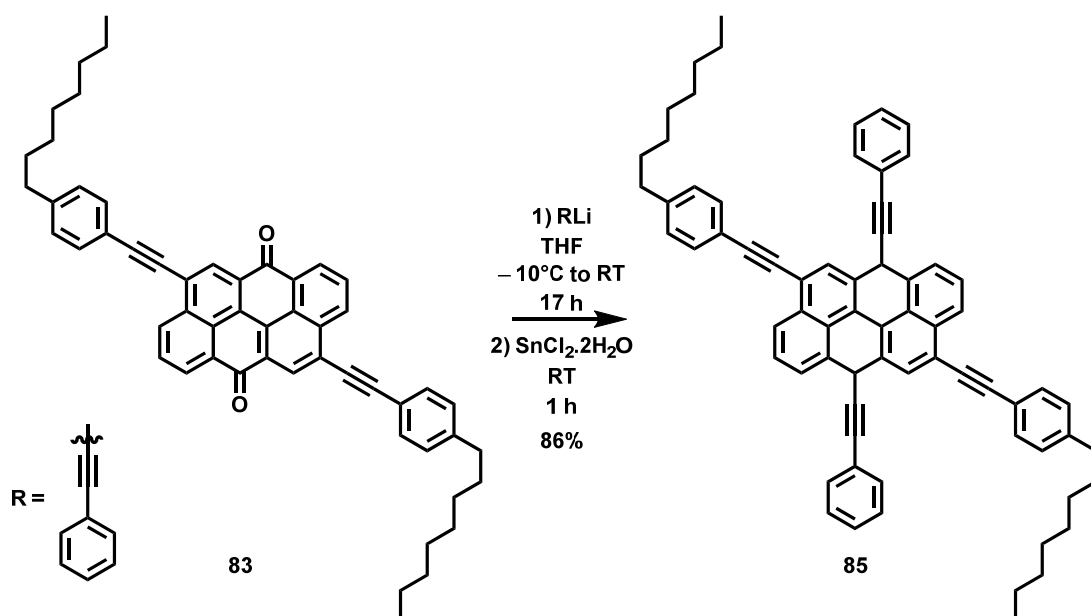
Scheme 3.29: Introduction of solubilizing groups to dibromoanthanthrone **73**.

Once we introduced the new solubilizing groups, we proceeded with the additions. Again, we used the di-*tert*-butylphenyl magnesium bromide as a nucleophile. The Grignard reagent was added at low temperature to the THF solution of **83**. Formation of two new spots was observed. Both yellow, but one of them was changing colour upon air atmosphere. This again suggested the formation of Michael addition product. After work-up and column chromatography, the two new spots were isolated. The minor product could not be identified as it did not give any signal in the 1H NMR spectrum. The second product was, however, identified as a product of double-fold Michael addition. Therefore, it is possible that the new solubilizing group is still too sterically demanding. In order to verify this, however, more data are needed.



Scheme 2.30: Addition of the excess of the nucleophile to anthanthrone **74**.

Last experiment, which we performed, was a control experiment with compact phenylethynyl substituent.



Scheme 3.31: Addition of two equivalents of lithium salt to anthanthrone **83**.

Similarly as in the previous case when compound **80** was formed, we observed only formation of double-fold 1,2-addition product **85** (Scheme 3.31).

3.3 CONCLUSION & OUTLOOK

In summary, we explored the possibility to protect the precious triangulene core by introducing bulky substituents at the specific positions to create a protective shell. Even though our original goal failed, we discovered the unexpected beauty of triangulene chemistry. We developed a novel methodology how five substituents can be successfully installed around triangulene core in a highly regioselective fashion, by means of nucleophilic aromatic substitutions and direct C_{sp2}-H activation. Nucleophilic aromatic substitutions on diketotriangulene do not proceed in expected 1,2-fashion, but rather in Michael 1,4-fashion. This chemistry allowed us to install bulky substituents at the α -positions of triangulene and to construct a more advanced protective shell around triangular core.

This unexpected behaviour inspired us to explore the addition pattern in other extended π -aromatic systems, such as heptauthrene and anthanthrone. Both these aromatic compounds react with the nucleophiles in an unexpected fashion. Especially in the case of anthanthrone, the chemistry is unpredictable. Our findings need to be supported by more advanced theoretical calculations and once we fully understand these systems, our findings will be published.

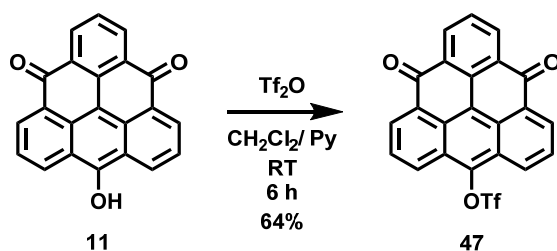
3.4 EXPERIMENTAL SECTION

3.4.1 GENERAL REMARKS

All chemicals and solvents were purchased from commercial sources and used without further purification unless stated otherwise. The reactions and experiments that are sensitive to oxygen were performed using Schlenk techniques and argon-saturated solvents. The solvents were saturated with argon by either passing argon gas through the solvent or using the freeze-pump-thaw technique in three cycles. All reactions were monitored by either thin-layer chromatography, GC-MS, LC-MS or MALDI-TOF MS. Yields refer to purified and spectroscopically pure (^1H NMR) compounds unless the crude product was used in the next step. For column chromatography, either silica gel Silicaflash[®] p60 (40 – 60 μm) from Silicycle or Alumina, activated (basic Brockmann Activity I) or neutral was used in dot was purchased from Fluka. The thin-layer chromatography was performed using silica-gel plates Silica Gel 60 F254 (0.2 mm thickness), purchased from Merck and visualized under a UV lamp (254 or 365). The NMR experiments were performed on Bruker Avance III NMR spectrometers operating at 400, 500, or 600 MHz proton frequencies. The instruments were equipped with a direct-observe 5 mm BBFO smart probe (400 and 600 MHz), an indirect-detection 5 mm BBI probe (500 MHz), or a five-channel cryogenic 5 mm QCI probe (600 MHz). All probes were equipped with actively shielded z -gradients (10 A). The experiments were performed at 295 or 298 K unless indicated otherwise and the temperatures were calibrated using a methanol standard showing accuracy within ± 0.2 K. Standard Bruker pulse sequences were used, and the data was processed on Topspin 3.2 (Bruker) using two-fold zero-filling in the indirect dimension for all 2D experiments. Chemical shifts (δ) are reported in parts per million (ppm) relative to the solvent residual peak. ^1H NMR titrations were performed by adding small amounts of dihydro triangulene **12** to a solution ExBox⁴⁺ in CD_3CN . Significant upfield shifts of ^1H resonances for c protons were observed to

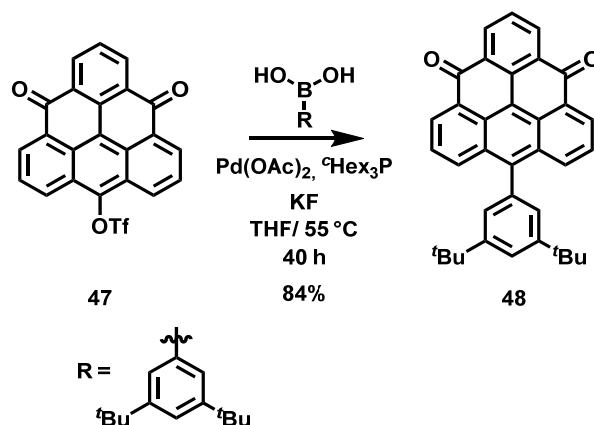
determine the association constant (K_a). The K_a values were calculated using Dynafit,^[P] a program which employs nonlinear least-squares regression on ligand–receptor binding data. The low-resolution mass spectra were recorded either on Bruker amaZon™ X for Electro Spray Ionization (ESI), on a Shimadzu GSMS-QP2010 SE gas chromatography system with ZB-5HT inferno column (30 mm x 0.25 mm x 0.25 mm) at 1 ml/ min He-flow rate (split = 20:1) with a Shimadzu electron ionization (EI 70 eV) mass detector, or Bruker microflex system for MALDI-TOF. High-resolution mass spectra (HRMS) were measured as HR-ESI-ToF-MS with a Maxis 4G instrument from Bruker with the addition of NaOAc. Data collections for the crystal structures were performed at low temperatures (123 K) using CuK α radiation on a Bruker APEX II diffractometer. Integration of the frames and data reduction was carried out using the APEX2 software. The structures were solved by the charge-flipping method using Superflip. All non-hydrogen atoms were refined anisotropically by full-matrix least-squares on F using CRYSTALS. Both structures were analyzed using Mercury.

3.4.2 EXPERIMENTAL PROCEDURES

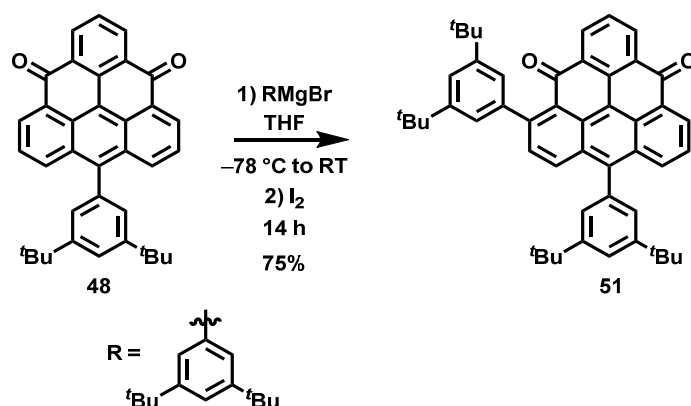


8,12-Dioxo-8,12-dihydrodibenzo[cd,mn]pyren-4-yl trifluoromethanesulfonate (**47**).

The solution 12-hydroxydibenzo[cd,mn]pyrene-4,8-dione (**11**, 500 mg, 1.55 mmol) was sonicated in dry pyridine (5mL) for 5 minutes under an argon atmosphere. Then dry CH₂Cl₂ was added, followed by dropwise addition of Tf₂O (312 μL, 1.86 mmol) under an argon atmosphere. The reaction mixture was then stirred for 6 h at room temperature before solvents were evaporated under reduced pressure. The residue was then purified by column chromatography over silica gel using CH₂Cl₂ then CH₂Cl₂/MeOH 50:1 as an eluent to afford the desired product (**47**, 449 mg, 64%) as a deep-red solid. ¹H NMR (400 MHz, CD₂Cl₂, ppm): δ 8.92 (dd, *J* = 7.1, 0.8 Hz, 2H), 8.75 (d, *J* = 7.7 Hz, 2H), 8.68 (dd, *J* = 8.7, 0.8 Hz, 2H), 8.04 (dd, *J* = 8.7, 7.2 Hz, 2H), 7.83 (t, *J* = 7.7 Hz, 1H). ¹⁹F NMR (376.5 MHz, CDCl₃, ppm): δ = -72.35. ¹³C NMR (150 MHz, CD₂Cl₂, ppm): Strong aggregation of **47** did not allow us to record an unequivocal ¹³C NMR spectrum of monomeric **47**. HRMS (EI) MS: *m/z* [*M*]⁺ calcd for C₂₃H₉O₅F₃S⁺: 454.01173; found 454.01250 (|Δ| = 1.71 ppm).

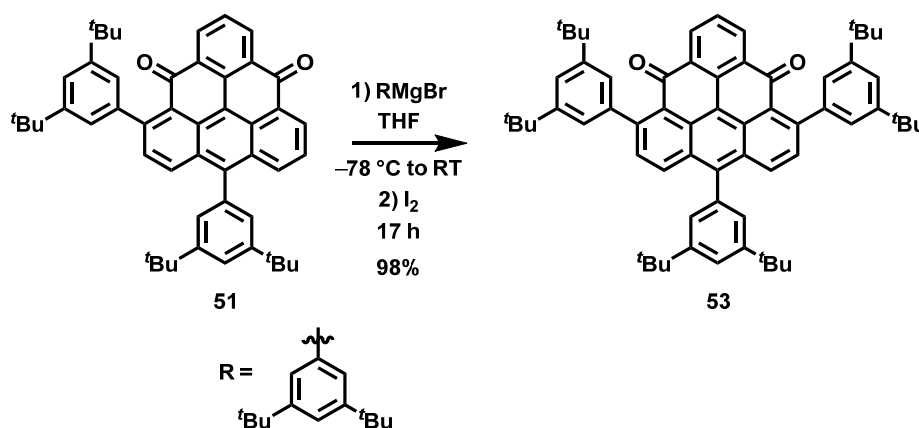


12-(3,5-Di-tert-butylphenyl)dibenzo[cd,mn]pyrene-4,8-dione (48). A solution of ^cHex₃P (15.3 mg, 0.11 mmol) in freshly argon bubbled dry THF (1 mL) was added to the solution of 8,12-dioxo-8,12-dihydrodibenzo[cd,mn]pyren-4-yl trifluoromethanesulfonate (**47**, 380 mg, 0.84 mmol), (3,5-Di-tert-butylphenyl)boronic acid (246 mg, 1.05 mmol), Pd(OAc)₂ (20.7 mg, 0.09 mmol) and anhydrous KF (161 mg, 2.77 mmol) in freshly argon bubbled dry THF (6 mL) under an argon atmosphere. The reaction vessel was then closed properly, and the mixture was heated at 55 °C for 40 h. Then few drops of water and solid Na₂CO₃ (25 mg) was added and the mixture was heated at 70 °C under air for 1 h to hydrolyse the unreacted triflate. Afterwards the solvents were evaporated under reduced pressure and the residue was then purified by column chromatography over silica gel using CH₂Cl₂ then CH₂Cl₂/MeOH 40:1 as an eluent to afford the desired product (**48**, 350 mg, 84%) as a deep-red solid. ¹H NMR (500 MHz, CD₂Cl₂, ppm): δ 8.82 (dd, *J* = 7.0, 1.2 Hz, 2H), 8.64 (d, *J* = 7.6 Hz, 2H), 8.21 (dd, *J* = 8.6, 1.2 Hz, 2H), 7.73 (dd, *J* = 8.6, 7.0 Hz, 2H), 7.71 (t, *J* = 1.9 Hz, 1H), 7.65 (t, *J* = 7.7 Hz, 1H), 7.43 (d, *J* = 1.9 Hz, 2H), 1.45 (s, 18H). ¹³C NMR (101 MHz, CD₂Cl₂, ppm): δ 182.9, 151.3, 146.5, 136.3, 136.2, 135.7, 133.1, 132.9, 130.8, 130.4, 128.8, 128.1, 126.9, 126.5, 126.2, 122.7, 115.9, 35.4, 31.71. HRMS (APCI): *m/z*: [*M* + H]⁺ calcd for C₃₆H₃₁O₂⁺: 495.23186; found 495.23114 (|Δ| = 1.45 ppm).

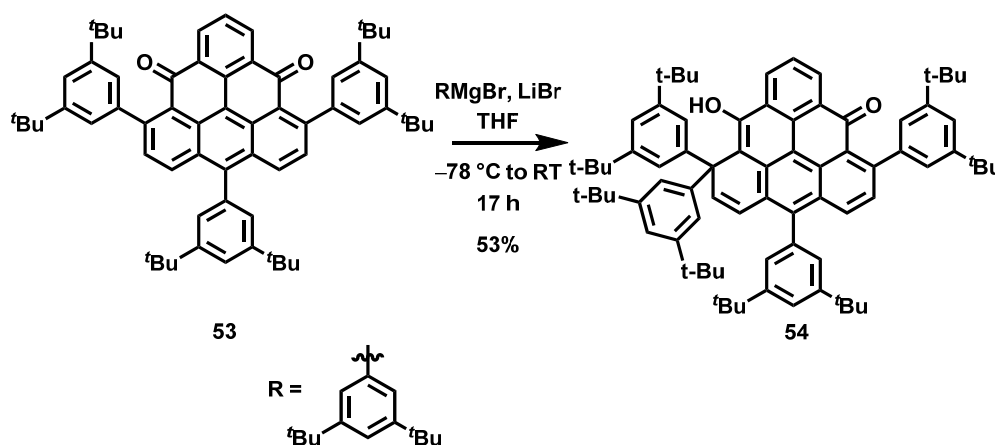


3,12-Bis(3,5-di-tert-butylphenyl)dibenzo[cd,mn]pyrene-4,8-dione (51). A solution of (3,5-di-tert-butylphenyl)magnesium bromide (2.47 ml, 0.81 mmol, 0.33 M solution in THF)

was added dropwise to the cooled ($-78\text{ }^{\circ}\text{C}$) solution of 12-(3,5-Di-tert-butylphenyl)dibenzo[cd,mn]pyrene-4,8-dione (**48**, 400 mg, 0.81 mmol) in dry THF under an argon atmosphere. The reaction mixture was stirred at $-78\text{ }^{\circ}\text{C}$ for 2 h before it was allowed to warm to room temperature over 12 h. Then iodine (123 mg, 0.49 mmol) was added and the reaction mixture was heated under air at $65\text{ }^{\circ}\text{C}$ for 2 h before 2 M NaOH (10 mL) was added and the mixture was extracted with CH_2Cl_2 (3x 10 ml). The combined organic layers were washed with water, brine, dried over anhydrous Na_2SO_4 , and filtered. After evaporation of the solvents, the residue was then purified by column chromatography over silica gel using cyclohexane/EtOAc 20:1 then cyclohexane/EtOAc 5:1 as an eluent to afford the desired product (**51**, 417 mg, 75%) as a deep-red solid. ^1H NMR (500 MHz, CD_2Cl_2 , ppm): δ 8.92 (dd, $J = 7.0, 1.3$ Hz, 1H), 8.73 (dd, $J = 7.6, 1.5$ Hz, 1H), 8.59 (dd, $J = 7.7, 1.5$ Hz, 1H), 8.24 (dd, $J = 8.6, 1.3$ Hz, 1H), 8.16 (d, $J = 8.9$ Hz, 1H), 7.77 (dd, $J = 8.5, 7.0$ Hz, 1H), 7.71 (t, $J = 7.6$ Hz, 1H), 7.71 (t, $J = 1.8$ Hz, 1H), 7.58 (d, $J = 8.8$ Hz, 1H), 7.53 (t, $J = 1.8$ Hz, 1H), 7.42 (d, $J = 1.8$ Hz, 2H), 7.35 (d, $J = 1.7$ Hz, 2H), 1.43 (s, 18H), 1.40 (s, 18H). ^{13}C NMR (126 MHz, CD_2Cl_2 , ppm): δ 183.6, 183.2, 151.4, 151.3, 151.1, 146.3, 143.0, 136.5, 136.2, 135.3, 134.5, 133.3, 133.0, 132.7, 132.5, 132.1, 130.5, 130.3, 129.9, 129.0, 128.5, 128.2, 127.2, 126.5, 126.2, 125.5, 122.9, 122.7, 121.6, 116.7, 35.37, 35.36, 31.68, 31.68. HRMS (ESI): m/z $[M + \text{H}]^+$ calcd for $\text{C}_{50}\text{H}_{51}\text{O}_2^+$: 683.3884; found 683.3875 ($|\Delta| = 1.2$ ppm).



3,9,12-Tris(3,5-di-tert-butylphenyl)-3,3a,8a,8a¹-tetrahydrodibenzo[cd,mn]pyrene-4,8-dione (53). A solution of (3,5-di-tert-butylphenyl)magnesium bromide (1.5 mL, 0.38 mmol, 0.25 M solution in THF) was added dropwise to the cooled ($-78\text{ }^{\circ}\text{C}$) solution of 3,12-bis(3,5-di-tert-butylphenyl)dibenzo[cd,mn]pyrene-4,8-dione (**51**, 260 mg, 0.38 mmol) in dry THF (30 mL) under an argon atmosphere. The reaction mixture was stirred at $-78\text{ }^{\circ}\text{C}$ for 5 h before it was allowed to warm to room temperature over 12 h. Then iodine (58.0 mg, 0.49 mmol) was added and the reaction mixture was heated under air at $65\text{ }^{\circ}\text{C}$ for 2 h before 2 M NaOH (10 mL) was added and the mixture was extracted with CH_2Cl_2 (3x 10 mL). The combined organic layers were washed with water, brine, dried over anhydrous Na_2SO_4 , and filtered. After evaporation of the solvents, the residue was then purified by column chromatography over silica gel using cyclohexane/ EtOAc 20:1 as an eluent to afford the desired product (**53**, 325 mg, 98%) as a deep-red solid. ^1H NMR (500 MHz, CDCl_3 , ppm): δ 8.64 (d, $J = 7.6$ Hz, 2H), 8.16 (d, $J = 8.9$ Hz, 2H), 7.69 (t, $J = 7.6$ Hz, 1H), 7.68 (t, $J = 1.8$ Hz, 1H), 7.64 (d, $J = 8.8$ Hz, 2H), 7.53 (t, $J = 1.8$ Hz, 2H), 7.40 (d, $J = 1.8$ Hz, 2H), 7.37 (d, $J = 1.8$ Hz, 4H), 1.44 (s, 18H), 1.42 (s, 36H). ^{13}C NMR (101 MHz, CDCl_3 , ppm): δ 183.7, 151.3, 151.0, 150.7, 145.5, 142.7, 136.5, 134.4, 134.0, 132.7, 131.8, 131.7, 129.3, 128.4, 127.9, 125.9, 125.4, 122.7, 122.2, 121.4, 117.1, 35.2 (two overlapped signals), 31.7 (two overlapped signals). HRMS (ESI): m/z $[M + \text{Na}]^+$ calcd for $\text{C}_{64}\text{H}_{71}\text{O}_2\text{Na}^+$: 893.5268; found 683.5279 ($|\Delta| = 1.2$ ppm).

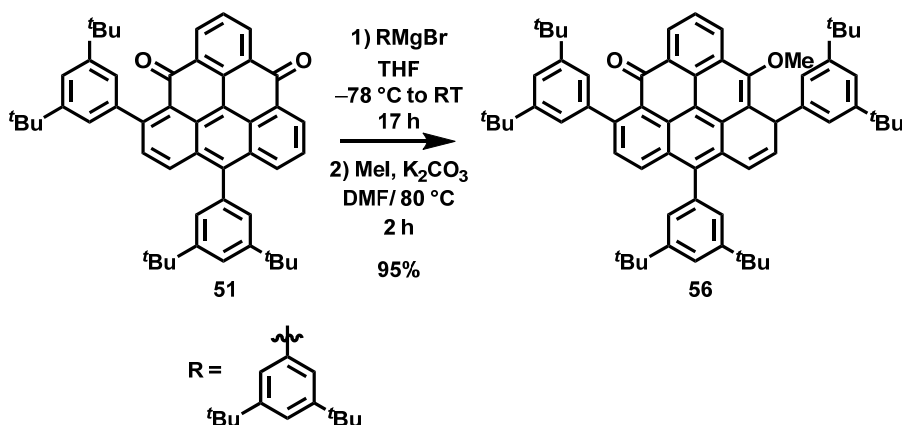


3a1,5,8,11-Tetrakis(3,5-di-tert-butylphenyl)-12-hydroxydibenzo[cd,mn]pyren-

4(3a1H)-one (54): Anhydrous LiBr (285 mg, 3.28 mmol) was dried at 100 °C under vacuum in an Schlenk tube for 3 h. After it was cooled down to room temperature and the Schlenk tube was evacuated and backfilled with argon three times. Then dry THF (1 mL) was added and the under an argon atmosphere. Afterwards, solution of 3,9,12-tris(3,5-di-tert-butylphenyl)-3,3a,8a,8a¹-tetrahydro-dibenzo[cd,mn]pyrene-4,8-dione (**53**, 25,0 mg, 28.7 μmol) in dry THF (1 mL) was added to the solution of LiBr in dry THF. The solution was cooled down to -78 °C and (3,5-di-tert-butylphenyl)magnesium bromide (38.9 μL, 24.5 μmol, 0.63 M solution in THF) was added dropwise under an argon atmosphere. The reaction mixture was stirred at -78 °C for 5 h before it was allowed to warm to room temperature over 12 h. Then sat. NH₄Cl (10 mL) was added and the mixture was extracted with EtOAc (3 x 10 mL). The combined organic layers were washed with, brine, dried over anhydrous Na₂SO₄, and filtered. After evaporation of the solvents, the residue was then purified by column chromatography over silica gel using cyclohexane/ EtOAc 30:1 as an eluent to afford the desired product (**54**, 14.6 mg, 53%) as a yellow film. ¹H NMR (500 MHz, CDCl₃, ppm): 8.67 (dd, *J* = 7.4, 1.3 Hz, 1H), 8.61 (dd, *J* = 8.1, 1.3 Hz, 1H), 7.83 (d, *J* = 8.4 Hz, 1H), 7.76 (dd, *J* = 8.1, 7.4 Hz, 1H), 7.54 (t, *J* = 1.8 Hz, 1H), 7.49 (d, *J* = 8.4 Hz, 1H), 7.46 (t, *J* = 1.8 Hz, 1H) 7.38 (d, *J* = 1.7 Hz, 4H), 7.34 (t, *J* = 1.7 Hz, 2H), 7.32 (d, *J* = 1.8 Hz, 2H), 7.28 (d, *J* = 1.8 Hz, 2H), 6.57 (d, *J* = 10.0 Hz, 1H), 6.23 (d, *J* = 10.0 Hz, 1H), 6.07 (s, 1H), 1.39 (s, 18H), 1.38 (s, 18H), 1.22 (s, 36H). ¹³C NMR (126 MHz, CD₂Cl₂, ppm): δ 184.8, 151.7, 151.3, 150.8, 150.1, 147.0, 143.2, 142.4, 138.1, 137.6, 137.5, 132.5, 130.9, 130.7, 130.3, 129.9, 129.4, 129.0, 128.5, 128.1, 126.5, 126.36, 126.34, 126.2, 125.6, 124.9, 123.3, 123.0, 121.3, 121.2, 120.9, 120.6, 119.5, 116.3, 54.8, 35.2 (two overlapped signals), 35.1 (two overlapped signals), 31.8, 31.7, 31.6 (two overlapped signals). HRMS (ESI): *m/z* [*M* + H]⁺ calcd for C₇₈H₉₃O₂⁺: 1061.7170; found 1061.7175 (|Δ| = 0.4 ppm).

3,3a1,5,8,11-Pentakis(3,5-di-tert-butylphenyl)-12-hydroxy-11,11a-dihydrodibenzo

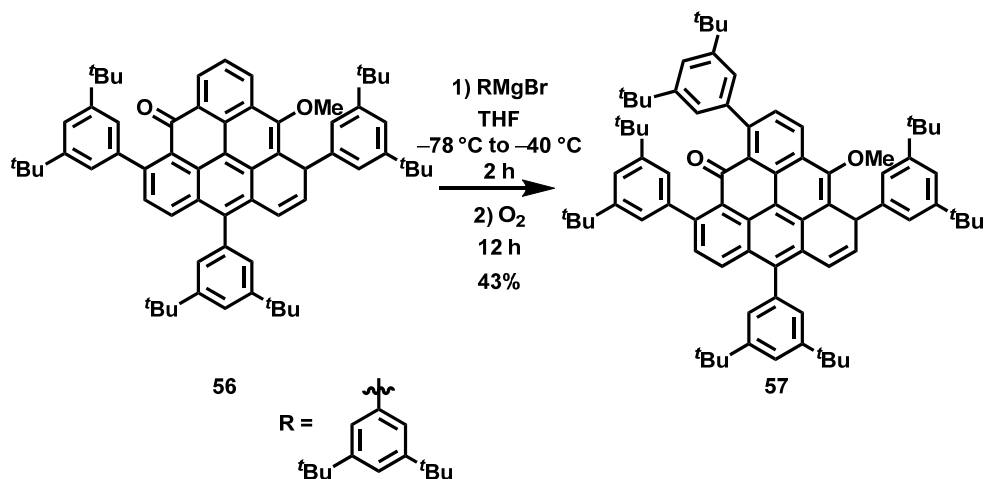
[cd,mn]pyren-4(3a1H)-one (55): A solution of (3,5-di-tert-butylphenyl)magnesium bromide (2.30 ml, 1.15 mmol, 0.50 M solution in THF) was added dropwise to the cooled ($-78\text{ }^{\circ}\text{C}$) solution of 3,9,12-tris(3,5-di-tert-butylphenyl)-3,3a,8a,8a¹-tetrahydrodibenzo[cd,mn]pyrene-4,8-dione (**53**, 25 mg, 28.7 μmol) in dry THF (1 mL) under an argon atmosphere. The reaction mixture was stirred at $-78\text{ }^{\circ}\text{C}$ for 2 h before it was allowed to warm to room temperature over 12 h. Then, the excess of unreacted Grignard reagent was quenched with sat. aq. NH_4Cl solution and the mixture was stirred upon air over night. Then CH_2Cl_2 (10 mL) was added and the organic layer separated, and the aqueous layer was extracted with CH_2Cl_2 (3x 10 mL). The combined organic layers were washed with water, brine, dried over anhydrous Na_2SO_4 , and filtered. After evaporation of the solvents, the residue was then purified by column chromatography over silica gel using cyclohexane to cyclohexane/ CH_2Cl_2 4:1 as an eluent to afford the product (**55**, 13.2 mg, 37%) as a yellow film. ^1H NMR (500 MHz, CDCl_3 , ppm): 8.70 (d, $J = 7.6$ Hz, 1H), 7.86 (d, $J = 8.4$ Hz, 1H), 7.56 (d, $J = 7.6$ Hz, 1H), 7.53 (t, $J = 1.8$ Hz, 1H), 7.51 (d, $J = 8.4$ Hz, 1H), 7.47 (t, $J = 1.8$ Hz, 1H), 7.37 (t, $J = 1.8$ Hz, 1H), 7.36 (d, $J = 1.8$ Hz, 2H), 7.29 (d, $J = 1.8$ Hz, 2H), 7.25 (d, $J = 1.8$ Hz, 4H), 7.18 (t, $J = 1.8$ Hz, 2H), 7.08 (d, $J = 1.8$ Hz, 2H), 6.46 (d, $J = 10.0$ Hz, 1H), 6.18 (d, $J = 10.0$ Hz, 1H), 6.06 (s, 1H), 1.40 (s, 18H), 1.39 (s, 18H), 1.20 (s, 18H), 1.16 (s, 36H). δ ^{13}C NMR (126 MHz, CDCl_3 , ppm): δ 185.0, 152.9, 151.1, 150.8, 150.1, 149.7, 146.6, 144.6, 143.5, 143.1, 141.3, 138.9, 137.7, 137.6, 132.6, 130.9, 130.5, 130.40, 130.37, 130.1, 129.9, 128.9, 126.5, 126.2, 125.6, 123.7, 123.13, 123.12, 122.5, 121.91, 121.85, 121.5, 121.2, 120.6, 119.7, 119.3, 55.3, 35.15, 35.13, 35.05, 34.99, 31.78, 31.7, 31.6, 31.5. HRMS (ESI): m/z [$M + \text{H}$]⁺ calcd for $\text{C}_{92}\text{H}_{113}\text{O}_2^+$: 1249.8735; found 1249.8732 ($|\Delta| = 0.2$ ppm).



3,9,12-Tris(3,5-di-tert-butylphenyl)-8-methoxydibenzo[cd,mn]pyren-4(9H)-one (56).

A solution of (3,5-di-tert-butylphenyl)magnesium bromide (2.05 ml, 0.55 mmol, 0.27 M solution in THF) was added dropwise to the cooled ($-78\text{ }^{\circ}\text{C}$) solution of 3,12-bis(3,5-di-tert-butylphenyl)dibenzo[cd,mn]pyrene-4,8-dione (**51**, 380 mg, 0.551 mmol) in dry THF (10 ml) under an argon atmosphere. The reaction mixture was stirred at $-78\text{ }^{\circ}\text{C}$ for 5 h before it was allowed to warm to room temperature over 12 h. Then the solvent was removed under reduced pressure. To the crude hydroxide, solid K₂CO₃ (457 mg, 3.31 mmol) was added, followed by freshly argon bubbled dry DMF (10 mL). The mixture was stirred under an argon at room temperature for 5 minutes before methyl iodide (104 μL , 1.65 mmol) was added dropwise under an argon atmosphere. The mixture was heated at $80\text{ }^{\circ}\text{C}$ for 2 h. Then the solvent was evaporated, water (10 mL) was added and the mixture was extracted with ethyl acetate (3 x 10 mL). The combined organic layers were washed with, brine, dried over anhydrous Na₂SO₄, and filtered. After evaporation of the solvents, the residue was then purified by column chromatography over silica gel using cyclohexane/ethyl acetate 60:1 as an eluent to afford the desired product (**56**, 466 mg, 95%) as a yellow solid. ¹H NMR (400 MHz, CD₂Cl₂, ppm): δ 8.59 (dd, $J = 7.4, 1.2$ Hz, 1H), 8.46 (dd, $J = 8.2, 1.3$ Hz, 1H), 7.89 (d, $J = 8.5$ Hz, 1H), 7.84 (dd, $J = 8.1, 7.5$ Hz, 1H), 7.59 (t, $J = 1.8$ Hz, 1H), 7.50 (d, $J = 8.7$ Hz, 2H), 7.49 (t, $J = 1.7$ Hz, 1H), 7.34 (t, $J = 1.6$ Hz, 1H), 7.31 (d, $J = 1.8$ Hz, 2H), 7.27 (t,

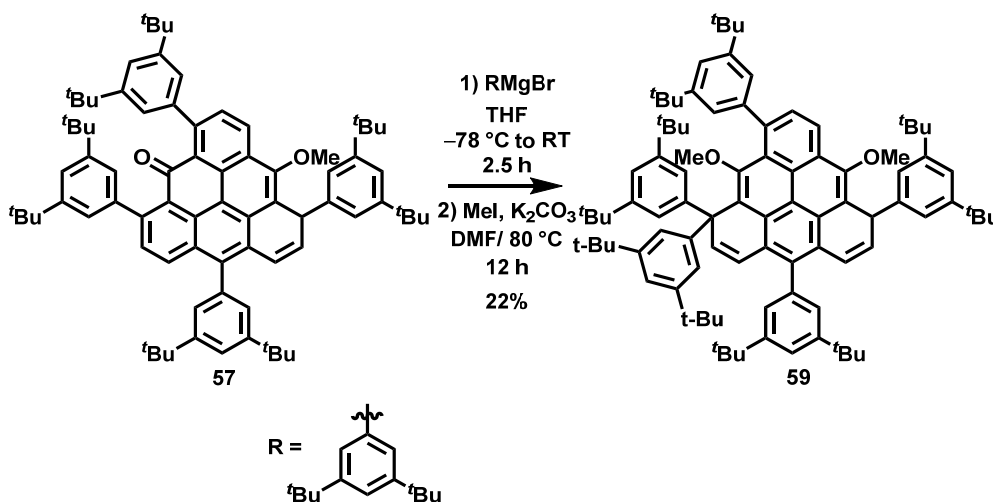
$J = 1.6$ Hz, 1H), 7.24 (t, $J = 1.7$ Hz, 1H), 7.19 (d, $J = 1.8$ Hz, 2H), 6.56 (dd, $J = 10.0, 1.3$ Hz, 1H), 6.24 (dd, $J = 10.0, 5.1$ Hz, 1H), 5.45 (dd, $J = 5.1, 1.2$ Hz, 1H), 3.72 (s, 3H), 1.40 (s, 9H), 1.39 (s, 18H), 1.38 (s, 9H), 1.22 (s, 18H). ^{13}C NMR (101 MHz, CD_2Cl_2 , ppm): δ 184.9, 154.8, 151.5, 151.4, 151.2, 150.6, 146.9, 144.7, 143.5, 138.0, 137.5, 133.5, 132.8, 131.8, 131.5, 131.4, 129.7, 129.6, 128.7, 128.6, 128.4, 128.1, 127.8, 126.98, 126.97, 126.8, 126.0, 125.6, 123.4, 123.3, 122.7, 121.9, 121.0, 120.8, 118.4, 62.4, 44.4, 35.33, 35.32, 35.28, 35.1, 31.74, 31.73, 31.69, 31.6. HRMS (ESI): m/z [$M + \text{H}$] $^+$ calcd for $\text{C}_{65}\text{H}_{75}\text{O}_2\text{Na}^+$: 909.5581; found 909.5578 ($|\Delta| = 0.3$ ppm).



3,5,9,12-Tetrakis(3,5-di-tert-butylphenyl)-8-methoxydibenzo[cd,mn]pyren-4(9H)-one

(57). A solution of (3,5-di-tert-butylphenyl)magnesium bromide (1.08 mL, 0.68 mmol, 0.63 M solution in THF) was added dropwise to the cooled ($-78\text{ }^\circ\text{C}$) solution of 3,9,12-tris(3,5-di-tert-butylphenyl)-8-methoxydibenzo[cd,mn]pyren-4(9H)-one (**56**, 200 mg, 0.225 mmol) in dry THF (2 mL) under an argon atmosphere. The reaction mixture was stirred at $-78\text{ }^\circ\text{C}$ for 1 h before it was allowed to $-40\text{ }^\circ\text{C}$ over 1 h. Then sat. NH_4Cl (10 mL) was added and the mixture was extracted with ethyl acetate (3 x 10 mL). The combined organic layers were washed with, brine, dried over anhydrous Na_2SO_4 , and filtered. After evaporation of the solvents, the residue was dissolved in THF (15 mL) and air was bubbled through the solution for 12 h. The solvent was evaporated, and the residue was then purified by column

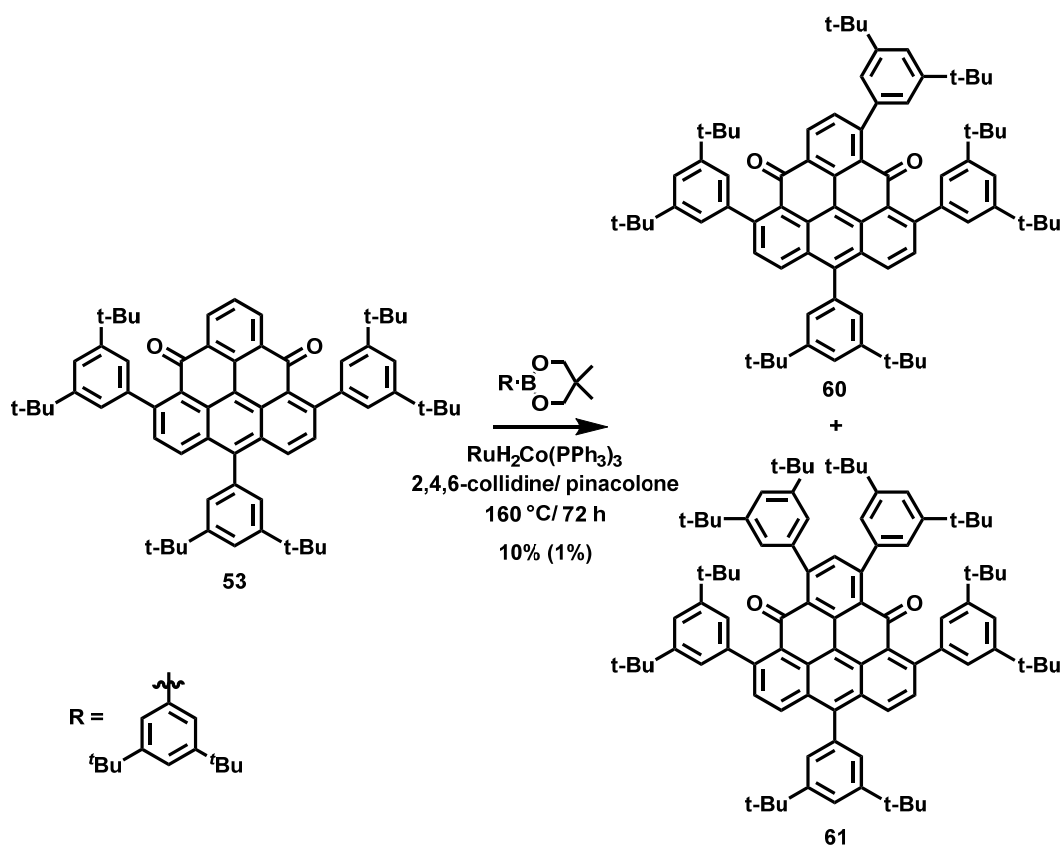
chromatography over silica gel using cyclohexane to cyclohexane/CH₂Cl₂10:1 as an eluent to afford the desired product (**57**, 105 mg, 43%) as a yellow solid. ¹H NMR (400 MHz, CD₂Cl₂, ppm): δ 8.40 (d, *J* = 8.5 Hz, 1H), 7.83 (d, *J* = 8.4 Hz, 1H), 7.60 (d, *J* = 8.5 Hz, 1H), 7.60 (t, *J* = 1.9 Hz, 1H), 7.40 (d, *J* = 8.4 Hz, 1H), 7.35 (m, 2H), 7.29 (t, *J* = 1.7 Hz, 1H), 7.26 (t, *J* = 1.8 Hz, 1H), 7.24 (d, *J* = 1.8 Hz, 2H), 7.21 (d, *J* = 1.9 Hz, 2H), 7.21 (d, *J* = 1.9 Hz, 2H), 6.59 (dd, *J* = 10.0, 1.4 Hz, 1H), 6.25 (dd, *J* = 10.0, 5.1 Hz, 1H), 5.49 (dd, *J* = 5.1, 1.3 Hz, 1H), 3.71 (s, 3H), 1.41 (s, 9H), 1.40 (s, 9H), 1.29 (s, 18H), 1.28 (s, 18H), 1.24 (s, 18). ¹³C NMR (101 MHz, CD₂Cl₂, ppm): δ 185.3, 154.6, 151.5, 151.4, 151.2, 150.0, 149.9, 146.7, 146.2, 144.9, 143.3, 143.1, 137.8, 137.6, 133.2, 132.6, 132.3, 131.7, 130.9, 129.7, 129.5, 129.2, 129.1, 128.4, 127.73, 127.69, 126.65, 126.01, 125.98, 125.5, 123.6, 123.5, 122.7, 121.9, 121.2, 121.1, 120.8, 119.1, 62.5, 44.4, 35.33, 35.29, 35.16, 35.13, 35.12, 31.76 (two overlapped signals), 31.74, 31.7, 31.6. HRMS (ESI): *m/z* [*M* + H]⁺ calcd for C₇₉H₉₅O₂⁺: 1075.7327; found 1075.7327 (|Δ| = 0.1 ppm).



1,3,5,8,11-Pentakis(3,5-di-tert-butylphenyl)-4,12-dimethoxy-1,5-dihydrodibenzo

[**cd,mn**] pyrene (**59**): A solution of (3,5-di-tert-butylphenyl)magnesium bromide (0.92 mL 0.58 mmol, 0.68 M solution in THF) was added dropwise to the stirred mixture of 3,5,9,12-tetrakis(3,5-di-tert-butylphenyl)-8-methoxydibenzo[**cd,mn**]pyren-4(9H)-one (**57**, 25.0 mg,

23.2 μmol) in dry THF (0.5 mL) at $-78\text{ }^{\circ}\text{C}$ under an argon atmosphere, and the mixture was stirred at the $-78\text{ }^{\circ}\text{C}$ for 30 min before it was allowed to warm to room temperature over 2 h. Then, the solvent was evaporated to dryness, K_2CO_3 (32.1 mg, 0.23 mmol) was added and the flask was evacuated and backfilled with argon five times. Freshly argon bubbled dry DMF (5 mL) was added and the mixture was bubbled with stream of argon for 10 min. Then MeI (7.22 μL , 0.12 mmol) was added and the mixture was gradually warmed to $80\text{ }^{\circ}\text{C}$ over night. Afterwards, the solvents were evaporated, water (10 mL) and EtOAc (10 mL) were added. Organic layer was separated, and the aqueous layer was extracted with EtOAc (3 x 10 mL). The combined organic layers were washed with water, brine, dried over anhydrous Na_2SO_4 , and filtered. After evaporation of the solvents, the residue was then purified by column chromatography over silica gel using cyclohexane/ CH_2Cl_2 20:1 as an eluent and additionally on the semipreparative HPLC (Hex/ CH_2Cl_2 / EtOAc 87.7:12:0.3) to afford the product (**59**, 12.2 mg, 41 %) as a yellow film. HRMS (ESI): m/z [$M + \text{Na}$] $^+$ calcd for $\text{C}_{94}\text{H}_{118}\text{O}_2\text{Na}^+$: 1301.9024; found 1301.9016 ($|\Delta| = 0.6$ ppm).

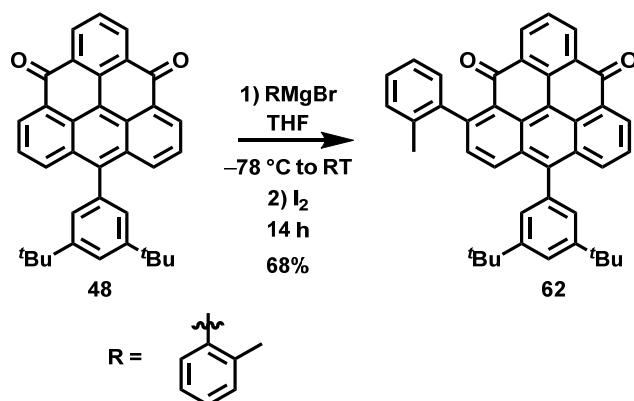


3,5,7,9,12-pentakis(3,5-di-tert-butylphenyl)dibenzo[cd,mn]pyrene-4,8-dione (61): The 3,9,12-tris(3,5-di-tert-butylphenyl)-3,3a,8a,8a¹-tetrahydro-dibenzo[cd,mn]pyrene-4,8-dione (**53**, 47.9 mg, 55 μmol) and boronic ester (74.8 mg, 248 μmol) were kept under vacuum in separate in two separate round-bottomed flask for 24 h. Then $\text{RuH}_2\text{Co}(\text{PPh}_3)_3$ (25.3 mg, 27.5 μmol) was added to the pinacol ester and the mixture was kept under vacuum for additional 2 h. Afterward freshly argon bubbled solvent mixture of 2,4,6-collidine/ pinacolone (3,3-dimethyl-2-butanone) (2 mL, 1:1) was added to the 3,9,12-tris(3,5-di-tert-butylphenyl)-3,3a,8a,8a¹-tetrahydro-dibenzo[cd,mn]pyrene-4,8-dione and the resulting mixture was added to the pinacol ester and catalyst. The reaction mixture was then heated at 160 °C under an argon atmosphere for 72 h. Afterwards, the solvents were evaporated with stream of nitrogen at 160 °C. The residue was dissolved in EtOAc (5 mL), washed with water (2x 10 mL), dried over Na_2SO_4 and filtered. After evaporation of the solvents, the residue was then

purified by column chromatography over silica gel using cyclohexane/ EtOAc, 60:1 as an eluent to afford desired product (**61**, 0.51 mg, 1%) as red film and the four substituted side product (**60**, 5.20 mg, 10%) as red film.

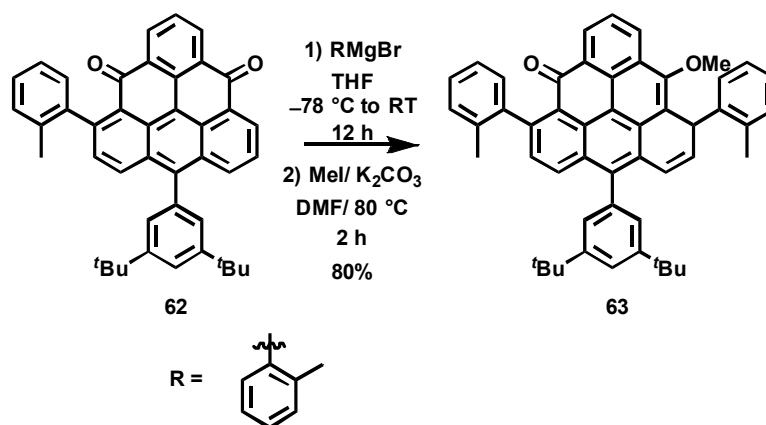
3,5,7,9,12-pentakis(3,5-di-tert-butylphenyl)dibenzo[cd,mn]pyrene-4,8-dione (61): ^1H NMR (500 MHz, CD_2Cl_2 , ppm): δ 8.09 (d, $J = 8.9$ Hz, 2H), 7.65 (t, $J = 1.8$ Hz, 1H), 7.58 (d, $J = 8.9$ Hz, 2H), 7.47 (s, 2H), 7.38 (d, $J = 1.8$ Hz, 2H), 7.37 (d, $J = 1.8$ Hz, 4H), 7.32 (t, $J = 1.8$ Hz, 2H), 7.29 (t, $J = 1.9$ Hz, 2H), 7.24 (d, $J = 1.8$ Hz, 4H), 1.42 (s, 18H), 1.25 (s, 36H), 1.20 (s, 36H).

3,5,9,12-tetrakis(3,5-di-tert-butylphenyl)dibenzo[cd,mn]pyrene-4,8-dione (60): ^1H NMR (500 MHz, CD_2Cl_2 , ppm): δ 8.60 (d, $J = 8.0$ Hz, 1H), 8.18 (d, $J = 8.8$ Hz, 1H), 8.09 (d, $J = 8.9$ Hz, 1H), 7.69 (d, $J = 1.8$ Hz, 1H), 7.68 (t, $J = 1.8$ Hz, 1H), 7.69 – 7.65 (m, 1H), 7.65 (d, $J = 8.8$ Hz, 1H), 7.59 (d, $J = 8.9$ Hz, 1H), 7.56 (d, $J = 8.0$ Hz, 1H), 7.53 (t, $J = 1.8$ Hz, 1H), 7.40 (t, $J = 1.7$ Hz, 4H), 7.33 (t, $J = 1.8$ Hz, 1H), 7.24 (d, $J = 1.8$ Hz, 2H), 1.45 (s, 18H), 1.43 (s, 18H), 1.26 (s, 18H), 1.25 (s, 18H).



12-(3,5-Di-tert-butylphenyl)-3-(o-tolyl)dibenzo[cd,mn]pyrene-4,8-dione (62). A solution of o-tolylmagnesium bromide (0.83 ml, 0.79 mmol, 0.95 M solution in THF) was added dropwise to the cooled (-78 °C) solution of 12-(3,5-di-tert-butylphenyl)dibenzo[cd,mn]pyrene-4,8-dione (**48**, 380 mg, 0.77 mmol) in dry THF (10 mL) under an argon atmosphere. The reaction mixture was stirred at -78 °C for 2 h before it was

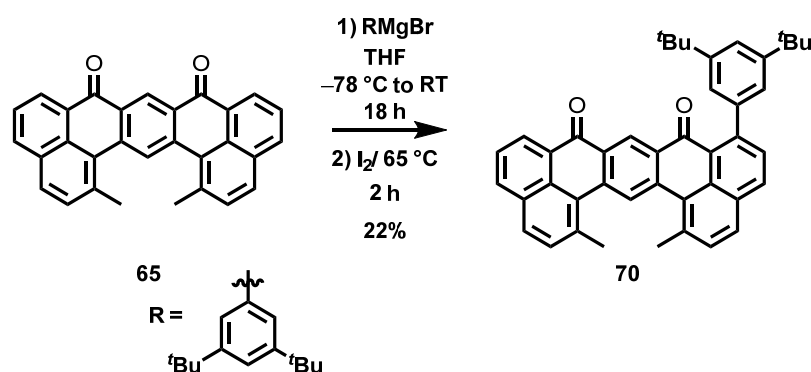
allowed to warm to room temperature over 12 h. Then iodine (123 mg, 0.49 mmol) was added and the reaction mixture was heated under air at 65 °C for 2 h before 2 M NaOH (10 mL) was added and the mixture was extracted with CH₂Cl₂ (3x 10 ml). The combined organic layers were washed with water, brine, dried over anhydrous Na₂SO₄, and filtered. After evaporation of the solvents, the residue was then purified by column chromatography over silica gel using cyclohexanethen cyclohexane/EtOAc 15:1 as an eluent to afford the desired product (**62**, 307 mg, 68%) as a deep-red solid. ¹H NMR (400 MHz, CDCl₃, ppm): δ 9.03 (dd, *J* = 7.0, 1.3 Hz, 1H), 8.84 (dd, *J* = 7.7, 1.5 Hz, 1H), 8.71 (dd, *J* = 7.7, 1.5 Hz, 1H), 8.24 (dd, *J* = 8.6, 1.3 Hz, 1H), 8.22 (d, *J* = 8.9 Hz, 1H), 7.80 (dd, *J* = 8.6, 7.0 Hz, 1H), 7.74 (t, *J* = 7.7 Hz, 1H), 7.68 (t, *J* = 1.8 Hz, 1H), 7.48 (d, *J* = 8.8 Hz, 1H), 7.42–7.33 (m, 5H), 7.20–7.15 (m, 1H), 2.13 (s, 3H), 1.44 (s, 9H), 1.43 (s, 9H). ¹³C NMR (101 MHz, CDCl₃, ppm): δ 183.33, 183.32, 151.1, 149.9, 146.1, 143.6, 136.2, 136.0, 135.2, 134.8, 134.3, 133.7, 133.2, 133.1, 131.4, 130.9, 130.3, 130.15, 130.1, 129.8, 128.8, 128.1, 127.8, 127.5, 127.1, 126.45, 125.44, 126.3, 125.9, 125.8, 125.3, 122.4, 116.7, 35.25, 35.24, 31.73, 31.72, 20.2.



12-(3,5-Di-tert-butylphenyl)-8-methoxy-3,9-di-o-tolyldibenzo[cd,mn]pyren-4(9H)-one (63). A solution of o-tolylmagnesium (0.45 ml, 0.50 mmol, 1.12 M solution in THF) was added dropwise to the cooled (-78 °C) solution of 12-(3,5-di-tert-butylphenyl)-3-(o-tolyl)dibenzo[cd,mn]pyrene-4,8-dione (**62**, 280 mg, 0.48 mmol) in dry THF (20 ml) under

an argon atmosphere. The reaction mixture was stirred at $-78\text{ }^{\circ}\text{C}$ for 5 h before it was allowed to warm to room temperature over 12 h. Then the solvent was removed under reduced pressure. To the crude hydroxide, solid K_2CO_3 (397 mg, 2.87 mmol) was added, followed by freshly argon bubbled dry DMF (30 mL). The mixture was stirred under an argon at room temperature for 5 minutes before methyl iodide (119 μL , 1.92 mmol) was added dropwise under an argon atmosphere. The mixture was heated at $80\text{ }^{\circ}\text{C}$ for 2 h. Then the solvent was evaporated, water (10 mL) was added and the mixture was extracted with ethyl acetate (3 x 10 mL). The combined organic layers were washed with, brine, dried over anhydrous Na_2SO_4 , and filtered. After evaporation of the solvents, the residue was then purified by column chromatography over silica gel using cyclohexane/ethyl acetate 30:1 as an eluent to afford the desired product (**63**, 265 mg, 80%) as a yellow solid. ^1H NMR (500 MHz, CDCl_3 , ppm): δ 8.70 (dt, $J = 7.4, 1.0$ Hz, 1H), 8.42 (dd, $J = 8.1, 1.3$ Hz, 1H), 7.93 (dd, $J = 8.3, 1.8$ Hz, 1H), 7.82 (dd, $J = 8.1, 7.4$ Hz, 1H), 7.58 (t, $J = 1.8$ Hz, 1H), 7.42 (dd, $J = 8.4, 0.8$ Hz, 1H), 7.39 – 7.33 (m, 4H), 7.25 – 7.22 (m, 2H), 7.10 (td, $J = 7.4, 1.6$ Hz, 1H), 7.00 (ddd, $J = 9.0, 6.7, 1.7$ Hz, 1H), 6.96 (d, $J = 6.6$ Hz, 1H), 6.59 (ddd, $J = 10.0, 1.7, 0.6$ Hz, 1H), 6.15 (ddd, $J = 10.0, 4.7, 3.2$ Hz, 1H), 5.74 (dt, $J = 4.3, 2.0$ Hz, 1H), 3.57 (d, $J = 0.9$ Hz, 3H), 2.64 (d, $J = 7.7$ Hz, 3H), 2.14 (d, $J = 12.1$ Hz, 3H), 1.42 (dd, $J = 3.6, 0.8$ Hz, 18H). ^{13}C NMR (101 MHz, CDCl_3 , ppm): 184.7, 154.44, 154.42, 151.0, 150.9, 145.4, 145.3, 144.3, 144.19, 144.18, 137.8, 137.1, 134.78, 134.75, 134.7, 133.3, 133.2, 131.40, 131.37, 131.35, 130.85, 130.82, 130.48, 130.46, 129.76, 129.74, 129.6, 129.2, 129.1, 128.7, 128.5, 128.4, 127.93, 127.91, 127.40, 129.39, 127.2, 127.1, 127.0, 126.9, 126.7, 126.63, 126.58, 126.5, 126.36, 126.35, 125.96, 125.94, 125.6, 125.49, 125.48, 125.4, 123.2, 121.5, 118.14, 118.12, 62.2, 35.18, 35.17 (two overlapped signals), 31.76, 31.74, 31.73, 20.4, 20.3, 19.82, 19.81. (out of 86 signals expected from two possible diastereomers (43 signals each), only 67 signals could be detected within the resolution limits of the NMR technique due to the signal overlap)

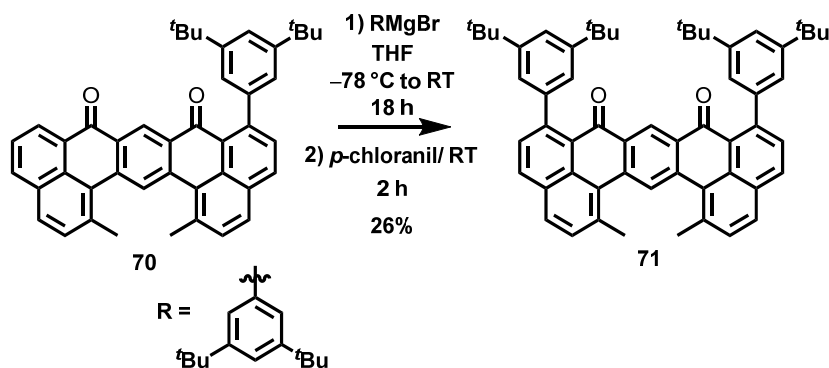
was not possible. HRMS (ESI): m/z $[M + H]^+$ calcd for $C_{58}H_{53}O_2^+$: 781.4040; found 781.4047 ($|\Delta| = 0.9$ ppm).



6-(3,5-Di-tert-butylphenyl)-1,15-dimethyldibenzo[de,jk]pentacene-7,9-dione (**70**):

A solution of (3,5-di-tert-butylphenyl)magnesium bromide (2.52 mL, 0.731 mmol, 0.29 M solution in THF) was added dropwise to the cooled ($-78\text{ }^{\circ}\text{C}$) solution of 1,15-dimethyldibenzo[de,jk]pentacene-7,9-dione (**65**, 300 mg, 0.731 mmol) in dry THF (50 mL) under an argon atmosphere. The reaction mixture was stirred at $-78\text{ }^{\circ}\text{C}$ for 6 h before it was allowed to warm to room temperature over 12 h. Then iodine (186 mg, 0.731 mmol) was added and the reaction mixture was heated under air at $65\text{ }^{\circ}\text{C}$ for 2 h before 2 M NaOH (25 mL) was added and the mixture was extracted with CH_2Cl_2 (3x 25 mL). The combined organic layers were washed with water, brine, dried over anhydrous Na_2SO_4 , and filtered. After evaporation of the solvents, the residue was then purified by column chromatography over silica gel using cyclohexane then cyclohexane/ CH_2Cl_2 4:1 as an eluent to afford the desired product (**65**, 98 mg, 22%) as a pale-orange powder. 1H NMR (500 MHz, $CDCl_3$, ppm): δ 9.35 (s, 1H), 8.99 (s, 1H), 8.75 (dd, $J = 7.2, 1.3$ Hz, 1H), 8.17 (dd, $J = 7.9, 1.3$ Hz, 1H), 8.10 (d, $J = 8.3$ Hz, 1H), 7.93 (d, $J = 8.4$ Hz, 1H), 7.92 (d, $J = 8.3$ Hz, 1H), 7.73 (dd, $J = 7.9, 7.2$ Hz, 1H), 7.66 (d, $J = 8.2$ Hz, 1H), 7.57 (d, $J = 8.3$ Hz, 1H), 7.57 ($J = 8.4$, Hz, 1H), 7.51 (t, $J = 1.8$ Hz, 1H), 7.34 (d, $J = 1.8$ Hz, 2H), 3.12 (s, 3H), 3.08 (s, 4H), 1.40 (s, 18H). ^{13}C NMR (126 MHz, $CDCl_3$, ppm): δ 185.5, 183.23, 150.7, 147.5, 141.7, 139.6, 139.4, 137.9, 137.5, 135.0, 134.1, 133.3, 132.6, 131.9, 131.7, 131.5, 130.8, 130.5, 130.1, 130.0,

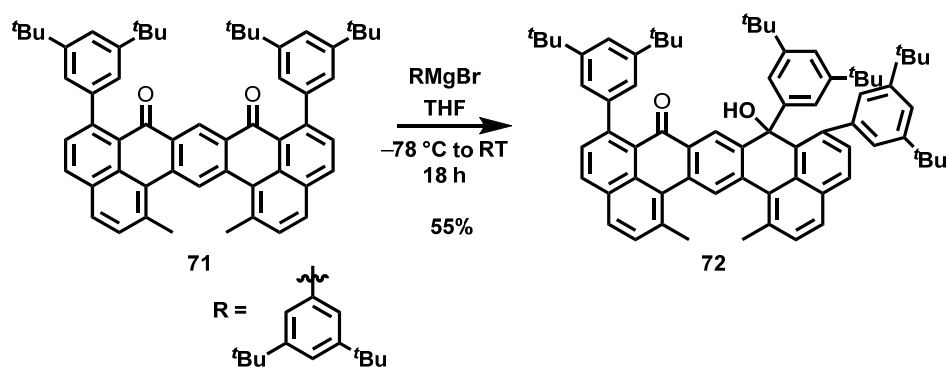
129.91, 129.86, 128.5, 128.2, 127.7, 126.7, 126.7, 126.09, 126.05, 123.7, 121.5, 35.2, 31.7, 26.7, 25.9. HRMS (ESI): m/z $[M + Na]^+$ calcd for $C_{44}H_{39}O_2Na^+$: 621.2764; found 621.2766 ($|\Delta| = 0.2$ ppm).



6,10-Bis(3,5-di-tert-butylphenyl)-1,15-dimethyldibenzo[de,jk]pentacene-7,9-dione

(71): A solution of (3,5-di-tert-butylphenyl)magnesium bromide (248 μL , 71.8 μmol , 0.29 M solution in THF) was added dropwise to the cooled (-78 $^{\circ}\text{C}$) solution of 6-(3,5-Di-tert-butylphenyl)-1,15-dimethyldibenzo[de,jk]pentacene-7,9-dione (**70**, 43 mg, 71.8 μmol) in dry THF (10 mL) under an argon atmosphere. The reaction mixture was stirred at -78 $^{\circ}\text{C}$ for 6 h before it was allowed to warm to room temperature over 12 h. Then *p*-chloranil (17.7 mg, 71.8 μmol) was added and the reaction mixture was stirred under air at room temperature for 2 h. Then 2M HCl (10 mL) was added and the mixture was extracted with CH_2Cl_2 (3x 25 ml). The combined organic layers were washed with water, brine, dried over anhydrous Na_2SO_4 , and filtered. After evaporation of the solvents, the residue was then purified by column chromatography over silica gel using cyclohexane then cyclohexane/ EtOAc 4:1 as an eluent to afford the desired product (**71**, 15.2 mg, 26%) as a pale-yellow powder. ^1H NMR (500 MHz, CD_2Cl_2 , ppm): δ 8.96 (s, 1H), 8.90 (s, 1H), 8.15 (d, $J = 8.3$ Hz, 2H), 7.97 (d, $J = 8.3$ Hz, 2H), 7.63 (d, $J = 8.3$ Hz, 4H), 7.49 (t, $J = 1.8$ Hz, 2H), 7.33 (d, $J = 1.8$ Hz, 4H), 3.09 (s, 6H), 1.38 (s, 36H). ^{13}C NMR (126 MHz, CD_2Cl_2 , ppm): δ 185.4, 151.1, 147.3, 142.4, 139.1, 138.2, 134.2, 133.6, 132.2, 131.2, 130.8, 130.6, 130.1, 128.3, 126.8, 126.7, 126.4, 119

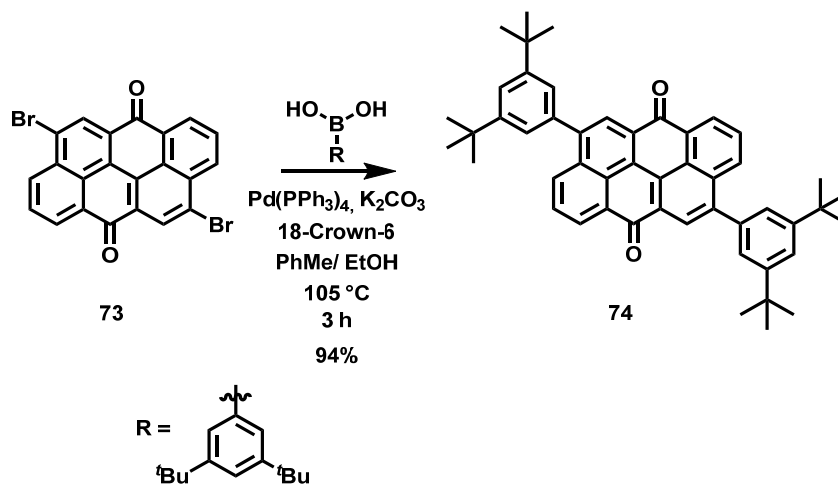
124.0, 121.6, 35.3, 31.7, 26.2. HRMS (ESI): m/z $[M + Na]^+$ calcd for $C_{58}H_{58}O_2Na^+$: 809.4329; found 809.4324 ($|\Delta| = 0.7$ ppm).



6,10,15-Tris(3,5-di-tert-butylphenyl)-9-hydroxy-1,15-dimethyldibenzo[de,jk]

pentacene-7(15H)-one (72): A solution of (3,5-di-tert-butylphenyl)magnesium bromide (1.75 mL, 0.964 mmol, 0.55 M solution in THF) was added dropwise to the cooled (-78°C) solution of 6,10-bis(3,5-di-tert-butylphenyl)-1,15-dimethyldibenzo[de,jk]pentacene-7,9-dione (**71**, 19 mg, 24.1 μmol) in dry THF (0.7 mL) under an argon atmosphere. The reaction mixture was stirred at -78°C for 2 h before it quenched with sat. aq. NH_4Cl solution (5 mL) and water (10 mL), CH_2Cl_2 (15 mL) was added and the organic layer was separated. The aqueous layer was extracted with CH_2Cl_2 (3 x 10 mL). The combined organic layers were washed with water, brine, dried over anhydrous Na_2SO_4 , and filtered. After evaporation of the solvents, the residue was then purified by column chromatography over silica gel using cyclohexane then cyclohexane/ CH_2Cl_2 3:2 as an eluent to afford the product (**72**, 13.1 mg, 55%) as a yellow solid. ^1H NMR (500 MHz, CD_2Cl_2 , ppm): δ 8.96 (s, 1H), 8.36 (s, 1H), 8.07 (d, $J = 8.2$ Hz, 1H), 7.90 (d, $J = 8.2$ Hz, 1H), 7.89 (d, $J = 8.1$ Hz, 1H), 7.86 (d, $J = 8.3$ Hz, 1H), 7.56 (d, $J = 8.4$ Hz, 1H), 7.53 (d, $J = 8.4$ Hz, 1H), 7.53 (d, $J = 8.2$ Hz, 1H), 7.47 (t, $J = 1.6$ Hz, 1H), 7.43 (t, $J = 1.5$ Hz, 1H), 7.39 (t, $J = 1.6$ Hz, 1H), 7.35 (d, $J = 8.2$ Hz, 1H), 7.27 (d, $J = 1.5$ Hz, 1H), 7.13 (t, $J = 1.5$ Hz, 1H), 6.72 (d, $J = 1.6$ Hz, 1H), 6.31 (t, $J = 1.5$ Hz, 1H), 3.06 (s, 1H), 3.03 (s, 2H), 2.97 (s, 2H), 1.39 (s, 9H), 1.38 (s, 18H), 1.03 (s, 18H), 0.92 (s, 9H). ^{13}C NMR (126 MHz, CD_2Cl_2 , ppm): δ 185.84 151.93 151.0, 150.90, 150.85, 149.2,

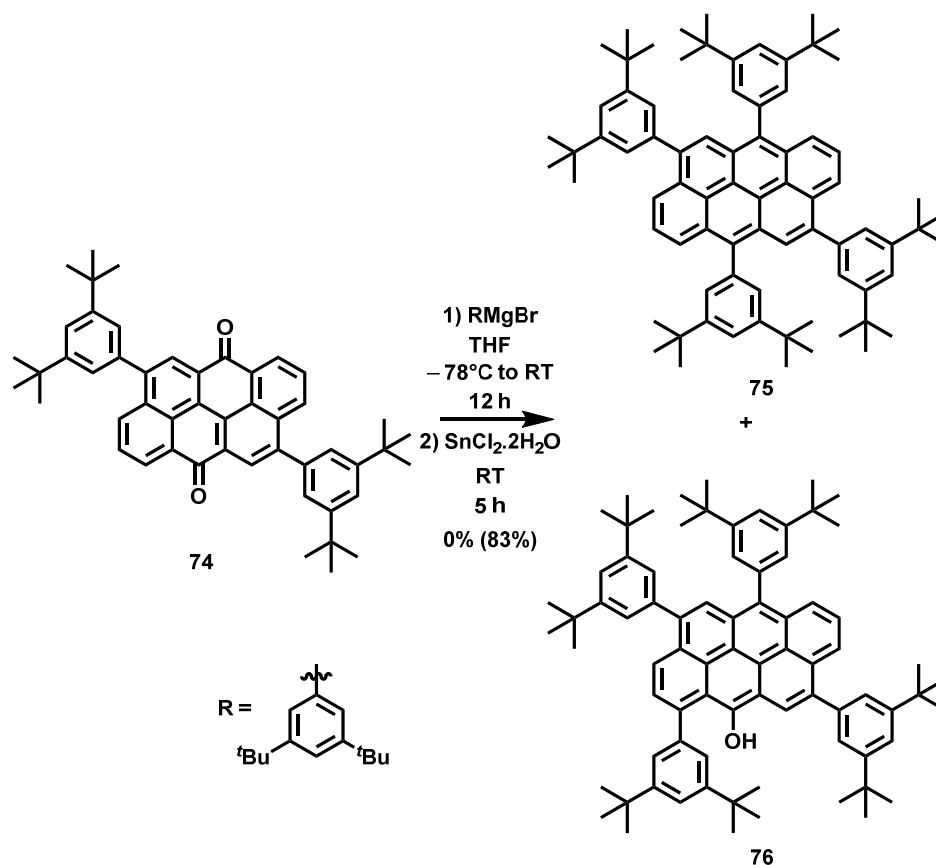
146.9, 144.0, 143.1, 142.7, 139.6, 137.1, 135.4, 134.93, 134.90, 134.6, 133.3, 133.2, 132.1, 131.3, 131.1, 130.94, 130.89, 130.54, 130.51, 130.3, 130.1, 129.1, 128.6, 128.3, 127.2, 126.8, 124.5, 123.8, 122.3, 121.7, 121.4, 121.2, 120.0, 77.6, 35.33, 35.30, 35.0, 34.9, 31.8, 31.6, 31.4, 31.3, 26.2, 24.2. HRMS (ESI): m/z $[M + H]^+$ calcd for $C_{72}H_{81}O_2^+$: 977.6231; found 977.6230 ($|\Delta| = 0.1$ ppm).



4,10-Bis(3,5-di-tert-butylphenyl)naphtho[7,8,1,2,3-nopqr]tetraphene-6,12-dione (74):

A solution of 4,10-dibromonaphtho[7,8,1,2,3-nopqr]tetraphene-6,12-dione (1.00 g, 2.15 mmol), (3,5-di-tert-butylphenyl)boronic acid (1.26 g, 5.37 mmol), $\text{Pd}(\text{PPh}_3)_4$ (0.50 g, 0.43 mmol), 18-Crown-6 (5.74 mg, 0.02 mmol), 2M K_2CO_3 (21.5 mL) and EtOH (13.5 mL) in toluene (135 mL) was degassed with stream of argon for 30 min. The mixture was then heated at 105 °C for 3 h under an argon atmosphere, before it was allowed to cool down to room temperature. 2 M HCl (100 mL) was added and the organic layer was separated, and the aqueous layer was extracted with toluene (3 x 25 mL). The combined organic layers were washed with brine, dried over anhydrous Na_2SO_4 , and filtered. After evaporation of the solvents, the residue was then purified by column chromatography over silica gel using cyclohexane/ CH_2Cl_2 3:2 to cyclohexane/ CH_2Cl_2 1:2 as an eluent to afford the desired product (**74**, 1.38 g, 94%) as a deep-red solid. ^1H NMR (500 MHz, CD_2Cl_2 , ppm): δ 8.57

(dd, $J = 7.2, 1.2$ Hz, 2H), 8.37 (s, 2H), 8.31 (dd, $J = 8.3, 1.2$ Hz, 2H), 7.76 (dd, $J = 8.3, 7.2$ Hz, 2H), 7.61 (t, $J = 1.8$ Hz, 2H), 7.48 (d, $J = 1.8$ Hz, 4H), 1.44 (s, 36H). ^{13}C NMR (126 MHz, CD_2Cl_2 , ppm): δ 183.3, 151.5, 144.7, 138.8, 134.5, 133.6, 130.7, 129.8, 129.6, 129.0, 128.3, 127.3, 125.1, 124.9, 122.5, 35.4, 31.7. HRMS (ESI): m/z $[M + \text{H}]^+$ calcd for $\text{C}_{50}\text{H}_{51}\text{O}_2^+$: 683.3884; found 683.3880 ($|\Delta| = 0.6$ ppm).

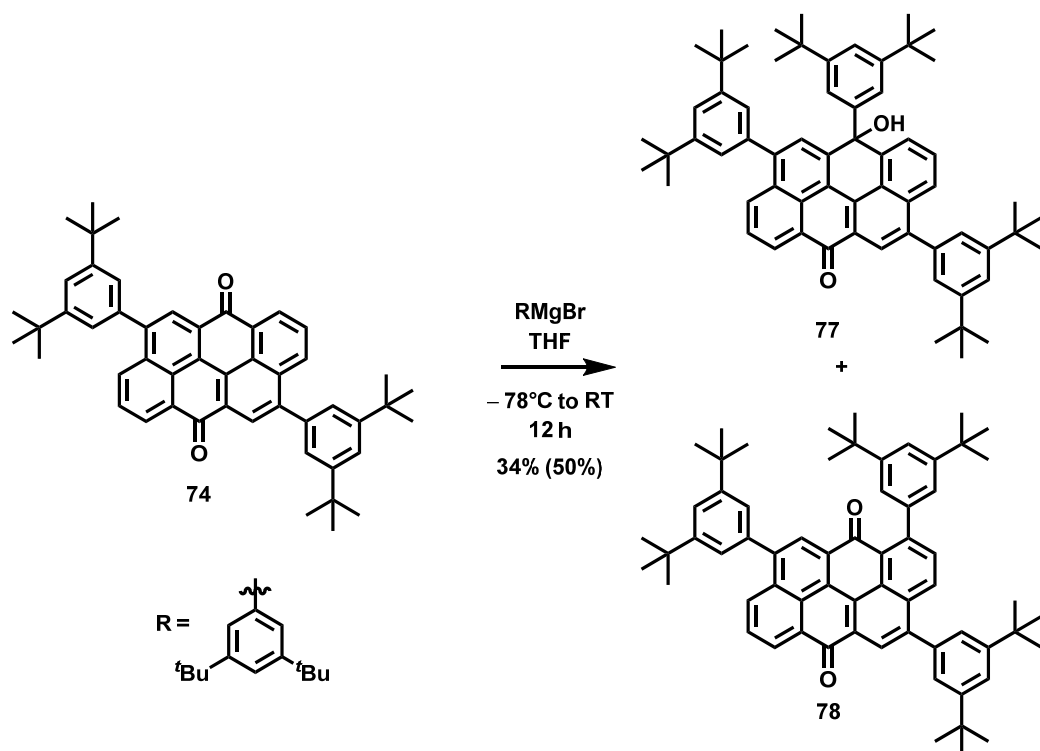


4,6,10,12-Tetrakis(3,5-di-tert-butylphenyl)naphtho[7,8,1,2,3-nopqr]tetraphene (75): A solution of (3,5-di-tert-butylphenyl)magnesium bromide (5.94 mL, 1.74 mmol, 0.29 M solution in THF) was added dropwise to the cooled (-78°C) solution of 4,10-bis(3,5-di-tert-butylphenyl)naphtho[7,8,1,2,3-nopqr]tetraphene-6,12-dione (74, 200 mg, 0.29 mmol) in dry THF (50 mL) under an argon atmosphere. The reaction mixture was stirred at -78°C for 2 h before it was allowed to warm to room temperature over 12 h. Then 3 M HCl (5 mL) and $\text{SnCl}_2 \cdot 2\text{H}_2\text{O}$ (267 mg, 1.16 mmol) was added and the reaction mixture was stirred at room temperature for additional 5 h. Afterwards, water (25 mL) was added and the organic layer

was separated, and the aqueous layer was extracted with CH₂Cl₂ (3 x 20 mL). The combined organic layers were washed with brine, dried over anhydrous Na₂SO₄, and filtered. After evaporation of the solvents, the residue was then purified by column chromatography over silica gel using cyclohexane/CH₂Cl₂ 4:1 and the undesired side product was isolated (**76**, 253 mg, 83%) as a yellow solid.

4,7,10,12-Tetrakis(3,5-di-tert-butylphenyl)naphtho[7,8,1,2,3-nopqr]tetraphen-6-ol

(76): ¹H NMR (500 MHz, CD₂Cl₂, ppm): δ 8.50 (s, 1H), 8.20 (d, *J* = 7.8 Hz, 1H), 8.19 – 8.15 (m, 2H), 7.96 (dd, *J* = 8.2, 7.5 Hz, 1H), 7.96 (s, 1H), 7.90 (d, *J* = 7.8 Hz, 1H), 7.73 (t, *J* = 1.8 Hz, 1H), 7.64 (t, *J* = 1.8 Hz, 1H), 7.63 (d, *J* = 1.8 Hz, 2H), 7.62 – 7.59 (m, 3H), 7.57 (t, *J* = 1.8 Hz, 1H), 7.56 (d, *J* = 1.8 Hz, 2H), 7.51 (d, *J* = 1.8 Hz, 2H), 1.45 (s, 36H, two overlapped signals), 1.44 (s, 18H), 1.41 (s, 18H). ¹³C NMR (126 MHz, CD₂Cl₂, ppm): δ 152.51, 151.34 (two overlapped signals), 151.3, 148.6, 141.2, 141.1, 140.9, 140.7, 140.3, 138.7, 136.0, 135.1, 132.3, 131.8, 131.7, 129.3, 128.5, 127.9, 126.6, 126.3, 125.0, 124.9, 124.8, 124.74, 124.70, 123.7, 123.5, 123.3, 123.2, 122.9, 122.4, 122.0, 121.8, 121.7, 119.0, 117.04, 116.98, 35.6, 35.39, 35.35, 35.3, 31.9, 31.8, 31.7, 31.6. HRMS (APCI): *m/z* [*M*]⁺ calcd for C₇₈H₉₂O₂⁺: 1044.71427; found 1044:71220 (|Δ| = 1.98 ppm).



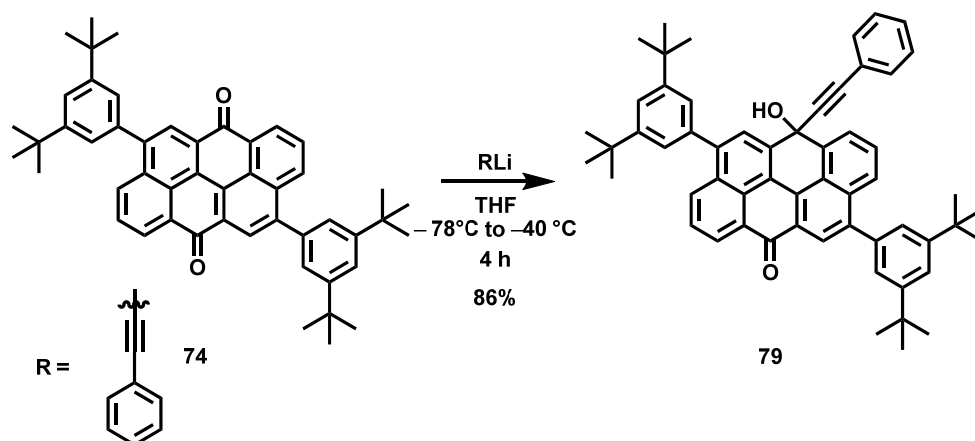
4,10,12-Tris(3,5-di-tert-butylphenyl)-12-hydroxynaphtho[7,8,1,2,3-nopqr]tetraphen-6(12H)-one (77): A solution of (3,5-di-tert-butylphenyl)magnesium bromide (252 μL , 73.2 μmol , 0.29 M solution in THF) was added dropwise to the cooled (-78°C) solution of 4,10-bis(3,5-di-tert-butylphenyl)naphtho[7,8,1,2,3-nopqr]tetraphene-6,12-dione (**74**, 50 mg, 73.2 μmol) in dry THF (10 mL) under an argon atmosphere. The reaction mixture was stirred at -78°C for 2 h before it was allowed to warm to room temperature over 12 h. Then 2 M HCl (10 mL) was added and the organic layer was separated. The aqueous layer was extracted CH_2Cl_2 (3 x 10 mL), the combined organic layers were washed with brine, dried over anhydrous Na_2SO_4 , and filtered. After evaporation of the solvents, the residue was then purified by column chromatography over silica gel using cyclohexane/ CH_2Cl_2 3:2 and two products were isolated, product of 1,2-addition as yellow solid (**77**, 22 mg, 34%) and product of 1,4-addition as red solid (**78**, 34 mg, 50 %).

4,10,12-Tris(3,5-di-tert-butylphenyl)-12-hydroxynaphtho[7,8,1,2,3-nopqr]tetraphen-6(12H)-one (77): $^1\text{H NMR}$ (500 MHz, CDCl_3 , ppm): δ 8.90 (dd, $J = 7.3, 1.3$ Hz, 1H), 8.55 (s, 1H), 8.34 (dd, $J = 8.3, 1.3$ Hz, 1H), 8.04 (dd, $J = 8.3, 1.2$ Hz, 1H), 7.81 (dd, $J = 6.2, 1.1$

Hz, 1H), 7.79 (dd, $J = 8.3, 7.3$ Hz, 1H), 7.69 (s, 1H), 7.63 (dd, $J = 8.3, 7.3$ Hz, 1H), 7.54 (t, $J = 1.8$ Hz, 1H), 7.50 (t, $J = 1.8$ Hz, 1H), 7.45 (d, $J = 1.8$ Hz, 2H), 7.30 – 7.27 (m, 3H), 7.26 (signal hidden under solvent), 2.86 (s, 1H, OH), 1.42 (s, 18H), 1.35 (s, 18H), 1.21 (s, 18H). ^{13}C NMR (126 MHz, CDCl_3 , ppm): δ 184.5, 150.90, 150.87, 150.6, 146.9, 144.5, 143.3, 142.3, 142.1, 139.4, 138.9, 134.0, 133.8, 130.7, 130.3, 129.6, 129.1, 129.0, 128.83, 128.79, 127.3, 127.02, 127.00, 126.9, 125.1, 124.6, 124.3, 121.9, 121.7, 121.0, 120.6, 120.1, 119.2, 75.5, 35.2, 35.1, 35.0, 31.7, 31.62, 31.60. HRMS (APCI): m/z $[M + \text{H}]^+$ calcd for $\text{C}_{64}\text{H}_{73}\text{O}_2^+$: 873.56051; found 873.56869 ($|\Delta| = 2.08$ ppm).

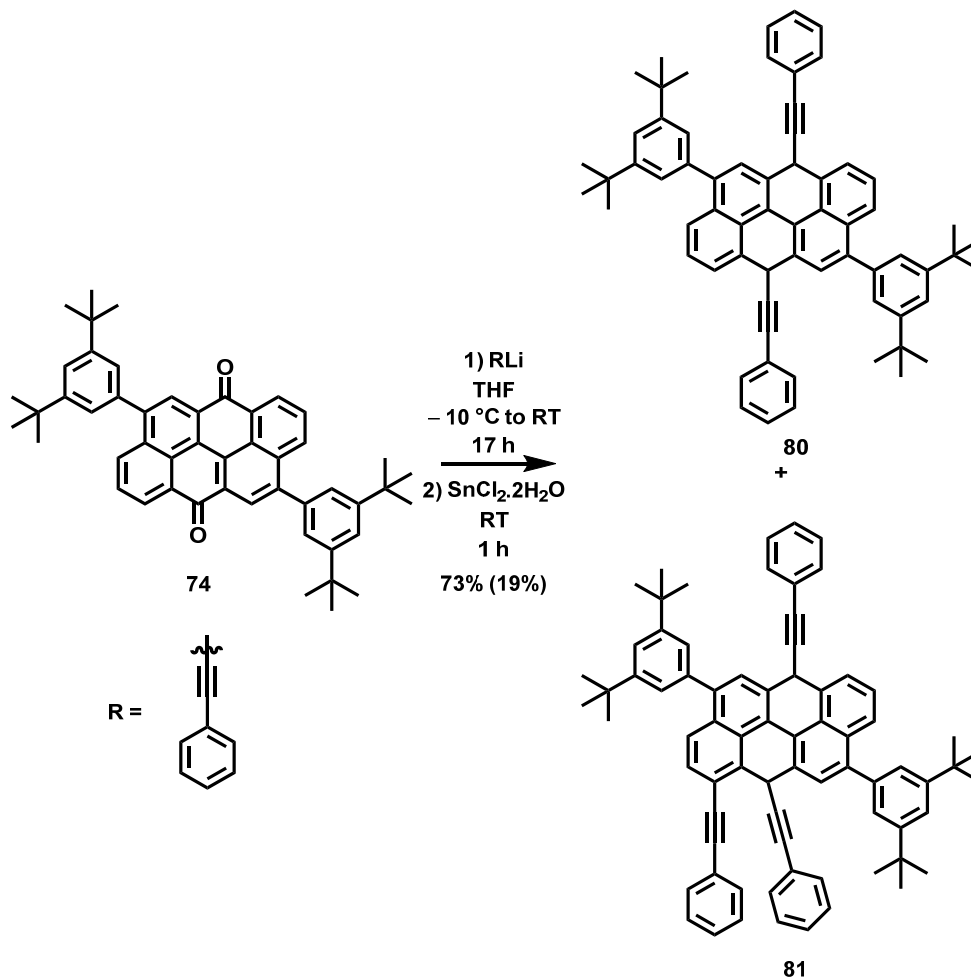
1,4,10-Tris(3,5-di-tert-butylphenyl)naphtho[7,8,1,2,3-nopqr]tetraphene-6,12-dione

(78): ^1H NMR (500 MHz, CDCl_3 , ppm): δ 8.82 (dt, $J = 7.2, 1.3$ Hz, 1H), 8.59 (s, 1H), 8.40 (dd, $J = 8.4, 1.2$ Hz, 1H), 8.39 (s, 1H), 8.31 (d, $J = 8.6$ Hz, 1H), 7.83 (dd, $J = 8.4, 7.3$ Hz, 1H), 7.66 (d, $J = 8.6$ Hz, 1H), 7.59 (t, $J = 1.8$ Hz, 1H), 7.55 (t, $J = 1.8$ Hz, 1H), 7.50 (t, $J = 1.8$ Hz, 1H), 7.45 (d, $J = 1.7$ Hz, 2H), 7.39 (d, $J = 1.8$ Hz, 2H), 7.31 (d, $J = 1.8$ Hz, 2H), 1.44 (s, 18H), 1.40 (s, 18H), 1.39 (s, 18H). ^{13}C NMR (126 MHz, CDCl_3 , ppm): δ 184.1, 184.0, 151.1, 151.06, 150.6, 149.4, 144.4, 144.3, 142.1, 138.5, 134.5, 134.0, 133.2, 133.0, 132.9, 131.1, 130.1, 129.9, 129.8, 129.5, 128.6, 128.1, 127.9, 126.7, 126.4, 125.2, 124.9, 124.8 (two overlapped signals), 122.6, 122.18, 122.16, 121.3, 35.21, 35.19, 35.16, 31.74 (two overlapped signals), 31.70. HRMS (APCI): m/z $[M + \text{H}]^+$ calcd for $\text{C}_{64}\text{H}_{71}\text{O}_2^+$: 871.54486; found 871.54397 ($|\Delta| = 1.02$ ppm).



4,10-Bis(3,5-di-tert-butylphenyl)-12-hydroxy-12-(phenylethynyl)naphtho[7,8,1,2,3-nopqr]tetraphen-6(12H)-one (79): A solution of (phenylethynyl)lithium (120 μL , 62.5 μmol , 0.58 M solution in THF) was added dropwise to the cooled ($-78\text{ }^\circ\text{C}$) solution of 4,10-bis(3,5-di-tert-butylphenyl)naphtho[7,8,1,2,3-nopqr]tetraphene-6,12-dione (**74**, 50 mg, 73.2 μmol) in dry THF (15 mL) under an argon atmosphere. The reaction mixture was stirred at $-78\text{ }^\circ\text{C}$ for 1 h before it was allowed to warm to $-40\text{ }^\circ\text{C}$ over 3 h. Then sat. aq. NH_4Cl (5 mL) was added and the organic layer was separated. The aqueous layer was extracted with CH_2Cl_2 (3 x 10 mL), the combined organic layers were washed with brine, dried over anhydrous Na_2SO_4 , and filtered. After evaporation of the solvents, the residue was then purified by column chromatography over deactivated silica gel (1 % Et_3N) using cyclohexane/ CH_2Cl_2 3:2 as an eluent to afford the desired product (**79**, 49.7 mg, 86%, partial decomposition on silica gel) as a yellow solid. ^1H NMR (500 MHz, CD_2Cl_2 , ppm): δ 8.74 (dd, $J = 7.3, 1.1$ Hz, 1H), 8.52 (dd, $J = 7.3, 1.0$ Hz, 1H), 8.42 (s, 1H), 8.35 (dd, $J = 8.3, 1.0$ Hz, 1H), 8.30 (s, 1H), 8.14 (dd, $J = 8.4, 0.9$ Hz, 1H), 7.83 (dd, $J = 8.3, 7.3$ Hz, 1H), 7.77 (dd, $J = 8.2, 7.3$ Hz, 1H), 7.61 (t, $J = 1.8$ Hz, 1H), 7.57 (t, $J = 1.7$ Hz, 1H), 7.49 (d, $J = 1.7$ Hz, 2H), 7.48 – 7.44 (m, 2H), 7.40 (d, $J = 1.8$ Hz, 2H), 7.36 – 7.27 (m, 3H), 2.82 (s, 1H), 1.43 (s, 18H), 1.41 (s, 18H). ^{13}C NMR (126 MHz, CD_2Cl_2 , ppm): δ 184.2, 151.6, 151.5, 145.6, 142.8, 139.6, 139.4, 139.1, 138.9, 134.34, 134.25, 132.2, 131.6, 130.7, 129.8, 129.5, 129.4,

129.0, 128.9, 128.7, 128.6, 128.4, 127.7, 127.63, 127.57, 125.3, 124.98, 124.96, 124.5, 122.72, 122.67, 122.4, 119.9, 92.8, 88.3, 68.7, 35.50, 35.48, 31.86, 31.85. HRMS (APCI): m/z $[M + H]^+$ calcd for $C_{58}H_{57}O_2^+$: 785.43531; found 785.43417 ($|\Delta| = 1.45$ ppm).



4,10-Bis(3,5-di-tert-butylphenyl)-6,12-bis(phenylethynyl)-6,12-dihydronaphtho

[7,8,1,2,3-nopqr]tetraphene (81): An 4,10-bis(3,5-di-tert-butylphenyl)naphtho[7,8,1,2,3-nopqr]tetraphene-6,12-dione (**74**, 50 mg, 73.2 μ mol) was added in one portion under an positive argon pressure to the cooled (-10 °C) mixture of lithium phenylacetylide (1.26 mL, 0.73 mmol, 0.58 M solution in THF) in dry THF (1 mL) and the mixture was stirred at -10 °C for 2 h before it was allowed to warm up to room temperature overnight. Then 3 M HCl (3 mL) and SnCl₂·2H₂O (66.1 mg, 0.29 mmol) was added and the reaction mixture was stirred at room temperature for additional 1 h. Afterwards, water (10 mL) was added, the

organic layer was separated. The aqueous layer was extracted with CH₂Cl₂ (3 x 10 mL) and the combined organic layers were washed with brine, dried over Na₂SO₄, and filtered. After evaporation of the solvents, the residue was then purified by column chromatography over silica gel using cyclohexane to cyclohexane/CH₂Cl₂ 95:5 as an eluent to afford the desired product (**80**, 45.7 mg, 73%) as a deep-red solid and product of triple addition (**81**, 13.5 mg, 19%) as deep-purple solid.

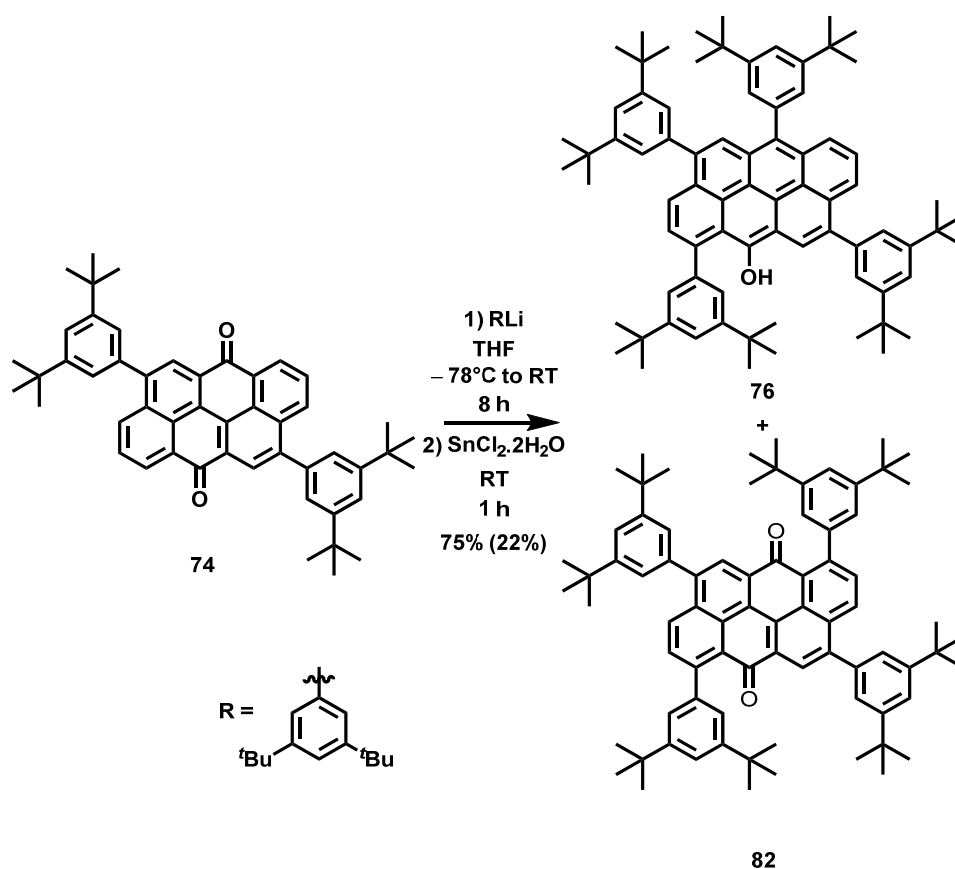
4,10-Bis(3,5-di-tert-butylphenyl)-6,12-bis(phenylethynyl)-6,12-dihydronaphtho

[7,8,1,2,3-nopqr]tetraphene (80): ¹H NMR (500 MHz, CDCl₃, ppm): δ 9.26 (dd, *J* = 8.0, 0.8 Hz, 2H), 8.89 (s, 2H), 8.48 (dd, *J* = 7.6, 0.7 Hz, 2H), 8.25 (t, *J* = 7.8 Hz, 2H), 7.85-7.82 (m, 4H), 7.73 (d, *J* = 1.8 Hz, 4H), 7.63 (t, *J* = 1.8 Hz, 2H), 7.50 – 7.39 (m, 6H), 1.49 (s, 36H). ¹³C NMR (126 MHz, CDCl₃, ppm): δ 151.1, 142.7, 140.0, 132.2, 131.9, 131.3, 131.3, 128.8, 128.70, 127.2, 126.7, 125.7, 124.9, 124.8, 123.8, 123.1, 121.8, 121.7, 116.9, 102.2, 87.8, 35.3, 31.8. (three signals could not have been identified due signal overlap) HRMS (APCI): *m/z* [M + H]⁺ calcd for C₆₆H₆₁O₂⁺: 853.47678; found 853.47580 (|Δ| = 1.15ppm).

4,10-Bis(3,5-di-tert-butylphenyl)-1,6,12-tris(phenylethynyl)-6,12-dihydronaphtho

[7,8,1,2,3-nopqr]tetraphene (81): ¹H NMR (500 MHz, CDCl₃, ppm): δ 9.25 (dd, *J* = 8.0, 0.7 Hz, 1H), 9.11 (s, 1H), 8.94 (s, 1H), 8.53 (dd, *J* = 7.6, 0.7 Hz, 1H), 8.48 (d, *J* = 8.1 Hz, 1H), 8.40 (d, *J* = 8.1 Hz, 1H), 8.25 (t, *J* = 7.9 Hz, 1H), 7.85 – 7.81 (m, 2H), 7.73 (d, *J* = 1.8 Hz, 2H), 7.71 (d, *J* = 1.8 Hz, 2H), 7.63 (t, *J* = 1.8 Hz, 1H), 7.61 (t, *J* = 1.8 Hz, 1H), 7.57 – 7.52 (m, 2H), 7.51 – 7.42 (m, 5H), 7.25 – 7.12 (m, 6H), 1.49 (s, 18H), 1.48 (s, 18H). ¹³C NMR (126 MHz, CDCl₃, ppm): δ 151.1, 151.0, 143.1, 142.5, 140.0, 139.9, 134.7, 134.0, 132.2, 131.9, 131.8, 131.4, 131.3, 131.2, 130.1, 128.8, 128.7, 128.3, 128.2, 128.1, 127.9, 127.5, 127.0, 125.9, 125.3, 124.8, 124.2, 124.0, 123.8, 123.7, 122.8, 121.9, 121.82, 121.80, 119.8, 117.6, 117.5, 116.8, 106.3, 102.6, 100.0, 92.3, 89.6, 87.8, 35.28, 35.25, 29.85 (two overlapped peaks), (out of 62 signals expected from this molecule, only 48 signals could be detected within the resolution limits of the NMR technique because of the signal overlap).

HRMS (APCI): m/z $[M + H]^+$ calcd for $C_{74}H_{65}^+$: 953.50808; found 953.50601 ($|\Delta| = 2.17$ ppm).



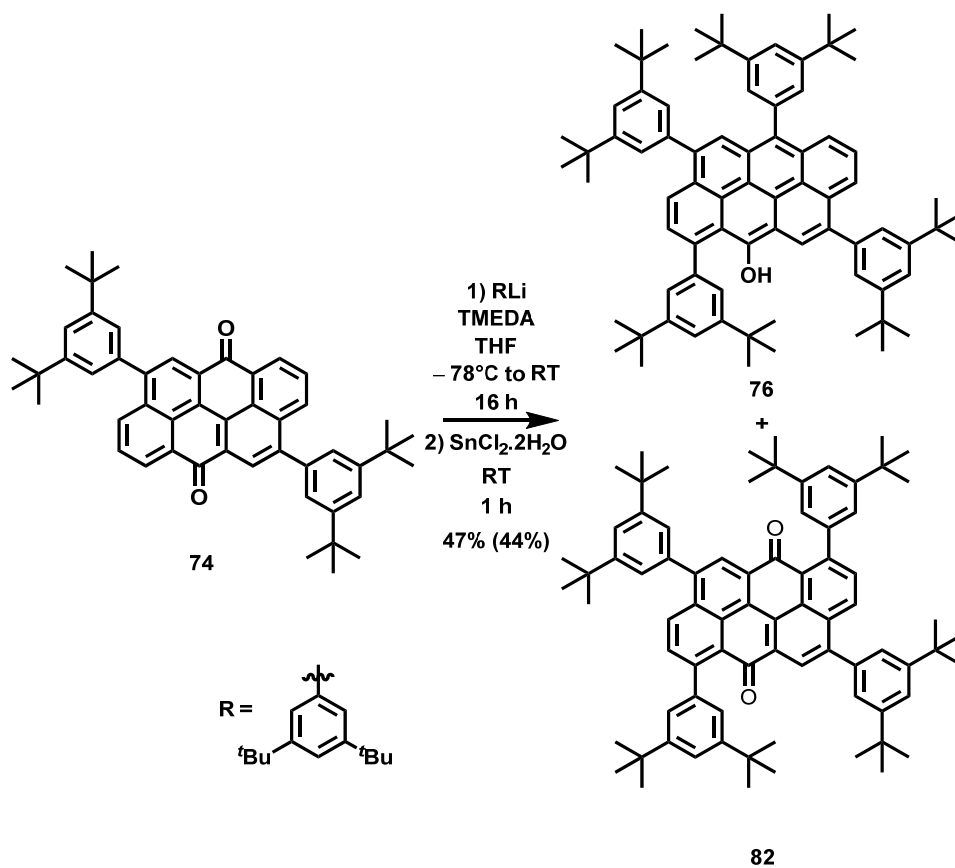
4,7,10,12-Tetrakis(3,5-di-tert-butylphenyl)naphtho[7,8,1,2,3-nopqr]tetraphen-6-ol

(76): *n*BuLi (448 μ L, 0.72 mmol, 1.6 M solution in hexanes) was added dropwise to the cooled (-78 °C) solution of 1-bromo-3,5-di-tert-butylbenzene (178 mg, 0.66 mmol) in dry THF (5 mL) and the mixture was stirred at -78 °C for 1 h. Then 4,10-bis(3,5-di-tert-butylphenyl)naphtho [7,8,1,2,3-nopqr]tetraphene-6,12-dione (74, 35 mg, 51.2 μ mol) was added in one portion under an positive argon pressure and the mixture was stirred at -78 °C for 2 h. Afterwards, the mixture was allowed to warm to room temperature over 5 h. Then 3 M HCl (3 mL) and SnCl₂·2H₂O (66.1 mg, 0.29 mmol) were added and the reaction mixture was stirred at room temperature for additional 1 h. Afterwards, water (10 mL) was added and the organic layer was separated. The aqueous layer was extracted with CH₂Cl₂ (3 x 10

mL) and the combined organic layers were washed with brine, dried over Na₂SO₄, and filtered. After evaporation of the solvents, the residue was then purified by column chromatography over silica gel using cyclohexane to cyclohexane/CH₂Cl₂ 4:1 and two products were isolated, product (**76**, 39.9 mg, 75%) as a yellow solid and product (**83**, 11.1mg, 22%) as orange solid.

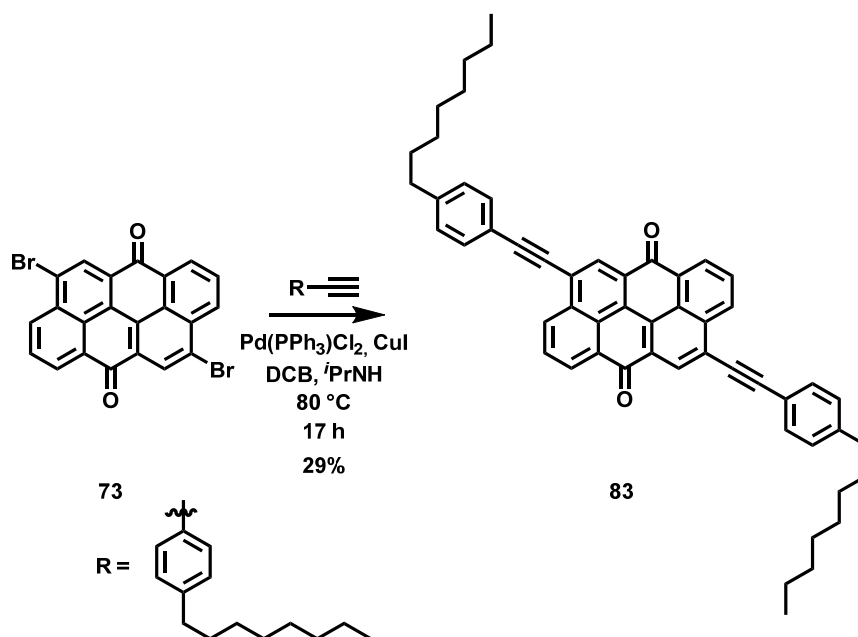
1,4,7,10-Tetrakis(3,5-di-tert-butylphenyl)naphtho[7,8,1,2,3-nopqr]tetraphene-6,12-

dione (82): ¹H NMR (500 MHz, CDCl₃, ppm): δ 8.43 (s, 2H), 8.32 (d, *J* = 8.6 Hz, 2H), 7.65 (d, *J* = 8.6 Hz, 2H), 7.55 (t, *J* = 1.8 Hz, 2H), 7.50 (t, *J* = 1.8 Hz, 2H), 7.40 (d, *J* = 1.8 Hz, 4H), 7.32 (d, *J* = 1.8 Hz, 4H), 1.40 (s, 36H), 1.40 (s, 36H). ¹³C NMR (126 MHz, CDCl₃, ppm): δ 184.3, 151.0, 150.5, 149.1, 144.1, 142.2, 138.7, 133.7, 132.8, 132.6, 131.3, 129.19, 129.18, 126.9, 126.6, 125.1, 124.9, 122.7, 122.1, 121.3, 120.6, 35.20, 35.16, 31.8, 31.7. (contains impurity of ditertbutyl phenyl nature) HRMS (ESI): *m/z* [*M* + Na]⁺ calcd for C₇₈H₉₀O₂Na⁺: 1081.6833; found 1081.6829 (|Δ| = 0.4 ppm).



4,7,10,12-Tetrakis(3,5-di-tert-butylphenyl)naphtho[7,8,1,2,3-nopqr]tetraphen-6-ol

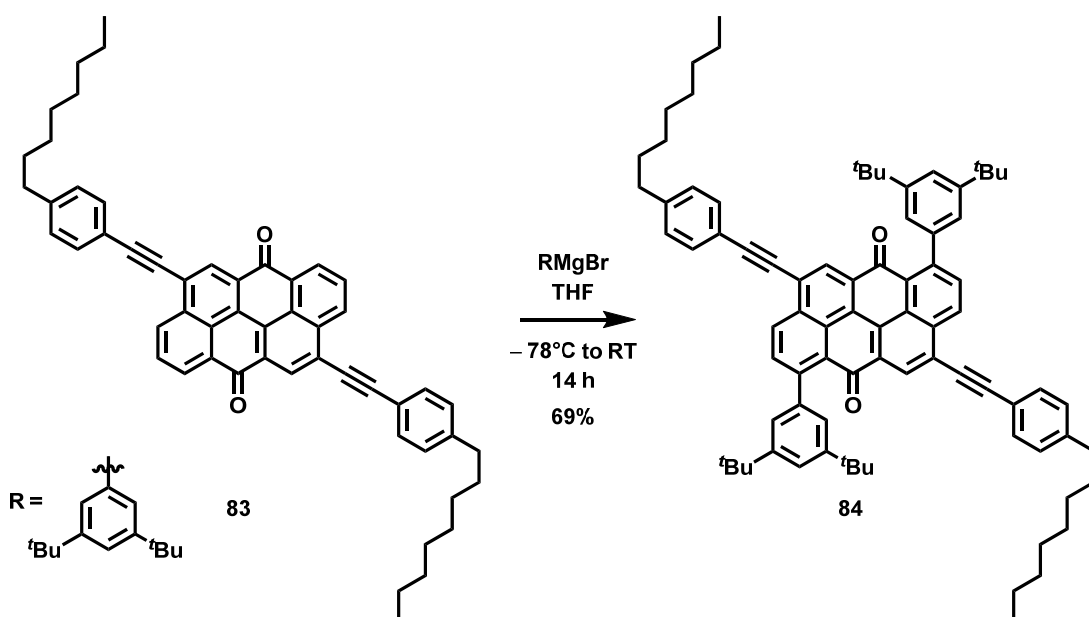
(76): *n*BuLi (448 μ L, 0.72 mmol, 1.6 M solution in hexanes) was added dropwise to the cooled (-78 $^{\circ}$ C) solution of 1-bromo-3,5-di-tert-butylbenzene (178 mg, 0.66 mmol) in dry THF (5 mL) and the mixture was stirred at -78 $^{\circ}$ C for 1 h before it was allowed to warm to -20 $^{\circ}$ C over 1 h. Then TMEDA (386 μ L, 2.56 mmol) was added dropwise and the mixture was stirred at -20 $^{\circ}$ C for 30 min and then it was cooled down again to -78 $^{\circ}$ C. Then 4,10-bis(3,5-di-tert-butylphenyl)naphtho[7,8,1,2,3-nopqr]tetraphene-6,12-dione (**74**, 35 mg, 73.2 μ mol) was added in one portion under an positive argon pressure and the mixture was stirred at -78 $^{\circ}$ C for 1 h. Afterwards, the mixture was allowed to warm to room temperature overnight. Then 3 M HCl (3 mL) and SnCl₂·2H₂O (66.1 mg, 0.29 mmol) was added and the reaction mixture was stirred at room temperature for additional 1 h. Afterwards, water (10 mL) and CH₂Cl₂ were added and the organic layer was separated. The aqueous layer was extracted with CH₂Cl₂ (3 x 10 mL) and the combined organic layers were washed with brine, dried over Na₂SO₄, and filtered. After evaporation of the solvents, the residue was then purified by column chromatography over silica gel using cyclohexane to cyclohexane/CH₂Cl₂ 4:1 and two products were isolated, product (**76**, 25.3 mg, 47%) as a yellow solid and product (**82**, 24.1mg, 44%) as orange solid.



4,10-Bis((4-octylphenyl)ethynyl)naphtho[7,8,1,2,3-nopqr]tetraphene-6,12-dione (83**):**

A dry Schlenk tube (50 mL) was charged with 4,10-dibromonaphtho[7,8,1,2,3-nopqr]tetraphene-6,12-dione (**73**, 500 mg, 1.08 mmol), 1-ethynyl-4-octylbenzene (509 mg, 2.38 mmol), Pd(PPh₃)₂Cl₂ (152 mg, 0.22 mmol), and CuI (32.9 mg, 0.173 mmol) and it was kept under vacuum for 30 min. before it was evacuated and backfilled with argon three times. Then freshly deaerated mixture of 1,2-dichlorobenzene (15 mL) and *i*Pr₂NH (2 mL) was added and the mixture was gradually heated to 80 °C over 45 min. The mixture was then stirred at 80 °C under an argon atmosphere for 16 h. The mixture was then allowed to cool down to room temperature, diluted with MeOH (100 mL) and filtered. The residue was purified by column chromatography over silica gel using CH₂Cl₂ to CH₂Cl₂/MeOH 95:5 as an eluent to afford the desired product (**83**, 232 mg, 29%) as a purple solid. ¹H NMR (500 MHz, CD₂Cl₂, ppm): δ 8.85 (dd, *J* = 8.2, 1.2 Hz, 2H), 8.76 (dd, *J* = 7.3, 1.2 Hz, 2H), 8.66 (s, 2H), 7.97 (dd, *J* = 8.2, 7.3 Hz, 2H), 7.64 (d, *J* = 8.2, 4H), 7.29 (*J* = 8.2, 4H), 2.68 (t, *J* = 7.7, 4H), 1.67 (p, *J* = 7.7 Hz, 4H), 1.40 – 1.27 (m, 20H), 0.89 (t, *J* = 6.9, 6H). ¹³C NMR (126 MHz, CDCl₃, ppm): δ 182.5, 144.7, 134.02, 134.01, 133.96, 132.0, 131.4, 129.6, 129.50, 129.45, 128.9, 128.4, 127.7, 127.2, 124.7, 119.9, 98.6, 86.3, 36.2, 32.1, 31.4, 29.6,

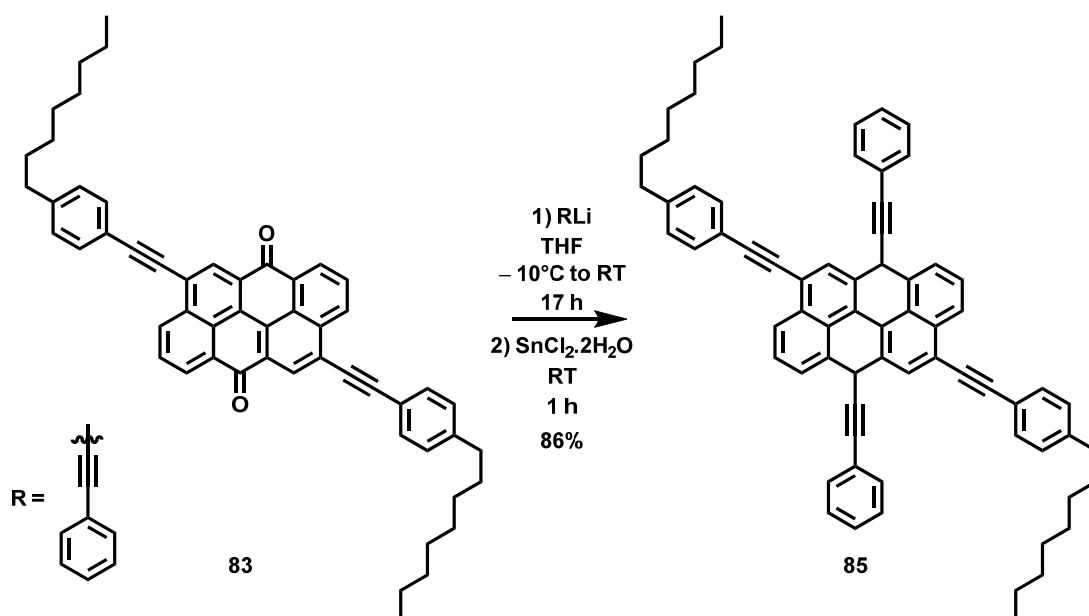
29.5, 29.4, 22.8, 14.3. (two signals could not have been identified due signal overlap) HRMS (APCI): m/z $[M + H]^+$ calcd for $C_{54}H_{51}O_2^+$: 731.38836; found 731.38688 ($|\Delta| = 2.02$ ppm).



1,7-bis(3,5-di-tert-butylphenyl)-4,10-bis((4-octylphenyl)ethynyl)naphtho[7,8,1,2,3-nopqr]tetraphene-6,12-dione (84): A solution of (3,5-di-tert-butylphenyl)magnesium bromide (1.09 mL, 0.54 mmol, 0.5 M solution in THF) was added dropwise to the cooled (-78°C) solution of 4,10-bis((4-octylphenyl)ethynyl)naphtho[7,8,1,2,3-nopqr]tetraphene-6,12-dione (**83**, 31.5 mg, 54.4 μmol) in dry THF (10 mL) under an argon atmosphere. The reaction mixture was stirred at -78°C for 2 h before it was allowed to warm to room temperature over 12 h. Then 3 M HCl (3 mL) and $\text{SnCl}_2 \cdot 2\text{H}_2\text{O}$ (50.1 mg, 218 μmol) was added and the reaction mixture was stirred at room temperature for additional 1 h. Afterwards, water (10 mL) was added, the organic layer was separated, and the aqueous layer was extracted with CH_2Cl_2 (3 x 10 mL). The combined organic layers were washed with brine, dried over anhydrous Na_2SO_4 , and filtered. After evaporation of the solvents, the residue was then purified by column chromatography over silica gel using cyclohexane to cyclohexane/ CH_2Cl_2 4:1 as an eluent to afford the product (**84**, 36.1 mg, 69%) as a purple solid. ^1H NMR (500 MHz, CD_2Cl_2 , ppm): δ 8.84 (d, $J = 8.4$ Hz, 2H), 8.56 (s, 1H), 7.80 (d,

133

$J = 8.4$ Hz, 2H), 7.61 (d, $J = 8.2$ Hz, 2H), 7.56 (t, $J = 1.8$ Hz, 2H), 7.35 (d, $J = 1.8$ Hz, 4H), 7.27 (d, 4H), 2.66 (t, $J = 7.6$ Hz, 4H), 1.64 (p, $J = 7.6$ Hz, 4H), 1.37 – 1.23 (m, 20H), 0.91 – 0.86 (m, 6H). ^{13}C NMR (126 MHz, CD_2Cl_2 , ppm): Strong aggregation and low solubility of **84** did not allow us to record an unequivocal ^{13}C NMR spectrum of monomeric **84**. HRMS (APCI): m/z $[M + \text{H}]^+$ calcd for $\text{C}_{82}\text{H}_{91}\text{O}_2^+$: 1107.70136; found 1107.70058 ($|\Delta| = 0.71$ ppm).



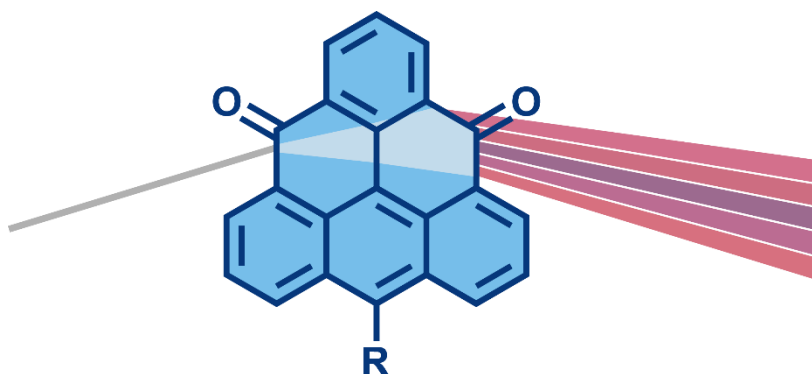
4,10-Bis((4-octylphenyl)ethynyl)-6,12-bis(phenylethynyl)-6,12-dihydronaphtho

[7,8,1,2,3-nopqr]tetraphene (85): An 4,10-bis((4-octylphenyl)ethynyl)naphtho[7,8,1,2,3-nopqr]tetraphene-6,12-dione (**83**, 31.5 mg, 43.1 μmol) was added in one portion under an positive argon pressure to the cooled (-10 °C) mixture of lithium phenylacetylide (0.74 mL, 0.43 mmol, 0.58 M solution in THF) in dry THF (1 mL) and the mixture was stirred at -10 °C for 2 h before it was allowed to warm up to room temperature overnight. Then 3 M HCl (2 mL) and $\text{SnCl}_2 \cdot 2\text{H}_2\text{O}$ (38.9 mg, 0.17 mmol) was added and the reaction mixture was stirred at room temperature for additional 1 h. Afterwards, water (10 mL) was added, the organic layer was separated. The aqueous layer was extracted with CH_2Cl_2 (3 x 10 mL) and the combined organic layers were washed with brine, dried over Na_2SO_4 , and filtered. After evaporation of the solvents, the residue was then purified by column chromatography over

silica gel using cyclohexane/toluene 4:1 to toluene as an eluent to afford the desired product (**85**, 33.4 mg, 86%) as a deep-purple solid. ^1H NMR (600 MHz, CD_2Cl_2 , ppm): δ 9.15 (d, $J = 8.0$ Hz, 2H), 9.02 (s, 2H), 8.88 (d, $J = 7.3$ Hz, 2H), 8.31 (t, $J = 7.7$ Hz, 2H), 8.00 – 7.93 (m, 4H), 7.76 (d, $J = 8.0$ Hz, 4H), 7.59 – 7.50 (m, 6H), 7.32 (d, $J = 8.0$ Hz, 4H), 2.75 (t, $J = 7.7$ Hz, 4H), 1.74 (p, $J = 7.7$ Hz, 4H), 1.48 – 1.32 (m, 20H), 0.97 – 0.94 (m, 6H). ^{13}C NMR (150 MHz, CD_2Cl_2 , ppm): δ 144.0, 131.84, 131.83, 130.8, 130.76, 130.75, 130.5, 130.3, 128.7, 128.54, 128.52, 126.8, 126.1, 124.7, 123.3, 122.6, 122.2, 120.7, 120.2, 116.8, 102.7, 99.5, 95.8, 87.4, 86.8, 79.5, 35.9, 31.7, 31.0, 29.3, 29.2, 29.1, 22.5, 14.0. HRMS (APCI): m/z $[M + \text{H}]^+$ calcd for $\text{C}_{70}\text{H}_{61}^+$: 901.47678; found 901.47742 ($|\Delta| = 0.71$ ppm).

CHAPTER IV:

DONOR–ACCEPTOR TRIANGLES



The following section has been published in

Synthesis **2017**, 47, 899–909.

Donor–Acceptor Molecular Triangles

Peter Ribar, Tomáš Šolomek^[173], Loïc Le Pleux, Daniel Häussinger, Alessandro Prescimone, Markus Neuburger, Michal Juríček*

University of Basel, Department of Chemistry, St. Johannis-Ring 19, 4056 Basel, Switzerland

michal.juricek@unibas.ch

Dedicated to Professor Paul Knochel on the occasion of his Presidency at the 51st Bürgenstock Conference

Key Words: donor–acceptor molecules, fluorescence, redox properties, solvatochromism, triangulene

4.1 IMPACT OF THE WORK

“Interest in triangulene and its precursors since its first prediction by Clar was due to its unique diradical character, as described in the previous two chapters. The precursors of triangulene, such as diketotriangulene, can absorb light and accept electrons and, therefore, these compounds might be of interest as acceptor units in donor–acceptor systems for different applications. Several groups have studied the redox properties of diketotriangulene for its use in secondary batteries, however, its optical properties remain unknown. Due to its unique triangular shape, diketotriangulene could be a very interesting material, as its packing in the solid state might be very different from other known acceptor systems, such as perylenediimide. As parent diketotriangulene is very poorly soluble, we synthesised its analogue with three tert-butyl groups. The enhanced solubility of this compound allowed us to prepare several donor–acceptor systems and to study their absorption, fluorescence, and redox properties.

Our findings were published two years ago in *Synthesis* **2017**, *47*, 899–909. and this manuscript is included as one chapter in the thesis. The chapter was reformatted to match the style of the thesis (such as compound, citation and page numbering as well as scheme and figure design). This work was highlighted in *Synfacts* **2017**, *13*, 0363. by Timothy M. Swager.”

4.2 ABSTRACT

The synthesis and optoelectronic properties of five donor–acceptor molecules, featuring an electron-acceptor unit made of six fused benzenoid rings that resembles an equilateral triangle, are described. These molecular ‘triangles’ were synthesized in eight steps from simple building blocks such that the electron-donor substituents could be installed in the last step by means of the Suzuki cross-coupling reaction. All molecules absorb and emit visible light in the region of around 450–650 and 550–850 nm, respectively, exhibit solvatochromism, and possess up to four redox states.

4.3 INTRODUCTION

Organic molecules that absorb or emit visible light play an important role in many research areas, including renewable-energy production,^[174] material science,^[175] and biological imaging,^[176] to name just a few. Their optoelectronic properties arise from the presence of a chromophoric unit, a metal or a π -conjugated core, that is embedded in the structure of these molecules, and are affected by various structural parameters of the chromophore. Parameters such as size and shape also affect the way in which molecules ‘pack’ within a bulk material or bind to a specific receptor, therefore, they need to be considered carefully when designing molecules for a specific application.

Most of the known π -conjugated chromophores have shapes reminiscent of a square (*e.g.*, porphyrins^{[174b], [177]}), a rectangle (*e.g.*, perylenediimides^[174b, 174d, 178]), or a sphere (*e.g.*, fullerenes^[179]). Chromophores with a shape that resembles an equilateral triangle, such as systems based on triangulene (Figure 1, top center, R = H), are far less common and rather unique. First proposed^[180] by Clar in 1953, triangulene represents an archetype of molecules with non-Kekulé structures. It contains two unpaired electrons, each occupying one of the two degenerate singly occupied molecular orbitals (SOMOs). Although the parent compound remains elusive and only two substituted derivatives of triangulene (*e.g.*, R = O⁻

) have been detected^[181] in solution this far, structural alterations of the highly reactive diradical triangulene core have led to the preparation of various types of stable triangulene-based chromophores (Figure 4.1).

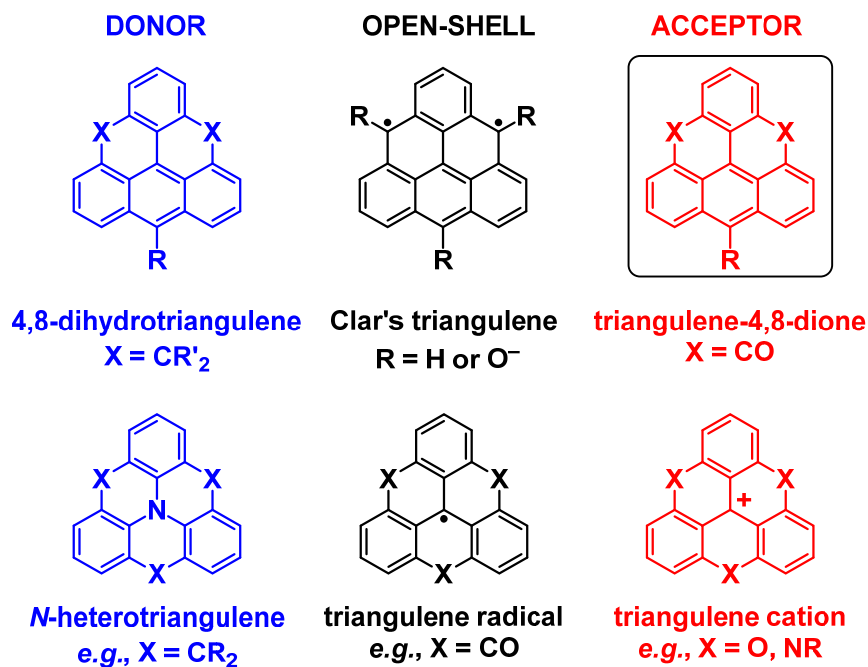
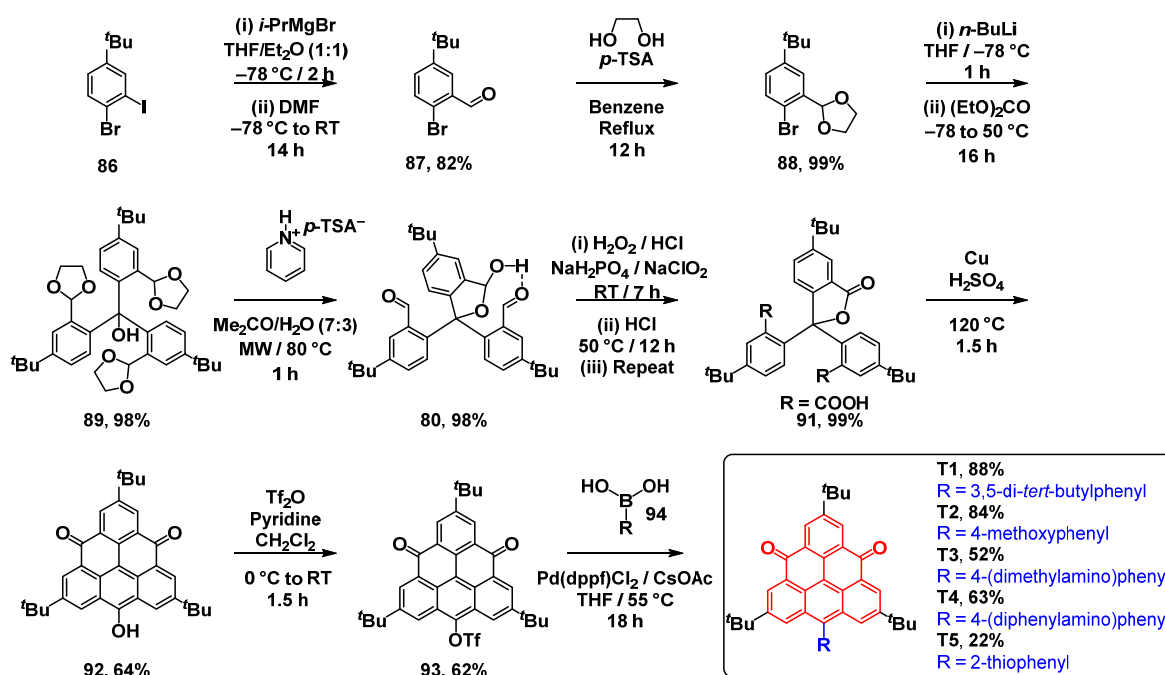


Figure 4.1: Structural formulae of various electron-donor (blue), open-shell (black), and electron-acceptor (red) derivatives of triangulene.

One type, obtained^[182] by peripheral installment of three oxo or dicyanomethylene functionalities in the center of each side of triangulene, is a triangulene monoradical system (Figure 1, bottom center, X is C=O or C=C(CN)₂). This type features one unpaired electron delocalized over the entire core and a pair of degenerate lowest unoccupied molecular orbitals (LUMOs). Substituted derivatives (Br and *tert*-butyl) of these triangulene radicals were found^[182] to be air-stable and redox-active, featuring as many as four (X is C=O) and eight (X is C=C(CN)₂) reversible redox states (the first oxidation species is shown in Figure 4.1, bottom right in red). When the carbon atoms in the center of each side of triangulene are replaced^[183] by X = O, S, NR, or CR₂, again, a triangulene radical system is obtained. In this case, however, the oxidized cationic forms, known as the triangulanium ions (Figure 4.1,

bottom right), are more stable. An additional replacement of the central carbon atom by a nitrogen atom gives^[184] a neutral *N*-hetero-triangulene system (Figure 4.1, bottom left), which has either electron-donating (X is CR₂) or electron-accepting (X is C=O) character. The triangulenium and *N*-heterotriangulene systems were shown to be redox-active, albeit to a lesser extent compared with triangulene radicals, highly fluorescent, as well as to exhibit^{183b} electrochemically induced chemiluminescence.



Scheme 1: Synthesis of the target compounds T1–T5.

Another type, formed when two carbon atoms in the center of each side of triangulene are replaced^[185] with X = CR'₂ (Figure 4.1, top left) is a neutral closed-shell triangulene system. Molecules of this type comprise a 9-phenylanthracene moiety, in which the phenyl subunit is co-planar with the anthracene subunit, in contrast to the parent compound 9-phenylanthracene that displays ~90° torsion angle between the two aryl subunits. On account of this planarization, substituted (R, R') 4,8-dihydrotriangulenes (blue) exhibit^[185] bathochromic shifts in their absorption and emission spectra, as well as higher quantum yields, compared to those of non-planar 9-phenylanthracene.

In addition to positively charged triangulenes, neutral electron-acceptor systems (Figure 4.1, top right) can be conceptualized, for example, when X is C=O, leading to triangulene-4,8-diones (red). Although the parent triangulene-4,8-dione was prepared^[180] more than 60 years ago, only its absorption spectrum reported in the original work by Clar ($\lambda_{\text{max}} \sim 500$ nm in benzene) is available to us as the source of information with regard to its optoelectronic properties. Based on this early seminal work, the lowest-energy absorption of triangulene-4,8-dione seems to be quite similar to that of perylenediimide (PDI; $\lambda_{\text{max}} = 526$ nm in CH_2Cl_2),^[186] one of the most widely used^[178] dyes and electron-acceptors. Inspired by this similarity, we examined the potential use of triangulene-4,8-dione as an electron-acceptor building block, by designing and synthesizing a series of compounds (**T1–T5**, Scheme 1), where triangulene-4,8-dione is linked to an electron-donor unit. In addition, we investigated the optoelectronic properties of these donor (blue)–acceptor (red) systems by means of UV/Vis spectroscopy, cyclic voltammetry (CV), and DFT calculations, and, based on these results, we compare triangulene-4,8-dione and PDI as electron-acceptors.

To favor the electron-communication between the donor and the acceptor units, the electron-donor unit (R) was introduced at the 12-position, at which triangulene-4,8-dione displays the highest coefficient in the LUMO. In addition, three bulky *tert*-butyl substituents were introduced in the apices of the triangle (positions 2, 6, and 10) to render sufficient solubilities of the target compounds. 12-Hydroxy-triangulene-4,8-dione **92** (Scheme 1) equipped with three *tert*-butyl substituents was chosen as the precursor for the preparation of the target compounds **T1–T5**, as its one-step transformation to a triflate derivative **93** would allow for a direct access to **T1–T5** by means of the Suzuki cross-coupling reaction. Compound **92** was reported^[182c] previously, however, only a brief summary of synthetic protocols for its preparation from 1-bromo-4-(*tert*-butyl)-benzene was described. The lack of experimental details did not allow us to successfully reproduce the original synthesis,

141

therefore, a new synthetic route for the preparation of **92** was developed in our laboratory (Scheme 4.1).

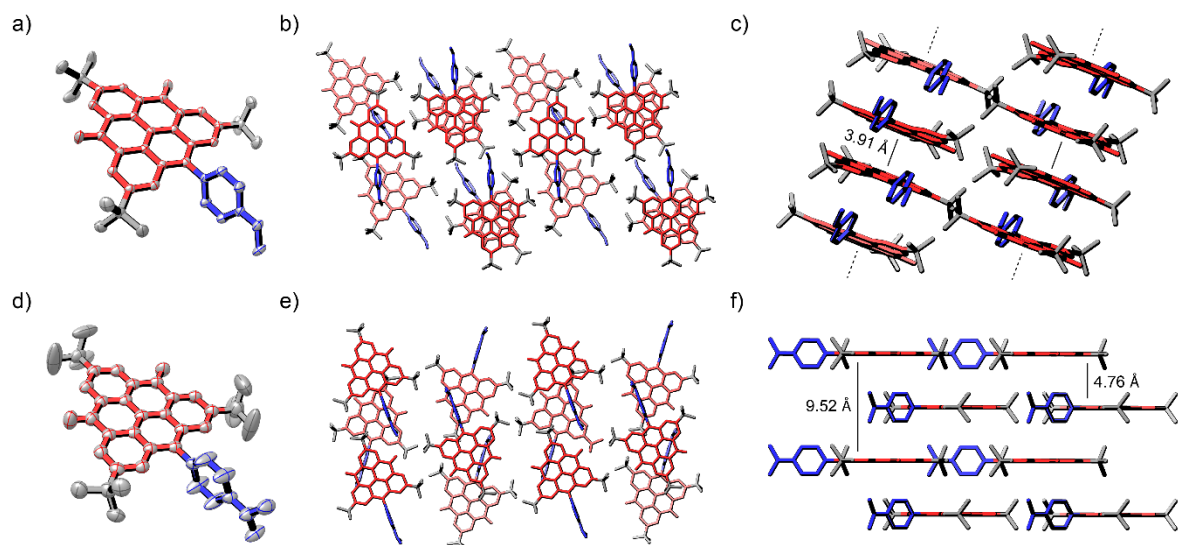


Figure 2: Different crystallographic views of the solid-state (super)structures of **T2** (a–c) and **T3** (d–f): (a,d) perspective, (b) along *c*-axis, (c) along *b*-axis, (e) along *a*-axis, and (f) along *b*-axis (thermal ellipsoids are shown at the 80% probability level).

4.4 RESULTS AND DISCUSSION

Our method employs 1-bromo-4-(*tert*-butyl)-2-iodobenzene (**86**) as the starting material, which was prepared in three steps from 1-bromo-4-(*tert*-butyl)benzene by following protocols reported^[187] previously. Selective iodine–magnesium bromide exchange was performed with isopropylmagnesium bromide at -78 °C, which upon the addition of DMF afforded the desired aldehyde **87** in 82% yield. Subsequent protection of the aldehyde moiety with ethylene glycol and bromine–lithium exchange with *n*-BuLi at -78 °C allowed us to prepare triphenylmethanol **89** by reacting slightly more than three equivalents of the lithium salt with one equivalent of diethyl carbonate. Notably, the desired intermediate **89** could be isolated in 98% yield by crystallization from hexane, without the need for purification by column chromatography. The removal of the ethylene glycol protecting groups proceeded best when pyridinium *para*-toluenesulfonate was employed^[188] as the acid under microwave irradiation (80 °C). Under these conditions, formation of unknown side-

products, which occurred on heating in an oil bath, was minimized and desired trisaldehyde **90** was obtained in 98% yield. Interestingly, one of the aldehyde functionalities in **90** forms a hemiacetal with the hydroxyl group localized at the central carbon atom and the hemiacetal hydroxyl group forms a hydrogen bond with one of the two remaining aldehyde functionalities. Accordingly, three sets of signals were observed for the phenyl and *tert*-butyl groups in the ^1H NMR spectrum of **90**, as well as two sets of signals for the two aldehyde moieties and one for the hemiacetal group. The three aldehyde moieties were subsequently oxidized^[189] to carboxylic acid functionalities by use of hydrogen peroxide and sodium chlorite as the oxidants in two cycles, affording compound **91** in 99% yield, again without the need for column chromatography. Similarly to **90**, one of the carboxylic acid functionalities in **91** forms a lactone with the hydroxyl group localized at the central carbon atom. In the sixth step, three-fold intramolecular Friedel–Crafts acylation in the presence of concentrated H_2SO_4 and Cu, which reduces the initially formed triarylmethyl cation, gave upon dilution with water and filtration, the hydroxyl compound **92** in 64% yield. Because of the limited solubility of **92**, its NMR spectra were acquired in D_2SO_4 . In the ^1H NMR spectrum, only one aromatic and one aliphatic signals were observed on account of the three-fold symmetry of the doubly protonated compound. Finally, a transformation of the hydroxyl group into the triflate group yielded compound **93**, a direct precursor of the target compounds **T1–T5**. Triflate **93** is prone to hydrolysis, therefore, no aqueous work-up was performed and deactivated silica gel (1% TEA) was used for column chromatography to achieve a yield of 62%.

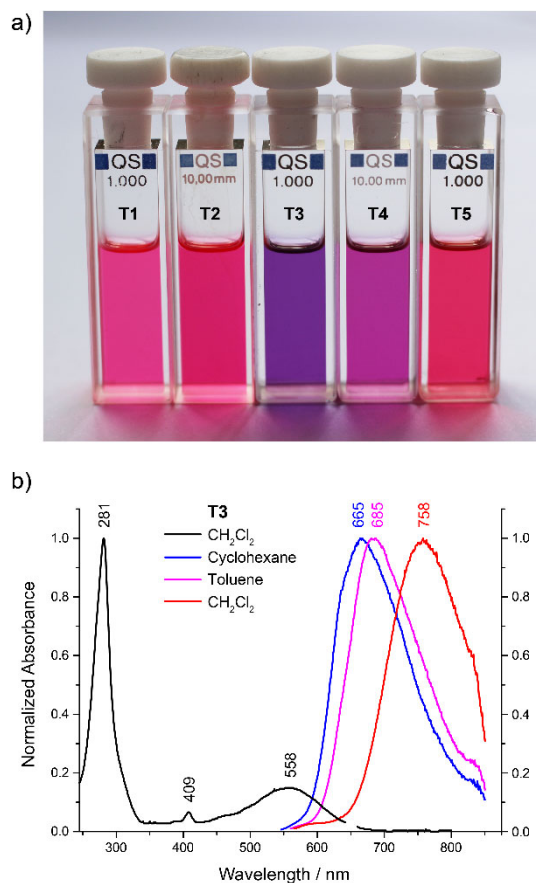


Figure 4.3: (a) Photographed solutions of the target compounds **T1–T5** in CH_2Cl_2 (~ 0.1 mM) and (b) normalized absorption (black) and emission (blue, purple, and red) spectra of **T3** in various solvents at room temperature.

Table 4.1: An Overview of Data Obtained from UV/Vis Spectroscopy, Cyclic Voltammetry, and DFT Calculations for **T1–T5**.

Entry	$\epsilon_{\text{abs-max}}$ (nm) ^a	$\epsilon / 10^3$ ($\text{M}^{-1} \cdot \text{cm}^{-1}$) ^a	$\epsilon_{\text{em-max}}$ (nm) ^b	E_{0-0} (eV) ^c	QY (%) ^d	E_{ox} (V) ^e	E_{red} (V) ^e	E_{HOMO} (eV) ^f	E_{LUMO} (eV) ^f	E_{g} (eV) ^g	$\Delta E_{\text{HOMO-LUMO}}$ (eV) ^h
T1	283	54.3									
	408	2.80	608	2.20	53	0.98	-1.38	-6.08	-3.72	2.36	2.68
	518	6.50	657				(-1.99)				(2.39)
	554	5.73									
T2	283	112									
	409	7.26	629	2.18	53	0.91	-1.41	-6.01	-3.69	2.32	2.64
	522	15.5	669				(-2.01)				(2.34)
	551	14.5									
T3	281	185									
	409	13.1	758	1.97	17	0.47	-1.43	-5.57	-3.67	1.9	2.25
	558	28.0				(0.98)	(-2.04)				(1.89)
T4	282	120									
	408	9.20	733	2.03	22	0.60	-1.38	-5.70	-3.72	1.98	2.16
	554	18.9				(1.03)	(-1.97)				(1.82)
T5	280	141									
	411	8.30	628	2.22	2	0.98	-1.32	-6.08	-3.78	2.30	2.68
	509	17.4	662				(-1.90)				(2.40)
	543	17.0									

^a Absorption maxima and the corresponding absorption coefficients in CH_2Cl_2 at room temperature.

^b Emission maxima in CH_2Cl_2 at room temperature. ^c Energy of the first electronic transition between zero vibrational states: $E_{0-0} = 1240/\lambda_{\text{inter}}$, where λ_{inter} is the intersection of normalized absorption and emission curves (see Figure S2). ^d Quantum yield. ^e The first (and second) oxidation and reduction

potential versus Fc^+/Fc .^f Energy of the HOMO and the LUMO calculated from the measured oxidation and reduction potentials: $E_{\text{HOMO}} = -e(E_{\text{ox}} + 5.1)$, $E_{\text{LUMO}} = -e(E_{\text{red}} + 5.1)$.^g $E_{\text{g}} = E_{\text{LUMO}} - E_{\text{HOMO}}$.^h The HOMO–LUMO gap energies obtained from B3LYP/6-311+G(2d,p)/PCM(CH_2Cl_2) single point calculation on B3LYP/6-31G(d) gas-phase geometries. The values in parentheses are the HOMO–LUMO gap energies obtained from TD-B3LYP/6-31G(d)/PCM(CH_2Cl_2) calculation on identical geometries.

The target compounds **T1** (R = 3,5-di-*tert*-butylphenyl), **T2** (R = 4-methoxyphenyl), **T3** (R = 4-(dimethylamino)phenyl), **T4** (R = 4-(diphenylamino)phenyl), and **T5** (thiophen-2-yl) were synthesized in one step, by the palladium-catalyzed Suzuki cross-coupling reaction of **8** and the corresponding boronic acid **9** in yields ranging from 22–88%. All compounds were characterized by $^1\text{H}/^{13}\text{C}$ NMR and IR spectroscopy and high-resolution mass spectrometry (HRMS; ESI), and the target compounds **T1–T5** also by 2D NMR spectroscopic techniques (COSY, NOESY, HMQC, HMBC). Compounds **T2**^[190] and **T3**^[191] were additionally characterized by X-ray diffraction (XRD) analysis (Figure 4.2) of their single crystals. The optoelectronic properties of **T1–T5** are first summarized and then discussed below.

The optical properties of **T1–T5** were investigated by UV/Vis spectroscopy in dilute CH_2Cl_2 solutions at room temperature and the results are summarized in Figure 4.3, Table 4.1, and Figures A1–A4. All compounds exhibit two major absorption bands, one very intense transition in the UV (maxima at ~ 280 nm) and one in the visible (maxima at ~ 510 – 560 nm) region. A vibrational progression of the lowest-energy absorption band is apparent in the case of **T1**, **T2**, and **T5**, while it is absent in the case of **T3** and **T4**. The absorption maxima of the amino-derivatives **T3** and **T4** display a bathochromic shift (~ 24 nm) relative to the averaged maxima of **T1**, **T2**, and **T5**, in accord with the color appearance of the corresponding solutions, which changes from pink–red (**T1**, **T2**, and **T5**) to purple–magenta (**T3** and **T4**; Figure 4.3a).

All molecules are fluorescent with moderate to low photo-luminescence quantum yields (2–53%) and possess a large Stokes shift (Table S1) that increases with increasing electron-donating ability of the donor substituent, following this order: **T1** (54 nm) < **T2** (78 nm) < **T5** (85 nm) < **T4** (179 nm) < **T3** (200 nm).

The Stokes shifts obtained from measurements of **T1–T5** in various solvents (cyclohexane, toluene, THF, CH₂Cl₂) also increase with increasing polarity of the solvent (Figures 4.3b and A2, and Table A1), and this effect is more pronounced for **T3** and **T4**. The energy of the first excited state, which was estimated from the zero–zero electronic transition (E_{0-0} ; Table A.1), is lower (~2 eV) for **T3** and **T4** compared with **T1**, **T2**, and **T5** (~2.2 eV).

The cyclic (CV) and differential pulse (DPV) voltammetry of CH₂Cl₂ solutions of **T1–T5** with ferrocenium/ferrocene (Fc⁺/Fc) couple as an internal standard (Figure 4.4, Table 1) showed one anodic and two cathodic waves, which can all be attributed to the triangulene-4,8-dione core. Compounds **T3** and **T4** exhibit an extra redox state with $E_{ox} = 0.47$ and 0.60 V for **T3** and **T4**, respectively, values that are comparable with those of analogous systems²⁰ with 4-(dimethylamino)phenyl ($E_{ox} = 0.48$ V) and 4-(diphenylamino)phenyl ($E_{ox} = 0.61$ V) donor substituents. The one-electron oxidations and the first one-electron reductions display electrochemical reversibility and chemical stability under the applied conditions for all derivatives, while the second one-electron reduction that occurs at more negative potentials (~ -2 V) is irreversible (Figures A5–A7).

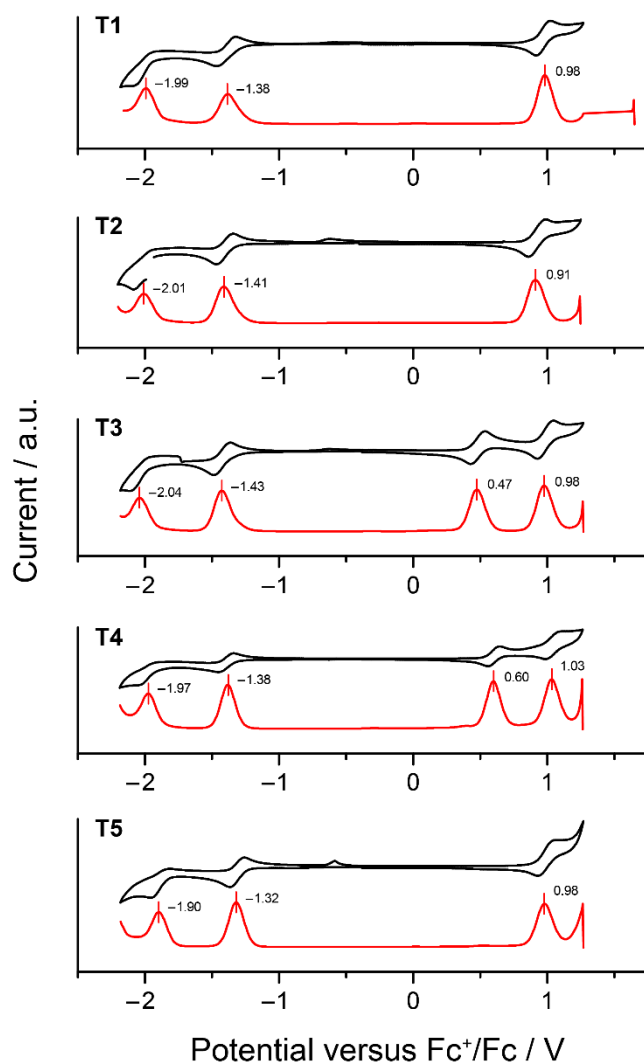


Figure 4.4: Cyclic voltammetry (CV) and square-wave traces recorded for **T1–T5** with reference to Fc^+/Fc in CH_2Cl_2 with TBAPF_6 as electrolyte. Scan rate = 100 mV s^{-1} .

The frontier molecular orbitals (FMOs) energies of **T1–T5** were estimated (Table 4.1) from their redox potentials, after correction of the vacuum energy level (5.1 eV). The LUMO energies (–3.78 to –3.69 eV) are comparable in all compounds. The HOMO energies of **T3** (–5.57 eV) and **T4** (–5.70 eV) are distinctly higher in energy compared to **T1** (–6.08 eV), **T2** (–6.01 eV), and **T5** (–6.08 eV). Consequently, the HOMO–LUMO gaps of **T3** (1.9 eV) and **T4** (1.98 eV) are lower than those of **T1**, **T2**, and **T5** (2.30–2.36 eV).

The DFT calculations (see Table 4.1, Figure 4.5, and the SI) were carried out to support the experimental observations. Because the induction effect of the three apex *tert*-butyl

groups was found to be negligible (see the SI), we used simplified structures of **T1–T5**, where the apex *tert*-butyl groups were replaced with hydrogen atoms to alleviate the computational costs, in all calculations. Inspection of the Kohn–Sham orbitals revealed that both the HOMO and the LUMO are localized primarily on the triangulene-4,8-dione unit in the case of **T1**, **T2**, and **T5** with a very small contribution from the donor substituent (Figures 4.5 and A8). In contrast, in the case of **T3** and **T4**, the FMOs are largely polarized: the HOMO is localized primarily on the donor substituent, while the LUMO is localized primarily on the triangulene-4,8-dione acceptor moiety. The energies of the first electronic transitions of **T1–T5** were calculated with TD-DFT approach (CAM-B3LYP and M06-2X, Tables A3–A8). The calculated energies (CH₂Cl₂) of the first electronic transitions follow the observed experimental trend and decrease in this order: **T5** (2.72 eV) > **T1** (2.71 eV) > **T2** (2.69 eV) > **T4** (2.63 eV) > **T3** (2.58 eV). They are, however, shifted by ~0.36 eV on average, on account of the possible incompleteness of the basis set, solvation effects, and systematic errors known to TD-DFT techniques.

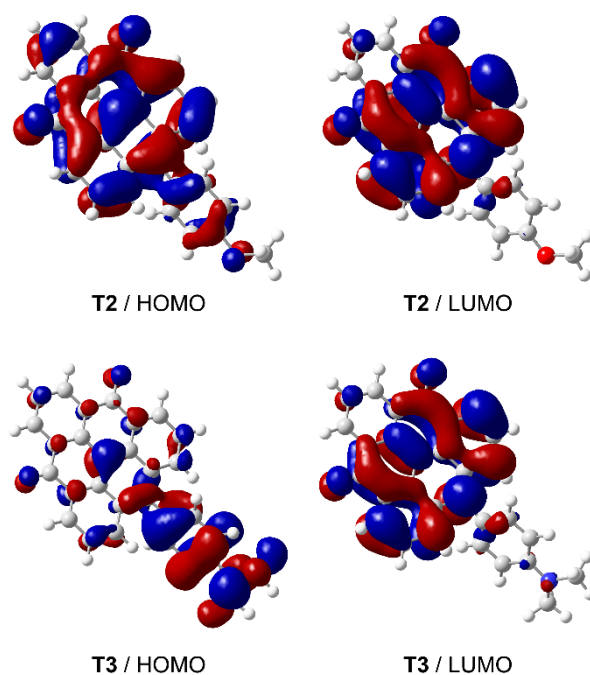


Figure 4.5: The HOMO and the LUMO of **T2** and **T3**.

In addition, the HOMO–LUMO energy gaps that were estimated directly from energies of the Kohn–Sham orbitals or from the TD-DFT calculations (B3LYP, CH₂Cl₂; Table 1) are in a good agreement with experimental values obtained from CV.

The differences in the solvatochromic behavior observed for both the absorption and emission of **T1–T5** solutions suggest that **T1–T5** can be divided into two families. Compounds **T1**, **T2**, and **T5** clearly possess a vibrationally resolved local first electronic transition, albeit with the band maxima shifted bathochromically when compared to the parent triangulene-4,8-dione reported^[180] by Clar. In contrast, the increasing admixture of the charge-transfer (CT) character in **T3** and **T4**, due to the presence of stronger electron-donating substituents, leads to loss of the vibrational progression in both absorption and emission spectra and markedly larger Stokes shifts in all solvents. Further support for the stronger CT state character of the lowest singlet excited state in **T3** and **T4** is provided by the decrease in their photoluminescence quantum yields ($\Phi \sim 20\%$) when compared to efficient fluorescence of **T1** and **T2** ($\Phi > 50\%$), which is a consequence of decreasing the energy of the singlet excited state of **T3** and **T4** (compare E_{0-0} , E_g , and $E_{\text{HOMO-LUMO}}$ in Table 1). The only exception is the very small Φ value (2%) found for **T5**, where other deactivation processes, presumably an intersystem crossing due to the heavy-atom effect of sulfur, must take place. The markedly different electron-donating strength of the substituents in **T3** and **T4** is expressed in the electrochemical data where the first one-electron oxidation takes place at these substituents, followed by the oxidation of the triangulene-4,8-dione core at more positive potential (>400 mV), in agreement with the DFT-calculated FMOs.

The optoelectronic properties of triangular **T1–T5** can be compared with those of the perylenediimide (PDI)-based chromophores. The parent PDI is highly fluorescent ($\Phi \sim 100\%$) and displays^[186] an intense lowest-energy π – π^* absorption band at 526 nm in CH₂Cl₂ ($\epsilon = 88 \times 10^3 \text{ M}^{-1} \cdot \text{cm}^{-1}$) and a very small Stokes shift of 7 nm. Installment of electron-

donating 4-(dimethyl-amino)phenyl substituents to the headland^[193] or bay^[194] positions of the PDI chromophore leads to a significantly red-shifted CT band (>600 nm) and a slight blue shift of the PDI-core π - π^* transition. Both transitions have markedly lower intensity due to PDI-chromophore symmetry perturbation. Note that the transition dipole moment of parent PDI is longitudinal with the PDI main molecular axis. The fluorescence is completely quenched^[195] as a result of the very fast electron transfer from the donor to the PDI acceptor. Compared with parent PDI, the lowest-energy absorption band of compounds **T1–T5** is slightly red-shifted and has a markedly lower absorption coefficient. The substituents in **T1–T5** are, however, positioned in the direction of the transition dipole moment and, as a result, the band intensity increases with the electron-donor strength in contrast to the PDIs. The much larger Stokes shifts in the case of **T1–T5** suggest a larger reorganization upon photoexcitation than that in PDIs. In contrast to 4-(dimethylamino)phenyl-substituted PDIs, **T3** still displays appreciable fluorescence. The reason is the shift of both one-electron reductions in **T1–T5**, which possess two electron-accepting carbonyl groups, to lower potentials (by ~300 and ~700 mV, respectively) compared to the case of the similarly substituted PDIs with four electron-accepting groups, despite comparable excited-state energies for both triangulene-4,8-dione and PDI chromophores. The electron-transfer quenching of the fluorescence in **T3** and **T4** is therefore inefficient.

Finally, the presented donor–acceptor systems possess a rather rare triangular shape, while PDIs possess a more conventional rectangular shape. Because triangles, in contrary to rectangles, cannot easily adopt a herringbone arrangement, the packing in the crystal structures of PDIs and triangulene-4,8-diones is expected to be different. As an example, compounds **T2** and **T3** display (Figure 4.2) a ‘layered’ packing mode in the solid state, where all layers are parallel to one another. In the case of **T2**, pairs of ‘dimeric’ stacks are formed in the solid state, while in the case of **T3**, the molecules are packed in a slipped-stack fashion.

This type of stack is scarce in the case of PDIs, which typically pack^[196] in a herringbone fashion. There are, however, examples^[197] where PDIs form parallel slipped stacks.

4.5 CONCLUSION AND OUTLOOK

In summary, we have synthesized a series of donor–acceptor molecular triangles, which absorb and emit visible light, as well as display solvatochromism and up to four redox states. All target compounds were prepared in one step from a common triflate precursor by means of the Suzuki cross-coupling reaction. The synthesis of the precursor was achieved in seven steps, including four with yields >98% and three where purification by column chromatography was not necessary. The results obtained from the photophysical and electrochemical studies indicate that triangulene-4,8-dione is a promising electron-acceptor chromophoric building block for applications in molecular electronics, adding diversity to the pool of known electron-acceptors on account of its triangular shape.

4.6 EXPERIMENTAL SECTION

4.6.1 GENERAL REMARKS

All chemicals and solvents, including 1-bromo-4-(*tert*-butyl)benzene [CAS Reg. No.: 3972-65-4], 1-bromo-3,5-di-*tert*-butylbenzene [CAS Reg. No.: 22385-77-9], (4-methoxyphenyl)boronic acid (**94b**) [CAS Reg. No.: 5720-07-0], (4-(dimethylamino)phenyl)boronic acid (**94c**) [CAS Reg. No.: 28611-39-4], (4-(diphenylamino)phenyl)boronic acid (**94d**) [CAS Reg. No.: 201802-67-7], and thiophen-2-ylboronic acid (**94e**) [CAS Reg. No.: 6165-68-0], were purchased from commercial sources and used without further purification unless stated otherwise. (3,5-Di-*tert*-butylphenyl)boronic acid (**94a**) [CAS Reg. No.: 197223-39-5] was prepared from 1-bromo-3,5-di-*tert*-butylbenzene according to previously reported^[187] protocols and spectroscopic data matched those in the literature. The reactions and experiments that are sensitive to oxygen were performed using Schlenk techniques and argon-saturated solvents. The solvents were saturated with argon by either passing argon gas through the solvent or using the freeze-pump-thaw technique in three cycles. For the GPC purification of **T5**, an automated Shimadzu Prominence System was used with SDV preparative columns from Polymer Standards Service (two Showdex columns in a series, 20 × 600 mm each, exclusion limit: 30'000 g mol⁻¹) with CHCl₃ as a solvent. For the preparation of compound **5**, Initiator Microwave System from Biotage was used. The NMR experiments were performed on Bruker Avance III NMR spectrometers operating at 400, 500, or 600 MHz proton frequencies. The instruments were equipped with a direct-observe 5 mm BBFO smart probe (400 and 600 MHz), an indirect-detection 5 mm BBI probe (500 MHz), or a five-channel cryogenic 5 mm QCI probe (600 MHz). All probes were equipped with actively shielded z-gradients (10 A). The experiments were performed at 295 or 298 K unless indicated otherwise and the temperatures were calibrated using a methanol standard showing accuracy

within ± 0.2 K. Standard Bruker pulse sequences were used and the data was processed on Topspin 3.2 (Bruker) using two-fold zero-filling in the indirect dimension for all 2D experiments. Chemical shifts (δ) are reported^[198] in parts per million (ppm) relative to the residual protonated solvent peak. High-resolution mass spectra (HRMS) were measured as HR-ESI-ToF-MS with a Maxis 4G instrument from Bruker with the addition of NaOAc. Data collections for the crystal structures of **T2** and **T3** were performed at low temperatures (123 K) using CuK α radiation on a Bruker APEX II diffractometer. Integration of the frames and data reduction was carried out using the APEX2 software.^[199] The structures were solved by the charge-flipping method using Superflip.^[200] All non-hydrogen atoms were refined anisotropically by full-matrix least-squares on F using CRYSTALS.^[201] Both structures were analyzed using Mercury.^[202] Melting points were measured on a Hund Weltzer V200 instrument and are uncorrected. The UV/Vis absorption spectra were recorded at room temperature on a Shimadzu UV-1800 spectrophotometer. Emission spectra were recorded on a Horiba Jobin-Yvon FluoroMax 4 fluorimeter. Quantum yields (CH₂Cl₂) were measured using a Hamamatsu absolute photoluminescence (PL) quantum yield spectrophotometer C11347 Quantaaurus-QY. The electrochemical measurements were performed with an AutoLab PGSTAT302 potentiostat-galvanostat controlled by resident NOVA 9.1 software using a conventional single-compartment three-electrode cell. A Pt disk ($\phi = 2$ mm) served as a working electrode, a Pt wire was used as an auxiliary, and the reference electrode was a saturated potassium chloride calomel electrode (SCE). The supporting electrolyte was 0.1M Bu₄NPF₆ in CH₂Cl₂. All potentials are quoted relative to ferrocenium/ferrocene (Fc⁺/Fc) couple as an internal standard. In all the experiments, the scan rate was 100 mV/s for cyclic voltammetry (CV) and the pulse frequency was 15 Hz for differential pulse voltammetry (DPV). All calculations were performed with Gaussian 09^[203] (version D.01) package of electronic structure programs. The gas-phase geometries were optimized with B3LYP functional, 6-31G(d) basis set, and a modified integration grid (Integral=Ultrafine keyword

in Gaussian). The frequency analysis of the minimum-energy geometries confirmed that all represent the potential-energy-surface minima. The electronic transitions were computed within the time-dependent density functional (TD-DFT) theory formalism. The 30 lowest transitions were calculated with 6-31G(d) basis set and the ultrafine integration grid. The collective solvation effects were accounted for with a polarizable continuum model (PCM) with the default settings implemented in Gaussian. Non-equilibrium solvation was assumed in electronic spectra calculations.

4.6.2 EXPERIMENTAL PROCEDURES

2-Bromo-5-(*tert*-butyl)benzaldehyde (87)

A solution of isopropylmagnesium bromide (20.1 mL, 58.4 mmol, 2.9 M solution in 2-methyltetrahydrofuran) was added dropwise to a cooled ($-78\text{ }^{\circ}\text{C}$) and vigorously stirred solution of 1-bromo-4-(*tert*-butyl)-2-iodobenzene (**86**, 20.4 g, 58.4 mmol) in a mixture of dry THF/Et₂O (400 mL, 1:1) under an argon atmosphere and the resultant mixture was stirred at $-78\text{ }^{\circ}\text{C}$ for 2 h before DMF (9.03 mL, 117 mmol) was added dropwise at $-78\text{ }^{\circ}\text{C}$. After the addition, the reaction mixture was stirred at $-78\text{ }^{\circ}\text{C}$ for an additional 2 h before it was allowed to warm to room temperature overnight. The reaction was quenched by the addition of water (400 mL). The organic layer was separated and the aqueous layer was extracted with Et₂O ($3 \times 100\text{ mL}$). The combined organic layers were washed with brine and dried over Na₂SO₄. After filtration and evaporation of the solvents, the residue was purified by column chromatography over silica gel using cyclohexane to cyclohexane/CH₂Cl₂ (1:1) as an eluent to afford the desired product.

Yield: 11.2 g (82%); colorless oil.

IR (neat): 2933, 2868, 1693, 1590, 1475, 1190, 1110, 1024, 826 cm^{-1} .

¹H NMR (400 MHz, CDCl₃): δ = 10.36 (s, 1H), 7.94 (d, J = 2.6 Hz, 1H), 7.57 (d, J = 8.4 Hz, 1H), 7.49 (dd, J = 8.4, 2.6 Hz, 1H), 1.33 (s, 9H) ppm.

¹³C NMR (101 MHz, CDCl₃): δ = 192.4, 151.6, 133.6, 133.04, 133.03, 126.9, 124.4, 35.0, 31.2 ppm.

HRMS (ESI): m/z [M + Na]⁺ calcd for C₁₁H₁₃BrONa⁺: 263.0042; found: 263.0043 ($|\Delta|$ = 0.5 ppm).

2-(2-Bromo-5-(*tert*-butyl)phenyl)-1,3-dioxolane (88)

A mixture of **87** (10.0 g, 40.2 mmol), ethylene glycol (2.70 mL, 48.2 mmol), and a catalytic amount of *p*-toluenesulfonic acid monohydrate in benzene (200 mL) was heated at reflux for 12 h by using the Dean–Stark apparatus to continuously remove water, which formed during the course of the reaction. After the reaction was completed, water (100 mL) was added and the organic layer was separated, washed with a saturated aqueous NaHCO₃ solution, and dried over Na₂SO₄. After filtration and evaporation of the solvents, the desired product was isolated and used in the next step without further purification.

Yield: 11.3 g (99%); colorless oil.

IR (neat): 2961, 2883, 1477, 1296, 1206, 1085, 1022, 822 cm⁻¹.

¹H NMR (400 MHz, CDCl₃): δ = 7.61 (d, *J* = 2.6 Hz, 1H), 7.48 (d, *J* = 8.4 Hz, 1H), 7.25 (dd, 8.4, 2.6 Hz, 1H), 6.07 (s, 1H), 4.23–4.13 (m, 2H), 4.13–4.04 (m, 2H), 1.31 (s, 9H) ppm.

¹³C NMR (101 MHz, CDCl₃): δ = 150.8, 135.7, 132.7, 128.1, 124.9, 119.9, 103.0, 65.6, 34.8, 31.4 ppm.

HRMS (ESI): *m/z* [M + H]⁺ calcd for C₁₃H₁₈BrO₂⁺: 285.0485; found: 285.0484 (|Δ| = 0.3 ppm).

Tris(4-(*tert*-butyl)-2-(1,3-dioxolan-2-yl)phenyl)methanol (89)

A solution of *n*-BuLi (27.2 mL, 43.6 mmol, 1.6 M solution in hexane) was added dropwise (over a period of 30 min) to a cooled (−78 °C) solution of **88** (11.3 g, 39.6 mmol) in dry THF (100 mL) under an argon atmosphere and the resulting mixture was stirred at −78 °C for 1 h before diethyl carbonate (1.63 mL, 13.2 mmol) was added dropwise. After the addition, the reaction mixture was stirred at −78 °C for an additional 1 h before the temperature was raised from −78 to 50 °C over 1 h. The mixture was heated at 50 °C for 16 h and then it was quenched by the addition of a saturated aqueous NH₄Cl solution (25 mL) and extracted with CH₂Cl₂ (3 × 25 mL). The combined organic layers were washed with brine and dried over

157

Na₂SO₄. After filtration, evaporation of the solvents gave the crude product that was crystallized from hexane to afford the desired product.

Yield: 8.38 g (98%); white solid; mp 254–255 °C.

IR (neat): 3442, 2954, 2871, 1408, 1393, 1362, 1208, 1108, 1062, 949, 894, 831 cm⁻¹.

¹H NMR (400 MHz, CD₃COCD₃): δ = 7.82 (d, *J* = 2.3 Hz, 3H), 7.19 (dd, *J* = 8.3, 2.3 Hz, 3H), 6.58 (d, *J* = 8.4 Hz, 3H), 5.94 (s, 3H), 5.86 (s, 1H), 4.10–3.94 (m, 6H), 3.83–3.68 (m, 6H), 1.32 (s, 27H) ppm.

¹³C NMR (101 MHz, CD₃COCD₃): δ = 150.8, 144.0, 137.6, 130.0, 125.9, 125.6, 102.1, 84.9, 65.6, 35.1, 31.6 ppm.

HRMS (ESI): *m/z* [M + Na]⁺ calcd for C₄₀H₅₂O₇Na⁺: 667.3605; found: 667.3609 (|Δ| = 0.6 ppm).

2,2'-(5-(*tert*-Butyl)-3-hydroxy-1,3-dihydroisobenzofuran-1,1-diyl)bis(5-(*tert*-butyl)benzaldehyde) (90)

A mixture of **89** (0.50 g, 0.77 mmol), pyridinium *p*-toluenesulfonate (0.58 g, 2.3 mmol), acetone (14 mL), and water (6 mL) was heated at 80 °C under a microwave irradiation for 1 h before it was diluted with a saturated aqueous NaHCO₃ solution (30 mL) and extracted with CH₂Cl₂ (3 × 25 mL). The combined organic layers were washed with brine and dried over Na₂SO₄. After filtration and evaporation of the solvents, the residue was purified by column chromatography over silica gel using CH₂Cl₂ to CH₂Cl₂/acetone (95:5) as an eluent to afford the desired product.

Yield: 389 mg (98%); white solid; mp 163–166 °C.

IR (neat): 3413, 2960, 2904, 2870, 1684, 1602, 1461, 1395, 1362, 1237, 979, 942, 834, 819 cm⁻¹.

^1H NMR (400 MHz, CD_3COCD_3): δ = 10.34 (s, 1H), 10.17 (s, 1H), 7.91 (d, J = 2.3 Hz, 1H), 7.85 (d, J = 2.3 Hz, 1H), 7.62–7.55 (m, 4H), 7.25 (d, J = 8.3 Hz, 1H), 7.21 (d, J = 7.9 Hz, 1H), 7.05 (d, J = 8.2 Hz, 1H), 6.60 (s, 1H), 6.42 (s, 1H), 1.37 (s, 9H), 1.32 (s, 9H), 1.31 (s, 9H) ppm.

^{13}C NMR (101 MHz, CD_3COCD_3): δ = 192.9, 192.5, 153.1, 152.3, 152.1, 145.5, 145.0, 142.1, 141.1, 135.4, 134.9, 130.52, 130.45, 128.8, 128.6, 127.5, 126.2 (two overlapped signals), 124.8, 121.2, 101.7, 92.0, 35.5, 35.3, 35.2, 31.7, 31.34, 31.31 ppm.

HRMS (ESI): m/z $[\text{M} + \text{Na}]^+$ calcd for $\text{C}_{34}\text{H}_{40}\text{O}_4\text{Na}^+$: 535.2819; found: 535.2821 ($|\Delta|$ = 0.3 ppm).

6,6'-(5-(*tert*-Butyl)-3-oxo-1,3-dihydroisobenzofuran-1,1-diyl)bis(3-(*tert*-butyl)benzoic acid) (91)

A mixture of hydrogen peroxide (9.85 mL, 347 mmol, 30% solution in water), sodium phosphate (3.84 g, 27.8 mmol), and water (10 mL) was acidified (pH ~ 2) with concentrated HCl and the resultant mixture was added into a solution of **90** (3.00 g, 5.79 mmol) in acetonitrile (60 mL). Afterwards, a solution of sodium chlorite (9.42 g, 11.6 mmol) in water (10 mL) was added over 5 h and the mixture was stirred at room temperature for 2 h, followed by the addition of concentrated HCl (2 mL). Subsequently, the mixture was stirred at 50 °C for 12 h before water (10 mL) was added. The mixture was extracted with ethyl acetate (3 × 25 mL) and the combined organic layers were washed with water and brine to afford, after evaporation of the solvents, a crude product mixture. The procedure described above was repeated one more time using the crude material obtained after the first round. During the second-round work-up, the ethyl acetate extract was dried over Na_2SO_4 . After filtration, evaporation of the solvents afforded the desired product.

Yield: 3.11 g (99%); white solid; mp 199–201 °C.

IR (neat): 3041, 2960, 2095, 2868, 1751.4, 1702, 1364, 1280, 1237, 1163, 937, 833, 655, 594 cm^{-1} .

^1H NMR (400 MHz, CD_3COCD_3): δ = 7.84 (dd, J = 8.1, 1.9 Hz, 1H), 7.80 (dd, J = 1.7, 0.6 Hz, 1H), 7.78 (dd, J = 8.2, 0.7 Hz, 1H), 7.56 (d, J = 2.2 Hz, 2H), 7.46 (dd, J = 8.4, 2.2 Hz, 2H), 7.28 (d, J = 8.4 Hz, 2H), 1.38 (s, 9H), 1.31 (s, 18H) ppm.

^{13}C NMR (101 MHz, CD_3COCD_3): δ = 170.4, 169.8, 153.8, 151.7, 150.4, 137.2, 133.3, 132.2, 129.1, 127.5, 127.18, 128.17, 125.9, 122.3, 91.1, 35.6, 35.1, 31.5, 31.3 ppm.

HRMS (ESI): m/z $[\text{M} + \text{Na}]^+$ calcd for $\text{C}_{34}\text{H}_{38}\text{O}_6\text{Na}^+$: 565.2561; found: 565.2562 ($|\Delta|$ = 0.3 ppm).

2,6,10-Tri-*tert*-butyl-12-hydroxydibenzo[*cd,mn*]pyrene-4,8-dione (92)

A mixture of **91** (1.50 g, 2.76 mmol), copper powder (193 mg, 3.04 mmol), and concentrated H_2SO_4 (5 mL) was heated at 120 $^\circ\text{C}$ for 1.5 h before the reaction mixture was filtered hot through a glass filter to remove the unreacted copper. The glass filter was washed with hot concentrated H_2SO_4 (5 mL) and the combined H_2SO_4 filtrates were poured on ice. The precipitate that formed was collected and washed with water, acetonitrile, and Et_2O to afford the desired product.

Yield: 864 mg (64%); deep blue solid; mp over 300 $^\circ\text{C}$.

IR (Neat): 3400, 2956, 2925, 2865, 1638, 1585, 1544, 1360, 1291, 1242, 1201, 1077, 459, 411 cm^{-1} .

^1H NMR (600 MHz, D_2SO_4): δ = 9.71 (s, 6H), 1.53 (s, 27H) ppm.

^{13}C NMR (151 MHz, D_2SO_4): δ = 175.0, 154.4, 142.0, 128.8, 121.3, 107.6, 35.8, 29.9, 29.8 ppm.

HRMS (ESI): m/z $[\text{M} - \text{H}]^-$ calcd for $\text{C}_{34}\text{H}_{33}\text{O}_3^+$: 489.2435; found: 489.2441 ($|\Delta|$ = 1.2 ppm).

2,6,10-Tri-*tert*-butyl-8,12-dioxo-8,12-dihydrodibenzo[*cd,mn*] pyren-4-yl trifluoromethanesulfonate (93)

To the cooled (0 °C) mixture of **92** (0.70 g, 1.43 mmol), dry pyridine (173 μ L, 2.15 mmol) and dry CH₂Cl₂ (35 mL), Tf₂O (364 μ L, 2.15 mmol) was added dropwise under an argon atmosphere. The mixture was stirred at 0 °C for 10 min and then it was allowed to warm to room temperature over 15 min. The mixture was then stirred at room temperature for 1 h before the solvents were evaporated. The residue was purified by column chromatography over silica gel (deactivated with 1% TEA) using cyclohexane/ethyl acetate (20:1) as an eluent to afford the desired product.

Yield: 550 mg (62%); dark red solid; mp over 300 °C.

IR (Neat): 2958, 2908, 2872, 1778, 1650, 1579, 1557, 1418, 1364, 1245, 1210, 1086, 1014, 828, 783, 647, 629 cm⁻¹.

¹H NMR (400 MHz, CDCl₃): δ = 9.09 (d, *J* = 1.9 Hz, 2H), 8.87 (s, 2H), 8.64 (d, *J* = 1.9 Hz, 2H), 1.59 (s, 18H), 1.54 (s, 9H) ppm.

¹⁹F NMR (376.5 MHz, CDCl₃, ppm): δ = -72.22.

¹³C NMR (150, CDCl₃, MHz): Strong aggregation of **93** did not allow us to record an unequivocal ¹³C NMR spectrum of monomeric **93**.

HRMS (ESI): *m/z* [M + Na]⁺ calcd for C₃₅H₃₃O₅F₃SNa⁺: 645.1893; found: 645.1898 ($|\Delta|$ = 0.8 ppm).

General procedure for T1–T5

Cesium acetate was pre-dried under vacuum at 100 °C for 30 min prior to setting up the reaction. Then, **93** (50 mg, 80.6 μ mol), boronic acid **94** (96.7 μ mol, 1.2 equiv.), cesium acetate (30.9 mg, 161 μ mmol), Pd(dppf)Cl₂ (11.8 mg, 16.2 μ mol), and a stirring bar were

placed in a Schlenk tube and kept under vacuum for 1 h at room temperature. Subsequently, the tube was evacuated and refilled with argon in three cycles and freshly distilled dry solvent (2.5 mL) was added. The reaction mixture was stirred under an argon atmosphere overnight at 55 °C before HCl (5 mL, 2 M) was added to quench the reaction. The mixture was then extracted with CH₂Cl₂ (3 × 10 mL) and the combined organic layers were washed with water and brine, and dried over Na₂SO₄. After filtration and evaporation of the solvents, the residue was purified by column chromatography over silica gel using cyclohexane to cyclohexane/ethyl acetate (30:1) as an eluent to afford the desired product.

2,6,10-Tri-*tert*-butyl-12-(3,5-di-*tert*-butylphenyl)dibenzo[*cd,mn*] pyrene-4,8-dione (T1)

Solvent: dry, freshly distilled THF.

Yield: 47.0 mg (88%); red solid; mp 139–141 °C.

IR (Neat): 2957, 2905, 2868, 1740, 1643, 1558, 1393, 1362, 1245, 865, 834, 647 cm⁻¹.

¹H NMR (400 MHz, CD₂Cl₂): δ = 9.09 (d, *J* = 2.0 Hz, 2H), 8.90 (s, 2H), 8.28 (d, *J* = 2.0 Hz, 2H), 7.68 (t, *J* = 1.8 Hz, 1H), 7.41 (d, *J* = 1.8 Hz, 2H), 1.56 (s, 9H), 1.43 (s, 18H), 1.42 (s, 18H) ppm.

¹³C NMR (101, CD₂Cl₂, MHz): δ = 183.7, 151.7, 151.1, 149.3, 145.0, 136.4, 133.8, 131.8, 131.1, 130.9, 130.6, 130.3, 129.1, 126.6, 125.3, 125.1, 122.3, 35.80, 35.77, 35.4, 31.7, 31.5, 31.2 ppm.

HRMS (ESI): *m/z* [M + H]⁺ calcd for C₄₈H₅₅O₂: 663.4197; found: 663.4185 (|Δ| = 1.7 ppm).

2,6,10-Tri-*tert*-butyl-12-(4-methoxyphenyl)dibenzo[*cd,mn*]pyrene-4,8-dione (T2)

Solvent: dry, freshly distilled THF.

Yield: 39.4 mg (84%); red solid; mp over 300 °C.

IR (Neat): 2958, 2905, 2870, 1660, 1643, 1557, 1511, 1242, 1031, 833, 803, 648 cm⁻¹.

^1H NMR (400 MHz, CD_2Cl_2): $\delta = 9.08$ (d, $J = 2.0$ Hz, 2H), 8.89 (s, 2H), 8.23 (d, $J = 2.0$ Hz, 2H), 7.52–7.43 (m, 2H), 7.23–7.18 (m, 2H), 3.99 (s, 3H), 1.56 (s, 9H), 1.43 (s, 18H) ppm.

^{13}C NMR (101, CD_2Cl_2 , MHz): $\delta = 183.7, 160.2, 151.8, 149.4, 143.4, 133.8, 133.1, 131.9, 131.1, 130.9, 130.5, 130.3, 129.5, 129.1, 125.1, 115.6, 114.2, 55.8, 35.81, 35.77, 31.5, 31.1$ ppm.

HRMS (ESI): m/z $[\text{M} + \text{H}]^+$ calcd for $\text{C}_{41}\text{H}_{41}\text{O}_3^+$: 581.3050; found: 581.3046 ($|\Delta| = 0.7$ ppm).

2,6,10-Tri-*tert*-butyl-12-(4-(dimethylamino)phenyl)dibenzo [cd,mn]pyrene-4,8-dione (T3)

Solvent: dry, freshly distilled 1,4-dioxane.

Yield: 25.1 mg (52%); purple solid; mp over 300 °C.

IR (Neat): 2960, 1874, 1732, 1642, 1606, 1556, 1523, 1392, 1353, 1245, 835, 801, 646, 600 cm^{-1} .

^1H NMR (400 MHz, CD_2Cl_2): $\delta = 9.08$ (d, $J = 2.0$ Hz, 2H), 8.89 (s, 2H), 8.37 (d, $J = 2.0$ Hz, 2H), 7.43 (d, $J = 8.6$ Hz, 2H), 7.02 (d, $J = 8.1$ Hz, 2H), 3.14 (s, 6H), 1.56 (s, 9H), 1.44 (s, 18H) ppm.

^{13}C NMR (101, CD_2Cl_2 , MHz): $\delta = 183.7, 151.5, 150.8, 149.1, 144.7, 133.8, 133.0, 132.4, 131.8, 131.1, 131.01, 130.98, 130.3, 129.1, 125.2, 114.9, 112.3, 40.8, 35.80, 35.76, 31.5, 31.2$ ppm.

HRMS (ESI): m/z $[\text{M} + \text{H}]^+$ calcd for $\text{C}_{42}\text{H}_{44}\text{NO}_2^+$: 594.3367; found: 594.3366 ($|\Delta| = 0.0$ ppm).

2,6,10-Tri-*tert*-butyl-12-(4-(diphenylamino)phenyl)dibenzo[cd,mn] pyrene-4,8-dione (T4)

Solvent: dry, freshly distilled THF.

Yield: 36.6 mg (63%); purple solid; 124–125 °C.

IR (Neat): 3060, 3034, 2954, 2905, 2868, 1736, 1643, 1590, 1577, 1490, 1392, 1269, 1245, 833, 749, 694, 646, 505 cm⁻¹.

¹H NMR (400 MHz, CD₂Cl₂): δ = 9.08 (d, *J* = 2.0 Hz, 2H), 8.89 (s, 2H), 8.31 (d, *J* = 2.0 Hz, 2H), 7.46–7.41 (m, 2H), 7.39–7.32 (m, 6H), 7.28–7.23 (m, 4H), 7.14–7.08 (m, 2H), 1.56 (s, 9H), 1.47 (s, 18H) ppm.

¹³C NMR (150, CD₂Cl₂, MHz.): δ = 183.7, 151.8, 149.42, 148.5, 148.1, 143.4, 133.7, 132.9, 131.9, 131.3, 131.1, 130.4, 130.3, 129.8, 129.2, 125.1, 125.0, 123.7, 123.5, 115.6, 35.9, 35.8, 31.5, 31.1 ppm.

HRMS (ESI): *m/z* [M + H]⁺ calcd for C₅₂H₄₈NO₂⁺: 718.3680; found: 718.3672 (|Δ| = 1.1 ppm).

2,6,10-Tri-*tert*-butyl-12-(thiophen-2-yl)dibenzo[*cd,mn*]pyrene-4,8-dione (T5)

Solvent: dry, freshly distilled THF.

This compound was additionally purified by GPC (CHCl₃).

Yield: 10.1 mg (22%); red solid; mp over 300 °C.

IR (Neat): 2958, 2920, 2870, 1729, 1660, 1644, 1579, 1553, 1413, 1391, 1362, 1246, 832, 717, 644.4 cm⁻¹.

¹H NMR (400 MHz, CD₂Cl₂): δ = 9.07 (d, *J* = 2.0 Hz, 2H), 8.89 (s, 2H), 8.35 (d, *J* = 2.0 Hz, 2H), 7.77 (dd, *J* = 5.2, 1.2 Hz, 1H), 7.41 (dd, *J* = 5.2, 3.4 Hz, 1H), 7.37 (dd, *J* = 3.4, 1.2 Hz, 1H), 1.56 (s, 9H), 1.45 (s, 18H) ppm.

¹³C NMR (101, CD₂Cl₂, MHz.): π = 183.6, 152.3, 150.0, 137.5, 135.0, 133.5, 132.0, 131.9, 131.3, 131.2, 130.37, 129.97, 129.08, 128.30, 127.63, 124.87, 116.99, 35.85, 35.80, 31.45, 31.05 ppm.

HRMS (ESI): m/z $[M + H]^+$ calcd for $C_{38}H_{37}O_2S^+$: 557.2509; found: 557.2506 ($|\Delta| = 0.5$ ppm).

4.7 ACKNOWLEDGEMENT

We are indebted to Prof. Dr. Marcel Mayor for generously hosting our group at the University of Basel and his invaluable support of our research, Angelo Lanzilotto, Prof. Dr. Edwin C. Constable, and Prof. Dr. Catherine E. Housecroft for the measurements of quantum yields, Mario Lehmann for his help with GPC purification of compound **T5**, and Martina Ribar Hesticová for taking the photograph shown in Figure 3a. The Swiss National Science Foundation (SNSF, M.J./PZ00P2_148043), the Novartis University of Basel Excellence Scholarship for Life Sciences (M.J.), and Experientia Foundation (T.Š.) are gratefully acknowledged for their financial support.

4.8 SUPPORTING INFORMATION

The full supporting information can be found in Appendix A.

SYNTHESIS OF DIBENZO[7₅]CETHRENE

5.1 INTRODUCTION

Interest in spin-delocalized π -conjugated molecules^[118,123, 204–208] that contain one or more unpaired electrons caught a significant attention of scientific community in recent years, as these systems are promising candidates as components of new materials, due to their magnetic and conducting properties^[209–213] that are usually associated with metals. The magnetism in these systems emerges from the presence^[214] of unpaired electrons, either in the ground state or low-lying excited states. Conductivity, on the other hand, arises on account of the short intermolecular distance between the molecules, which are held together via multi-centred n -electron π bonds, usually referred to as “pancake bond”.^[115, 116, 215–221] As briefly mentioned in section 1.5.2., the pancake bond can be formed by favourable overlap of SOMOs in odd-electron systems^[215–216] or by favourable overlap of partially occupied frontier molecular orbitals (namely, HOMO and LUMO), which are close in energy in Kekulé^[222] systems. As a consequence, a pair of electrons from HOMO partially occupies also the LUMO, to minimize the electron repulsion. The latter systems are called “diradicaloid” Kekulé systems.^[223] The ground state of the diradicaloid systems is singlet as they have no unpaired electrons, however, they usually possess a low-lying triplet excited state that can be populated^[204] thermally.^[223]

Phenalenyl-based systems zethrene and its analogues are one class of diradicaloid molecules.^[224–225] These extended delocalized systems can be formally obtained^[226–229] by

fusing two or more phenalenyl units by using a spacer such as benzene. If two phenalenyl units are fused together via a central benzene ring, five possible isomers can be formed (Figure 5.1).^[226]

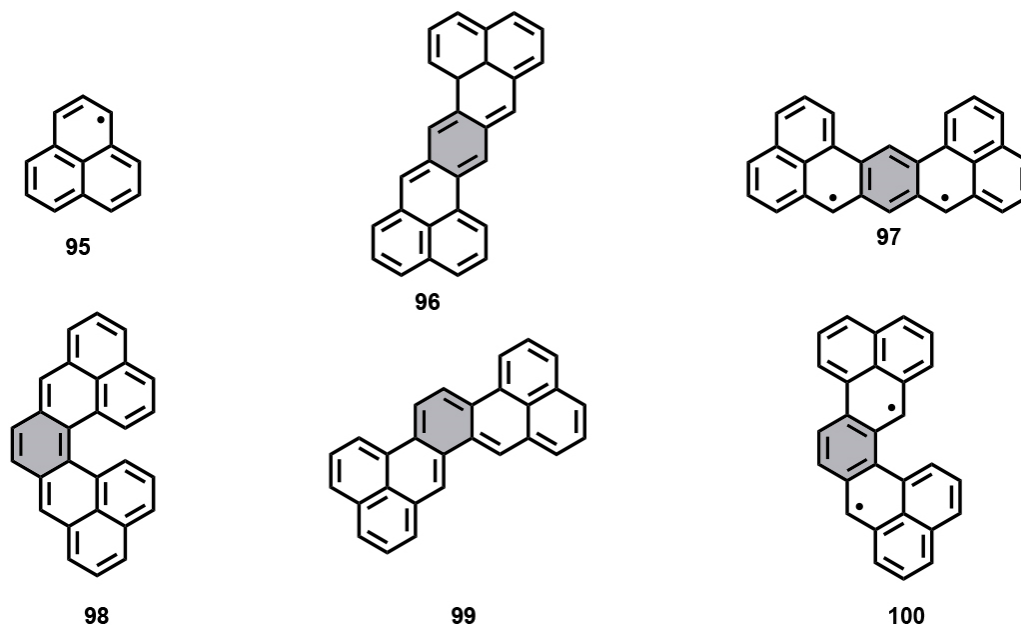
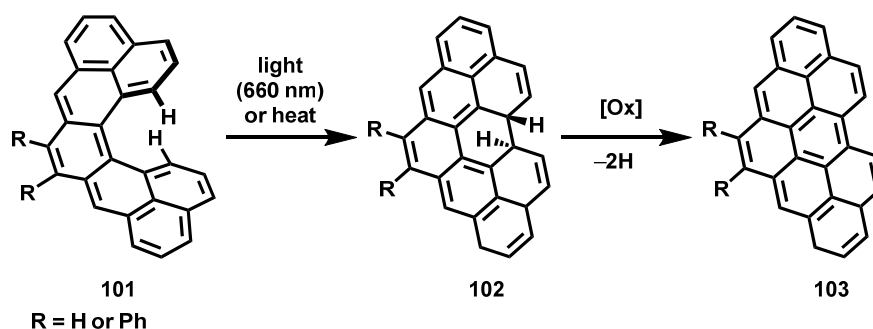


Figure 5.1: Five isomers formed by fusion of two phenalenyl units via benzene central molecule (marked grey).

Depending on the fusing mode, two distinguished sets of molecules can be made, namely, Kekulé diradicaloid molecules **96**, **98** and **99**, where two unpaired electrons of phenalenyl can couple to form a double bond or non-Kekulé molecules **97** and **100**, where the two electrons remain unpaired. The Kekulé diradicaloid molecules are predicted to have a singlet ground state with low HOMO–LUMO gap, on the other hand, the non-Kekulé molecules are predicted to have a triplet ground state. The derivatives of **96** (heptazetherene, Z-shaped)^[230], **97** (heptauthrene, U-shaped)^[231] and **98** (heptacethrene, C-shaped)^[232] are known, while the derivatives of **99** and **100** still remain to be made until this day. From the five possible isomers of heptazetherene **96-100**, isomer **98** is the only one to have a [5]helicene^[233] backbone. This compound, therefore, possesses properties which arise from both its electronic structure as well as helical chirality^[234]. This makes the heptacethrene (or

simply cethrene as it is the first compound of this series) an ideal candidate to investigate the effect of helical twist on its electronic structure.

In order to explore this effect, our group has recently synthesised the first derivative of cethrene, namely, diphenyl cethrene (Scheme 5.1),^[232] and was able to demonstrate several of its unique features.^[232, 235–236] One of the consequences of the helical geometry in cethrene is that intramolecular through-space orbital interaction arise within the frontier molecular orbitals, specifically, an antibonding interaction within the HOMO and a bonding interaction within the LUMO, which is not the case in planar isomer heptazethrene. These through-space interactions are responsible for the increase of the energy of HOMO, as well as the lowering of the energy of the LUMO, and therefore decrease^[232] the HOMO–LUMO gap of cethrene compared to heptazethrene.^[237]

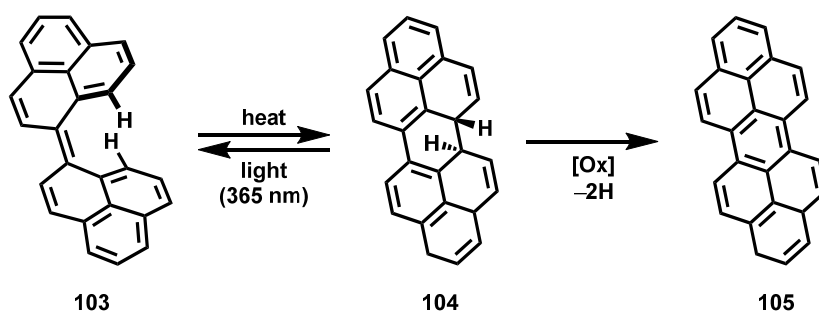


Scheme 5.1: Electrocyclic ring closure of cethrene and its oxidation to the closed flat form.

Another consequence of the through-space orbital interactions is the decrease of the singlet–triplet gap of cethrene (~ 5.6 kcal mol⁻¹, EPR; 5.9 kcal mol⁻¹, DFT), compared to heptazethrene (8.9 kcal mol⁻¹, DFT).^[11] A consequence of such decrease in singlet–triplet gap of cethrene is, that cethrene gives signal in EPR, while the heptazethrene is EPR silent. The reason behind this drop can be rationalized by the fact that in the singlet ground state, the two electrons occupy mainly the HOMO, while in the triplet state, both HOMO and LUMO are occupied by one electron each. Therefore, the singlet state suffers more from the

antibonding interaction within HOMO than the triplet state and this increase the energy of the singlet state in comparison to triplet state, and thus lowers the singlet–triplet gap.^[232]

During the course of the studies of diphenyl cethrene **101**, it was found out that it is not stable, and it undergoes a clean electrocyclic ring-closure transformation to the more stable closed form **102** (Scheme 5.1).^[232] This transformation proceeds in a conrotatory mode on account of steric constraints enforced by the helical geometry. Unlike in the case of most electrocyclic reactions, however, the conrotatory ring closure of open cethrene **101** proceeds both by symmetry-allowed^[238] photochemical reaction, as well as by formally thermally forbidden^[P1] reaction with a surprisingly low activation barrier ($\sim 14 \text{ kcal mol}^{-1}$). The mechanism of the thermally forbidden reaction is yet not fully understood.^[223, 235] Unfortunately, the closed form of cethrene **102** is not stable and it undergoes a facile oxidation to the planar hydrocarbon **103** (Scheme 5.1). Therefore, it was not possible to perform the reverse photochemical ring opening reaction of the closed cethrene **102** to its open form **103**.^[232]

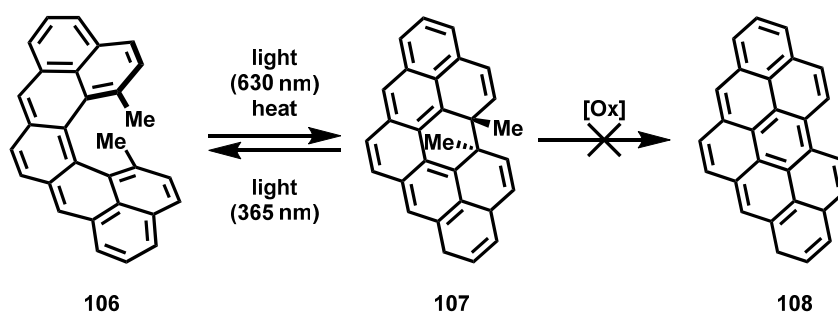


Scheme 5.2: Electrocyclic ring closure of biphenalenylidene and electrocyclic ring opening and oxidation to its closed form.

This process, however, could be validated in a simplified system biphenalenylidene, which is an analogue of cethrene short of two carbon atoms (Scheme 5.2).^[239–240] Kubo *et al.*^[238] demonstrated that the closed form **104** underwent an electrocyclic ring-opening reaction to give an open form **103** upon an UV light irradiation. Similarly to the open cethrene **101**, the open form **103** also underwent a thermal ring-closure reaction that

proceeds with a barrier ($\sim 16 \text{ kcal mol}^{-1}$) similar to that of open cethrene **101**. However, in this case, the closing reaction did not proceed upon irradiation with visible light. Similarly as in the case of closed cethrene **102**, also the closed form of biphenalenylidene **104** undergoes a facile oxidation to the planar hydrocarbon **105** (Scheme 5.2). Our results and the results of Kubo *et al.* indicated that cethrene and related molecules could be employed as a switch that can be operated solely by light.^[223]

With a goal to construct a stable chiroptical switch, which would not undergo the transformation to the flat hydrocarbon, our group recently synthesized a dimethyl derivative **106** of cethrene (Scheme 5.3). The two methyl groups were installed in the fjord region of the molecule, to suppress the oxidation to the flat hydrocarbon **108**.^[223]



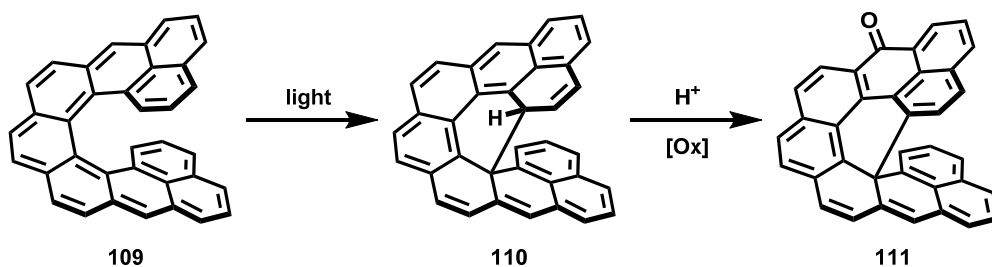
Scheme 5.3: Electrocyclic ring closure of dimethylcethrene and electrocyclic ring opening to its closed form.

Similarly to the open cethrene **101**, open dimethylcethrene undergoes ring-closure that can be induced both by light (630 nm) and heat. However, in contrast to the closed cethrene **102**, the closed form of dimethylcethrene **107** is a stable compound that can be purified by column chromatography and the structure of which was confirmed by X-ray crystallography. Also in contrast to the closed cethrene **102**, this process can be reversed by light irradiation (365 nm) and the whole photochemical cycle could be repeated up to 100 times with 10–20% observed decomposition. It was therefore demonstrated that the instalment of two methyl substituents in the fjord region of the parent cethrene leads to a robust system, and that cethrene can act as a switch operated solely by light.^[223] Despite the fact that both optical

and chiroptical properties of the open and closed form of dimethylcethrene are significantly different, the open form is, unfortunately EPR silent. The reason for this is that open dimethyl cethrene **101** possesses a singlet–triplet gap (10 kcal mol^{-1}) too large for the detection of an EPR signal.

The reason for such a significant increase of the singlet–triplet gap compared to parent cethrene molecule ($5.9 \text{ kcal mol}^{-1}$) can be rationalized by two factors. The first one is the higher degree of helical twist imposed by steric repulsion of the methyl substituents that are significantly bulkier than hydrogen atoms. This larger helical twist is responsible for a larger distance between the carbon atoms in the fjord region and results in a less efficient through-space orbital overlap, that is essential for decreasing the singlet–triplet gap compared to the planar isomer. The second reason for this singlet–triplet gap increase is the electronic effect of the methyl substituents.^[223] As the methyl groups are vital for stability, the singlet–triplet gap must be decreased by other terms, for example, by instalment of additional substituents around the periphery, in other to use the dimethylcethrene also as magnetic switch.

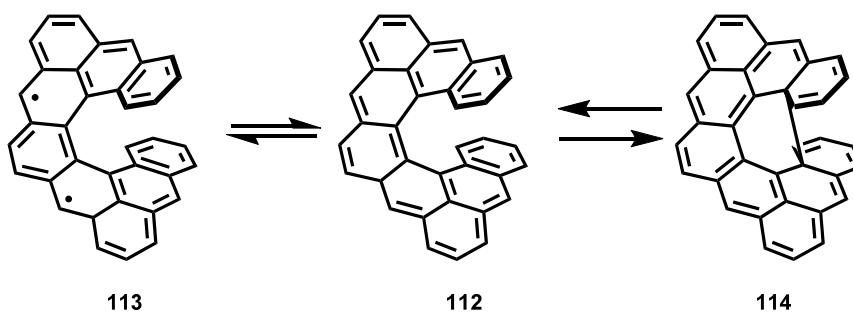
With the aim to explore the effect of elongation of the helical backbone on the electronic properties of the parent cethrene molecule, the higher homolog, nonacethrene **109** (Scheme 5.4) containing phenanthrene instead of benzene as a spacer between two phenalenyl molecules, was synthesized. This nonacethrene molecule **109** (Scheme 5.4) is predicted to have a singlet ground state, similarly to the parent cethrene **98** but the prolongation of the helical backbone should further decrease the HOMO–LUMO gap as well as decrease the singlet–triplet gap. This is because the prolongation of the paternal helical backbone results in the increase of the cofacial overlap between the spin units, which should lead to an increase of the effect of the through-space interactions.



Scheme 5.4: The decomposition cascade of nonacethrene **109** (unpublished results).

During the course of the studies of nonacethrene **109**, it was found out that the molecule is not stable. We hypothesized that the proton (highlighted in bold), in the closed form of nonacethrene **110** (Scheme 5.4), first isomerizes under the acidic conditions (column chromatography) to the position where upon oxidation (traces of oxygen on silica column), the keto group is formed, which leads to the formation of the keto molecule **111**.

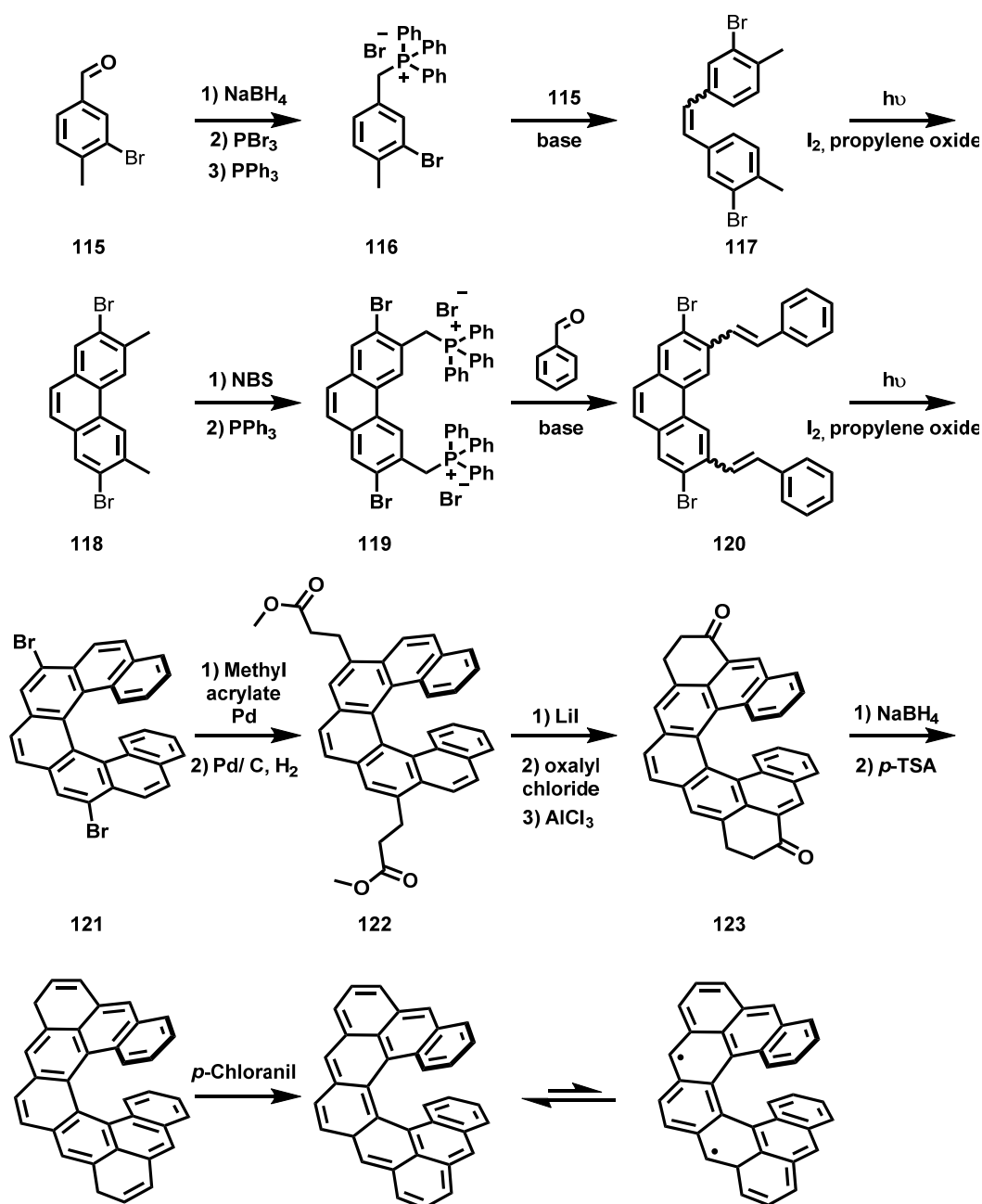
To overcome this problem with a migrating proton, we proposed to move one six-membered ring on each side of the helical backbone to form dibenzo[7₅]cethrene **112**. This should contribute to the stabilization of the system towards oxidation, as two quaternar centers will be formed upon ring closure.



Scheme 5.5: Isomer of the nonacethrene **112** with two benzene rings moved in different position.

5.2 RESULTS & DISCUSSION

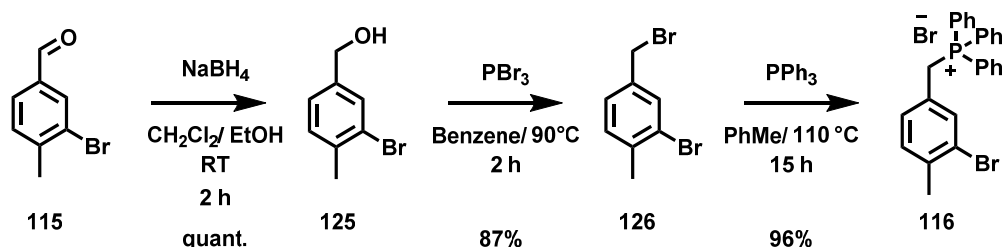
Our synthetic strategy for preparation of the nonacethrene **113** is based on a knowledge gained from previous projects such as cethrene **101** and dimethylcethrene **106**.



Scheme 5.6: Proposed synthesis for diradicaloid nonacethrene **113**.

The general idea for the synthesis was to first build the [7]helicene precursor **121** and then attach two alkyl chains to the backbone to form molecule **122**, which can be

intramolecularly closed to form the two remaining rings **123**. The crucial step towards the helicene **121** represents the successful preparation of the phenanthrene **118**, which can be prepared via photocyclodehydrogenation of the styryl compound **117**. A simple way how to prepare the styryl compound **117** is via Wittig reaction of one equivalent of aldehyde **115** and phosphonium salt **116**. Once the phenanthrene **118** is prepared, the two methyl groups can be brominated and converted to the diphosphonium salt **119**. The distyryl compound **120** can be prepared via double-fold Wittig reaction using two equivalents of the benzaldehyde and the diphosphonium salt **119**. The helicene precursor **121** can be then prepared via two-fold photocyclodehydrogenation of the distyryl compound **120** upon light irradiation.



Scheme 5.7: Three-step synthesis towards triphenyl phosphonium salt **116**.

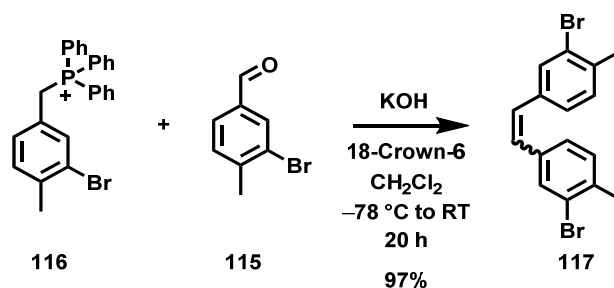
The synthesis of the heptacetherene **121** starts from commercially available 3-bromo-4-methylbenzaldehyde **115**, that was first reduced by NaBH₄ according to modified procedure previously described in literature^[241] (Scheme 5.7). Methanol was substituted for CH₂Cl₂/EtOH to boost the solubility of the starting material and therefore improve the yield. The desired (3-bromo-4-methylphenyl)methanol **125** was isolated after aqueous work up in quantitative yield. The ¹H NMR spectrum revealed, that the isolated material is in high purity and therefore no additional purification was required. Moreover, the reaction can be performed on a large scale with similar yield and purity of the desired product.

In next step, the crude (3-bromo-4-methylphenyl)methanol **125** was converted to the corresponding bromo derivative **126** by S_N2 substitution step, using PBr₃ in benzene as reagent (Scheme 5.7). This procedure is known in the literature.^[242] After aqueous work-up,

the desired 2-bromo-4-(bromomethyl)-1-methylbenzene **126** was isolated in very good 87% yield and high purity. The 2-bromo-4-(bromomethyl)-1-methylbenzene is not stable under ambient conditions and it slowly decomposed. Therefore, it needs to be used right away, or it can be temporally stored under an argon atmosphere in freezer for several days.

The bromo-4-(bromomethyl)-1-methylbenzene **126** was subsequently converted to the triphenyl phosphonium salt **116** using the literature known procedure (Scheme 5.7).^[243] The reaction was carried in anhydrous PhMe, with excess of triphenyl phosphine (PPh₃) under reflux. The desired triphenyl phosphonium salt was obtained after filtration and drying in *vacuo* in excellent 96% yield, and it was used in the next step without further purification.

Two building blocks, one equivalent of aldehyde **115** and one equivalent of the phosphonium salt **116** were condensed together via Wittig reaction, using KOH as a base to provide stilbene **117**, where two possible geometric isomers with either *E* or *Z* configuration could be formed (Scheme 5.8).

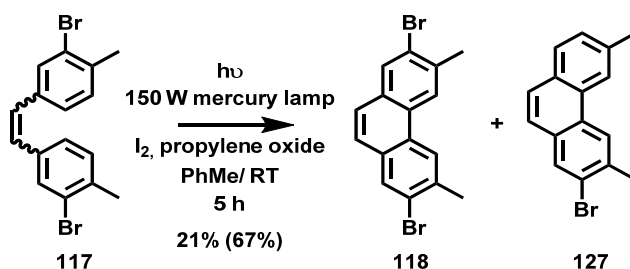


Scheme 5.8: Preparation of the stilbene **117** by Wittig reaction using KOH as a base.

The reaction mixture needs to be degassed extensively prior the addition of the base, otherwise formation of the unwanted side reaction occurs. After aqueous work-up, the crude product was purified by column chromatography using cyclohexane as eluent to obtain the desired product **117** as mixture of *E* and *Z* isomers in ratio 2.6:1 in favour of the *E* isomer in excellent 97% yield. It is possible to separate the two isomers from one another, however, it is not necessary as the mixture of the isomers does not hamper the following photocyclodehydrogenation. Therefore, only small sample of the isomer mixture of the

products was separated, to obtain sufficient amounts of the isomers for spectral characterization.

The photocyclodehydrogenation of the isomer mixture **117** (Scheme 5.9) was carried on in an immersion well photo reactor system with quartz cooling tube and quartz immersion tube containing 150 W medium pressure mercury lamp. The photocyclodehydrogenation was performed according to the procedure developed by Katz *et al.*^[244] where stoichiometric amount of iodine is used instead of catalytic amount and the reaction is performed under an inert atmosphere. Additionally, propylene oxide is used as HI scavenger, that is built during the reaction course, to avoid the photoreduction by HI.



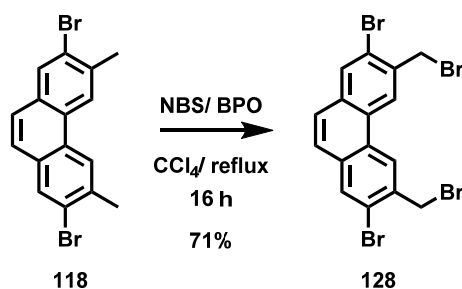
Scheme 5.9: Photodehydrocyclization of stilbene **117**.

The stilbene **117** was consumed within 5 h of irradiation, however, the TLC analysis as well as GS MS analysis revealed formation of two compounds, namely, desired dibromophenanthrene **118** and undesired monodehalogenated side product **127** (Scheme 5.9). We attempted to avoid the formation of the undesired side product **127** by adjusting the concentration and the reaction time, however, these changes were unsuccessful. The change of the concentration of the reaction did not affect the reaction at all and the shorten reaction time only decreased the yields of both products. We also switched the quartz cooling system to a glass one, to avoid the UV irradiation. This, however, lead only to prolongation of the reaction time and formation of more side products. The bromine is most likely to be lost after the cyclization as bromine or HBr is lost in radical or elimination mechanism to restore

the aromaticity before it can be oxidized. Alternatively, the bromine could be lost prior the photocyclization.

We were not able to eliminate the formation of the unwanted dehalogenated side product **127**. Nevertheless, we decided to continue to use these conditions as the desired **118** and undesired side product **127** could be easily separated by column chromatography. Moreover, the starting material **117** can be prepared in large quantities extremely quickly and in very good yields, as well as the photocyclodehydrogenation can be performed on 1 g scale at the time producing more than 200 mg of the desired product at the time. Furthermore, the monofunctionalized phenanthrenes such as side product **127** are very rarely obtainable, therefore, the undesired side product **127** can serve as a starting material for different project which are under investigation in the Juríček group. To obtain sufficient amount of the desired product **118**, the photocyclization is simply performed several times.

In the next step, the dibromophenatrene **118** was brominated by terms of radical bromination. NBS was used as source of bromine and BPO was used as radical starter. The reaction mixture was heated under reflux in CCl₄ overnight.

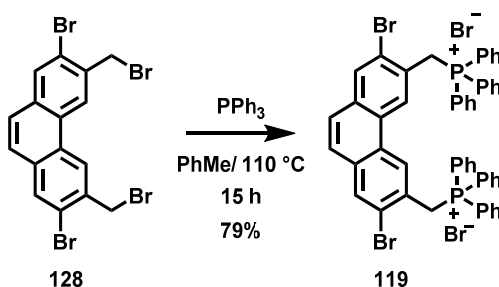


Scheme 5.10: Radical bromination of the dibromophenatrene **118**.

Both TLC and GC MS analysis confirmed full conversion of the starting material and formation of the desired product **128**, with traces of monobrominated species. The crude product was purified by column chromatography and the desired dibrominated product **128** was isolated in good 71% yield. Small amount of monobrominated product was also isolated,

however, it is not stable under ambient and acidic conditions and it decomposes on silica column.

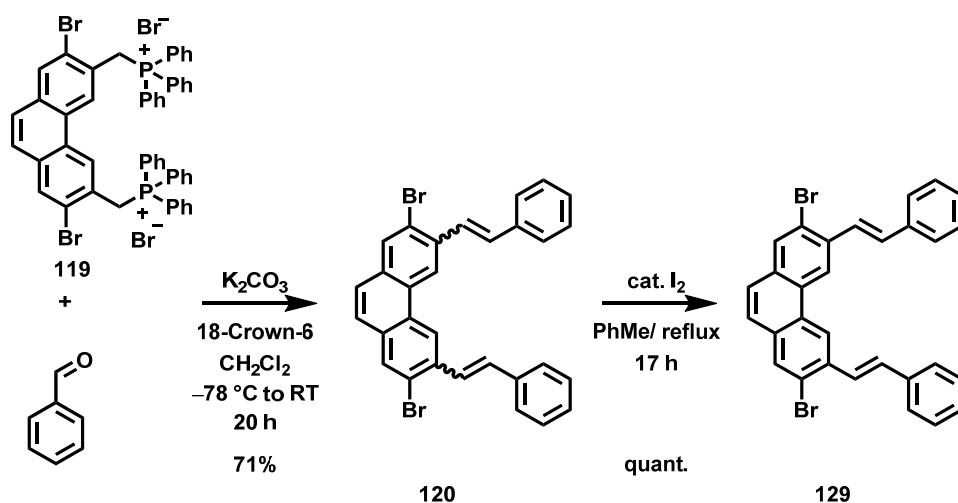
The dibrominated phenanthrene **128** was converted to its phosphonium salt **119**. The reaction was carried in anhydrous PhMe, with excess of triphenyl phosphine (PPh_3) under reflux (Scheme 5.11).



Scheme 5.11: Preparation of the phosphonium salt **119**.

The desired triphenyl phosphonium salt was obtained after filtration and drying in *vacuo* in good 79% yield, and it was used in the next step without further purification. The phosphonium salt is not stable under ambient conditions, neither in solution, and it needs to be used in next step right after isolation. The spectral characterization is also challenging as it decomposes in the NMR solvent. Therefore, the phosphonium salt is only characterized by its HR ESI MS.

In the next step, two building blocks, two equivalents of benzaldehyde and one equivalent of phosphonium salt **119** were condensed together via a double-Wittig reaction with KOH as a base to provide stilbene-type compound **120**. In this reaction formation of three possible geometric isomers with either (*E,E*), (*E,Z*) or (*Z,Z*) could be formed (Scheme 5.12).



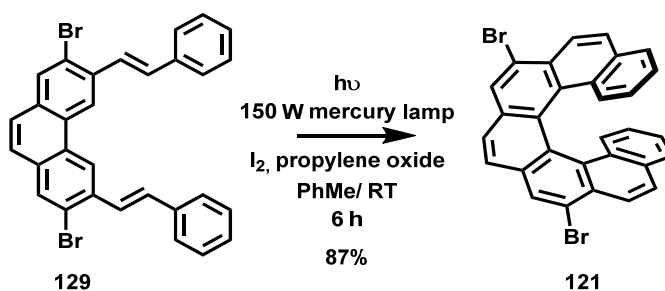
Scheme 5.12: Preparation of the compound **CV** and its subsequent isomerization to its (*E,E*) isomer.

Accordingly, the TLC analysis of the crude mixture showed three compounds possessing very similar R_f values. The column chromatography provided a mixture of three possible isomers. Therefore, the determination of the purity by ^1H NMR spectroscopy was complicated.

Similarly, to the photocyclodehydrogenation of stilbene **117**, having a mixture of isomers does not represent a problem for the following photocyclodehydrogenation. The mixture was isomerised in order to obtain single, thermodynamically most stable (*E,E*) isomer and with a goal to confirm the structure and purity of the Wittig product. The isomerisation was achieved by heating the mixture of isomers at 90–95 °C in PhMe overnight with a catalytic amount of iodine (Scheme 5.12). The most stable (*E,E*) isomer **129** was obtained via reversible radical addition of iodine to the double bond and subsequent elimination in the quantitative yield. The structure of the product **129** was confirmed by its ^1H NMR spectrum, which contained coupling constants (ca. 16 Hz) of the double-bond protons typical for vicinal *trans* coupling.

The subsequent photocyclodehydrogenation was again performed according to the procedure developed by Katz *et al.*,^[244] by using immersion well photo reactor system with

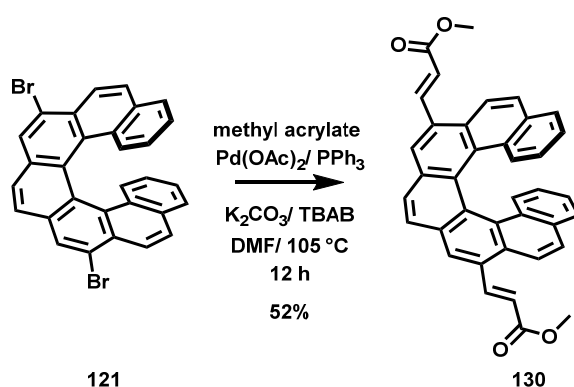
quartz cooling tube and 150 W medium pressure mercury lamp. This time the glass immersion tube was used in order to avoid the UV light irradiation.



Scheme 5.13: Photocyclodehydrogenation of compound **129**.

The compound **129** was smoothly cyclized within 6 h of irradiation in the presence of stoichiometric amount of iodine and large excess of propylene oxide to the corresponding dibromo [7]helicene **121**. The crude mixture was purified by column chromatography and the desired dibromo [7]helicene was isolated in excellent 87% yield. The reaction can be scaled up to 750 mg with retention of excellent yield and purity, however, the reaction needs to be deaerated extensively prior irradiation to avoid formation of undesired side products.

In the next step, the α,β -unsaturated side chain had to be introduced by means of double-fold Heck cross-coupling reaction with an *in situ* generated palladium catalyst to obtain the diester **130** (Scheme 5.14).



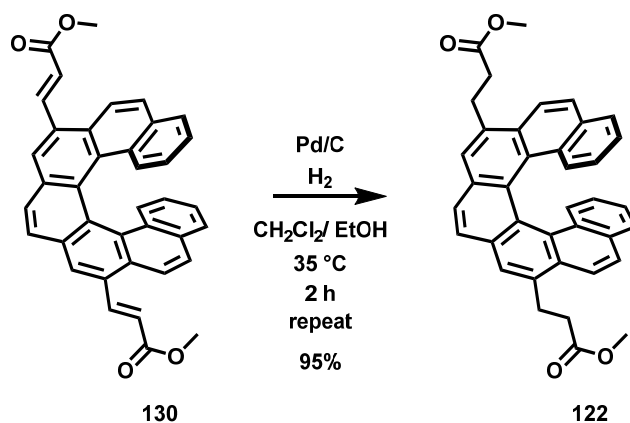
Scheme 5.14: Preparation of the diester **122**.

The desired diester **130** was obtained after column chromatography in moderate 52% yield.

The lower yield could be caused by insufficient deaerated as this was provided only by 181

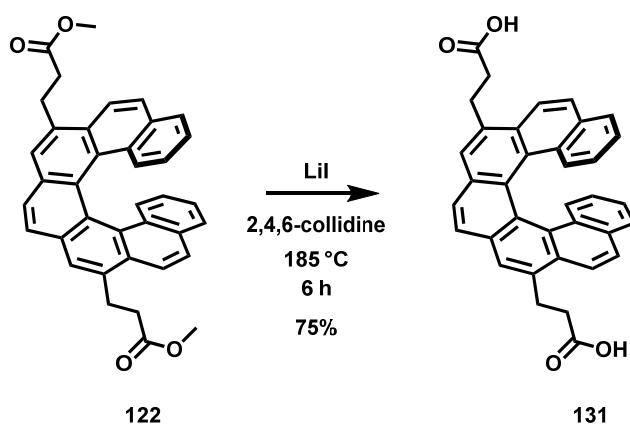
bubbling of argon for 15 min. Changing the deaerating method to freeze-pump-thaw in several cycles might be a solution for improving the reaction yield.

Subsequently, the double bonds of the diester **130** were attempted to be reduced by Pd/C hydrogen in CH₂Cl₂/ EtOH at room temperature (Scheme 5.15). However, only a very small conversion of the starting material was observed.



Scheme 5.15: Reduction of the double bond of the diester **122**.

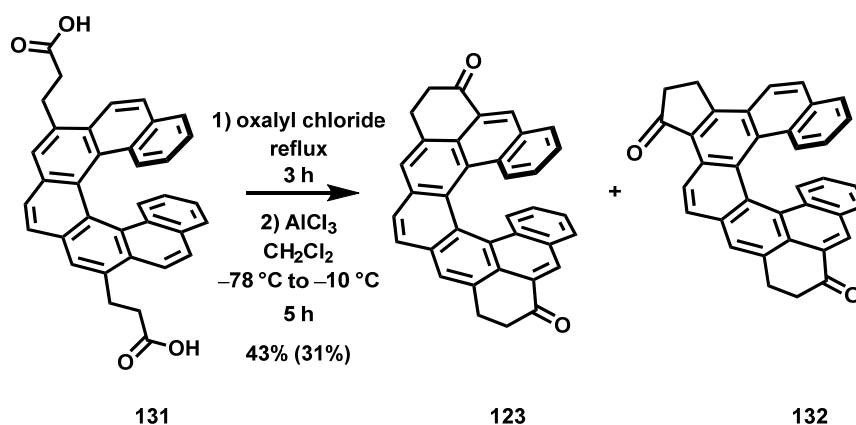
The increase of the reaction temperature to 35 °C significantly improved the conversion, but full conversion was still not observed. Therefore, the reaction mixture was passed through small pad of celite to remove the Pd/C and the crude mixture was subjected to the same condition as previously described. This procedure had to be repeated for three more times until the starting material was fully consumed. After final filtration and evaporation of the solvents, the crude was purified by column chromatography and the desired reduced diester **122** was isolated in excellent 95% yield and high purity.



Scheme 5.16: Deesterification of the diester **122**.

The deesterification of the diester **122** was attempted, according to previously reported procedure in our group.^[232] The diester **122** and LiI were heated at 185 °C in 2,4,6-collidine for 6 h (Scheme 5.16). After evaporation of the solvent and subsequent acidification, the formed precipitate was collected. After drying in *vacuo*, the desired diacid **131** was obtained in good 75% yield and it was used in next step without further purification.

The diacid **131** was subsequently transformed to its corresponding acid chloride, using oxalyl chloride. After evaporation of the excess oxalyl chloride the crude acid chloride was closed by Friedel–Crafts acylation, using AlCl₃ in CH₂Cl₂ at low temperature (Scheme 5.17).

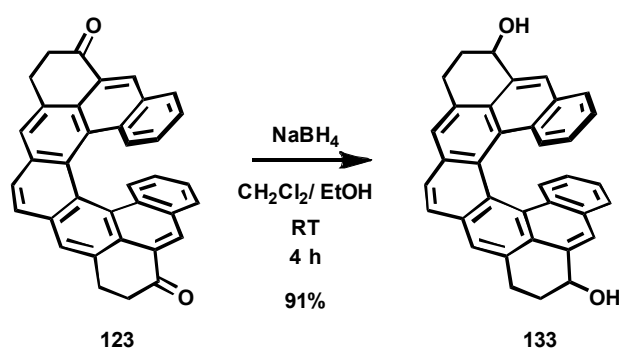


Scheme 5.17: Friedel–Crafts acylation of the diacid **131**.

The MALDI-TOF MS analysis revealed formation of the single compound. The crude mixture was purified by column chromatography. The subsequent ¹H NMR spectral analysis,

however, showed presence of two compounds, that were identified as desired symmetrical compound **123** and unsymmetrical compound **132**. The TLC analysis of the mixture revealed that these two compounds are partly separable, therefore, a new larger column chromatography, using Isolera column machine was performed. The two compounds could be separated using CH₂Cl₂ 7:3 to cyclohexane:CH₂Cl₂:EtOAc 63:30:7 as eluents in sufficient purity. As we performed this reaction only once, the optimization of the reaction conditions is required. We hypothesise that the formation of the undesired unsymmetrical compound **132** could be minimized by adjusting the concentration or reaction temperature. However, further experiments are required to support this speculation.

In next step, the two keto groups were smoothly reduced by NaBH₄ in CH₂Cl₂/ EtOH at room temperature.



Scheme 5.18: Reduction of the diketo compound **123**.

The desired dihydroxy compound **133** was obtained after column chromatography in high purity and in excellent 91% yield. The compound is not stable under ambient conditions and it decomposes within two days. Unfortunately, we discovered this later and we lost most of the compound.

The last reaction, which we were able to perform is the dehydroxylation of the dihydroxy compound **133**. The reaction was carried on in degassed PhMe with *p*-TSA (Scheme 5.19).

The presence of the two doublets at 3.96 and 3.63 ppm, characteristic for the $-\text{CH}_2-$ group, with combination of the obtained mass, strongly support the preparation of the desired helicene **124**. Due to decomposition of the compound **124**, obtained in the previous step and short period before the finishing of the lab work, we were not able to reproduce this reaction. However, the resynthesis and further investigation is ongoing in the research group of Prof. Juriček.

5.3 CONCLUSION & OUTLOOK

Unfortunately, we were not able to finish the synthesis of the diradicaloid nonacethrene **113** and prove its switching abilities, due to lack of time and series of unfortunate events. However, we were able to establish a synthetic strategy towards the precursor of nonacethrene **124** consisting of 15 steps, featuring two photocyclodehydrogenations as crucial synthetic steps. Even though, the first photocyclization step provided only a low amounts of the desired dibromophenatrene **118**, we decided to continue in this approach as the stilbene precursor can be easily prepared on a large scale and the obtained debrominated side **127** product can serve as a valuable starting material for other projects, which are ongoing in the research group of Prof. Juríček.

The dibrominated [7]helicene was then prepared in four steps in very good overall yield. The two additional six-membered rings were installed in four steps in the similar fashion as was already demonstrated in previous projects involving helical backbone.

Even though we have no final confirmation of the structure of the precursor **124**, the obtained mass and recorded ^1H NMR spectra, featuring two doublets typical for $-\text{CH}_2-$ groups strongly support that the final precursor was prepared. After successful preparation of the final precursor, the final oxidation to the diradicaloid nonacetherene **113** will be conducted and the switching abilities will be investigated. The resynthesis of the precursor is ongoing in the research group of Prof. Juríček.

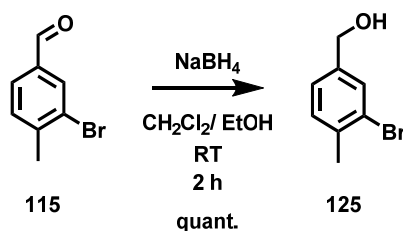
5.4 EXPERIMENTAL SECTION

5.4.1 GENERAL REMARKS

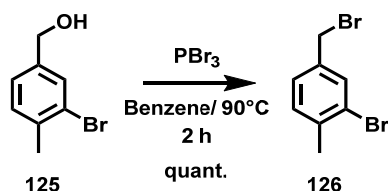
All chemicals and solvents were purchased from commercial sources and used without further purification unless stated otherwise. The reactions and experiments that are sensitive to oxygen were performed using Schlenk techniques and argon-saturated solvents. The solvents were saturated with argon by either passing argon gas through the solvent or using the freeze-pump-thaw technique in three cycles. All reactions were monitored by either thin-layer chromatography, GC MS, LC MS or Maldi-TOF. Yields refer to purified and spectroscopically pure (^1H NMR) compounds unless the crude product was used in the next step. For column chromatography either silica gel Silicaflash[®] p60 (40 – 60 μm) from Silicycle or Alumina, activated (basic Brockmann Activity I) or neutral was used in dot was purchased from Fluka. The thin-layer chromatography was performed using silica-gel plates Silica Gel 60 F254 (0.2 mm thickness), purchased from Merck and visualized under a UV lamp (254 or 365). The NMR experiments were performed on Bruker Avance III NMR spectrometers operating at 400, 500, or 600 MHz proton frequencies. The instruments were equipped with a direct-observe 5 mm BBFO smart probe (400 and 600 MHz), an indirect-detection 5 mm BBI probe (500 MHz), or a five-channel cryogenic 5 mm QCI probe (600 MHz). All probes were equipped with actively shielded z -gradients (10 A). The experiments were performed at 295 or 298 K unless indicated otherwise and the temperatures were calibrated using a methanol standard showing accuracy within ± 0.2 K. Standard Bruker pulse sequences were used, and the data was processed on Topspin 3.2 (Bruker) using two-fold zero-filling in the indirect dimension for all 2D experiments. Chemical shifts (δ) are reported in parts per million (ppm) relative to the solvent residual peak. The low-resolution mass spectra were recorded either on Bruker amaZon[™] X for Electro Spray Ionization (ESI), on a Shimadzu GSMS-QP2010 SE gas chromatography system with ZB-5HT inferno

column (30 mm x 0.25 mm x 0.25 mm) at 1 ml/ min He-flow rate (split = 20:1) with a Shimadzu electron ionization (EI 70 eV) mass detector, or Burkert microflex system for MALDI-TOF. High-resolution mass spectra (HRMS) were measured as HR-ESI-ToF-MS with a Maxis 4G instrument from Bruker with the addition of NaOAc.

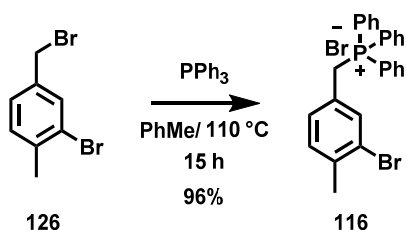
5.3.2 EXPERIMENTAL PROCEDURES



(3-bromo-4-methylphenyl)methanol (125): A solution of 3-bromo-4-methylbenzaldehyde (**115**, 5.50 g, 26.8 mmol) and NaBH₄ (1.52 g, 38.7 mmol) in CH₂Cl₂/ EtOH (90 mL, 2:1) was stirred at room temperature for 2 h before the reaction was carefully quenched by addition of sat. aq. Na₂CO₃. The organic layer was separated, and the aqueous layer was extracted with EtOAc (3 x 20 mL). The combined organic layers were washed with saturated aqueous Na₂CO₃, water and brine, dried over anhydrous Na₂SO₄, and filtered. After evaporation of the solvents, the desired product (**125**, 5.40 g, 100%) was afforded as a lightly-pink oil and was used in next step without further purification. This compound was also prepared and characterized elsewhere. The recorded spectra are in agreement with those reported previously.^[204] ¹H NMR (400 MHz, CDCl₃, ppm): δ 7.53 (d, *J* = 1.3 Hz, 1H), 7.21 (d, *J* = 7.7 Hz, 1H), 7.17 (dd, *J* = 7.8, 1.7 Hz, 1H), 4.61 (s, 2H), 2.38 (s, 3H). ¹³C NMR (101 MHz, CDCl₃, ppm): δ 140.4, 137.3, 131.02, 130.98, 126.0, 125.1, 64.5, 22.8.

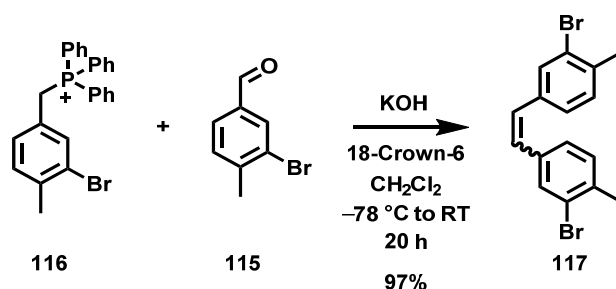


2-bromo-4-(bromomethyl)-1-methylbenzene (126): A solution of (3-bromo-4-methylphenyl)methanol (**125**, 5.40 g, 26.9 mmol) in dry benzene (50 mL) was deaerated with stream of argon for 15 min before PBr_3 (3.79 mL, 40.3 mmol) was added dropwise at room temperature. The mixture was heated at 90°C for 1 h under argon atmosphere before it was allowed to cool down to room temperature and the reaction was quenched by slow addition of sat. aq. Na_2CO_3 solution. The organic layer was separated and the aqueous layer was extracted with EtOAc (3 x 20 mL). The combined organic layers were washed brine, dried over anhydrous Na_2SO_4 , and filtered. After evaporation of the solvents, the desired product (**126**, 6.16 g, 87%) was afforded as a white crystalline solid and was used in next step without further purification. This compound was also prepared and characterized elsewhere. The recorded spectra are in agreement with those reported previously.^[205] ^1H NMR (400 MHz, CDCl_3 , ppm): δ 7.57 (d, $J = 1.7$ Hz, 1H), 7.23 (dd, $J = 7.8, 1.7$ Hz, 1H), 7.20 (d, $J = 7.8$, Hz, 1H), 4.42 (s, 2H), 2.39 (s, 3H). ^{13}C NMR (101 MHz, CDCl_3 , ppm): δ 138.4, 137.2, 132.9, 131.2, 128.0, 125.0, 32.3, 22.8.



(3-Bromo-4-methylbenzyl)triphenylphosphonium bromide (116): A solution of 2-bromo-4-(bromomethyl)-1-methylbenzene (**126**, 6.00 g, 22.7 mmol) and triphenylphosphine (9.62 g, 36.3 mmol) in dry toluene (100 mL) was deaerated with stream of argon for 15 min. The mixture was then heated under reflux over night before it was allowed to cool down to

the room temperature. The white precipitate was filtered and washed with toluene to afford the desired product (**116**, 11.5 g, 96%) as a white solid, which was used in the next step without further purification. This compound was also prepared and characterized elsewhere. The recorded spectra are in agreement with those reported previously.^[206] ¹H NMR (250 MHz, CD₃OD, ppm): δ 7.97–7.86 (m, 3H), 7.81–7.61 (m, 12H), 7.17 (d, $J = 7.8$, Hz, 1H), 7.09 (t, $J = 2.3$ Hz, 1H), 6.94 (dt, $J = 7.8, 2.3$ Hz, 1H), 4.92 (d, $J = 7.8$, Hz, 2H), 2.34 (d, $J = 14.9$, Hz, 2H). ¹³C NMR (63 MHz, CD₃OD, ppm): δ 140.0 (d, $J = 4.1$ Hz), 136.6 (d, $J = 3.1$ Hz), 135.9 (d, $J = 5.3$ Hz), 135.4 (d, $J = 9.7$ Hz), 132.3 (d, $J = 3.1$ Hz), 131.4 (d, $J = 12.7$ Hz), 131.1 (d, $J = 5.4$ Hz), 128.2 (d, $J = 8.7$ Hz), 126.0 (d, $J = 3.9$ Hz), 118.9 (d, $J = 86.4$ Hz), 29.8 (d, $J = 48.5$ Hz), 22.6. HRMS (ESI): m/z [M]⁺ calcd for C₂₆H₂₃BrP⁺: 445,0715; found 445,0711 ($|\Delta| = 0.1$ ppm).

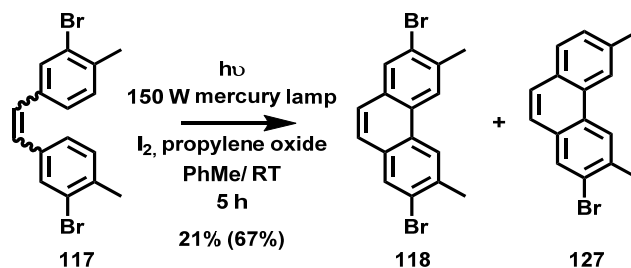


1,2-Bis(3-bromo-4-methylphenyl)ethene (117): To a cooled (-78 °C) solution of (3-bromo-4-methylbenzyl)triphenylphosphonium bromide (**116**, 11.5 g, 21.9 mmol), 3-bromo-4-methylbenzaldehyde (**115**, 4.58 g, 23.0 mmol), and 18-crown-6 (0.58 g, 2.19 mmol) in dry CH₂Cl₂ (60 mL), freshly powdered KOH (3.20 g, 56.9 mmol) was added in one portion under an argon atmosphere. The mixture was stirred at -78 °C for 2 h before it was allowed to warm to room temperature overnight. The solution was decanted to remove the white precipitate and the organic layer was washed with sat. aq. NH₄Cl, brine, and dried over anhydrous Na₂SO₄. After filtration and evaporation of the solvent, the residue was purified

by column chromatography over silica gel using cyclohexane as an eluent to afford desired product (**117**, 7.75 g, 97%) as a mixture (2.6:1) of two possible isomers.

(Z)-1,2-bis(3-bromo-4-methylphenyl)ethene (133): ^1H NMR (400 MHz, CDCl_3 , ppm): δ 7.44 (t, $J = 1.0$ Hz, 2H), 7.07 (m, 4H), 6.48 (s, 2H), 2.37 (s, 6H). ^{13}C NMR (101 MHz, CDCl_3 , ppm): δ 137.0, 136.4, 130.7, 129.3, 127.7, 124.9, 22.8. HRMS (APCI): m/z : $[\text{M}]^+$ calcd for $\text{C}_{16}\text{H}_{14}\text{Br}_2^+$: 363.94568; found 363.94538 ($|\Delta| = 0.82$ ppm).

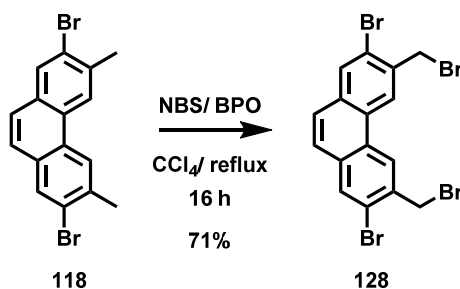
(E)-1,2-bis(3-bromo-4-methylphenyl)ethene (134): ^1H NMR (400 MHz, CDCl_3 , ppm): δ 7.67 (d, $J = 1.8$ Hz, 2H), 7.31 (dd, $J = 7.8, 1.8$ Hz, 2H), 7.21 (d, $J = 7.8$ Hz, 2H), 6.95 (s, 2H), 2.40 (s, 4H). ^{13}C NMR (101 MHz, CDCl_3 , ppm): δ 137.4, 136.7, 131.1, 130.3, 129.3, 127.6, 125.5, 22.8. HRMS (APCI): m/z : $[\text{M}]^+$ calcd for $\text{C}_{16}\text{H}_{14}\text{Br}_2^+$: 363.94568; found 363.94544 ($|\Delta| = 0.64$ ppm).



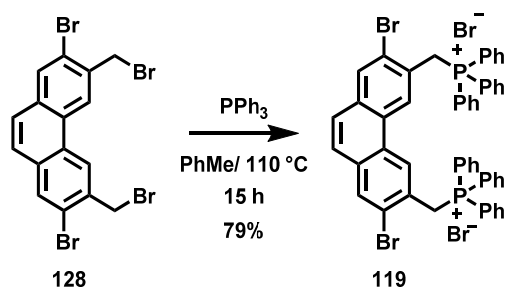
2,7-dibromo-3,6-dimethylphenanthrene (118): A solution of 1,2-bis(3-bromo-4-methylphenyl)ethene (**117**, 1.00 g, 2.73 mmol) and I_2 (0.83 g, 3.28 mmol) in dry toluene (700 mL) was stirred vigorously and deaerated with stream of argon for 40 min. before propylene oxide (9.6 mL, 137 mmol) was added and the mixture was degassed for additional 5 min. Afterwards the mixture was stirred upon UV light irradiation (quartz cooling system) for 5 h. Then the mixture was washed with sat. aq. $\text{Na}_2\text{S}_2\text{O}_3$ (3x 100 mL), brine, and dried over anhydrous Na_2SO_4 . After filtration and evaporation of the solvent, the residue was purified by column chromatography over silica gel using cyclohexane as an eluent to afford desired product (210 mg, 21%) as a white solid and a dehalogenated by-product (520 mg, 67%) as a white solid.

2,7-Dibromo-3,6-dimethylphenanthrene (118): ^1H NMR (400 MHz, CDCl_3 , ppm): δ 8.46 (s, 2H), 8.05 (s, 2H), 7.57 (s, 2H), 2.66 (s, 6H). ^{13}C NMR (101 MHz, CDCl_3 , ppm): δ 136.4, 131.8, 131.7, 128.9, 125.9, 124.2, 22.8. HRMS (APCI): m/z : $[\text{M}]^+$ calcd for $\text{C}_{16}\text{H}_{12}\text{Br}_2^+$: 361.9003; found 363.92978 ($|\Delta| = 0.68$ ppm).

2-Bromo-3,6-dimethylphenanthrene (127): ^1H NMR (400 MHz, CDCl_3 , ppm): δ 8.50 (s, 1H), 8.41 (s, 1H), 8.05 (s, 1H), 7.76 (d, $J = 8.1$, 1H), 7.65 (d, $J = 8.8$ Hz, 1H), 7.54 (d, $J = 8.8$ Hz, 1H), 7.43 (dd, $J = 8.1$, 1.2 Hz, 1H), 2.66 (s, 3H), 2.63 (s, 3H). ^{13}C NMR (101 MHz, CDCl_3 , ppm): δ 136.7, 135.7, 132.0, 131.5, 129.26, 128.7 (two overlapped signals), 127.2, 124.6, 124.4, 123.8, 122.4, 23.7, 22.3.

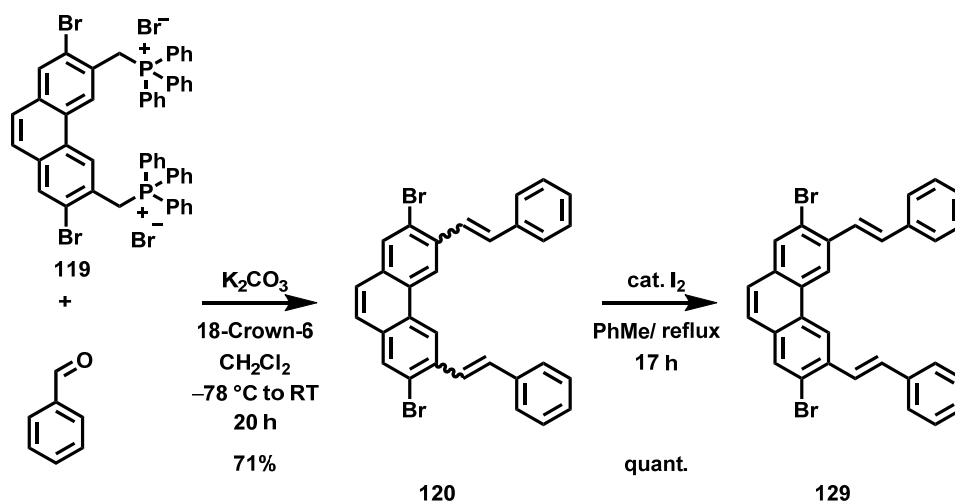


2,7-dibromo-3,6-bis(bromomethyl)phenanthrene (128): A solution of 2,7-dibromo-3,6-dimethylphenanthrene (**118**, 1.50 g, 4.12 mmol), NBS (1.76 g, 9.89 mmol), and dibenzoyl peroxide (120 mg, 0.49 mmol) in dry CCl_4 (150 mL) was deaerated with stream of argon for 20 min. Then the solution was heated under reflux overnight before it was allowed to cool down to room temperature. The solvent was evaporated, and the residue was purified by column chromatography over silica gel using cyclohexane as an eluent to afford desired product (**128**, 1.53 g, 71%) as a white solid. ^1H NMR (400 MHz, CDCl_3 , ppm): 8.69 (s, 2H), 8.12 (s, 2H), 7.66 (s, 2H), 4.88 (s, 4H). ^{13}C NMR (101 MHz, CDCl_3 , ppm): 135.8, 133.4, 133.1, 129.1, 127.3, 125.6, 123.2, 34.0. HRMS (APCI): m/z : $[\text{M}]^+$ calcd for $\text{C}_{16}\text{H}_{10}\text{Br}_4^+$: 517.75105; found 517.75085 ($|\Delta| = 0.38$ ppm).



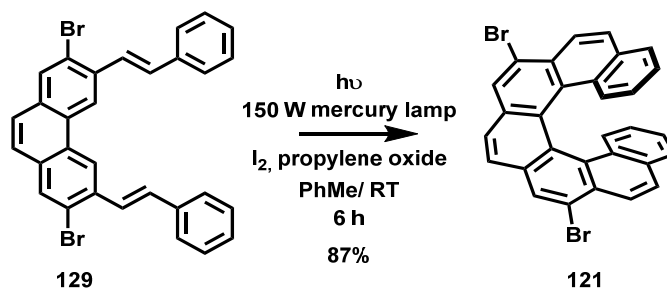
((2,7-Dibromophenanthrene-3,6-diyl)bis(methylene))bis(triphenylphosphonium)

dibromide (119): A solution of 2,7-dibromo-3,6-bis(bromomethyl)phenanthrene (**128**, 1.50 g, 2.87 mmol) and triphenylphosphine (2.43 g, 9.18 mmol) in dry toluene (350 mL) was deaerated with stream of argon for 15 min. The mixture was then heated under reflux overnight before it was allowed to cool down to the room temperature. The white precipitate was filtered and washed with toluene to afford the desired product (**119**, 2.37 g, 79%) as a pale brown solid, which was used in the next step without further purification. HRMS (ESI): m/z $[\text{M}]^+$ calcd for $\text{C}_{52}\text{H}_{40}\text{Br}_2\text{P}_2^{2+}$: 442,0481; found 442,0482 ($|\Delta| = 0.4$ ppm).



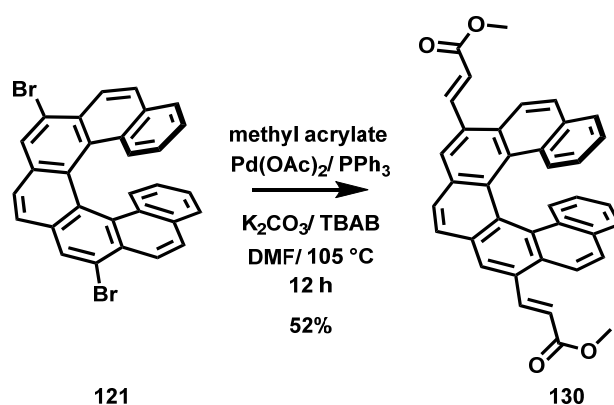
2,7-Dibromo-3,6-di((E)-styryl)phenanthrene (129): To a cooled ($-78 ^\circ\text{C}$) solution of ((2,7-dibromophenanthrene-3,6-diyl)bis(methylene)) bis(triphenylphosphonium) dibromide (**119**, 2.30 g, 2.2 mmol), benzaldehyde (0.61 g, 5.72 mmol), and 18-crown-6 (0.12 g, 0.44 mmol) in dry CH_2Cl_2 (100 mL), freshly powdered K_2CO_3 (0.64 g, 11.4 mmol) was added in one portion under an argon atmosphere. The mixture was stirred at $-78 ^\circ\text{C}$ for 3 h before it

was allowed to warm to room temperature overnight. The solution was decanted to remove the white precipitate and the organic layer was washed with sat. aq. NH_4Cl , brine, dried over anhydrous Na_2SO_4 . After filtration and evaporation of the solvent, the residue was purified by column chromatography over silica gel using cyclohexane/ CH_2Cl_2 9:1 as an eluent to afford desired product (0.81 g, 71%) as a mixture of isomers. The isomeric product was then dissolved in PhMe (100 mL) and stirred for 17 h at 95 °C in the presence of a catalytic amount of iodine. The resulting solution was washed with aqueous $\text{Na}_2\text{S}_2\text{O}_3$ (10%) and brine and dried over anhydrous Na_2SO_4 . After filtration and evaporation of the solvents, the pure (*E,E*) isomer (**129**, 0.81 g, quant.) was obtained as white solid. ^1H NMR (400 MHz, CDCl_3 , ppm): 8.89 (s, 2H), 8.10 (s, 2H), 7.69 – 7.66 (m, 4H), 7.67 (d, $J = 16.1$ Hz, 2H), 7.59 (s, 2H), 7.47 – 7.40 (m, 4H), 7.38 – 7.33 (m, 2H), 7.30 (d, $J = 16.1$ Hz, 2H). ^{13}C NMR (101 MHz, CDCl_3 , ppm): 137.1, 136.1, 132.9, 132.5 (two overlapped signals), 129.3, 129.0, 128.5, 128.1, 127.2, 126.7, 123.2, 120.7. HRMS (APCI): m/z [M] $^+$ calcd for $\text{C}_{30}\text{H}_{20}\text{Br}_2^+$: 537.99263; found 537.99225 ($|\Delta| = 0.70$ ppm).



7,12-Dibromobenzo[1,2-*c*:4,3-*c'*]diphenanthrene (121): A solution of 2,7-dibromo-3,6-di(styryl)phenanthrene (**129**; 0.75 g, 1.39 mmol, mixture of isomers) and I_2 (0.74 g, 2.9 mmol) in dry toluene (700 mL) was stirred vigorously and deaerated with a stream of argon for 40 min before propylene oxide (9.73 mL, 139 mmol) was added and the mixture was degassed for additional 5 min. Afterwards, the mixture was stirred upon light irradiation (glass cooling system) for 6 h. Then the mixture was washed with sat. aq. $\text{Na}_2\text{S}_2\text{O}_3$ (3×100

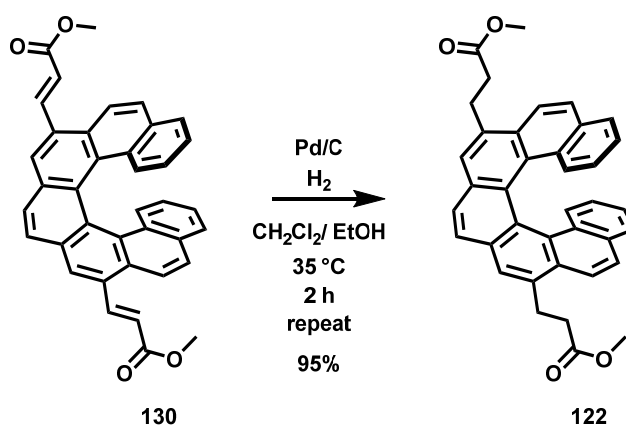
mL), brine, and dried over anhydrous Na₂SO₄. After filtration and evaporation of the solvent, the residue was purified by column chromatography over silica gel using cyclohexane to cyclohexane:CH₂Cl₂ (8:1) as an eluent to afford the desired product (**121**, 650 mg, 87%) as a yellow solid. ¹H NMR (500 MHz, CDCl₃, ppm): δ 8.28 (s, 2H), 8.16 (d, *J* = 8.8 Hz, 2H), 7.92 (s, 2H), 7.54 (dt, *J* = 8.7, 0.6 Hz, 2H), 7.34–7.28 (m, 2H), 7.19–7.11 (m, 2H), 6.94 (ddd, *J* = 8.0, 6.8, 1.1 Hz, 1H), 6.44 (ddd, *J* = 8.4, 6.8, 1.4 Hz, 1H). ¹³C NMR (101 MHz, CDCl₃, ppm): δ 132.2, 131.7, 130.2, 130.1, 129.4, 129.1, 128.5, 126.8, 126.72, 125.9, 124.9, 124.5, 124.34, 124.33, 122.4. HRMS (APCI): *m/z* [*M*]⁺ calcd for C₃₀H₁₆Br₂⁺: 533.96133; found 533.96090 (|Δ| = 0.80 ppm).



Dimethyl 3,3'-(benzo[1,2-*c*:4,3-*c'*]diphenanthrene-7,12-diyl) (2*E*,2'*E*)-diacrylate (130**):**

A mixture of 7,12-dibromobenzo[1,2-*c*:4,3-*c'*]diphenanthrene (**121**, 0.30 g, 0.56 mmol), PPh₃ (0.15 g, 0.56 mmol), Pd(OAc)₂ (63 mg, 0.28 mmol), K₂CO₃ (232 mg, 1.68 mmol), and TBAB (541 mg, 1.68 mmol) in dry DMF (10 mL) was deaerated with a stream of argon for 40 min before methyl acrylate (1.44 g, 16.8 mmol) was added. The flask was properly closed, and the mixture was heated at 105 °C for 12 h. Then, the mixture was allowed to cool to room temperature and the reaction was quenched by the addition of 1 M HCl (15 mL) and CH₂Cl₂ (20 mL). The organic layer was separated, and the aqueous layer was extracted with CH₂Cl₂ (3 × 10 mL). The combined organic layers were washed with 1 M HCl (15 mL), brine, and dried over anhydrous Na₂SO₄. After filtration and evaporation of the solvents, the

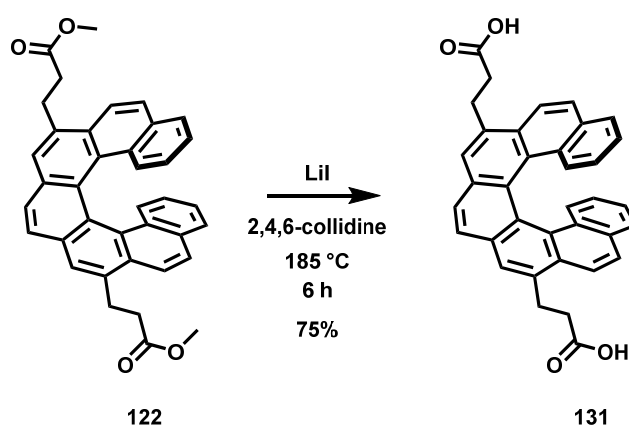
residue was purified by column chromatography over silica gel using cyclohexane to cyclohexane: EtOAc (8:1) as an eluent to afford desired product (**130**, 159 mg, 52%) as a pale yellow solid. ¹H NMR (500 MHz, CDCl₃, ppm): δ 8.67 (d, *J* = 15.7 Hz, 2H), 8.23 (d, *J* = 0.6 Hz, 2H), 8.05 (d, *J* = 8.9 Hz, 2H), 8.05 (s, 2H), 7.55 (d, *J* = 8.7, 2H), 7.31 (m, 2H), 7.12 (m, 2H), 6.93 (ddd, *J* = 7.9, 6.9, 1.1 Hz, 2H), 6.79 (d, *J* = 15.7 Hz, 2H), 6.41 (ddd, *J* = 8.4, 6.9, 1.4 Hz, 1H), 3.93 (s, 6H). ¹³C NMR (101 MHz, CDCl₃, ppm): δ 167.5, 142.2, 131.7, 131.6, 131.5, 129.4, 129.03, 128.98, 128.1, 127.6, 126.62, 126.60, 126.1, 126.6, 124.6, 124.2, 121.5, 120.9, 52.1. HRMS (ESI): *m/z* [*M* + H]⁺ calcd for C₃₈H₂₇O₄⁺: 547.1904; found 547.1897 (|Δ| = 1.2 ppm).



Dimethyl 3,3'-(benzo[1,2-*c*:4,3-*c'*]diphenanthrene-7,12-diyl)diacrylate (130):

Dimethyl 3,3'-(benzo[1,2-*c*:4,3-*c'*]diphenanthrene-7,12-diyl) (2*E*,2'*E*)-diacrylate (**130**, 220 mg, 0.366 mmol) and Pd/C (171 mg, 0.161 mmol, 10%) were suspended in CH₂Cl₂/EtOH (20 mL, 4:3) and hydrogen gas was passed through the suspension for 30 min. The reaction mixture was then stirred at 35 °C under a hydrogen atmosphere for 2 h. Then it was passed through a short plug of celite and concentrate in vacuum. The procedure described above was repeated four more times until full conversion of starting material was achieved. The crude product was purified by column chromatography over silica gel using cyclohexane to cyclohexane:EtOAc (4:1) as an eluent to afford the desired product (**122**, 210 mg, 95%) as

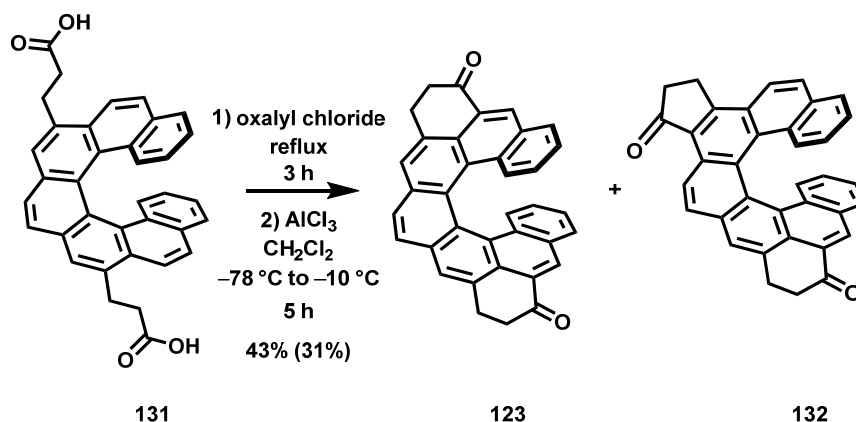
a yellow solid. ^1H NMR (500 MHz, CDCl_3 , ppm): δ 7.95 (s, 2H), 7.91 (d, $J = 8.8$ Hz, 2H), 7.82 (s, 2H), 7.51 (d, $J = 8.8$ Hz, 2H), 7.30–7.27 (m, 2H), 7.10 (d, $J = 8.5$, 2H), 6.90 (ddd, $J = 7.9, 6.9, 1.1$ Hz, 2H), 6.38 (ddd, $J = 8.3, 6.9, 1.3$ Hz, 2H), 3.73 (s, 6H), 3.63 (ddt, $J = 30.6, 11.7, 4.0$ Hz, 4H), 2.95 (ddd, $J = 8.8, 7.4, 1.6$ Hz, 4H). ^{13}C NMR (126 MHz, CDCl_3 , ppm): δ 173.6, 135.3, 131.4, 131.2, 129.7, 129.29, 129.1, 127.4, 126.7, 126.6, 126.4, 125.0, 124.8, 124.7, 123.7, 120.9, 51.9, 35.3, 28.6. HRMS (ESI): m/z $[M + \text{Na}]^+$ calcd for $\text{C}_{38}\text{H}_{30}\text{O}_4\text{Na}^+$: 575.2036; found 573.2033 ($|\Delta| = 0.5$ ppm).



3,3'-(Benzo[1,2-*c*:4,3-*c'*]diphenanthrene-7,12-diyl)dipropionic acid (131): A mixture of dimethyl 3,3'-(benzo[1,2-*c*:4,3-*c'*]diphenanthrene-7,12-diyl)dipropionate (**122**, 200 mg, 0.363 mmol), LiI (340 mg, 2.54 mmol), and 2,4,6-collidine was heated at 185 °C for 6 h under an argon atmosphere. Afterwards, the reaction was cooled to room temperature and the solvent was evaporated to dryness. To the residue, 2 M HCl (20 mL) was added, and the precipitate that formed was filtered and washed with water to give the desired product (**131**, 142 mg, 75%) as a brown solid, which was used in the next step without further purification. ^1H NMR (500 MHz, CDCl_3 , ppm): δ 8.01 (s, 2H), 8.00 (d, $J = 8.9$ Hz, 2H), 7.92 (s, 2H), 7.54 (d, $J = 8.8$ Hz, 2H), 7.28 (d, $J = 7.8$, 2H), 7.01 (d, $J = 8.4$ Hz, 2H), 6.86 (ddd, $J = 7.9, 6.8, 0.8$ Hz, 2H), 6.36 (ddd, $J = 8.3, 6.8, 1.1$ Hz, 2H), 3.61 (ddt, $J = 43.9, 15.2, 7.7$ Hz, 4H), 2.94 (t, $J = 7.7$ Hz, 4H). ^{13}C NMR (101 MHz, CDCl_3 , ppm): δ 176.8, 136.9, 134.64, 134.63,

130.9, 130.5, 130.1, 126.4, 127.63, 127.55, 127.5, 125.9, 125.8, 124.8, 122.0, 36.3, 29.5.

HRMS (ESI): m/z $[M + H]^+$ calcd for $C_{36}H_{25}O_4^+$: 521.1758; found 521.1759 ($|\Delta| = 0.2$ ppm).



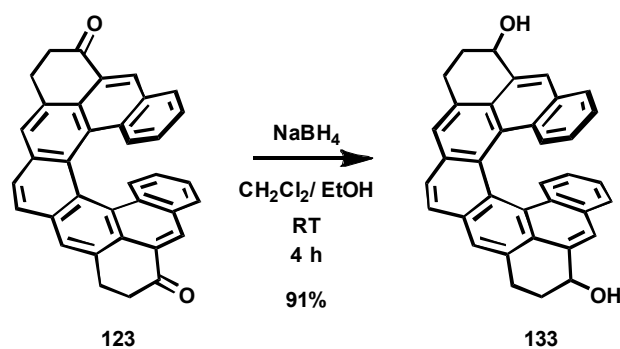
2,3,8,9-Tetrahydrodinaphtho[3,2,1-*pq*:1',2',3'-*uv*]pentaphene-1,10-dione (123): A solution of 3,3'-(benzo[1,2-*c*:4,3-*c'*]diphenanthrene-7,12-diyl)dipropionic acid (**131**, 70 mg, 0.13 mmol) in oxalyl chloride (10 mL) was heated at reflux for 3 h before the excess of oxalyl chloride was removed under reduced pressure. The crude product was dissolved in dry CH_2Cl_2 (20 mL) and the solution was cooled to -78 °C. $AlCl_3$ (268 mg, 2.01 mmol) was added in one portion and the reaction mixture was allowed to warm to -10 °C over 5 h before it was poured onto ice and acidified with 2 M HCl. The organic layer was separated, and the aqueous layer was extracted with CH_2Cl_2 (3×10 mL). The combined organic layers were washed with sat. aq. $NaHCO_3$ (10 mL), brine, and dried over anhydrous Na_2SO_4 . After filtration and evaporation of the solvent, the residue was purified by column chromatography over silica gel using cyclohexane: CH_2Cl_2 7:3 to cyclohexane: CH_2Cl_2 :EtOAc 63:30:7 as an eluent to afford the desired product (**123**, 28 mg, 43%) as a pale yellow solid and a side product (**131**, 20.1 mg, 31%) as a yellow solid.

2,3,8,9-Tetrahydrodinaphtho[3,2,1-*pq*:1',2',3'-*uv*]pentaphene-1,10-dione (123): 1H NMR (500 MHz, $CDCl_3$, ppm): δ 8.18 (s, 2H), 7.99 (s, 2H), 7.88 (t, $J = 1.2$ Hz, 2H), 7.43–7.36 (m, 2H), 7.11 (dq, $J = 8.5, 0.9$ Hz, 2H), 6.88 (ddd, $J = 8.0, 6.9, 1.1$ Hz, 2H), 6.40 (ddd,

$J = 8.4, 6.9, 1.3$ Hz, 2H), 3.64–3.43 (m, 4H), 3.10–2.96 (m, 4H). ^{13}C NMR (126 MHz, CDCl_3 , ppm): δ 198.6, 133.1, 132.3, 130.9, 129.6, 129.2, 129.90, 128.09, 128.06, 127.7, 126.6, 126.3, 126.0, 124.7, 124.4, 39.2, 28.9. * One signal is missing due overlapping. HRMS (ESI): m/z $[M + \text{H}]^+$ calcd for $\text{C}_{36}\text{H}_{23}\text{O}_2^+$: 487.1693; found 487.1698 ($|\Delta| = 1.1$ ppm).

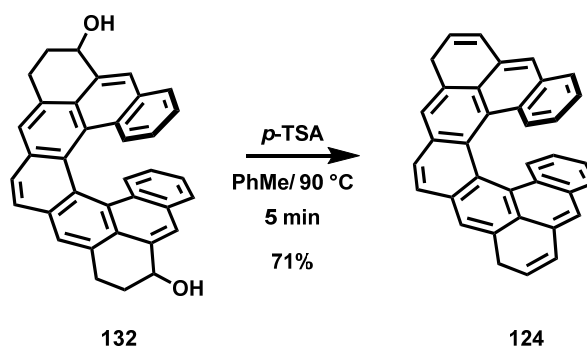
1,2,7,8-Tetrahydrocyclopenta[*c*]dinaphtho[1,2-*a*:3',2',1'-*no*]tetraphene-3,9-dione

(131): ^1H NMR (500 MHz, CDCl_3 , ppm): δ 9.47 (d, $J = 8.3$ Hz, 1H), 8.25 (t, $J = 0.7$ Hz, 1H), 8.17 (d, $J = 8.4$ Hz, 1H), 7.98 (t, $J = 1.1$ Hz, 1H), 7.95 (d, $J = 8.5$ Hz, 1H), 7.61 (m, 1H), 7.51–7.47 (m, 1H), 7.36–7.32 (m, 1H), 7.23–7.19 (m, 1H), 7.14–7.10 (m, 1H), 7.01–6.94 (m, 2H), 6.55 (ddd, $J = 8.5, 6.8, 1.3$ Hz, 1H), 6.40 (ddd, $J = 8.4, 6.8, 1.4$ Hz, 1H), 3.74–3.50 (m, 4H), 3.19–2.93 (m, 4H). ^{13}C NMR (126 MHz, CDCl_3 , ppm): δ 207.7, 198.6, 158.6, 133.6, 133.2, 133.0, 132.4, 132.2, 130.8, 130.3, 129.7, 129.5, 129.2, 129.0, 120.7, 128.6, 128.3, 128.2, 128.03, 128.02, 127.4, 126.9, 126.7, 126.1, 126.0, 125.64, 125.56, 124.9, 124.8, 124.6, 123.1, 121.5, 38.9, 37.9, 28.9, 24.9.



1,2,3,8,9,10-Hexahydrodinaphtho[3,2,1-*pq*:1',2',3'-*uv*]pentaphene-1,10-diol (133): A mixture of 2,3,8,9-tetrahydrodinaphtho[3,2,1-*pq*:1',2',3'-*uv*]pentaphene-1,10-dione (**123**, 23.0 mg, 47.4 μmol) in dry $\text{CH}_2\text{Cl}_2/\text{EtOH}$ (30 mL, 2:1) was deaerated with stream of argon for 30 min. before NaBH_4 (9.00 mg, 0.24 mmol) was added in one portion. The mixture was stirred at room temperature for 4 h under an argon atmosphere. Then 2 M HCl (10 mL) was added and the organic layer was separated. The aqueous layer was extracted with CH_2Cl_2 (3 x 10 mL). The combined organic layers were washed with sat. aq. NaHCO_3 solution, brine

and dried over anhydrous Na₂SO₄. After filtration and evaporation of the solvent, the residue was purified by column chromatography over silica gel using cyclohexane to cyclohexane: EtOAc 4:1 as an eluent to afford desired product (**133**, 21 mg, %) as a pale-yellow solid. ¹H NMR (500 MHz, CDCl₃, ppm): δ 7.99 – 7.94 (m, 2H), 7.84 – 7.81 (m, 2H), 7.60 – 7.53 (m, 2H), 7.32 – 7.28 (m, 2H), 7.14 – 7.06 (m, 2H), 6.94 – 6.86 (m, 2H), 6.41 – 6.31 (m, 2H), 5.13 – 5.08 (m, 1H), 3.70 – 3.17 (m, 4H), 2.49 – 2.15 (m, 4H). ¹³C NMR (101 MHz, CDCl₃, ppm): 135.52, 135.49, 135.18, 135.16, 133.9, 131.10, 131.09, 131.04, 131.02, 131.01, 130.99, 129.36, 129.34, 129.29, 128.6, 128.49, 128.47, 127.1, 126.7, 126.47, 126.45, 125.02, 124.99, 124.97, 124.95, 124.89, 124.88, 124.8, 124.53, 124.49, 124.4, 124.3, 124.20, 124.18, 124.17, 123.9, 123.44, 123.35, 123.3, 123.2, 69.8, 69.7, 32.0, 31.2, 26.9, 26.2. (out of 54 signals expected from three possible diastereomers (18 signals each), only 46 signals could be detected within the resolution limits of the NMR technique because of the signal overlap) | HRMS (ESI): m/z [M + Na]⁺ calcd for C₃₆H₂₆O₂Na⁺: 513.1825; found 513.1828 (|Δ| = 0.6 ppm).



3,8-Dihydrodinaphtho[3,2,1-pq:1',2',3'-uv]pentaphene (124): *p*-Toluenesulfonic acid monohydrate (0.58 mg, 3.06 μmol) was added to a hot (90 °C) solution 1,2,3,8,9,10-hexahydrodinaphtho[3,2,1-pq:1',2',3'-uv]pentaphene-1,10-diol (**132**, 5.00 mg, 10.2 μmol) in PhMe (5 mL) and the reaction mixture was heated at 90 °C for 5 min. before it was cooled in an ice bath, diluted with ^oHex (5 mL) and passed through a pad of silica gel using

^oHex/PhMe (95:5) as an eluent. Evaporation of the solvents afforded the desired product (3.30 mg, 71%) as a pale-yellow solid. ¹H NMR (400 MHz, C₆D₆, ppm): δ 7.84 (d, *J* = 2.4 Hz, 2H), 7.68 (d, *J* = 8.3 Hz, 2H), 7.44 – 7.41 (m, 2H), 7.35 – 7.27 (m, 4H), 7.12 (d, *J* = 7.6 Hz, 3H), 6.84 (d, *J* = 7.7 Hz, 2H), 6.75 (td, *J* = 7.3, 3.9 Hz, 2H), 6.20 (t, *J* = 7.8 Hz, 2H), 3.96 (d, *J* = 18.6 Hz, 2H), 3.63 (dd, *J* = 18.7, 2H).

REFERENCES

- [1] Castro Neto, A. H. *Materials Today* **2010**, *13*, 12–17.
- [2] Valladas, H.; *Meas. Sci. Technol.* **2003**, *14*, 1487–1492.
- [3] Georgakilas, V.; Perman, J. A.; Tucek, K.; Zboril, R. *Chem. Rev.* **2015**, *4744–4822*.
- [4] Downloaded from: https://en.wikipedia.org/wiki/Allotropes_of_carbon (accessed september 2018)
- [5] Hirsch, A. *Nature Mat.* **2010**, *9*, 868–871.
- [6] Kroto, H. W.; Heath, J. R.; O'brien, S. C. Curl, R. F.; Smalley, R. E. *Nature* **1985**, *318*, 162–163.
- [7] Tiwari, S. K.; Kumar, V.; Huczko, A.; Oraon, R.; De Adhikari, A.; Nayak, G. C. *Crit. Rev. Solid State, Mater. Sci.* **2016**, *41*, 257–317.
- [8] Zeynalov, E. B.; Allen, N. S.; Salmanova, N. I. *Polym. Degrad. Stab.* **2009**, *94*, 1183–1189.
- [9] Czochara, R.; Kusio, J.; Litwinienko, G. *RCS Adv.* **2017**, *7*, 44021–44025.
- [10] Xiao, L.; Takada, H.; Maeda, K.; Haramato, M.; Miwa, N. *Biomed. Pharmacother.* **2005**, *59*, 351–358.
- [11] Cai, X.; Jia, Z.; Liu, Z.; Hou, B.; Luo, C.; Li, W.; Liu, J. *J. Neurosci. Res.* **2008**, *86*, 3622–3634.
- [12] Gharbi, N.; Pressac, M.; Hadchouel, M.; Szwawac, H.; Wilson, S. R.; Mousa, F. *Nano Lett.* **2005**, *5*, 2578–2585.
- [13] Bonifazi, D.; Enger, O.; Diederich, F. *Chem. Soc. Rev.* **2007**, *36*, 309–414.
- [14] Imahori, H. *J. Phys. Chem. B* **2004**, *108*, 6130–6134.
- [15] Guldi, D. M.; Aminur Rahman, G. M. Sgobba, V. Ehli, C. *Chem. Soc. Rev.* **2006**, *35*, 471–487.
- [16] Li, G.; Shrotriya, V.; Huang, J. S.; Yao, Y.; Moriarty, T.; Emery, K.; Yang, Y. *Nature. Mat.* **2005**, *4*, 864–868.
- [17] Kim, J. Y.; Lee, K.; Coates, N. E.; Moses, D.; Nguyen, T. Q.; Dante, M; Heeger, A. J. *Science*, **2007**, *317*, 222–225.R,

- [18] Guenes, S.; Neugebauer, H.; Saricifici, N. S.; *Chem. Rev.* **2007**, *107*, 1324–1338.
- [19] Iijima, S. *Nature* **1991**, *354*, 56–58.
- [20] Terranova, M. L.; Sessa, V, Rossi, M. *Chem. Vap. Deposition.* **2006**, *12*, 315–325.
- [21] Dai, H. *Acc. Chem. Res.* **2002**, *35*, 1035–1044.
- [22] Bahr, J.; Mickelson, E. T. Bronikowski, M. J.; Smalley, R. E.; Tour, J. M. *Chem. Commun.* **2001**, *21*, 193–194.
- [23] Agnihitri, S.; Mota, J. P. B.; Abadi, M. R.; Rood, M. J. *Langmuir* **2005**, *21*, 896–904.
- [24] Tans, S. J.; Devoret, M. H.; Dai, H.; Thess, A.; Smalley, R. E.; Georliga, L. J.; Dekker, C. *Nature* **1997**, *386*, 474–477.
- [25] Bockrath, M.; Cobden, D. H.; McEuen, P. L.; Chopra, N. G.; Zettl, A.; Thess, A.; Smalley, R. E. *Science* **1997**, *275*, 1922–1925.
- [26] Tans, S. J.; Verschueren, R. M.; Dekker, C. *Nature* **1998**, *393*, 49–52.
- [27] Mizuno, K.; Ishii, K.; Kishida, H.; Hayamizu, Y.; Yasuda, S; Futaba, D. N. Yumura, M.; Hata, K. *Proc. Natl. Acad. Sci. USA* **2009**, *106*, 6044–6047.
- [28] Wallace, P. R. *Phys. Rev.* **1947**, *72*, 622–634.
- [29] Boehm, H. P.; Clauss, A.; Fischer, G. O.; Hofmann, U. *Z. Naturforsch.* **1962**, *17*, 150–153.
- [30] Sun, Z.; Chi, C.; Wu, J. *Chem. Soc. Rev.* **2012**, *41*, 7857–7889
- [31] Singh, V.; Joung, D.; Zhai, L.; Das, S.; Khondaker, S. I.; Seal, S. *Prog. Mater. Sci.* **2011**, *56*, 1178–1271.
- [32] Stankovich, S.; Dikin, D. A.; Dommett, G.; Kohlhaas, K.; Zimney, E. J. Stach, E. A. Piner, R. D. Nguyen, S. T.; Ruoff, R. S. *Nature* **2006**, *442*, 282–286.
- [33] Nag, A.; Mitra, A.; Mukhopadhyay, S. C. *Sens. Actuators, A* **2018**, *270*, 177–194.
- [34] Justino, C. I. L.; Gomes, A. R.; Fritas, A. C.; Duarte, A. C.; Rocha-Santos, T. A. P. *Trends Anal. Chem.* **2017**, *91*, 53–66.
- [35] Yadav, R.; Subhash, A.; Chemmenchery, N.; Kandasubramanian, B. *Ind. Eng. Chem. Res.* **2018**, *57*, 9333–9350.
- [36] Roy-Mayhew, A. D.; Aksay, I. A. *Chem. Rev.* **2014**, *144*, 6323–6348.
- [37] Xu, Y.; Liu, J. *Small* **2016**, *12*, 1400–1419.
- [38] Chee, W. K.; Lim, H. N.; Huang, N. M.; Harrison, I. *RCS Adv.* **2015**, *83*, 1–93.

- [39] For more information, visit <https://www.nobelprize.org/> (accessed september 2018).
- [40] Scott, L. T.; Boorum, M. M.; McMahon, B. J.; Hagen, S.; Mack, J.; Blank, J.; Wegner, H.; de Meijere, A. *Science* **2002**, *295*, 1500–1503.
- [41] Segawa, Y.; Ito, H.; Itami, K. *Nature Rev.* **2016**, *1*, 1–14.
- [42] Jasti, R.; Bhattecharjee, J.; Neaton, J. B.; Bertozzi, C. R. *J. Am. Chem. Soc.* **2008**, *130*, 17646–17647.
- [43] Takaba, H.; Omachi, H.; Bouffard, J.; Itami, K. *Angew. Chem. Int. Ed.* **2009**, *48*, 6112–6116.
- [44] Omachi, H.; Segawa, Y.; Itami, K. *Org. Lett.* **2011**, *13*, 2480–2483.
- [45] Hitosugi, S.; Nakanishi, W.; Yamasaki, T.; Isobe, H. *Nature Commun.* **2011**, *2*, 1–5.
- [46] Matsuno, T.; Kamata, S.; Hitogusi, S.; Isobe, H. *Chem. Sci.* **2013**, *4*, 3179–3183.
- [47] Kekulé, A. *Bull. Soc. Chim. Fr.* **1865**, *3*, 98–110.
- [48] von Ragué Schleyer, P.; Jiao, H. *Pure Appl. Chem.* **1996**, *68*, 209–218.
- [49] Krygowski, T. M.; Cyrański, M. K.; Czarnocki, Z.; Häfelinger, G.; Kartotzky, A. *R. Tetrahedron* **2000**, *56*, 1783–1796.
- [50] von Ragué Schleyer, P. *Chem. Rev.* **2001**, *101*, 1115–1118.
- [51] Hückel, E. *Z. Physik.* **1931**, *70*, 204–286.
- [52] Hückel, E. *Z. Physik.* **1931**, *72*, 310–337.
- [53] Hückel, E. *Z. Physik.* **1932**, *76*, 628–648.
- [54] Hückel, E. *Z. Elektrochem. Angew. Phys. Chem.* **1937**, *43*, 752–788.
- [55] Hückel, E. *Z. Elektrochem. Angew. Phys. Chem.* **1937**, *43*, 827–849.
- [56] Armitt, T. W.; Robinson, R. *J. Chem. Soc. Trans.* **1925**, *127*, 1604–1618.
- [57] *The Aromatic Sextet*, Clar, E. John Wiley & Sons, New York, **1972**.
- [58] Randić, M. *Chem. Rev.* **2003**, *103*, 3449–3605.

- [59] Solà, M. *Front. Chem.* **2013**, *1*, 1–8.
- [60] Portella, G.; Poater, J.; Solà, M.; *J. Phys. Org. Chem.* **2005**, *18*, 785–791.
- [61] Schulman, J. M.; Disch, R. L. *J. Phys. Chem. A* **1999**, *103*, 6669–6672.
- [62] Cyrański, M. K.; Stępień, B. T.; Krygowski, T. M. *Tetrahedron* **2000**, *56*, 9663–9667.
- [63] Suresh, C. H.; Gadre, S. R. *J. Org. Chem.* **1999**, *64*, 2505–2512.
- [64] von Ragué Schleyer, P.; Manoharan, M.; Jio, H.; Stahl, F. *Org. Lett.* **2001**, *3*, 3643–3646.
- [65] Behrens, S.; Köster, M.; Jug, K. *J. Org. Chem.* **1994**, *59*, 2546–2551.
- [66] Pater, J.; Visser, R.; Solà, M.; Bickelhaupt, M. F. *J. Org. Chem.* **2006**, *72*, 1134–1142.
- [67] Kato, T.; Yoshizawa, K.; Hirao, K. *J. Chem. Phys.* **2002**, *116*, 3420–3429.
- [68] Dabestani, R.; Ivanov, I. N. *Photochem. Photobiol.* **1999**, *70*, 10–34.
- [69] Chien, S.-U.; Cheng, M.-F.; Lau, K.-C.; Li, W.-K. *J. Phys. Chem. A* **2005**, *109*, 7509–7518.
- [70] Randić, M. *Chem. Phys. Lett.* **2014**, *601*, 1–5.
- [71] Balaban, A. T.; Klein, D. *J. Phys. Chem.* **2009**, *113*, 19123–19133.
- [72] Mo, Y.; Lin, Z.; Wu, W.; Zhang, Q. *J. Phys. Chem.* **1996**, *100*, 6469–5474.
- [73] Longuet-Higgins, H. C. *J. Chem. Phys.* **1950**, *18*, 265–274.
- [74] Juríček, M. *Chimia* **2018**, *72*, 322–327.
- [75] Borden, W. T.; Davidson, E. R. *J. Am. Chem. Soc.* **1977**, *99*, 4587–4594.
- [76] Borden, W.T. *Mol. Cryst. Liq. Cryst.* **1993**, *232*, 195–218.
- [77] Borden, W. T. *J. Org. Chem.* **2011**, *76*, 2943–2963.
- [78] Coulson, C. A.; Rushbrooke, G. S. *Proc. Cambridge Phil.*, **1940**, 137–200.
- [79] Clar, E.; Macpherson *Tetrahedron*, **1962**, *18*, 1411–1416.

- [80] Rule, M.; Marlin, A. R.; Seeger, D. E.; Hilinski, E. F.; Dougherty, D. A.; Berson, J. A. *Tetrahedron*, **1982**, *38*, 787–798.
- [81] Ovchinnikov, A. A. *Theor. Chim. Acta*. **1978**, *47*, 297–304.
- [82] Dowd, P. *Acc. Chem. Rev.* **1972**, *5*, 242–248.
- [83] Jordan, K. D.; Nachtigall, P. *J. Am. Chem. Soc.* **1993**, *115*, 270–271.
- [84] a) Gomberg, M. *J. Am. Chem. Soc.* **1900**, *22*, 757–771. b) Gomberg, M. *Ber. Dtsch. Chem. Ges. 1900*, **33**, 3150–3163.
- [85] *Stable Radicals: Fundamentals and Applied Aspects of Odd-Electron Compounds*, Ed.: Hicks, R. G. John Wiley & Sons, Chichester, **2010**.
- [86] Jacobsen, P. *Ber. Dtsch. Chem. Ges.* **1905**, *38*, 196–199.
- [87] Heintschel, E. *Ber. Dtsch. Chem. Ges.* **1903**, *38*, 320–322.
- [88] Heintschel, E. *Ber. Dtsch. Chem. Ges.* **1903**, *38*, 579.
- [89] Maki, A. H.; Allendoerfer, R. D.; Dannem, J. C.; Keys, R. T. *J. Am. Chem. Soc.* **1968**, *90*, 4225–4231.
- [90] Lankamp, H.; Nauta, W. T.; MacLean, C. *Tetrahedron Lett.* **1968**, *9*, 249–254.
- [91] Neumann, W. P.; Uzick, W.; Zarkadis, A. K. *J. Am. Chem. Soc.* **1986**, *108*, 3762–3770.
- [92] Neumann, W. P.; Penenory, A.; Stewen, U., Lehning, M. *J. Am. Chem. Soc.* **1989**, *111*, 5845–5851.
- [93] Ballester, M.; Riera-Figueras, J.; Castaner, J.; Badfa, C.; Monso, J. M. *J. Am. Chem. Soc.* **1971**, *93*, 2215–2225.
- [94] Ballester, M. *Acc. Chem Res.* **1985**, *18*, 380–87.
- [95] Keckmann, A.; Lambert, C. *J. Am. Chem. Soc.* **2007**, *129*, 5515–5527.
- [96] Sedó, J.; Ventosa, N.; Molins, M. A.; Pons, M.; Rovira, C.; Veciana, J. *J. Org. Chem.* **2001**, *66*, 1567–1578.
- [97] Ratera, I.; Ruiy-Molina, D.; Vidal-Gancedo, J.; Novoa, J. J.; Wurst, K.; Letard, J.-F.; Rovira, C.; Veciana, J. *Chem. Eur. J.* **2004**, *10*, 603–616.

- [98] Uchida, K.; Kubo, T. *J. Synth. Org. Chem. Jpn.* **2016**, *74*, 1069–1077.
- [99] Sogo, P. B.; Nakazaki, M.; Calvin, M. *J. Chem. Phys.* **1957**, *26*, 1343–1345.
- [100] Reid, D. H. *Tetrahedron*, **1958**, *3*, 339–352.
- [101] Reid, D.H. *Q. Rev. Chem. Soc.* **1965**, *19*, 274–302.
- [102] Gerson, F.; Heilbronner, E.; Reddoch, H. A.; Paskovich, D. H.; Das, N. C. *Helv. Chim. Acta* **1967**, *50*, 813–821.
- [103] Preuss, K. E. *Polyhedron*, **2014**, *79*, 1–15.
- [104] Dwyer, D. W.; Ciralo, M. F.; Gilbert, D. C.; Doetschman, D. C. *J. Phys. Chem. A* **2000**, *104*, 7629–7634.
- [105] Small, D.; Rosokha, S. V.; Kochi, J. K.; Head-Gordon, M. *J. Phys. Chem. A* **2005**, *109*, 11261–11267.
- [106] Zaitsev, V.; Rosokha, S. V.; Head-Gordon, M.; Kochi, J.K. *J. Org. Chem.* **2006**, *71*, 520–526.
- [107] Haddon, R. C.; Wudl, F.; Kaplan, M. L.; Marshall, J. H.; Cais, R. E.; Bramwell, F. B. *J. Am. Chem. Soc.* **1978**, *100*, 7629–7633.
- [108] Goto, K.; Kubo, T.; Yamamoto, K.; Nakasuji, K.; Sato, K.; Shiomi, D.; Takui, T.; Kubota, M.; Kobayashi, T.; Yakusi, K.; Ouyang, J. *J. Am. Chem. Soc.* **1999**, *121*, 1619–1620.
- [109] Fukui, K.; Sato, K.; Shiomi, D.; Takui, T.; Itoh, K.; Gotoh, K.; Kubo, T.; Yamamoto, K.; Nakasuji, K.; Naito, A. *Synth. Met.* **1999**, *103*, 2257–2258.
- [110] Fukui, K.; Sato, K.; Shiomi, D.; Takui, T.; Itoh, K.; Kubo, T.; Gotoh, K.; Yamamoto, K.; Nakasuji, K.; Naito, A. *Mol. Cryst. Liq. Cryst.* **1999**, *334*, 49–58.
- [111] Takano, Y.; Taniguchi, T.; Isobe, H.; Kubo, T.; Morita, Y.; Yamamoto, K.; Nakasuji, K.; Takui, T.; Yamaguchi, K. *J. Am. Chem. Soc.* **2002**, *124*, 11122–11130.
- [112] Suzuki, S.; Morita, Y.; Fukui, K.; Sato, K.; Shiomi, D.; Takui, T.; Nakasuji, K. *J. Am. Chem. Soc.* **2006**, *128*, 2530–2531.
- [113] Tian, Y.-H.; Kertesz, M. *J. Am. Chem. Soc.* **2010**, *132*, 10648–10649.
- [114] Zhongyu, M.; Kertesz, M. *Angew. Chem. Int. Ed.* **2017**, *56*, 10188–10191.

- [115] Mandal, S. K.; Samanta, S.; Itkis, M. E.; Jensen, D. W.; Reed, R. W.; Okley, R. T.; Tham, F. S.; Donnadiou, B.; Haddo, R. C. *J. Am. Chem. Soc.* **2006**, *128*, 1982-1994.
- [116] Pal, S. K.; Itkis, M. E.; Tham, F. S.; Reed, R. W.; Oakley, T. T.; Haddon, R. C. *Science* **2005**, *309*, 281-284.
- [117] Chi, X.; Itkis, M. E.; Kirchbaum, K.; Pinkerton, A. A.; Oakley, R. T.; Cordes, A. W.; Haddon, R. C. *J. Am. Chem. Soc.* **2001**, *123*, 4041-4048.
- [118] Morita, Y.; Suzuki, S.; Sato, K.; Takui, T. *Nature Chem.* **2011**, *3*, 197-204.
- [119] Abe, M. *Chem. Rev.* **2013**, *113*, 7011-7088.
- [120] Yeh, C.-N.; Chai, J.-D. *Sci. Rep.* **2016**, *6*, 1-14.
- [121] Sun, Z.; Ye, Q.; Chi, C.; Wu, J. *Chem. Soc. Rev.* **2012**, *41*, 7857-7889.
- [122] Chikamatsu, M.; Mikami, Chisaka, J.; Yoshida, Y.; Azumi, R. Yase, K. *App. Phys. Lett.* **2007**, *91*, 043506.
- [123] Chase, D. T.; Fix, A. G.; Kang, S. J.; Rose, B. D.; Weber, C. D.; Zhong, Y.; Zakharov, L. N.; Lonergan, M. C.; Nuckolls, C.; Haley, M. M. *J. Am. Chem. Soc.* **2012**, *134*, 10349-10352.
- [124] Lee, J.; Jadhav, P.; Reusswig, P. D.; Yost, S. R.; Thompson, N. J.; Congreve, D. N.; Hontz, E.; van Vooris, T.; Baldo, M. A. *Acc. Chem. Res.* **2012**, *46*, 1300-1311.
- [125] Son, Y.-W.; Cohen, M. L.; Louie, S. *Phys. Rev. Lett.* **2006**, *97*, 216803.
- [126] Kamada, K.; Ohta, K.; Kubo, T.; Shimizu, A.; Morita, Y.; Nakasuji, K.; Kishi, R.; Ohta, S.; Furukawa, S.; Takahashi, H.; Nakano, M. *Angew. Chem. Int. Ed.* **2007**, *46*, 3544-3546.
- [127] Harigaya, K. *Chem. Phys. Lett.* **2001**, *339*, 23-28.
- [128] Philpott, M. R.; Cimpoesu, F.; Kawazoe, Y. *Chem. Phys.* **2008**, *354*, 1-15.
- [129] Philpott, M. R.; Cimpoesu, F.; Kawazoe, Y. *Mat. Trans.* **2008**, *49*, 2448-2456.
- [130] Sharma, V.; Som, N.; Dabhi, S. D.; Jha, P. K. *Chemistry Select.* **2018**, *3*, 2390-2397.

- [131] Allison, G.; Bushby, R. J.; Paillaud, J.-L.; Thornton-Pett, M. *J. Chem. Soc., Perkin Trans 1*, **1995**, *0*, 385–390.
- [132] *Aromatische Kohlenwasserstoffe*, Clar, E. Springer-Verlag, Berlin, **1941**.
- [133] Inoue, J.; Fukui, K.; Kubo, T.; Nakazawa, S.; Sato, K.; Shiomi, D.; Morita, Y.; Yamamoto, K.; Takui, T.; Nakasuji, K. *J. Am. Chem. Soc.* **2001**, *123*, 12702–12703.
- [134] Bearpark, M. J.; Robb, M. A.; Bernardi, F.; Olivucci, M. *Chem. Phys. Rev.* **1994**, *217*, 513–519.
- [135] Allison, G.; Bushby, R. J.; Jesudson, M.; Paillaud, J.-L.; Taylor, N. *Chem. Soc., Perkin Trans 2*, **1997**, *0*, 147–156.
- [136] Gapurenko, O. A.; Starikov, A. G.; Minyaev, R. M.; Minkin, V. I. *Russ. Chem. Bull.* **2011**, *60*, 1517–1524.
- [137] Clar, E.; Stewart, D. G. *J. Am. Chem. Soc.* **1951**, *0*, 3215–3218.
- [138] Clar, E.; Stewart, D. G. *J. Am. Chem. Soc.* **1953**, *75*, 2667–2672.
- [139] Clar, E.; Stewart, D. G. *J. Am. Chem. Soc.* **1954**, *76*, 3504–3507.
- [140] Clar, E.; Kemp, W.; Stewart, D. G. *Tetrahedron*, **1958**, *3*, 325–333.
- [141] Allison, G.; Bushby, R. J.; Paillaud, J.-L. *J. A. Chem. Soc.* **1993**, *115*, 2062–2064.
- [142] Allison, G.; Bushby, R. J.; Paillaud, J.-L. *J. Mater. Sci. Mater. Electron.* **1994**, *5*, 67–74.
- [143] Fukui, K.; Inoue, J.; Nakazawa, S.; Aoki, T.; Morita, Y.; Yamamoto, K.; Sato, K.; Shiomi, D.; Nakasuji, K.; Takui, T. *Synth. Met.* **2001**, *121*, 1824–1825.
- [144] Trinquier, G.; Chilkuri, V. G.; Malrieu, J.-P. *J. Chem. Phys.* **2014**, *140*, 204113.
- [145] Morita, Y.; Nishida, S.; Murata, T.; Moriguchi, M.; Ueda, A.; Satoh, M.; Arifuku, K.; Sato, K.; Takui, T. *Nature Mat.* **2011**, *10*, 947–951.
- [146] Morita, Y. Okafuji, T.; Satoh, M.; *JP2007227186 A*, **2007**.
- [147] Morita, Y.; Murata, T.; Ueda, A.; Yamada, C.; Kanzaki, Y.; Shiomi, D.; Sato, K.; Takui, T. *Bull. Chem. Soc. Jpn.* **2018**, *91*, 922–931.
- [148] Iwabata, Y.; Wang, Q.; Yoshikawa, T.; Ueda, A.; Murata, T.; Kariyazono, K.; Moriguchi, M.; Okamoto, H.; Morita, Y.; Nakai, H. *Njp Quantum Mat.* **2017**, *2*, 1–7.

- [149] Buimaga-Iarinca, L.; Floare, C. G.; Morari, C. *Chem. Phys. Lett.* **2014**, *598*, 48–52.
- [150] Ueda, A.; Wasa, H.; Nishida, S.; Kanzaki, Y.; Sato, K.; Shiomi, D.; Takui, T.; Morita, Y. *Chem. Eur. J.* **2012**, *18*, 16272–16276.
- [151] Ueda, A.; Wasa, H.; Nishida, S.; Kanzaki, Y.; Sato, K.; Takui, T.; Morita, Y. *Chem. Asian J.* **2013**, *8*, 2057–2063.
- [152] Pavliček, N.; Mistry, A.; Majzik, Y.; Moll, N. Meyer, G.; Fox, D. J. Gross, L. *Nature Nanotechnol.* **2017**, *12*, 308–312.
- [153] Gaudioso, H.; Lee, H. J.; Ho, W. *J. Am. Chem. Soc.* **1999**, *121*, 8479–8485.
- [154] Pavliček, N.; Schuler, B.; Collazos, S.; Moll, N.; Pérez, D.; Guitián, E.; Meyer, G.; Peña, D. Gross, L. *Nat. Chem.* **2015**, *7*, 623–628.
- [155] Schuler, B.; Fatayer, S.; Mohn, F.; Moll, N.; Paclíček, N.; Meyer, G.; Peña, D.; Gross, L. *Nature Chem.* **2016**, *8*, 220–224.
- [156] Barnes, J. C.; Juriček, M.; Strutt, N. L.; Frasconi, M.; Sampath, S.; Giesener, M. A.; McGrier, P. L.; Burns, L. C.; Stern, C. L.; Sarjeant, A. A.; Stodart, J. F. *J. Am. Chem. Soc.* **2013**, *135*, 183–192.
- [157] Hara, O.; Tanaka, K.; Yamamoto, K.; Nakazawa, T.; Murata, I. *Tetrahedron Lett.* **1977**, *18*, 2435–2436.
- [158] Wiggins, J. M. *Synth. Commun.* **1988**, *18*, 741–749.
- [159] Azzena, U.; Demartis, S.; Melloni, G. *J. Org. Chem.* **1996**, *61*, 4913–4919.
- [160] Kuzmic, P. *Anal. Biochem.* **1996**, *237*, 260–273.
- [161] Dale, E. j.; Vermeulen, N. A.; Thomas, A. A.; Barnes, J. C.; Juriček, M.; Blackburn, A. K.; Strutt, N. L.; Sarjent, A. A.; Stern, C. L.; Denmark, S. E.; Stoddart, J. F. *J. Am. Chem. Soc.* **2014**, *136*, 10669–10682.
- [162] Krasovskiy, A.; Knochel, P. *Synthesis* **2006**, *5*, 890–891.
- [163] Li, Y.; Huang, K-W.; Webster, R. D.; Zeng, Z.; Zeng, W.; Chi, C.; Furukawa, K.; Wu, J. *Chem. Sci.* **2014**, *5*, 1908–1914.
- [164] Koelsch, C. F.; Rosenwald, R. H. *J. Am. Chem. Soc.* **1937**, *59*, 2166–2169.
- [165] Koelsch, C. F.; Anthes, J. A. *J. Org. Chem.* **1941**, *6*, 558–565.

- [166] Wang, M.-Z.; Ku, C.-F.; Si, T.-X.; Tsang, S.-W.; Lv, X.-M.; Li, X.-W.; Li, Z.-M.; Zhang, H.-J.; Chan, A. S. C. *J. Nat. Prod.* **2018**, *81*, 98–105.
- [167] Quiñones, W.; Escobar, G.; Echeverri, F.; Torres, F.; Rosero, Y.; Arango, V.; Cardona, G.; Gallego, A. *Molecules* **2000**, *5*, 974-980.
- [168] Rosquete, L. I.; Cabrera-Serra, G. M.; Piñero, J. S.; Martín-Rodríguez, P.; Fernández-Pérez, L.; Luis, J. G.; McNaughton-Smith, G.; Abad-Grillo, T. *Bioorg. Med. Chem.* **2010**, *18*, 4530–4534.
- [169] Zhu, X.-H.; Peng, J.; Cao, Y.; Roncali, J. *Chem. Soc. Rev.* **2011**, *40*, 3509–3524.
- [170] Schwenn, E.; Gui, K.; Nardes, A.; Krueger, K. B.; Lee, K. H.; Mutkins, K.; Rubinstein-Dunlop, H.; Shaw, P. E.; Kopidakis, N.; Burn, P. L.; Meredith, P. *Adv. Eng. Mater.* **2011**, *1*, 73–81.
- [171] Wang, C.; Dong, H.; Hu, W.; Liu, Y.; Zhu, D. *Chem. Rev.* **2012**, *112*, 2208–2267.
- [172] Reich, H. *J. Chem. Rev.* **2013**, *113*, 7130–7178.
- [173] New address: T. Šolomek, Department of Chemistry and Argonne-Northwestern Solar Energy Research Center, Northwestern University, 2145 Sheridan Road, Evanston, Illinois 60208-3113, United States.
- [174] a) Pashaei, B.; Shahroosvand, H.; Grätzel, M.; Nazeeruddin, M. K. *Chem. Rev.* **2016**, *116*, 9485. b) Nielsen, C. B.; Holliday, S.; Chen, H.-Y.; Cryer, S. J.; McCulloch, I. *Acc. Chem. Res.* **2015**, *48*, 2803. c) Urbani, M.; Grätzel, M.; Nazeeruddin, M. K.; Torres, T. *Chem. Rev.* **2014**, *114*, 12330. d) Frischmann, P. D.; Mahata K.; Würthner, F. *Chem. Soc. Rev.* **2013**, *42*, 1847. e) Chen, X.; Li, C.; Grätzel, M.; Kostecki, R.; Mao, S. S. *Chem. Soc. Rev.*, **2012**, *41*, 7909.
- [175] Schwoerer, M.; Wolf, H. C. *Organic Molecular Solids*; Wiley-VCH: Weinheim, **2007**.
- [176] a) Sun, M.; Müllen, K.; Yin, M. *Chem. Soc. Rev.* **2016**, *45*, 1513. b) Lavis, L. D.; Raines, R. T. *ACS Chem. Biol.* **2008**, *3*, 142.
- [177] a) *The Porphyrin Handbook*, Vols. 15–20; Kadish, K. M.; Smith, K. M.; Guillard, R., Eds.; Academic: San Diego, **2003**. b) de la Torre, D.; Nicolau, M.; Torres, T. *In Supramolecular Photosensitive and Electroactive Materials*; Nalwa, H. S., Ed.; Academic: New York, **2001**, 1–111.
- [178] a) Würthner, F.; Saha-Möller, C. R.; Fimmel, B.; Ogi, S.; Leowanawat, P.; Schmidt, D. *Chem. Rev.* **2016**, *166*, 962. b) Görl, D. Zhang, X.; Würthner, F.

- Angew. Chem. Int. Ed.* **2012**, *51*, 6328. c) Zhan, X.; Facchetti, A.; Barlow, S.; Marks, T. J.; Ratner, M. A.; Wasielewski, M. R.; Marder, S. R. *Adv. Mater.* **2011**, *23*, 268. d) Safont-Sempere, M. M.; Fernández, G.; Würthner, F. *Chem. Rev.* **2011**, *111*, 5784.
- [179] *Fullerenes: Principles and Applications*; Langa, F.; Nierengarten, J.-F., Eds.; The Royal Society of Chemistry: Cambridge, **2007**.
- [180] Clar, E.; Stewart, D.G. *J. Am. Chem. Soc.* **1953**, *75*, 2667.
- [181] a) Inoue, J.; Fukui, K.; Kubo, T.; Nakazawa, S.; Sato, K.; Shiomi, D.; Morita, Y.; Yamamoto, K.; Takui, T.; Nakasuji, K. *J. Am. Chem. Soc.* **2001**, *123*, 12702. (b) Allinson, G.; Bushby, R. J.; Paillaud, J.-L.; Thornton-Pett, M. *J. Chem. Soc., Perkin Trans. 1* **1995**, *4*, 385.
- [182] a) Ueda, A.; Wasa, H.; Nishida, S.; Kanzaki, Y.; Sato, K.; Takui, T.; Morita, Y. *Chem.–Asian J.* **2013**, *8*, 2057. b) Ueda, A.; Wasa, H.; Nishida, S.; Kanzaki, Y.; Sato, K.; Shiomi, D.; Takui, T.; Morita, Y. *Chem.–Eur. J.* **2012**, *18*, 16272. c) Morita, Y.; Nishida, S.; Murata, T.; Moriguchi, M.; Ueda, A.; Satoh, M.; Arifuku, K.; Sato, K.; Takui, T. *Nat. Mater.* **2011**, *10*, 947.
- [183] a) Wallabregue, A.; Moreau, D.; Sherin, P.; Moneva Lorente, P.; Jarolímová, Z.; Bakker, E.; Vauthey, E.; Gruenberg, J.; Lacour, J. *J. Am. Chem. Soc.* **2016**, *138*, 1752. b) Adam, C.; Wallabregue, A.; Li, H.; Gouin, J.; Vanel, R.; Grass, S.; Bosson, J.; Bouffier, L.; Lacour, J.; Sojic N. *Chem.–Eur. J.* **2015**, *21*, 19243. c) Bosson, J.; Gouin, J.; Lacour, J. *Chem. Soc. Rev.* **2014**, *43*, 2824. d) Hamacek, J.; Besnard, C.; Mehanna, N.; Lacour, J. *Dalton Trans.* **2012**, *41*, 6777. e) Nicolas, C.; Bernardinelli, G.; Lacour, J. *J. Phys. Org. Chem.* **2010**, *23*, 1049. f) Laursen, B. W.; Krebs, F. C. *Chem.–Eur. J.* **2001**, *7*, 1773. g) Hellwinkel, D.; Aulmich, G.; Melan, M. *Chem. Ber.* **1981**, *114*, 86.
- [184] a) Hammer, N.; Schaub, T. A.; Meinhardt, U.; Kivala, M. *Chem. Rec.* **2015**, *15*, 1119. b) Kivala, M.; Pisula, W.; Wang, S.; Marvinskiy, A.; Gisselbrecht, J.-P.; Feng, X.; Müllen, K. *Chem.–Eur. J.* **2013**, *19*, 8117.
- [185] Iwahara, H.; Kushida, T.; Yamaguchi, S. *Chem. Commun.* **2016**, *52*, 1124.
- [186] Huang, C.; Barlow, S.; Marder, S. R. *J. Org. Chem.* **2011**, *76*, 2386.

- [187] Wegner, H. A.; Reisch, H.; Rauch, K.; Demeter, A.; Zachariasse, K. A.; de Meijere, A.; Scott, L. T. *J. Org. Chem.* **2006**, *71*, 9080.
- [188] a) Hoffmann, V.; Jenny, N.; Häussinger, D.; Neuburger, M.; Mayor, M. *Eur. J. Org. Chem.* **2016**, *16*, 2187. b) He, Y.; Johansson, M.; Sterner, O. *Synth. Commun.* **2004**, *32*, 4153.
- [189] Dalcanale, E.; Montanari, F. *J. Org. Chem.* **1986**, *51*, 567.
- [190] Compound **T2** was crystallized from a solution in CH₂Cl₂/MeOH (1:1) by slow evaporation of the solvent mixture. Crystallographic parameters: C₄₁H₄₀O₃; 0.06 × 0.06 × 0.11 mm; monoclinic, C₂/c (No. 15); a = 17.6046(12), b = 15.1726(10), and c = 24.4615(16) Å; α = 90, β = 107.854(2), and γ = 90°; V = 6219.2(7) Å³; Z = 8; T = 123 K; ρ_{calc} = 1.240 g cm⁻³; μ = 0.595 mm⁻¹. CCDC no.: 1513957.
- [191] Compound **T3** was crystallized from a solution in CH₂Cl₂/MeCN (1:1) by slow evaporation of the solvent mixture. Crystallographic parameters: [C₄₂H₄₃NO₂]_{0.5}(CH₂Cl₂); 0.07 × 0.09 × 0.10 mm; orthorhombic, Pnnm (No. 58); a = 14.8990(11), b = 25.4300(19), and c = 9.5165(7) Å; α = 90, β = 90, and γ = 90°; V = 3505.6(5) Å³; Z = 4; T = 123 K; ρ_{calc} = 1.1600 g cm⁻³; μ = 1.196 mm⁻¹. CCDC no.: 1513958.
- [192] An, Z.; Odom, S. A.; Kelley, R. F.; Huang, C.; Zhang, X.; Barlow, S.; Padilha, L. A.; Fu, J.; Webster, S.; Hagan, D. J.; Van Stryland, E. W.; Wasielewski, M. R.; Marder, S. R.; *J. Phys. Chem. A* **2009**, *113*, 5585.
- [193] Nakazono, S.; Easwaramoorthi, S.; Kim, D.; Shinokubo, H.; Osuka, A. *Org. Lett.* **2009**, *11*, 5426.
- [194] Dey, S.; Efimov, A.; Lemmetyinen, H. *Eur. J. Org. Chem.* **2012**, 2367.
- [195] Shoer, L. E.; Eaton, S. W.; Margulies, E. A.; Wasielewski, M. R. *J. Phys. Chem. B* **2015**, *119*, 7635.
- [196] Zhan, X.; Facchetti, A.; Barlow, S.; Marks, T. J.; Ratner, M. A.; Wasielewski, M. R.; Marder, S. R. *Adv. Mater.* **2011**, *23*, 268.
- [197] a) Hartnett, P. E.; Margulies, E. A.; Matte, H. S. S. R.; Hersam, M. C.; Marks, T. J.; Wasielewski, M. R. *Chem. Mater.* **2016**, *28*, 3928. b) Eaton, S. W.; Shoer, L. E.; Karlen, S. D.; Dyar, S. M.; Margulies, E. A.; Veldkamp, B. S.; Ramanan, C.; Hartzler, D. A.; Savikhin, S.; Marks, T. J.; Wasielewski, M. R. *J. Am. Chem. Soc.* **2013**, *135*, 14701.

- [198] Fulmer, G. R.; Miller, A. J. M.; Sherden, N. H.; Gottlieb, H. E.; Nudelman, A.; Stoltz, B. M.; Bercaw, J. E.; Goldberg, K. I. *Organometallics* **2010**, *29*, 2176.
- [199] Bruker Analytical X-ray Systems, Inc., *APEX2*, Version 2 User Manual, M86–E01078; Bruker: Madison, WI, **2006**.
- [200] Palatinus, L.; Chapuis, G. *J. Appl. Cryst.* **2007**, *40*, 786.
- [201] Betteridge, P. W.; Carruthers, J. R.; Cooper, R. I.; Prout, K.; Watkin, D. J. *J. Appl. Cryst.* **2003**, *36*, 1487.
- [202] a) Macrae, C. F.; Bruno, I. J.; Chisholm, J. A.; Edgington, P. R.; McCabe, P.; Pidcock, E.; Rodriguez-Monge, L.; Taylor, R.; van de Streek, J.; Wood, P. A. *J. Appl. Cryst.* **2008**, *41*, 466. b) Bruno, I. J.; Cole, J. C.; Edgington, P. R.; Kessler, M.; Macrae, C. F.; McCabe, P.; Pearson, J.; Taylor, R. *Acta Cryst.* **2002**, *58*, 389.
- [203] Gaussian 09, Revision D.01, Frisch, M. J.; Trucks, G. W.; Schlegel, H. B.; Scuseria, G. E.; Robb, M. A.; Cheeseman, J. R.; Scalmani, G.; Barone, V.; Mennucci, B.; Petersson, G. A.; Nakatsuji, H.; Caricato, M.; Li, X.; Hratchian, H. P.; Izmaylov, A. F.; Bloino, J.; Zheng, G.; Sonnenberg, J. L.; Hada, M.; Ehara, M.; Toyota, K.; Fukuda, R.; Hasegawa, J.; Ishida, M.; Nakajima, T.; Honda, Y.; Kitao, O.; Nakai, H.; Vreven, T.; Montgomery, Jr., J. A.; Peralta, J. E.; Ogliaro, F.; Bearpark, M.; Heyd, J. J.; Brothers, E.; Kudin, K. N.; Staroverov, V. N.; Kobayashi, R.; Normand, J.; Raghavachari, K.; Rendell, A.; Burant, J. C.; Iyengar, S. S.; Tomasi, J.; Cossi, M.; Rega, N.; Millam, J. M.; Klene, M.; Knox, J. E.; Cross, J. B.; Bakken, V.; Adamo, C.; Jaramillo, J.; Gomperts, R.; Stratmann, R. E.; Yazyev, O.; Austin, A. J.; Cammi, R.; Pomelli, C.; Ochterski, J. W.; Martin, R. L.; Morokuma, K.; Zakrzewski, V. G.; Voth, G. A.; Salvador, P.; Dannenberg, J. J.; Dapprich, S.; Daniels, A. D.; Farkas, Ö.; Foresman, J. B.; Ortiz, J. V.; Cioslowski, J.; Fox, D. J. Gaussian, Inc., Wallingford CT, **2009**.
- [204] Konishi, A.; Kubo, T. *Top. Curr. Chem.* **2017**, *375*, 83.
- [205] Konishi, A.; Kubo, T. *In Chemical Science of π -Electron Systems*; Akasaka, T., Osuka, A., Fukuzumi, S., Kandori, H., Aso, Y., Eds.; Springer: Tokyo, Japan, **2015**; 337–360.
- [206] Kubo, T. *Chem. Rec.* **2015**, *15*, 218–232.

- [207] Sun, Z.; Zeng, Z.; Wu, J. *Acc. Chem. Res.* **2014**, *47*, 2582–2591.
- [208] Morita, Y.; Nishida, S. In *Stable Radicals: Fundamentals and Applied Aspects of Odd-Electron Compounds*; Hicks, R. G., Ed.; Wiley: Wiltshire, U.K., **2010**; 81–145.
- [209] Ravat, P.; Marszalek, T.; Pisula, W.; Müllen, K.; Baumgarten, M. *J. Am. Chem. Soc.* **2014**, *136*, 12860–12863.
- [210] Shimizu, A.; Kubo, T.; Uruichi, M.; Yakushi, K.; Nakano, M.; Shiomi, D.; Sato, K.; Takui, T.; Hirao, Y.; Matsumoto, K.; Kurata, H.; Morita, Y.; Nakasuji, K. *J. Am. Chem. Soc.* **2010**, *132*, 14421–14428.
- [211] Pal, S. K.; Itkis, M. E.; Tham, F. S.; Reed, R. W.; Oakley, R. T.; Haddon, R. C. *Science* **2005**, *309*, 281–284.
- [212] Kubo, T.; Shimizu, A.; Sakamoto, M.; Uruichi, M.; Yakushi, K.; Nakano, M.; Shiomi, D.; Sato, K.; Takui, T.; Morita, Y.; Nakasuji, K. *Angew. Chem., Int. Ed.* **2005**, *44*, 6564–6568.
- [213] Itkis, M. E.; Chi, X.; Cordes, A. W.; Haddon, R. C. *Science* **2002**, *296*, 1443–1445.
- [214] Michl, J.; Bonačić-Koutecký, V. *Tetrahedron* **1988**, *44*, 7559–7585.
- [215] Kubo, T.; Katada, Y.; Shimizu, A.; Hirao, Y.; Sato, K.; Takui, T.; Uruichi, M.; Yakushi, K.; Haddon, R. C. *J. Am. Chem. Soc.* **2011**, *133*, 14240–14243.
- [216] Goto, K.; Kubo, T.; Yamamoto, K.; Nakasuji, K.; Sato, K.; Shiomi, D.; Takui, T.; Kubota, M.; Kobayashi, T.; Yakushi, K.; Ouyang, J. *J. Am. Chem. Soc.* **1999**, *121*, 1619–1620.
- [217] Cui, Z.-H.; Lischka, H.; Beneberu, H. Z.; Kertesz, M. *J. Am. Chem. Soc.* **2014**, *136*, 5539–5542.
- [218] Mou, Z.; Uchida, K.; Kubo, T.; Kertesz, M. *J. Am. Chem. Soc.* **2014**, *136*, 18009–18022.
- [219] Cui, Z.-H.; Lischka, H.; Beneberu, H. Z.; Kertesz, M. *J. Am. Chem. Soc.* **2014**, *136*, 12958–12965.
- [220] Tian, Y.-H.; Huang, J.; Kertesz, M. *Phys. Chem. Chem. Phys.* **2010**, *12*, 5084–5093.
- [221] Miller, J. S.; Novoa, J. *Acc. Chem. Res.* **2007**, *40*, 189–196.
- [222] Mou, Z.; Kertesz, M. *Angew. Chem., Int. Ed.* **2017**, *56*, 10188–10191.

- [223] Ravat, P.; Šolomek, T.; Häussinger, D.; Blacque, O.; Juríček, M. *J. Am. Chem. Soc.* **2018**, *140*, 10839–10847.
- [224] Hu, P.; Wu, J. *Can. J. Chem.* **2016**, *95*, 223–233.
- [225] Mitchell, R. H.; Sondheimer, F. *Tetrahedron* **1970**, *26*, 2141–2150.
- [226] Sun, Z.; Zeng, Z.; Wu, J. *Acc. Chem. Res.* **2014**, *47*, 2582–2591.
- [227] Shimizu, A.; Kubo, T.; Uruichi, U.; Yakushi, K.; Nakano, M.; Shiomi, D.; Sato, K.; Takui, T.; Hirao, Y.; Matsumoto, K.; Kurata, K.; Morita, Y.; Nakasuji, K. *J. Am. Chem. Soc.* **2010**, *132*, 14421–14428
- [228] Kubo, T.; Shimizu, A.; Uruichi, M.; Yakushi, K.; Nakano, M.; Shiomi, D.; Sato, K.; Takui, T.; Morita, Y.; Nakasuji, K. *Org. Lett.* **2007**, *9*, 81–84.
- [229] Kubo, T.; Shimizu, A.; Sakamoto, M.; Uruichi, M.; Yakushi, M.; Nakano, M.; Shiomi, D.; Sato, K.; Takui, T.; Morita, Y.; Nakasuji, K. *Angew. Chem. Int. Ed.* **2005**, *44*, 6564–6568.
- [230] a) Sun, Z.; Lee, S.; Park, K. H.; Zhu, X.; Zhang, W.; Zheng, B.; Hu, P.; Zeng, Z.; Das, S.; Li, Y.; Chi, C.; Li, R-W.; Huang, K-W.; Ding, J.; Kim, D. Wu, J. *J. Am. Chem. Soc.* **2013**, *135*, 18229–18236. b) Li, Y.; Heng, K-W.; Lee, B.S.; Aratani, N.; Zafra, J. L.; Bao, N.; Lee, R.; Sung, Y. M.; Sun, Z.; Huang, K-W.; Webster, R. D.; López Navarrete, J. T.; Kim, D.; Osuka, A.; Casado, J.; Ding, J.; Wu, J. *J. Am. Chem. Soc.* **2012**, *134*, 14913–14922. c) Sun, Z.; Huang, K-W.; Wu, J. *J. Am. Chem. Soc.* **2011**, *133*, 11896–11899.
- [231] Li, Y.; Huang, K-W.; Sun, Z.; Webster, R. D.; Zeng, Z.; Zeng, W.; Chi, C.; Furukawa, K.; Wu, J. *Chem. Sci.* **2014**, *5*, 1908–1914.
- [232] Ravat, P.; Šolomek, T.; Rickhaus, M.; Häussinger, D.; Neuburger, M.; Baumgarten, M.; Juríček, M. *Angew. Chem. Int. Ed.* **2016**, *55*, 1183–1186.
- [233] Goedicke, C.; Stegemeyer, H. *Tetrahedron Lett.* **1970**, *11*, 937–940.
- [234] Ueda, A.; Wasa, H.; Suzuki, S.; Okada, K.; Sato, K.; Takui, T.; Morita, Y. *Angew. Chem. Int. Ed.* **2012**, *51*, 6691–6695.
- [235] Šolomek, T.; Ravat, P.; Mou, Z.; Kertesz, M.; Juríček, M. *J. Org. Chem.* **2018**, *83*, 4769–4774.
- [236] Ravat, P.; Šolomek, T.; Ribar, P.; Juríček, M. *Synlett* **2016**, *27*, 1613–1617.

- [237] Li, Y.; Heng, W.-K.; Lee, B. S.; Aratani, N.; Zafra, J. L.; Bao, N.; Lee, R.; Sung, Y. M.; Sun, Z.; Huang, K.-W.; Webster, R. D.; López Navarrete, J. T.; Kim, D.; Osuka, A.; Casado, J.; Ding, J.; Wu, J. *J. Am. Chem. Soc.* **2012**, *134*, 14913–14922.
- [238] a) Woodward, R. B.; Hoffmann, R. *The Conservation of Orbital Symmetry*; Verlag Chemie: Weinheim, Germany, **1970**. b) Fleming, I. *Molecular Orbitals and Organic Chemical Reactions*; Wiley: Chichester, U.K., **2010**; 253–368. c) Woodward, R. B.; Hoffmann, R. *Angew. Chem., Int. Ed.* **1969**, *8*, 781–932. d) Woodward, R.; Hoffmann, R. *J. Am. Chem. Soc.* **1965**, *87*, 395–397.
- [239] Uchida, K.; Ito, S.; Nakano, M.; Abe, M.; Kubo, T. *J. Am. Chem. Soc.* **2016**, *138*, 2399–2410.
- [240] Pogodin, S.; Agranat, I. *J. Am. Chem. Soc.* **2003**, *125*, 12829–12835.
- [241] Bishnupada, S.; Ramasastry, S. S. V. *Angew. Chem. Int. Ed.* **2008**, *47*, 9708–9710.
- [242] Yao, D.; Liu, X.; Jiang, H.; Hua, J.; Bao, J. *J. Org. Chem.* **2011**, *76*, 10068–10077.
- [243] Norito, T.; Robindro Singh, S.; Bujor, C. *Angew. Chem. Int. Ed.* **2008**, *47*, 9708–9710.
- [244] Liu, L.; Yang, B.; Katz, T. J.; Poindexter, M. K. *J. Org. Chem.* **1991**, *56*, 3769–3775.

APPENDIX A

Supporting information for *Synthesis* **2017**, *47*, 899–909.

Donor–Acceptor Molecular Triangles

Peter Ribar, Tomáš Šolomek, Loïc Le Pleux, Daniel Häussinger, Alessandro Prescimone, Markus Neuburger, Michal Juríček

A1. Table of Contents

A1. Table of Contents	A2
A2. UV/Vis Spectroscopy	A4
Figure A1	A4
Figure A2	A5
Table A1	A6
Figure A3	A7
Figure A4	A8
A3. Cyclic Voltammetry	A9
Figure A5	A9
Figure A6	A10
Figure A7	A11
A4. Theoretical Calculations	A12
Table A2	A13
Table A3	A14
Table A4	A15
Table A5	A16
Table A6	A17
Table A7	A18
Table A8	A19
Figure A8	A20
A5. Assignment of Proton and Carbon Resonances	A21
A6. Copies of the NMR Spectra	A22

A2. UV/Vis Spectroscopy

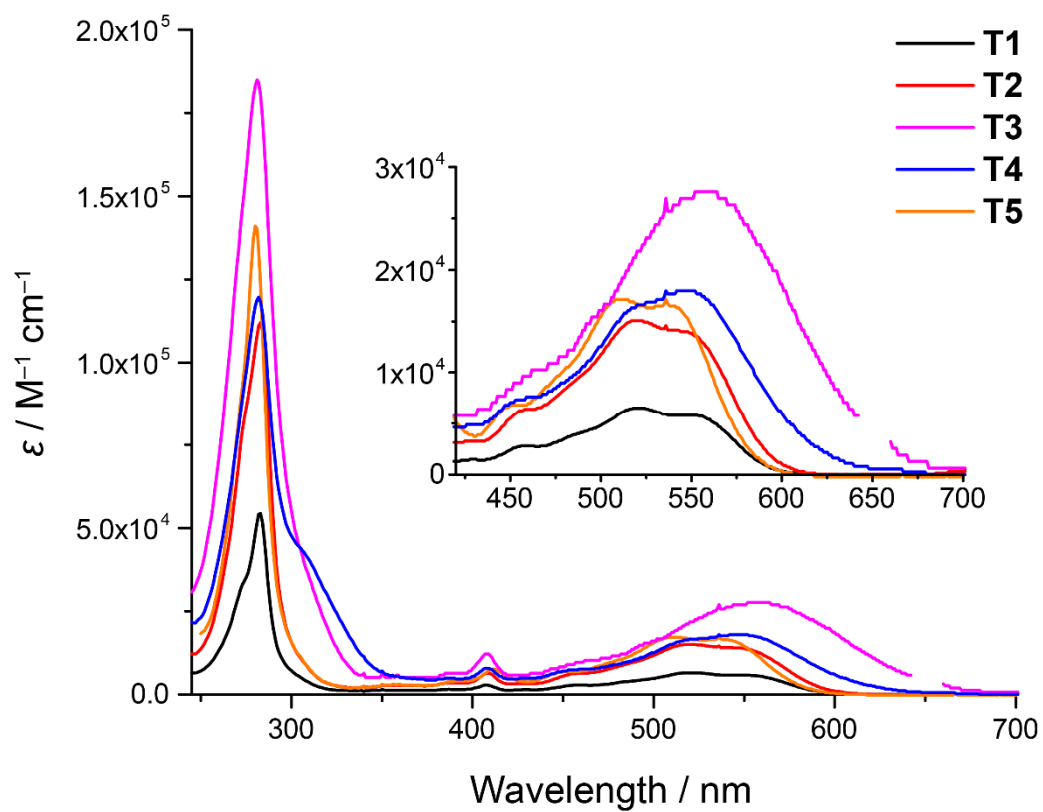


Figure A1: UV/Vis Absorption spectra of T1–T5 in CH_2Cl_2 at room temperature.

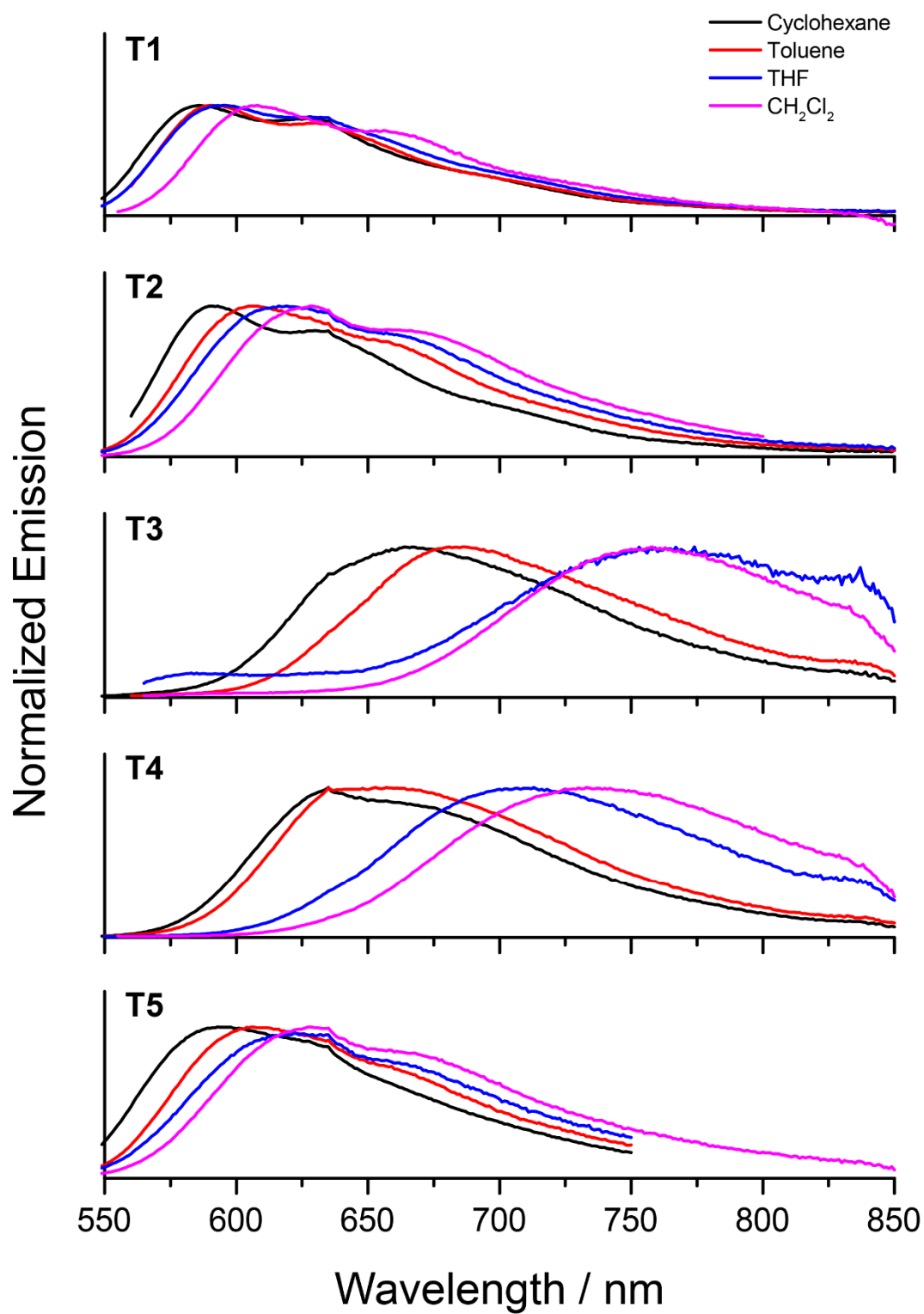


Figure A2: Fluorescence spectra of T1–T5 in various solvents of different polarity.

Table A1: Absorption and Emission Maxima, and Stokes Shifts^a of **T1–T5** in Different Solvents.

Compound	Cyclohexane	Toluene	THF	CH ₂ Cl ₂		
T1	$\lambda_{\text{abs-max}}$ (nm)	510 542	514 549	512 547	518 554	
	$\lambda_{\text{em-max}}$ (nm)	585 628	590 630	596 628	608 657	
	Stokes shift (nm)	43	41	49	54	
	T2	$\lambda_{\text{abs-max}}$ (nm)	509 546	515 546	510 548	522 551
		$\lambda_{\text{em-max}}$ (nm)	590 630	607 652	619 657	629 669
Stokes shift (nm)		44	61	71	78	
T3		$\lambda_{\text{abs-max}}$ (nm)	541	549	550	558
		$\lambda_{\text{em-max}}$ (nm)	664	686	774	758
	Stokes shift (nm)	123	137	224	200	
	T4	$\lambda_{\text{abs-max}}$ (nm)	540	542	542	554
		$\lambda_{\text{em-max}}$ (nm)	635	657	713	733
Stokes shift (nm)		95	115	171	179	
T5		$\lambda_{\text{abs-max}}$ (nm)	501 530	507 537	506 536	509 543
		$\lambda_{\text{em-max}}$ (nm)	593 628	606 657	625 663	628 662
	Stokes shift (nm)	63	69	89	85	

^a Stokes shift = $\lambda_{\text{em-max}}$ (highest energy) – $\lambda_{\text{abs-max}}$ (lowest energy).

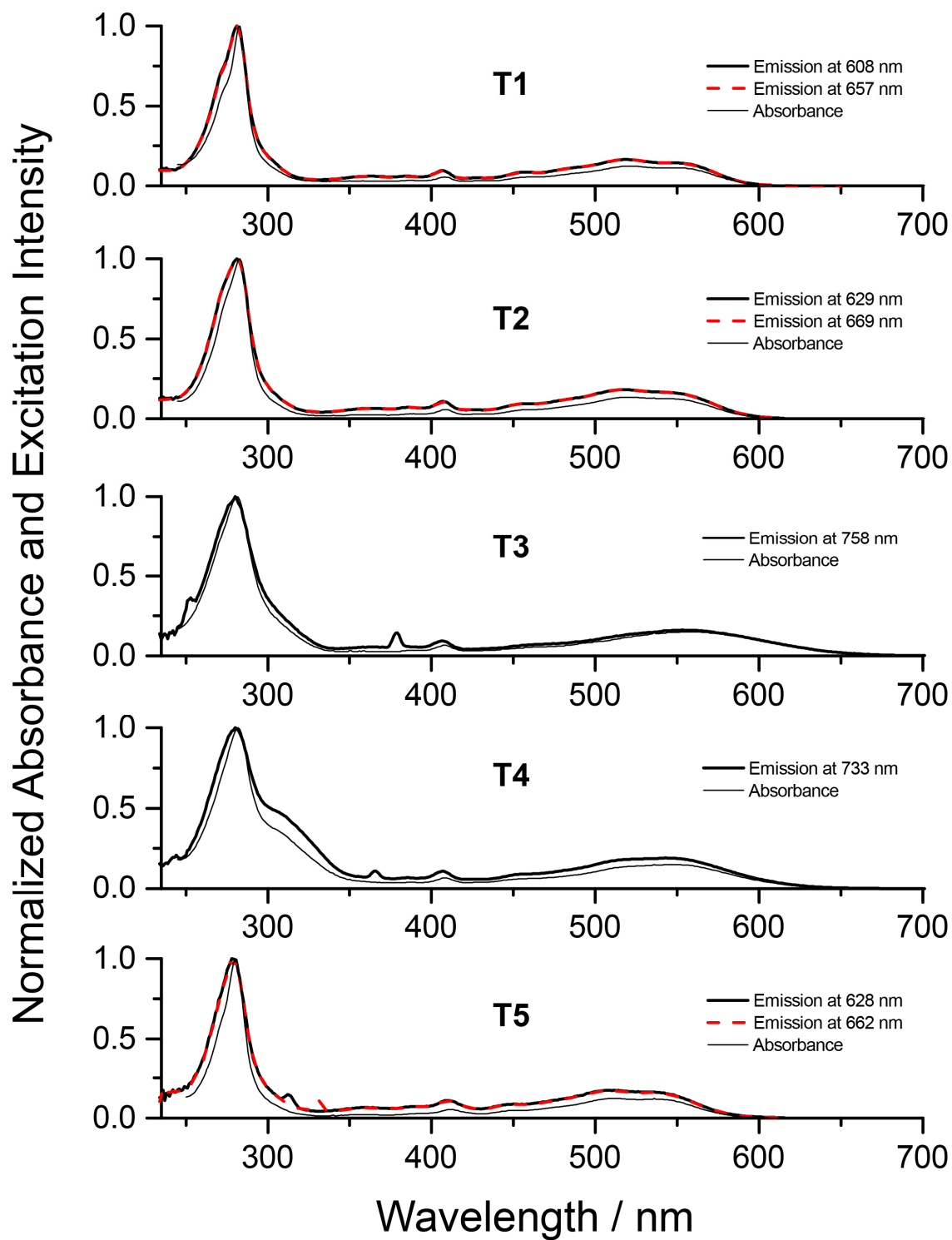


Figure A3: Normalized excitation and absorption spectra of **T1–T5** in CH_2Cl_2 at room temperature.

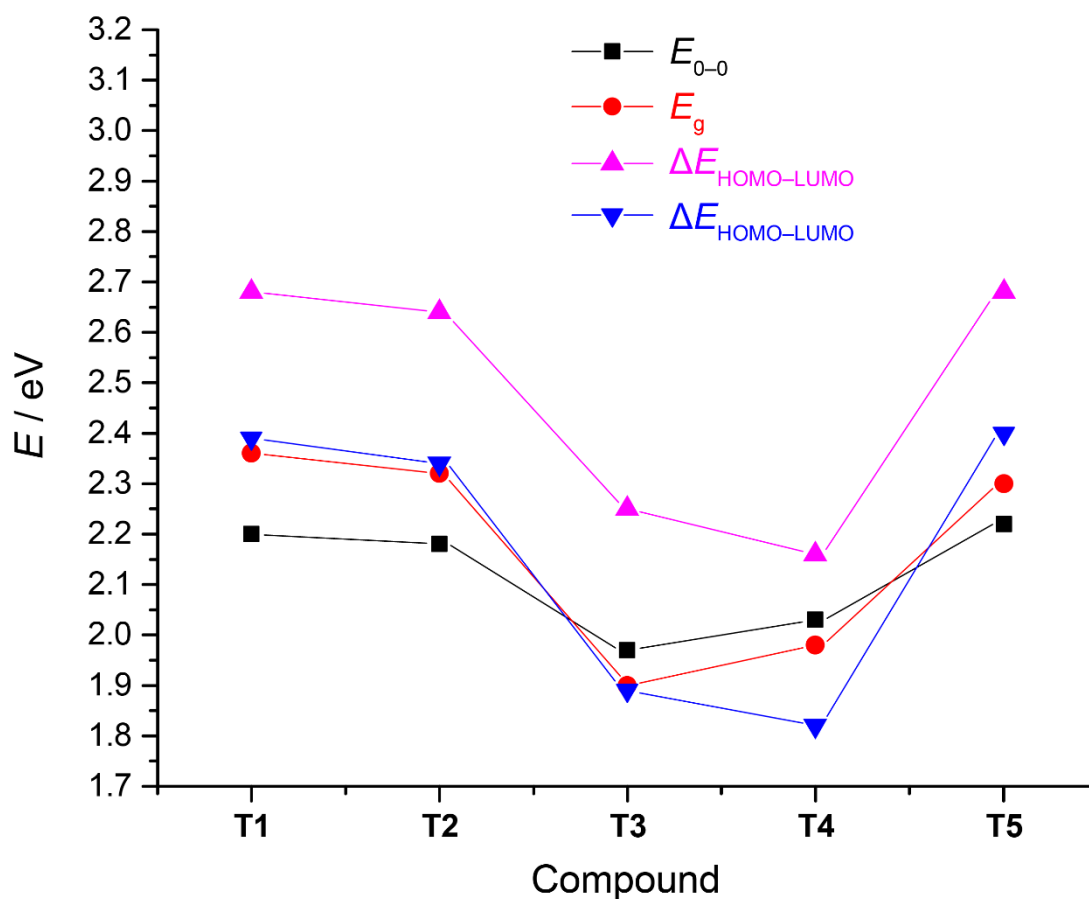


Figure A4: Comparison of E_{0-0} (black) obtained from UV/Vis spectroscopic measurements, E_g (red) obtained from cyclic voltammetry measurements, and $\Delta E_{\text{HOMO-LUMO}}$ obtained from DFT calculations (B3LYP/6-311+G(2d,p)/PCM(CH₂Cl₂) single point calculation in magenta and TD-B3LYP/6-31G(d)/PCM(CH₂Cl₂) calculation in blue) on B3LYP/6-31G(d) gas-phase geometries for **T1–T5**.

A3. Cyclic Voltammetry

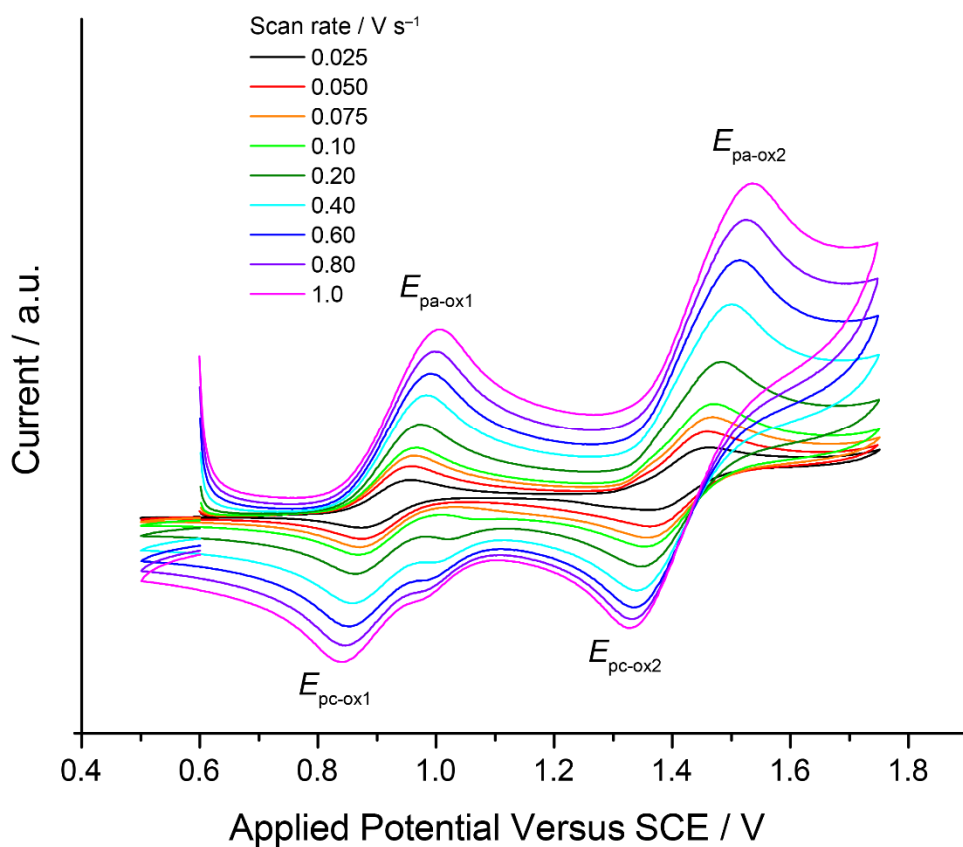


Figure A5: Cyclic voltammetry traces ($E > 0V$) for **T3** at different scan rates (CH₂Cl₂ / TBAPF₆).

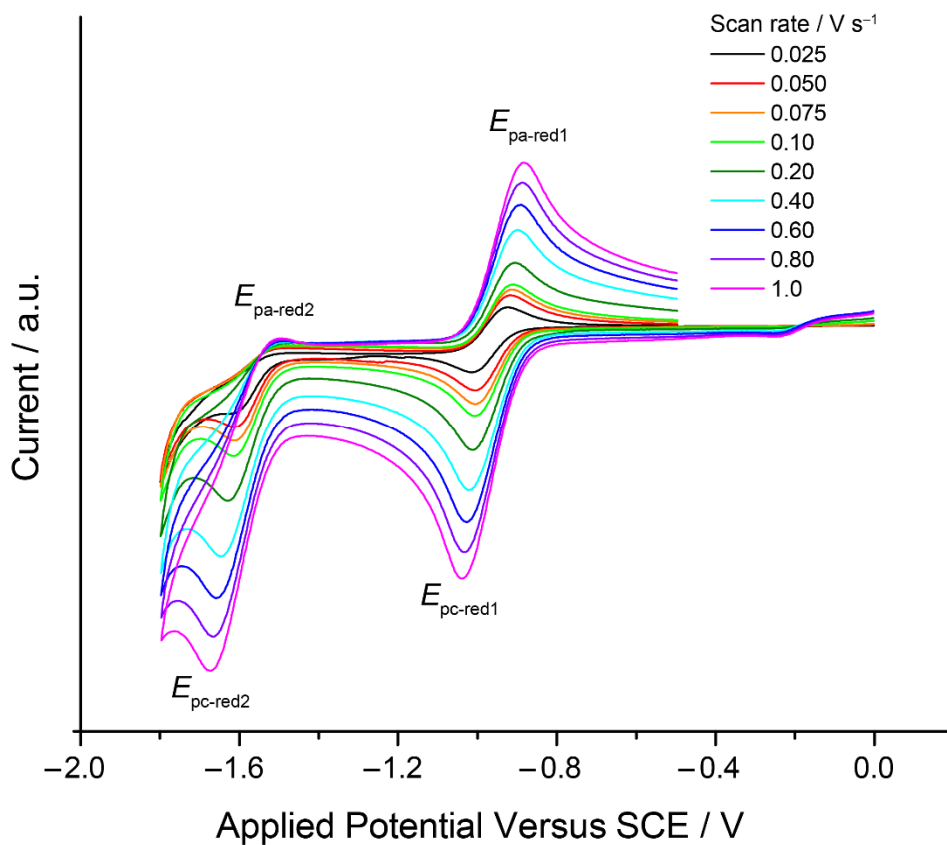


Figure A6: Cyclic voltammety traces ($E < 0V$) for **T3** at different scan rates ($\text{CH}_2\text{Cl}_2 / \text{TBAPF}_6$).

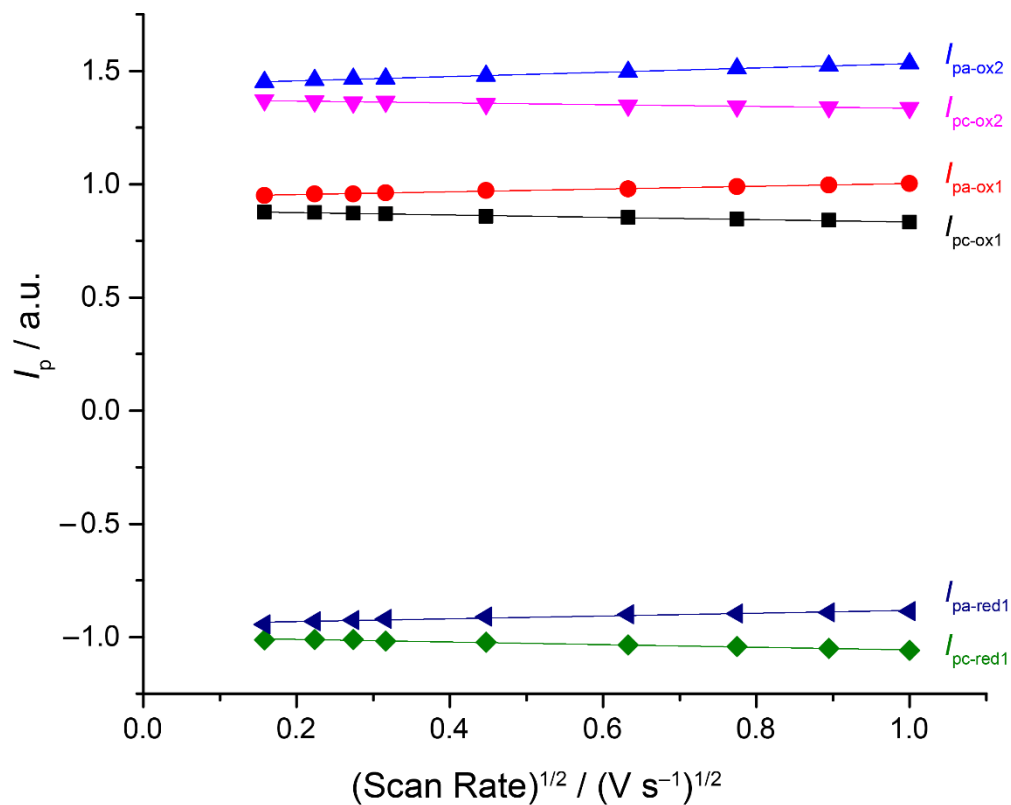
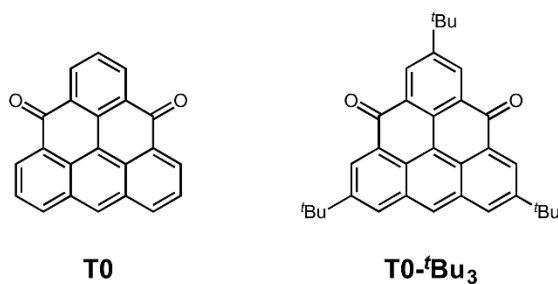


Figure A7: Plots of peak anodic (I_{pa}) and cathodic (I_{pc}) current versus $(\text{scan rate})^{1/2}$ for the first ('ox1') and second ('ox2') oxidation and the first reduction ('red1') of **T3** by using the data from Figures S5 and S6.

A4. Theoretical Calculations

Molecules **T1–T5** were simplified to alleviate the computational costs by substitution of the three apex *tert*-butyl groups in positions 2, 6, and 10 (**T1_H–T5_H**) by hydrogen atoms. The effect of the *tert*-butyl groups on the calculated absorption spectra was tested on the parent triangulene-4,8-dione (**T0**) in the gas phase and CH₂Cl₂ as a model solvent. The results obtained with four different functionals (PBE1PBE, B3LYP, CAM-B3LYP, and M06-2X) are summarized in Table S2. The induction effect of the three *tert*-butyl groups causes a bathochromic shift of the energy of the first electronic transition by ~0.06 eV for all considered functionals irrespective of the solvation, and can therefore be neglected.

The first electronic transition in the series of donor–acceptor molecules **T1_H–T5_H** was calculated with the CAM-B3LYP and M06-2X functionals that showed^{S1–S3} previously a balanced performance in evaluating both the local and charge-transfer (CT) electronic transitions. The results obtained from these calculations are summarized in Tables S3–S8.

Table A2: Comparison of Energies^a of the First Electronic Transitions in **T0** and **T0-^tBu₃**.

Molecule	PBE1PBE		B3LYP		CAM-B3LYP		M06-2X	
	λ (nm)	ΔE (eV)						
T0-^tBu₃ (gas)	494	2.5097	510	2.4327	445	2.7853	445	2.7886
T0-^tBu₃ (PCM)	502	2.4680	518	2.3933	455	2.7267	454	2.7286
T0 (gas)	482	2.5699	498	2.4917	436	2.8409	435	2.8490
T0 (PCM)	490	2.5293	505	2.4527	446	2.7824	445	2.7887

^a Calculated with the TD-DFT formalism with the 6-31G(d) basis set in the gas phase and CH₂Cl₂ modeled as a polarizable continuum (PCM).

Table A3: The 10 Lowest Electronic Transitions^a in **T1_H** in CH₂Cl₂ with Oscillator Strength Higher than 0.015 ($f > 0.015$).

Excited state	CAM-B3LYP			Excited state	M06-2X		
	λ (nm)	ΔE (eV)	f		λ (nm)	ΔE (eV)	f
1	457	2.7104	0.4396	1	457	2.7144	0.4315
2	350	3.5387	0.0377	4	352	3.5232	0.0472
5	336	3.6912	0.0952	5	333	3.7186	0.0818
8	295	4.1983	0.0196	8	294	4.2196	0.0134
9	285	4.3564	0.0333	9	285	4.3509	0.0333
11	262	4.7314	0.2958	10	273	4.5372	0.0038
16	240	5.1603	1.1426	11	263	4.7197	0.3356
17	240	5.1703	0.4324	15	241	5.1426	1.1057
18	231	5.3691	0.0157	17	239	5.1915	0.4466
19	229	5.4216	0.0455	18	230	5.3843	0.0444

^a Calculated with the TD-DFT formalism with the 6-31G(d) basis set and CH₂Cl₂ modeled as a polarizable continuum.

Table A4: The 10 Lowest Electronic Transitions^a in **T2_H** in CH₂Cl₂ with Oscillator Strength Higher than 0.015 ($f > 0.015$).

Excited state	CAM-B3LYP			Excited state	M06-2X		
	λ (nm)	ΔE (eV)	f		λ (nm)	ΔE (eV)	f
1	461	2.6885	0.4448	1	461	2.6903	0.4361
2	351	3.5275	0.0393	4	353	3.5109	0.0484
5	336	3.6908	0.0927	6	333	3.7202	0.0793
7	296	4.1953	0.0183	8	289	4.2956	0.0475
8	289	4.2878	0.0573	10	267	4.6392	0.1132
10	266	4.6693	0.1775	11	261	4.7432	0.2421
11	259	4.7886	0.1377	15	244	5.0915	0.0523
16	241	5.1486	0.8724	16	242	5.1338	1.0647
17	240	5.1578	0.3201	18	239	5.1882	0.445
18	240	5.1644	0.444	19	234	5.3091	0.043

^a Calculated with the TD-DFT formalism with the 6-31G(d) basis set and CH₂Cl₂ modeled as a polarizable continuum.

Table A5: The 10 Lowest Electronic Transitions^a in **T3_H** in CH₂Cl₂ with Oscillator Strength Higher than 0.015 ($f > 0.015$).

Excited state	CAM-B3LYP			Excited state	M06-2X		
	λ (nm)	ΔE (eV)	f		λ (nm)	ΔE (eV)	f
1	481	2.5772	0.4941	1	488	2.5397	0.4645
3	358	3.4648	0.0511	2	408	3.0372	0.0277
6	336	3.6943	0.0819	3	363	3.4185	0.0237
7	295	4.2065	0.0186	5	360	3.4471	0.0315
8	290	4.2774	0.0408	6	333	3.723	0.0715
11	271	4.5809	0.0378	9	288	4.3054	0.0165
12	263	4.7094	0.3378	11	272	4.5665	0.0295
13	258	4.8082	0.0447	12	265	4.6768	0.3861
14	255	4.8686	0.0406	13	258	4.8131	0.0449
16	246	5.0461	0.0165	14	256	4.8481	0.0932

^a Calculated with the TD-DFT formalism with the 6-31G(d) basis set and CH₂Cl₂ modeled as a polarizable continuum.

Table A6: The 10 Lowest Electronic Transitions^a in **T4_H** in CH₂Cl₂ with Oscillator Strength Higher than 0.015 ($f > 0.015$).

Excited state	CAM-B3LYP			Excited state	M06-2X		
	λ (nm)	ΔE (eV)	f		λ (nm)	ΔE (eV)	f
1	472	2.628	0.5524	1	477	2.5997	0.5266
3	353	3.5094	0.0432	5	356	3.4863	0.0492
6	336	3.6898	0.0858	6	333	3.7188	0.0738
7	296	4.1924	0.0236	8	294	4.2137	0.0172
8	290	4.2765	0.0478	9	289	4.2874	0.0423
10	281	4.4126	0.6266	10	284	4.3653	0.6408
11	275	4.5073	0.0182	13	271	4.5767	0.2206
13	269	4.6094	0.1947	14	269	4.6059	0.1493
14	267	4.6461	0.223	16	262	4.7238	0.3312
15	260	4.7601	0.233	18	249	4.9781	0.052

^a Calculated with the TD-DFT formalism with the 6-31G(d) basis set and CH₂Cl₂ modeled as a polarizable continuum.

Table A7: The 10 Lowest Electronic Transitions^a in **T5_H** in CH₂Cl₂ with Oscillator Strength Higher than 0.015 ($f > 0.015$).

Excited state	CAM-B3LYP			Excited state	M06-2X		
	λ (nm)	ΔE (eV)	f		λ (nm)	ΔE (eV)	f
1	456	2.7198	0.4129	1	455	2.7264	0.4048
4	344	3.6006	0.015	4	346	3.5871	0.037
5	338	3.6642	0.1231	6	335	3.6961	0.0857
8	294	4.214	0.07	8	296	4.1838	0.0431
11	260	4.7623	0.2279	9	283	4.3809	0.0203
12	249	4.9705	0.0184	11	261	4.7493	0.2811
16	240	5.1658	1.2704	15	241	5.1447	0.0199
17	239	5.1939	0.3639	16	241	5.1499	1.2055
18	228	5.4317	0.0605	17	238	5.2091	0.3834
21	221	5.5996	0.1366	19	228	5.4309	0.1006

^a Calculated with the TD-DFT formalism with the 6-31G(d) basis set and CH₂Cl₂ modeled as a polarizable continuum.

Table A8: Energies^a of the Lowest Electronic Transition in **T1_H**– **T5_H** in different solvents.

	CAM-B3LYP						M06-2X					
	Toluene		CH ₂ Cl ₂		DMSO		Toluene		CH ₂ Cl ₂		DMSO	
	λ (nm)	ΔE (eV)	λ (nm)	ΔE (eV)	λ (nm)	ΔE (eV)	λ (nm)	ΔE (eV)	λ (nm)	ΔE (eV)	λ (nm)	ΔE (eV)
T1_H	459 (0.4483)	2.7029	457 (0.4396)	2.7104	457 (0.4393)	2.7112	458 (0.4399)	2.7084	457 (0.4315)	2.7144	457 (0.4314)	2.7148
T2_H	462 (0.4535)	2.6829	461 (0.4448)	2.6885	461 (0.4447)	2.6884	461 (0.4443)	2.6868	461 (0.4361)	2.6903	461 (0.4361)	2.6896
T3_H	478 (0.5105)	2.5961	481 (0.4941)	2.5772	483 (0.4893)	2.5669	482 (0.4933)	2.5733	488 (0.4645)	2.5397	491 (0.4540)	2.5235
T4_H	471 (0.5617)	2.6306	472 (0.5524)	2.6280	472 (0.5514)	2.6250	475 (0.5462)	2.6117	477 (0.5266)	2.5997	478 (0.5212)	2.5932
T5_H	457 (0.4240)	2.7113	456 (0.4129)	2.7198	456 (0.4119)	2.7208	456 (0.4156)	2.7191	455 (0.4048)	2.7264	455 (0.4039)	2.7270

^a Calculated with the TD-DFT formalism with the 6-31G(d) basis set and solvent modeled as a polarizable continuum.

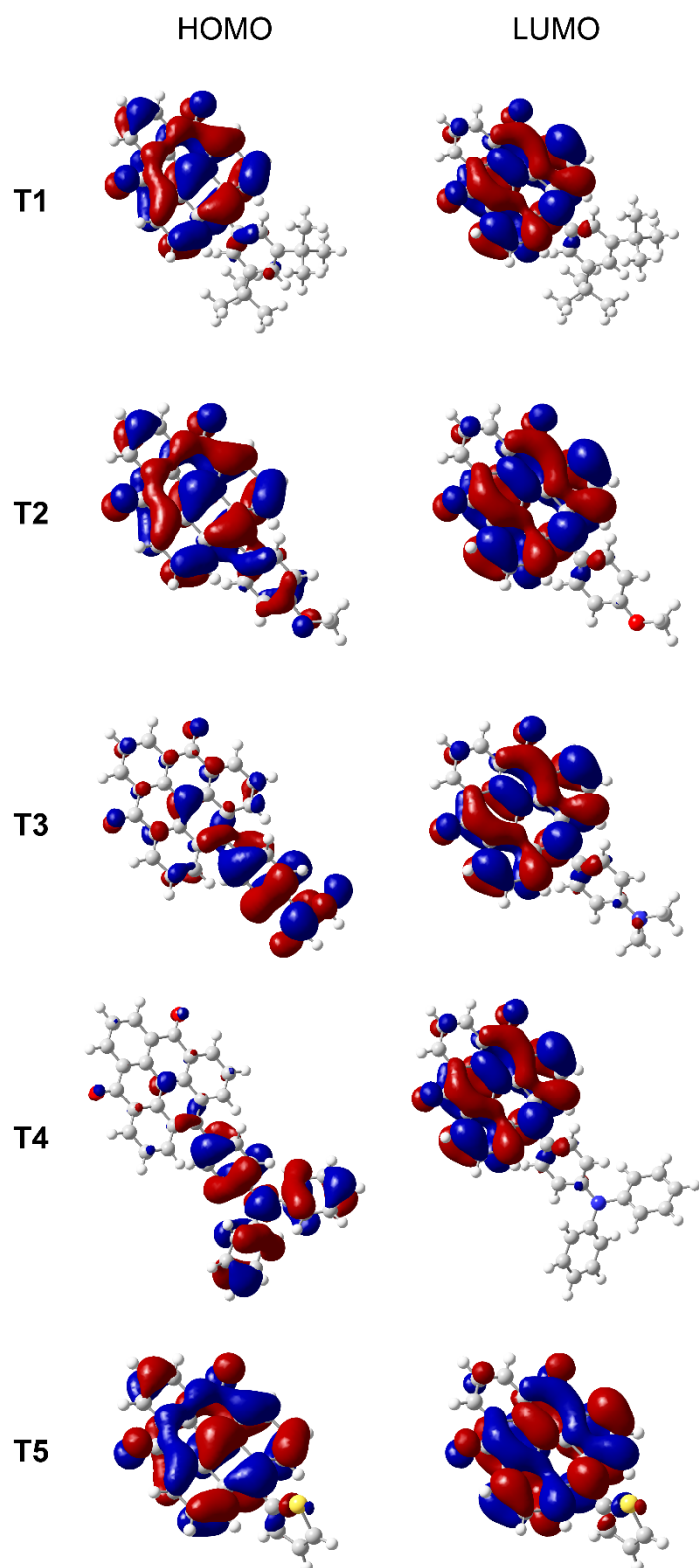
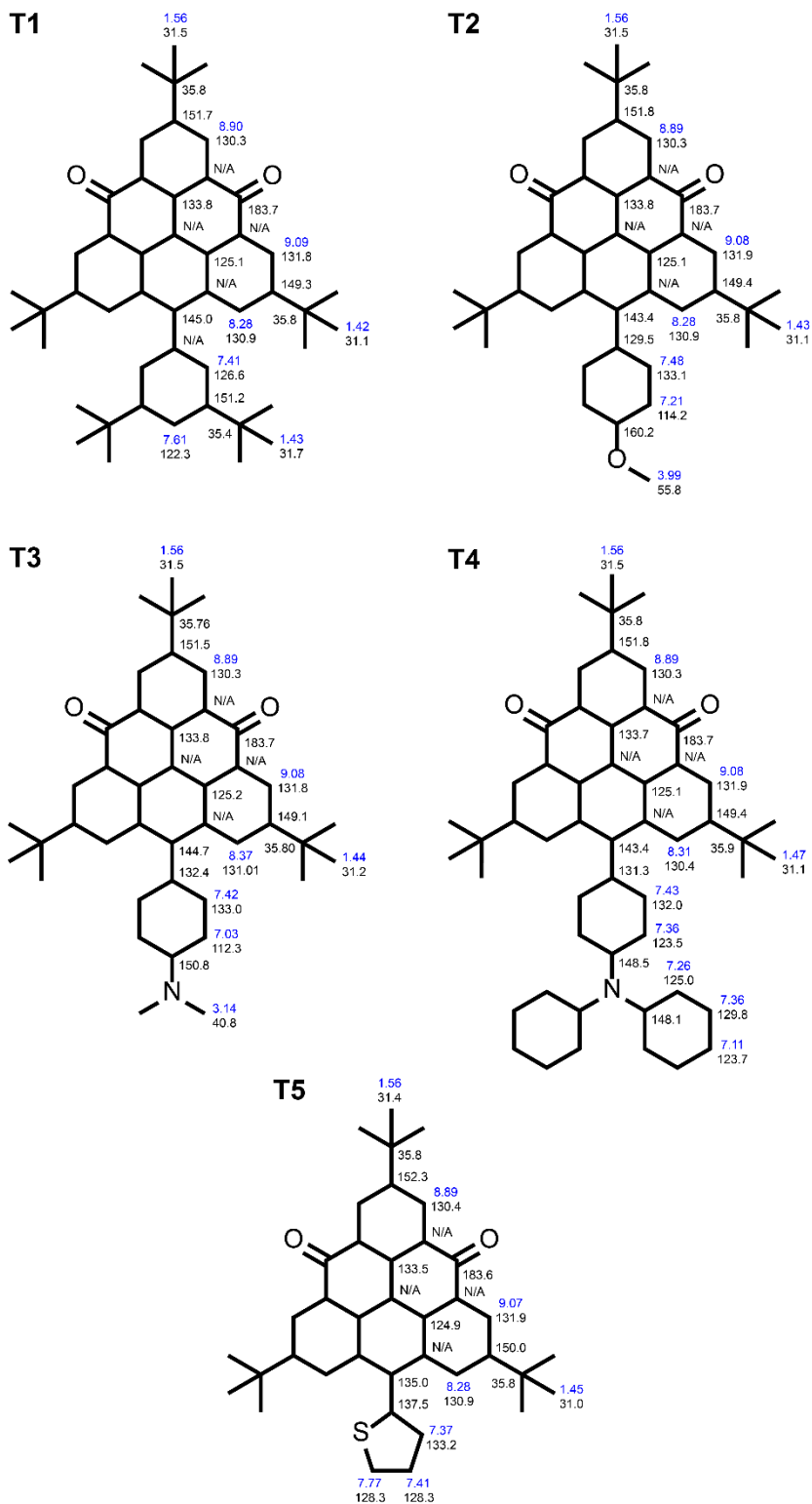


Figure A8: The HOMO and the LUMO of T1–T5 (DFT, B3LYP/6-31G(d), gas phase).

A5. Assignment of Proton and Carbon Resonances

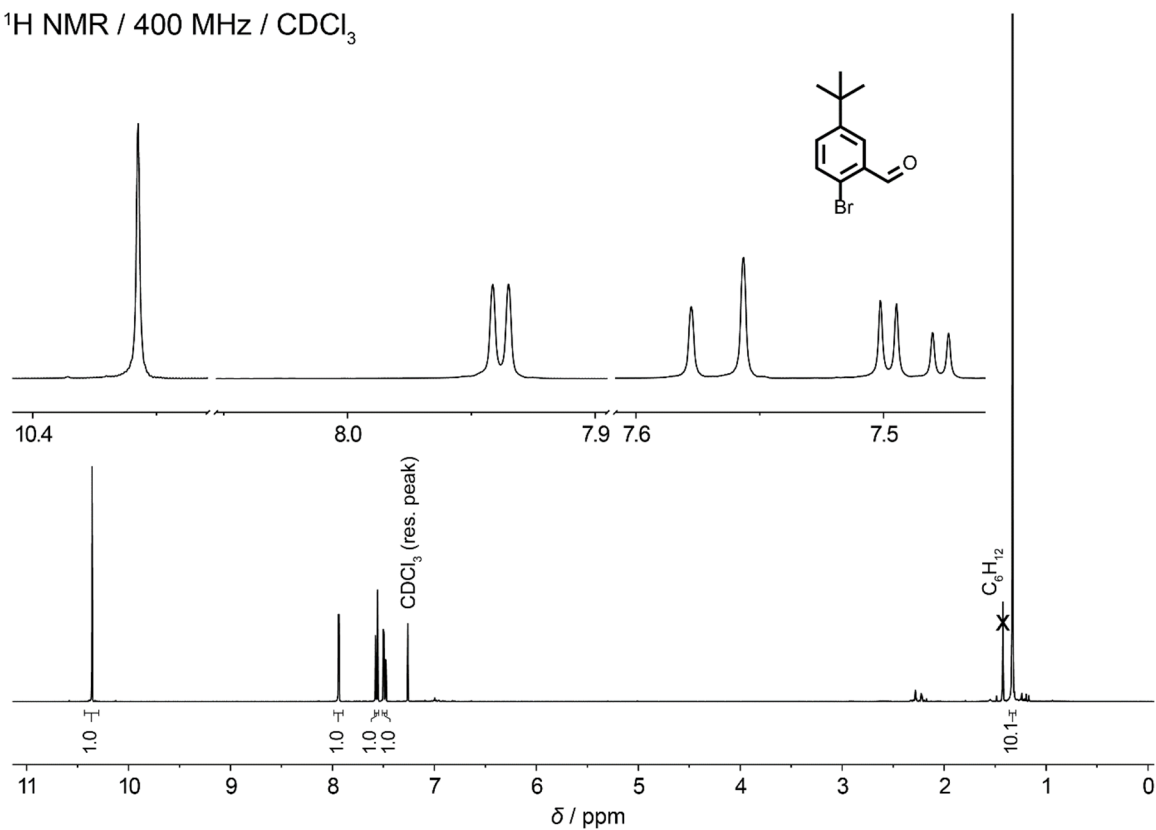
^1H / ^{13}C NMR



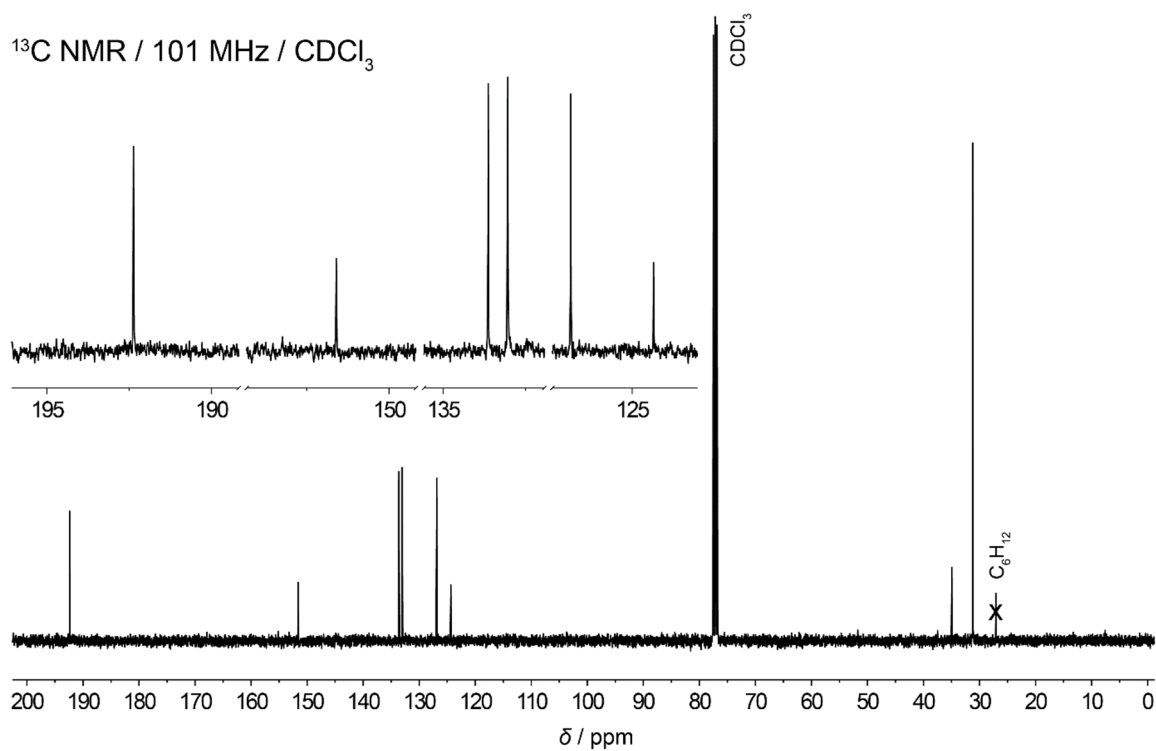
A6. Copies of the NMR Spectra

2-Bromo-5-(*tert*-butyl)benzaldehyde (2)

^1H NMR / 400 MHz / CDCl_3

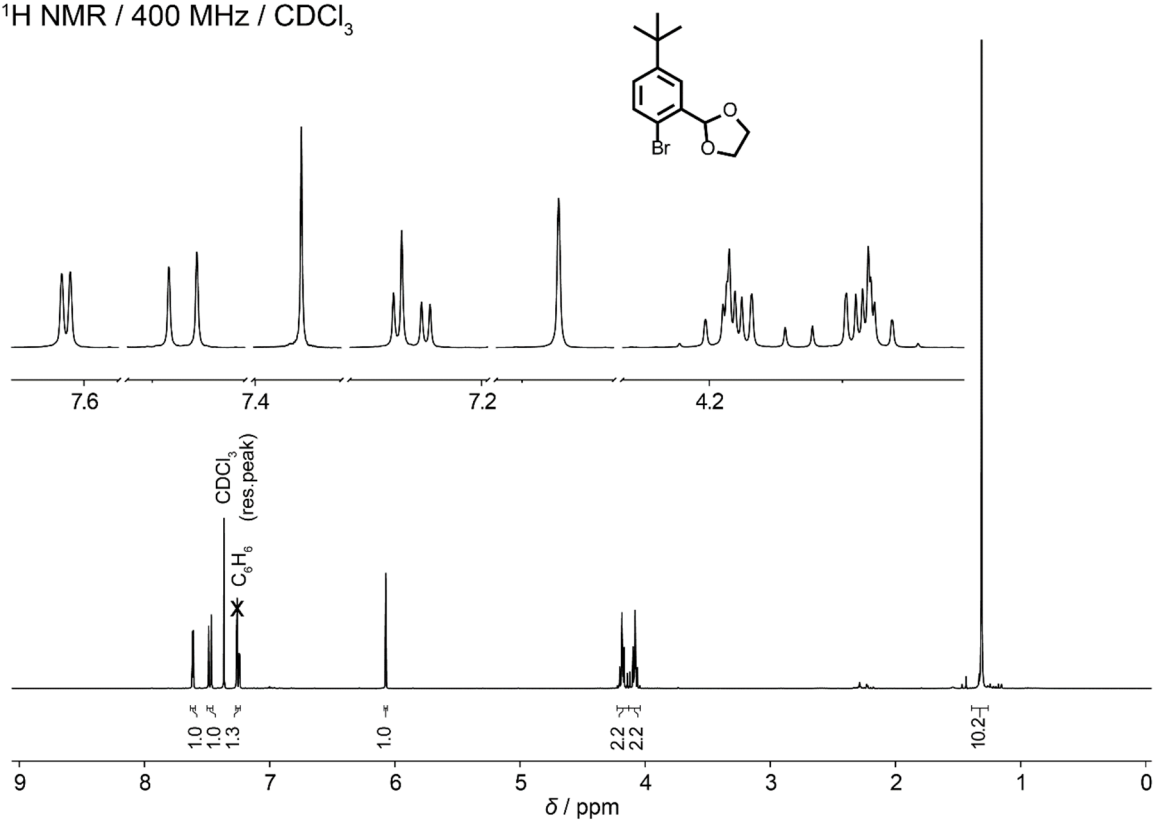


^{13}C NMR / 101 MHz / CDCl_3

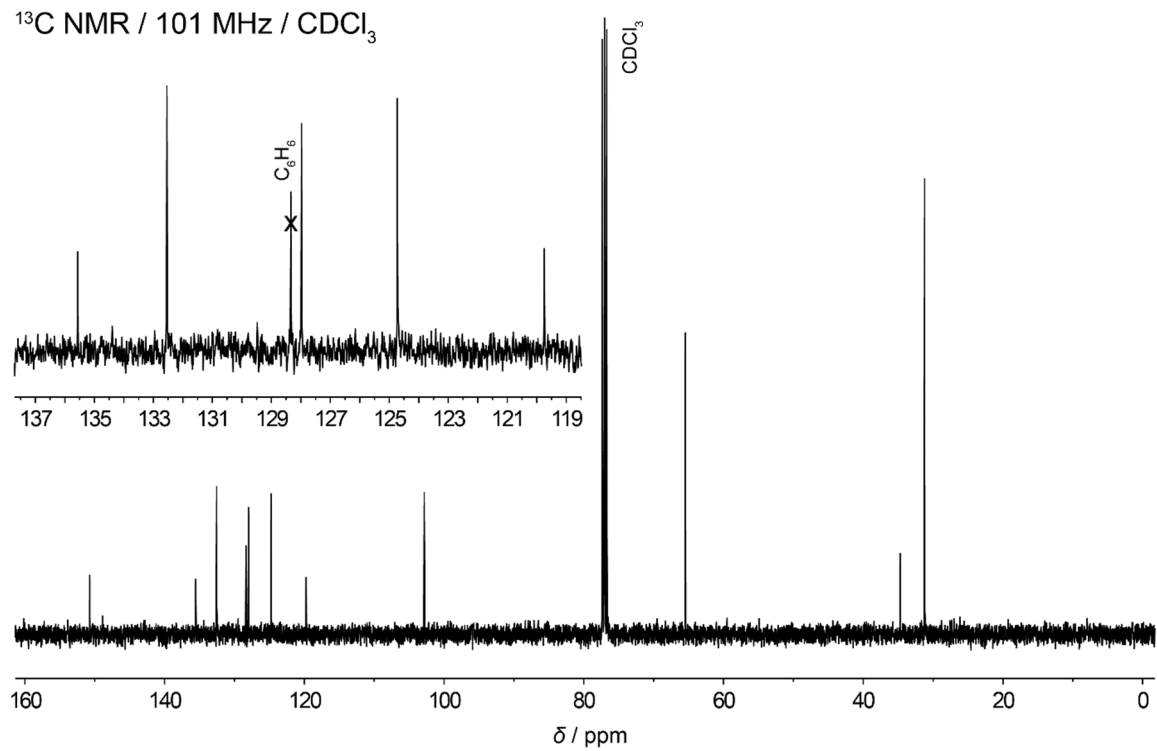


2-(2-Bromo-5-(*tert*-butyl)phenyl)-1,3-dioxolane (3)

$^1\text{H NMR}$ / 400 MHz / CDCl_3

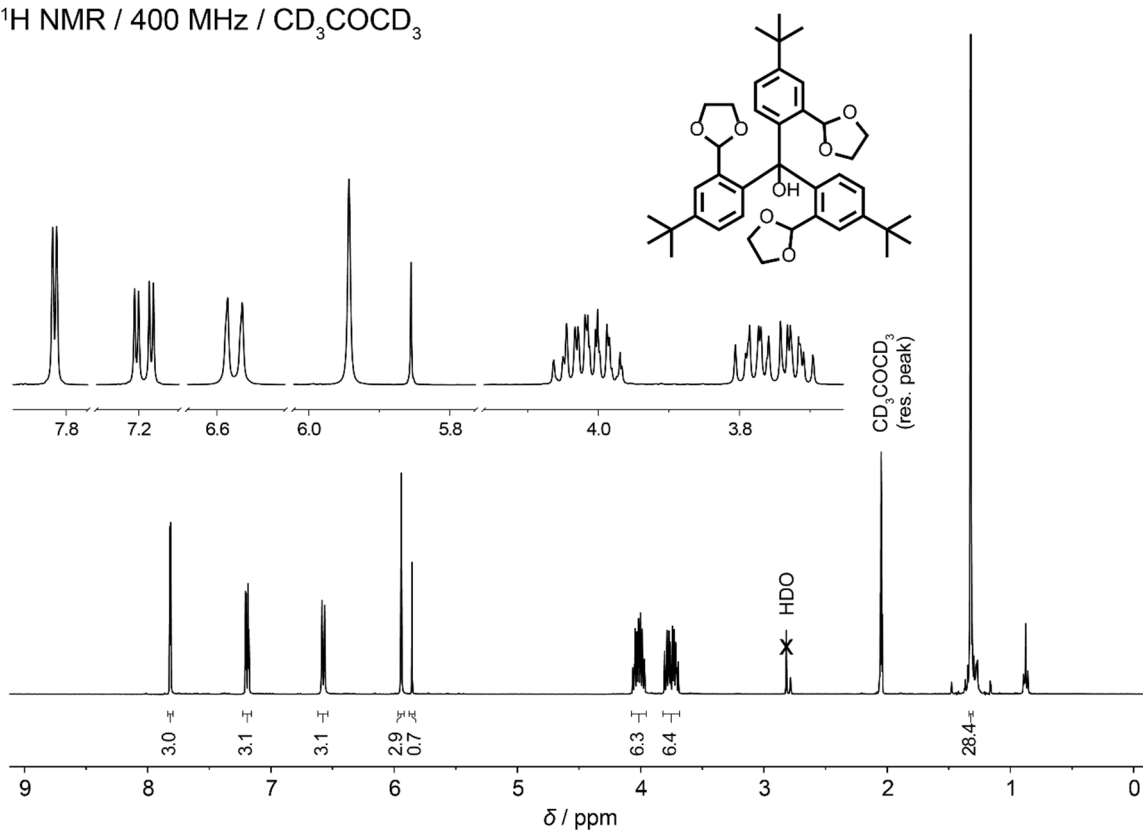


$^{13}\text{C NMR}$ / 101 MHz / CDCl_3

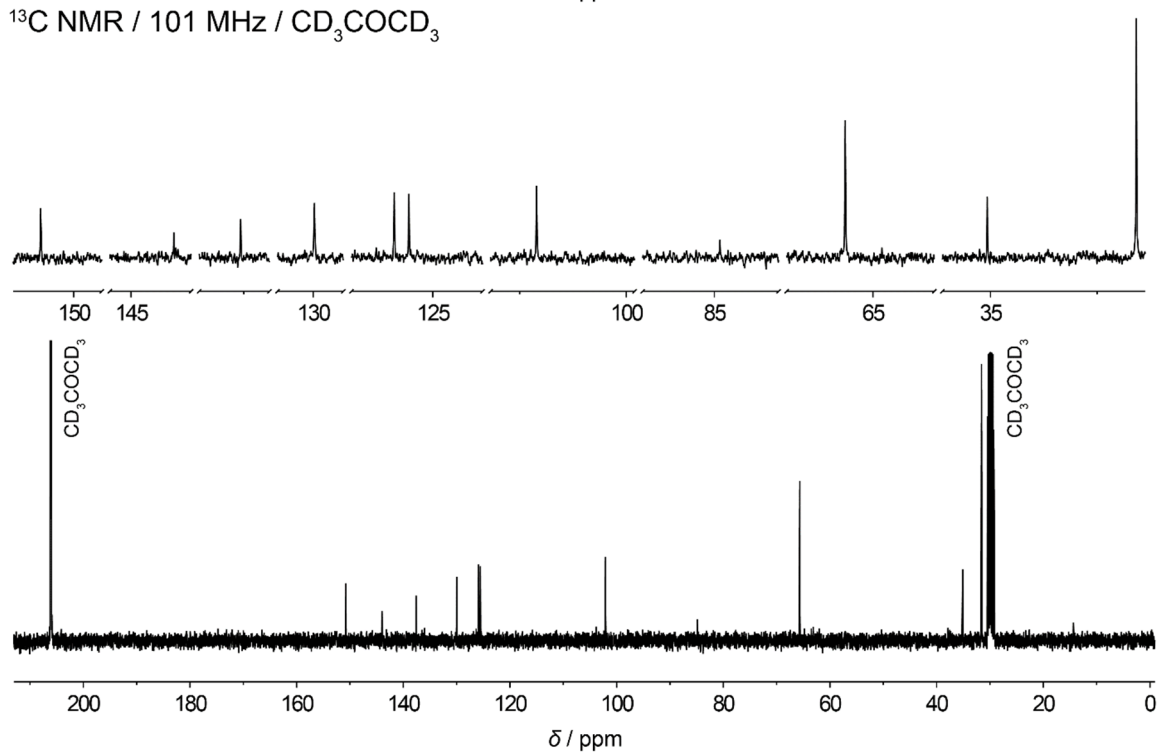


Tris(4-(*tert*-butyl)-2-(1,3-dioxolan-2-yl)phenyl)methanol (4)

^1H NMR / 400 MHz / CD_3COCD_3

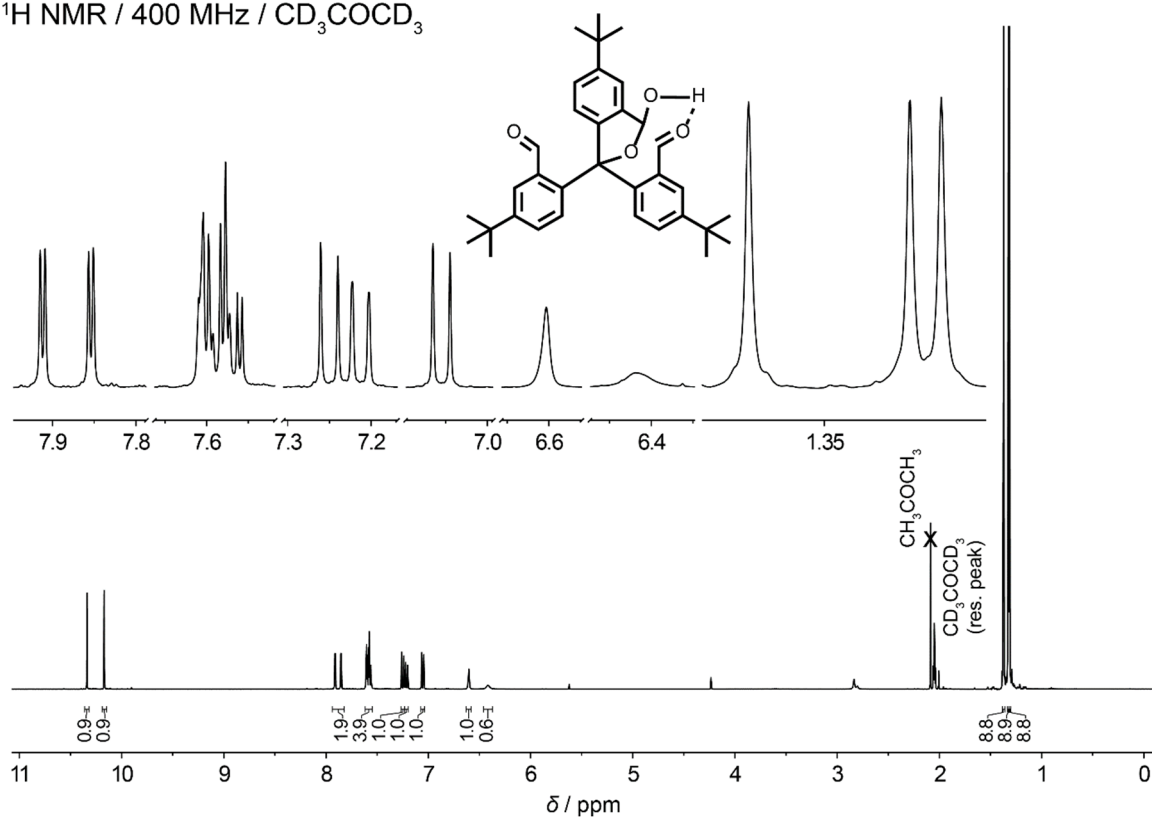


^{13}C NMR / 101 MHz / CD_3COCD_3

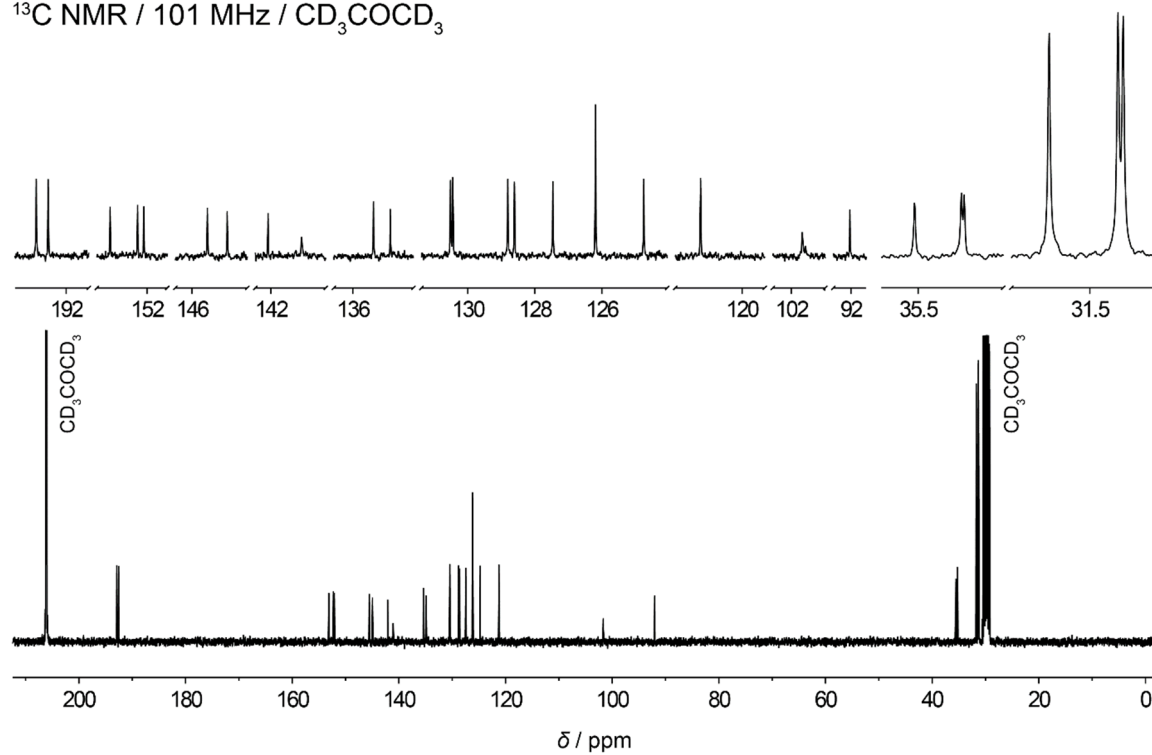


2,2'-(5-(*tert*-Butyl)-3-hydroxy-1,3-dihydroisobenzofuran-1,1-diyl)bis(5-(*tert*-butyl)benzaldehyde) (5)

$^1\text{H NMR}$ / 400 MHz / CD_3COCD_3

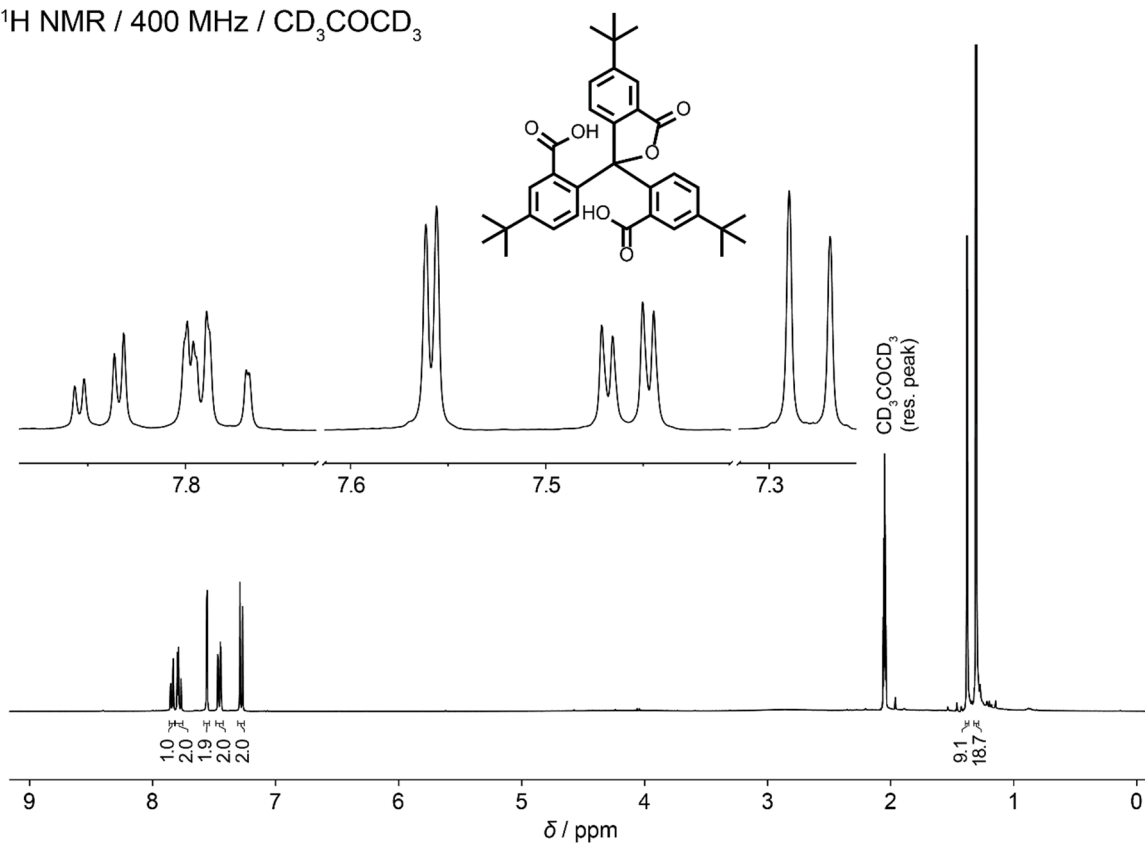


$^{13}\text{C NMR}$ / 101 MHz / CD_3COCD_3

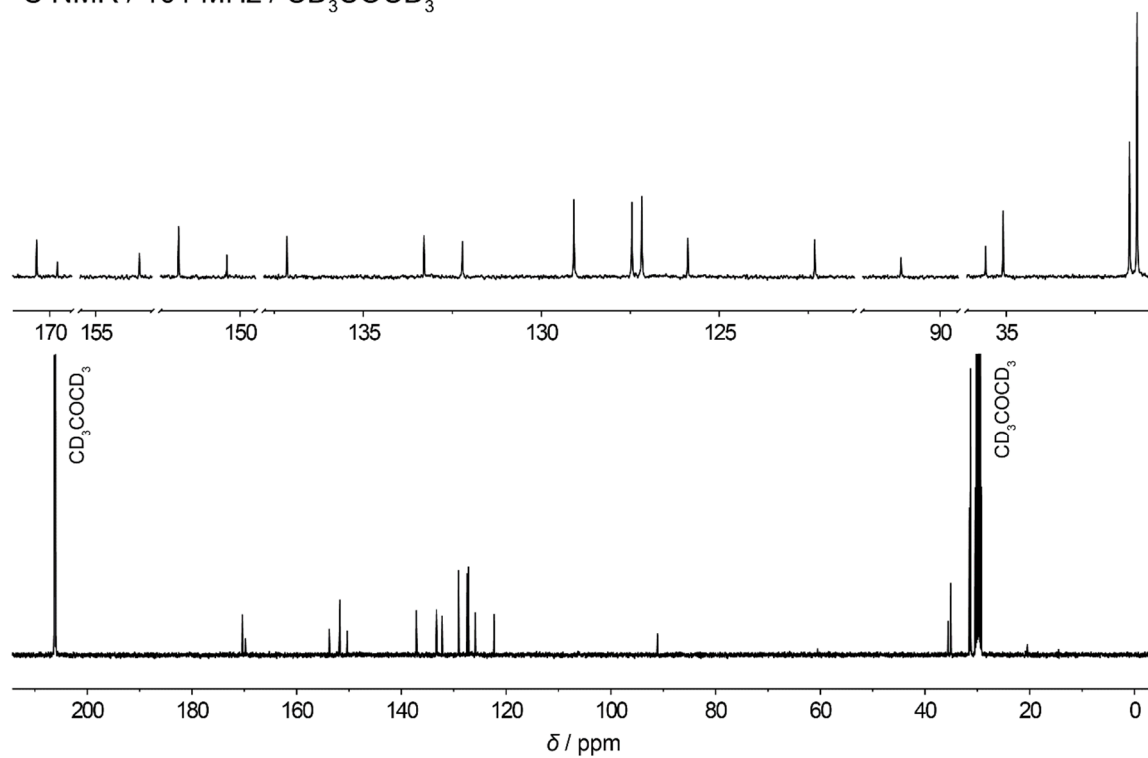


6,6'-(5-(*tert*-Butyl)-3-oxo-1,3-dihydroisobenzofuran-1,1-diyl)bis(3-(*tert*-butyl)benzoic acid) (6)

$^1\text{H NMR}$ / 400 MHz / CD_3COCD_3

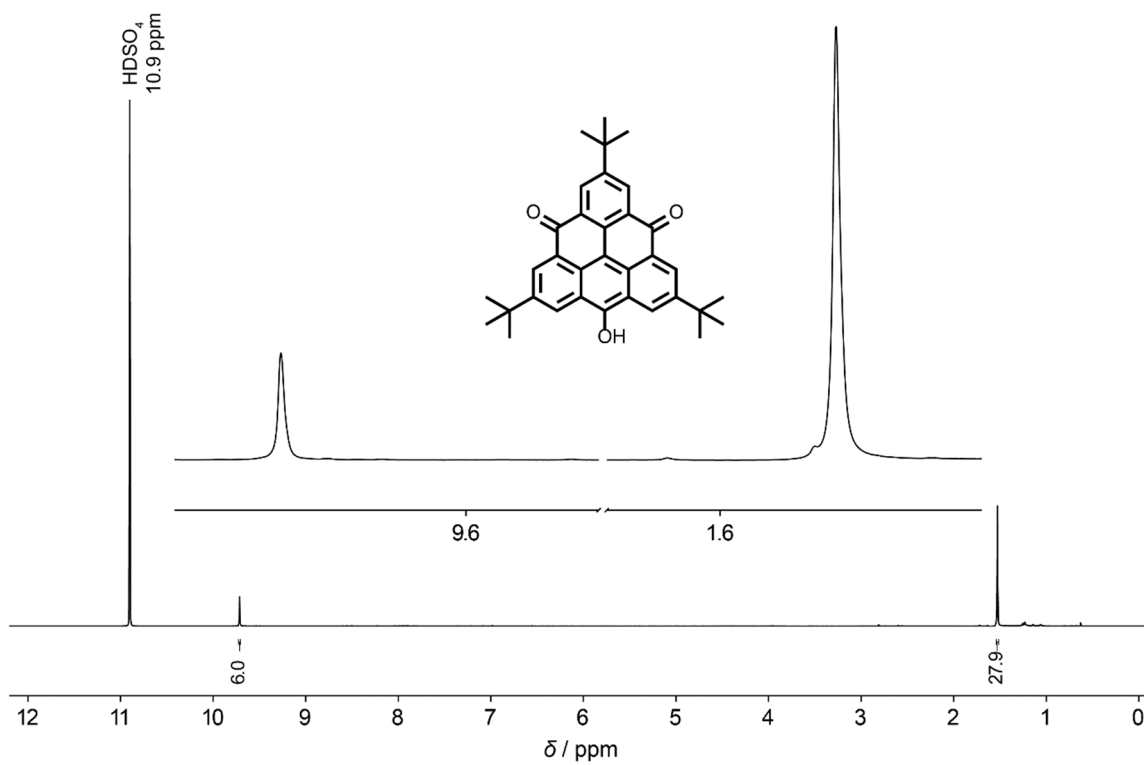


$^{13}\text{C NMR}$ / 101 MHz / CD_3COCD_3

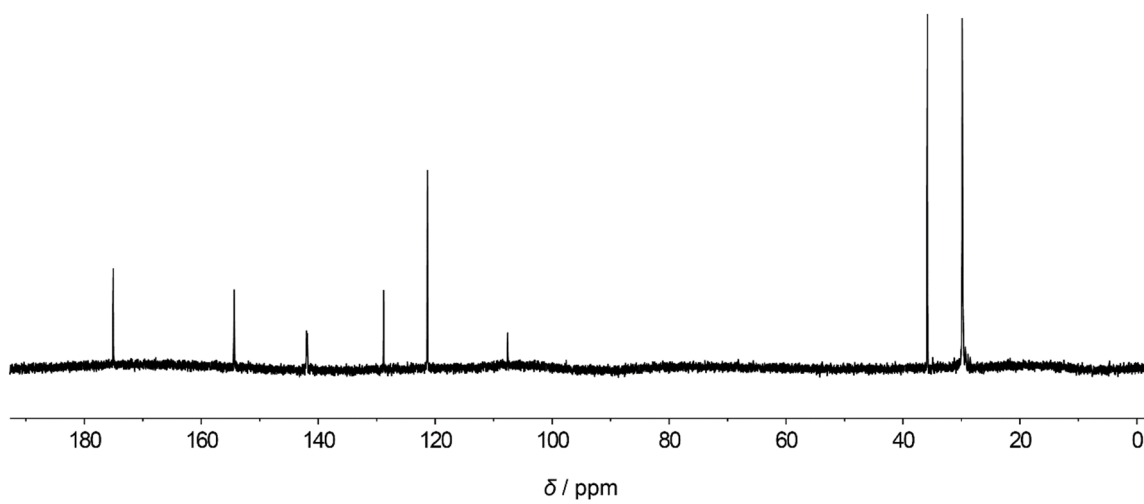


2,6,10-Tri-*tert*-butyl-12-hydroxydibenzo[*cd,mn*]pyrene-4,8-dione (7)

^1H NMR / 600 MHz / D_2SO_4

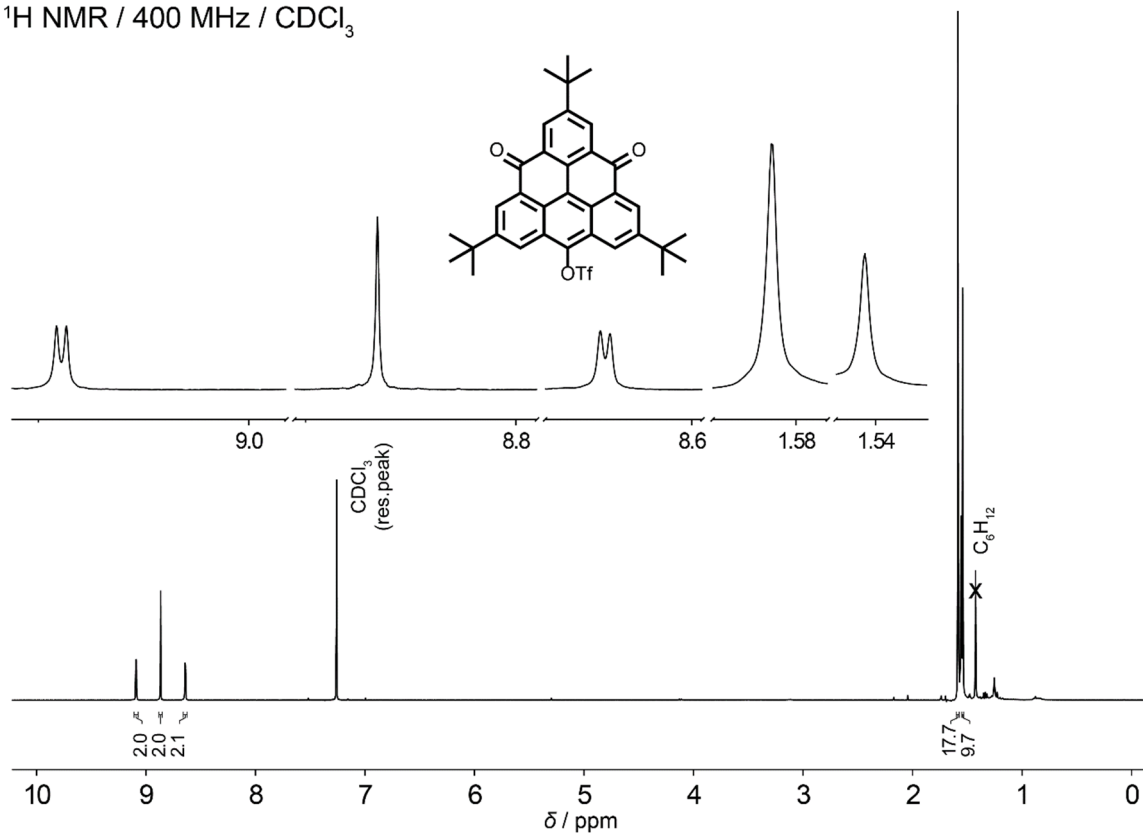


^{13}C NMR / 151 MHz / D_2SO_4

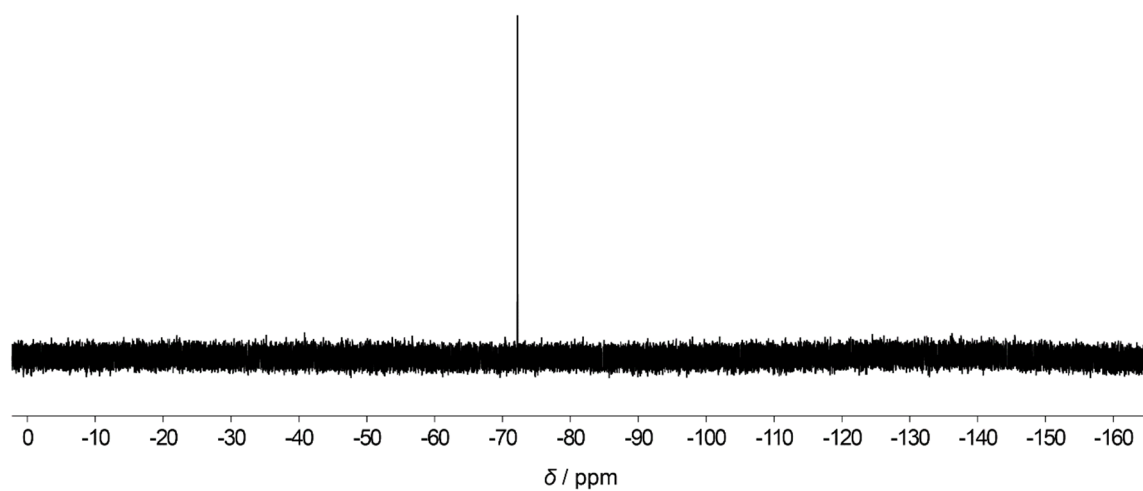


2,6,10-Tri-*tert*-butyl-8,12-dioxo-8,12-dihydrodibenzo[*cd,mn*] pyren-4-yl trifluoromethanesulfonate (8)

$^1\text{H NMR}$ / 400 MHz / CDCl_3

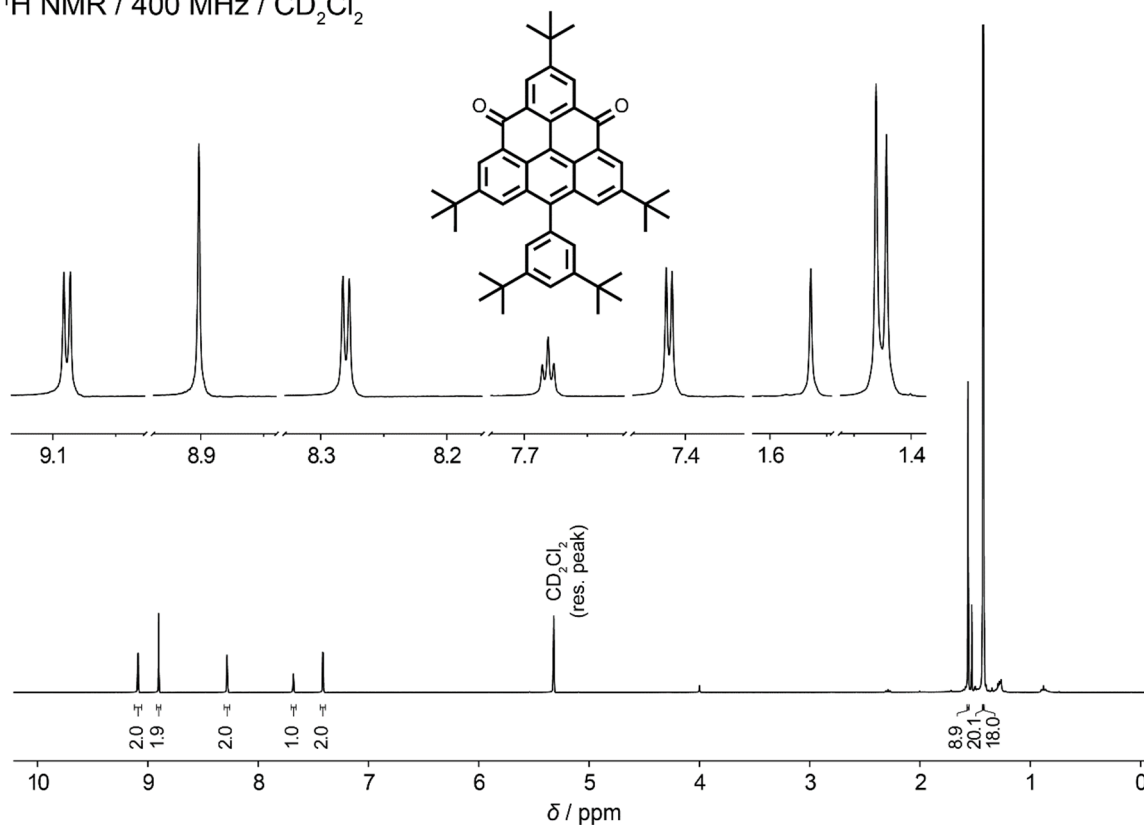


$^{19}\text{F NMR}$ / 376.5 MHz / CDCl_3

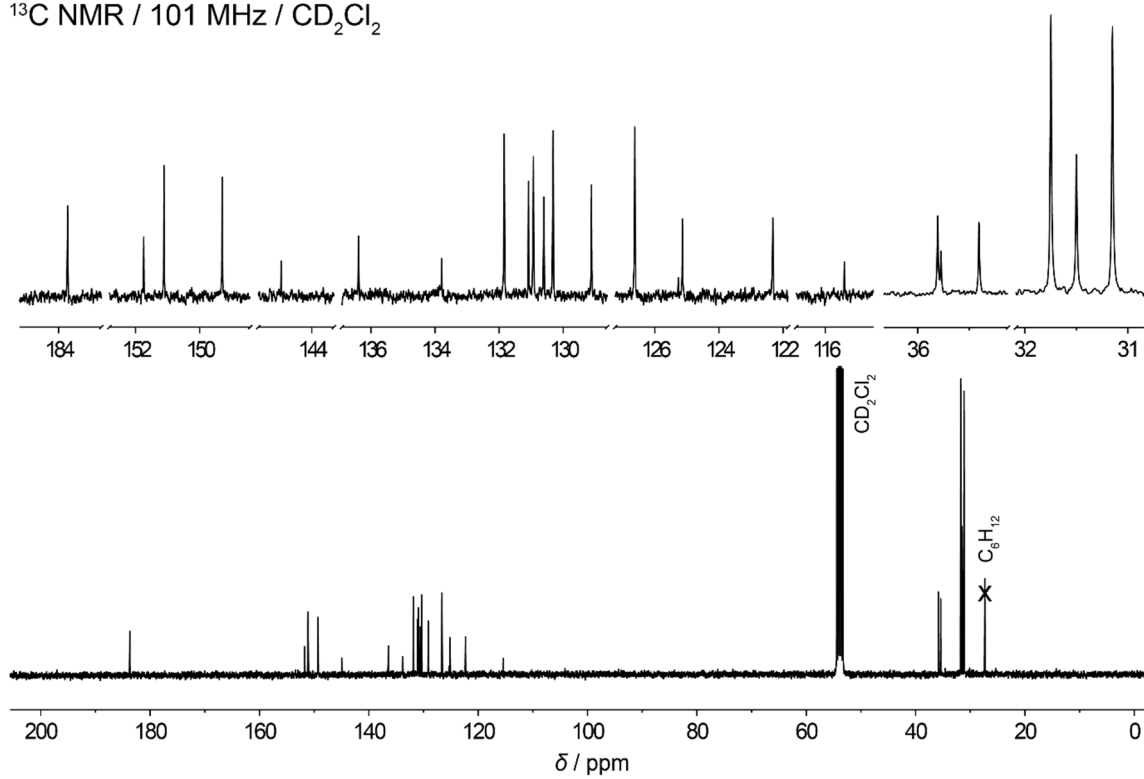


2,6,10-Tri-*tert*-butyl-12-(3,5-di-*tert*-butylphenyl)dibenzo[*cd,mn*] pyrene-4,8-dione (T1)

$^1\text{H NMR}$ / 400 MHz / CD_2Cl_2

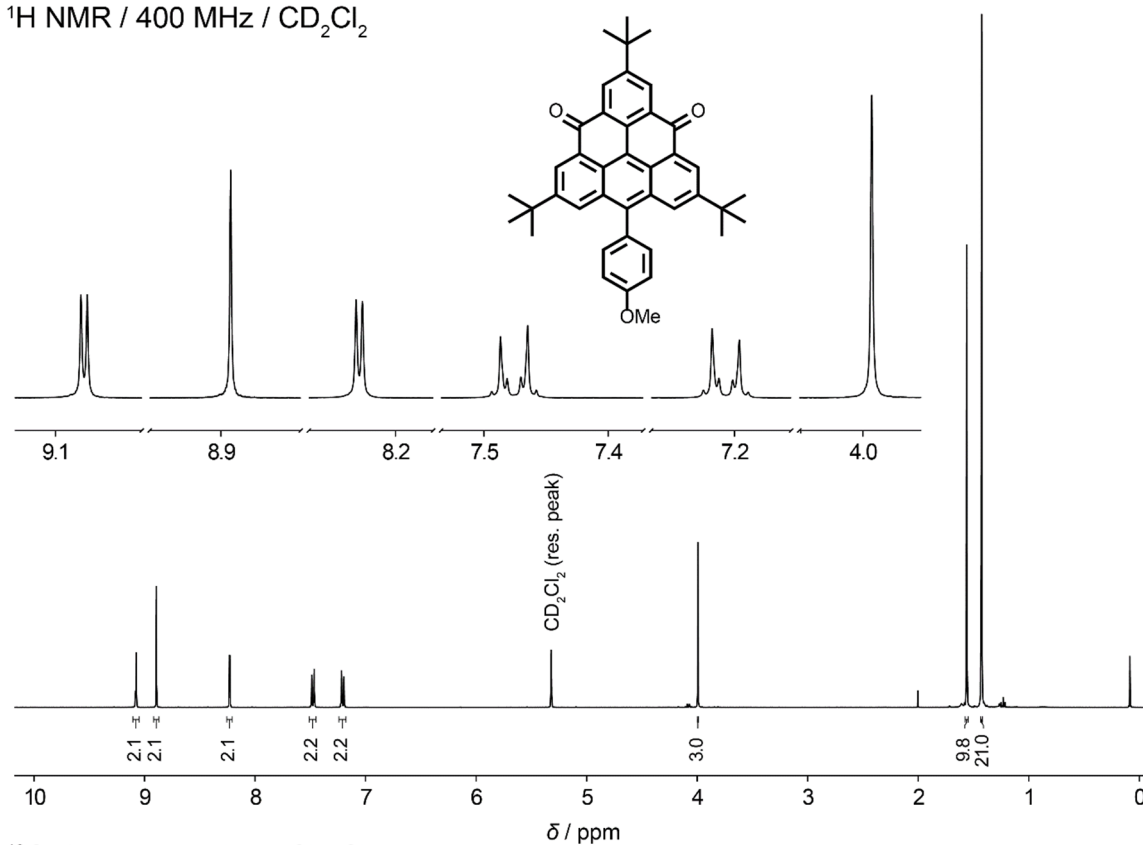


$^{13}\text{C NMR}$ / 101 MHz / CD_2Cl_2

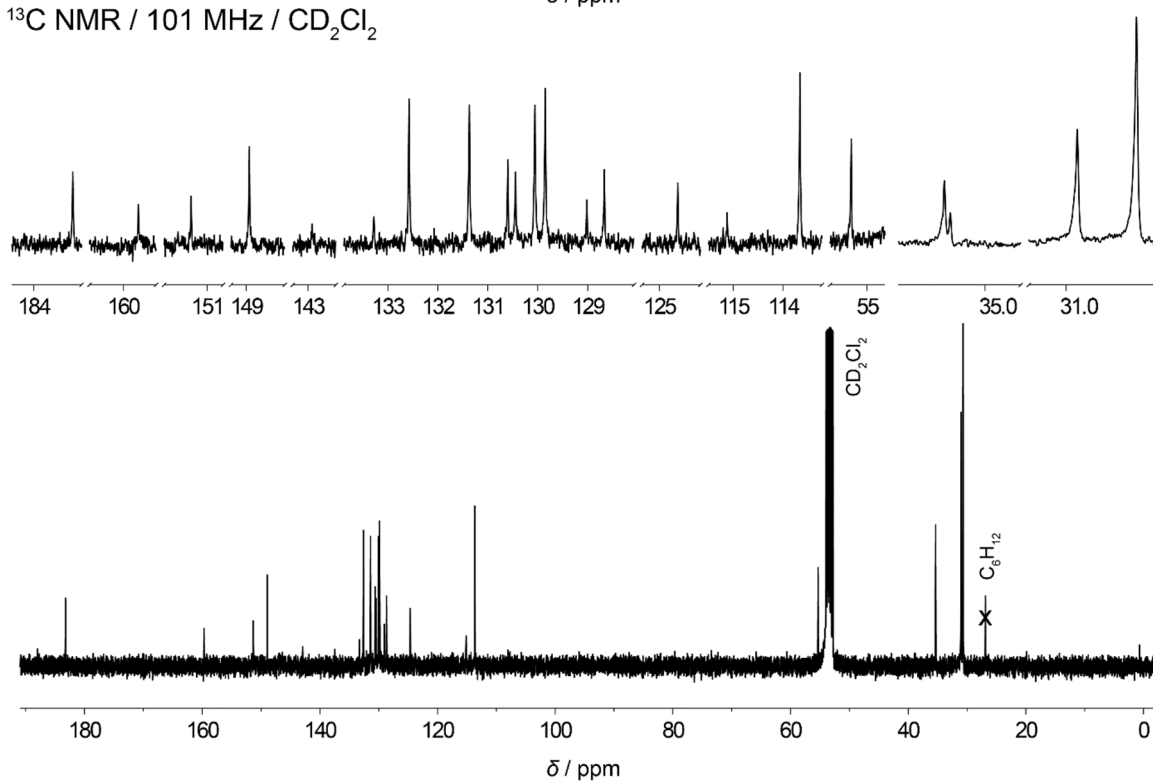


2,6,10-Tri-*tert*-butyl-12-(4-methoxyphenyl)dibenzo[*cd,mn*]pyrene-4,8-dione (T2)

$^1\text{H NMR}$ / 400 MHz / CD_2Cl_2

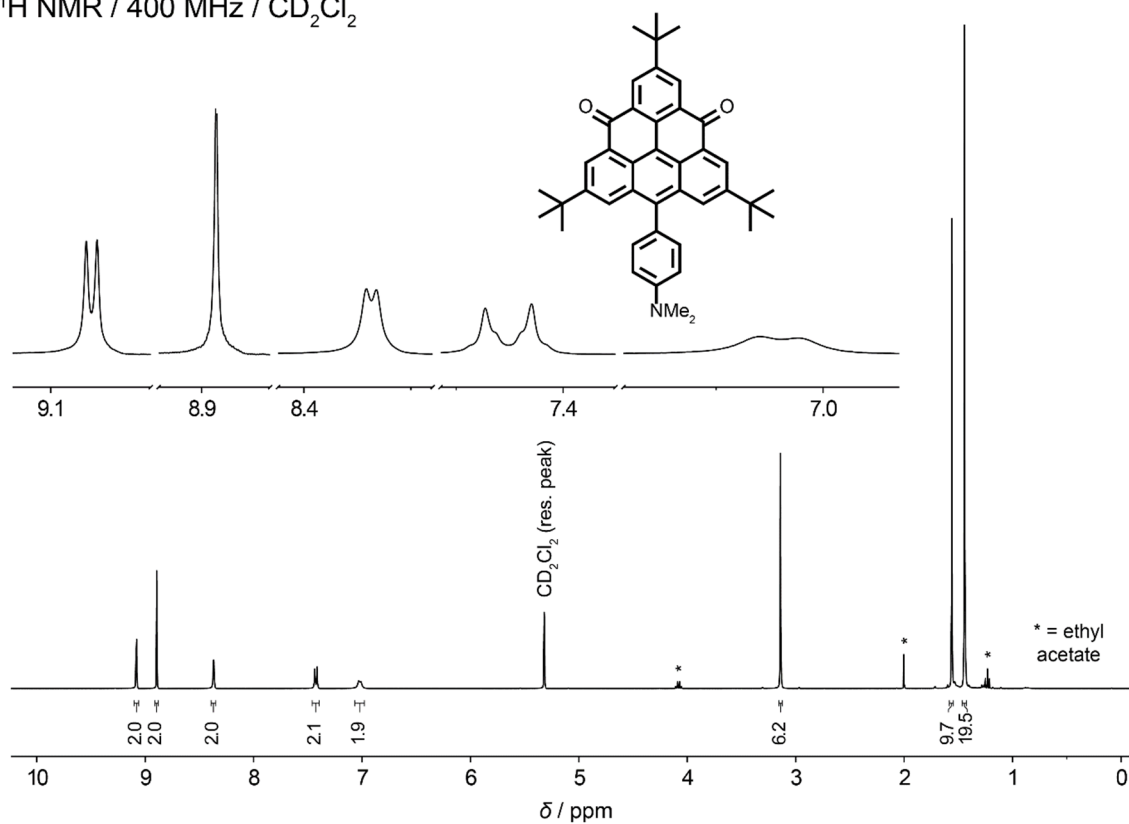


$^{13}\text{C NMR}$ / 101 MHz / CD_2Cl_2

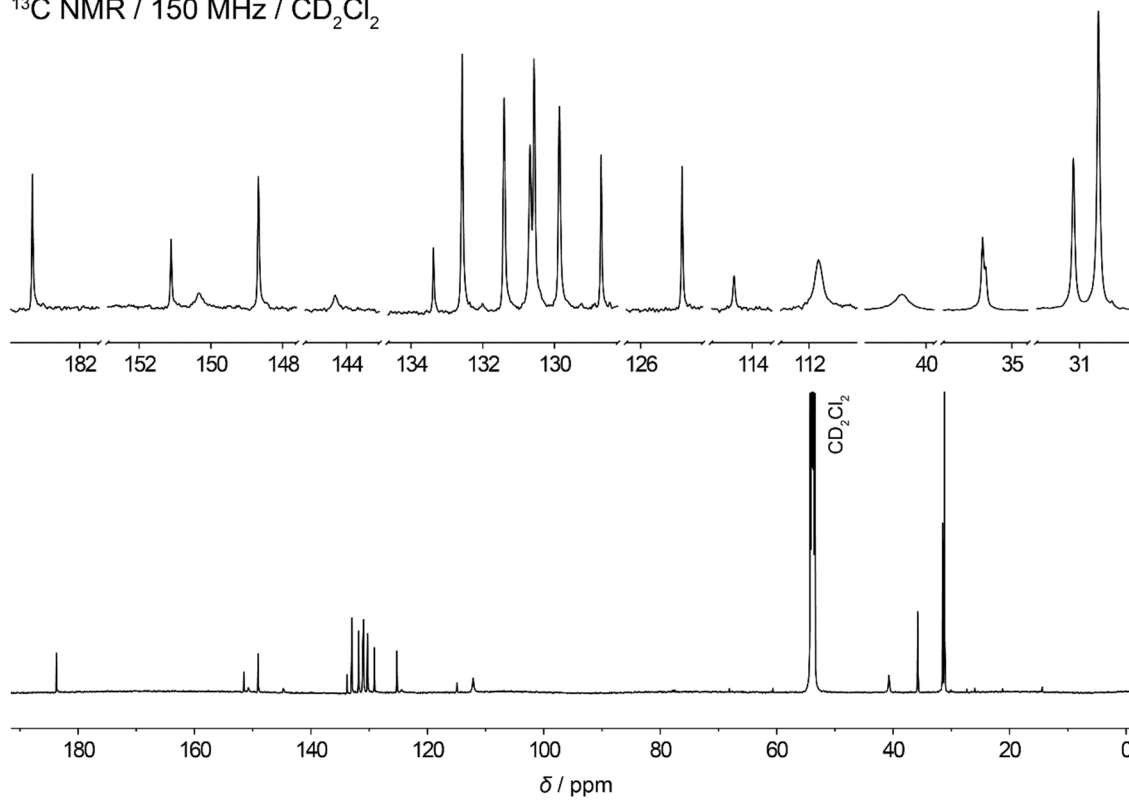


2,6,10-Tri-*tert*-butyl-12-(4-(dimethylamino)phenyl)dibenzo [cd,mn]pyrene-4,8-dione (T3)

$^1\text{H NMR}$ / 400 MHz / CD_2Cl_2

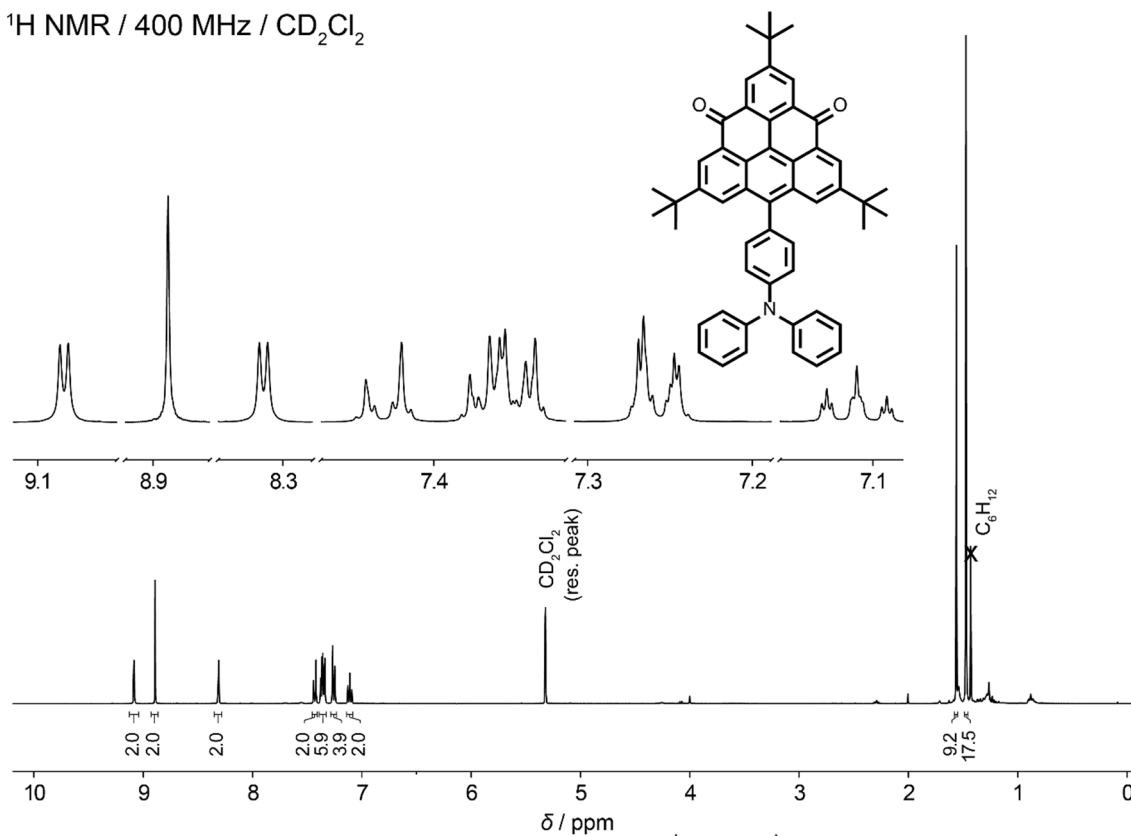


$^{13}\text{C NMR}$ / 150 MHz / CD_2Cl_2

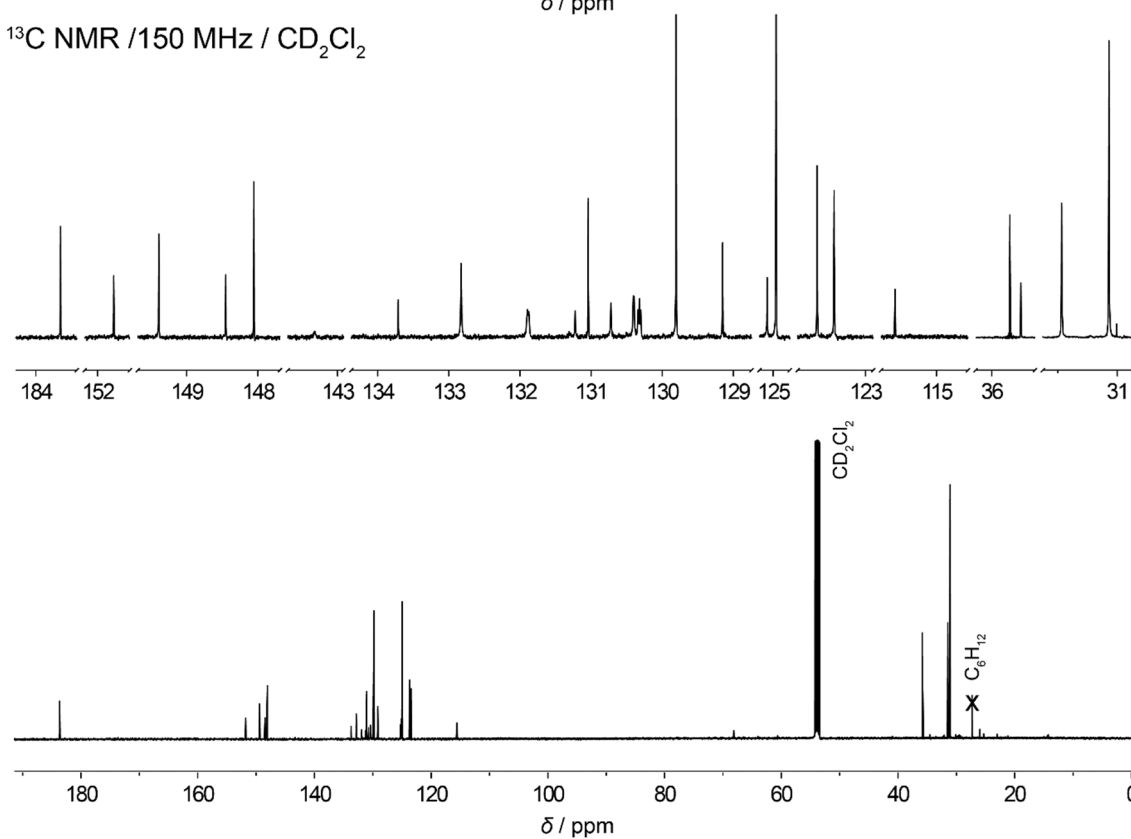


2,6,10-Tri-*tert*-butyl-12-(4-(diphenylamino)phenyl)dibenzo[*cd,mn*] pyrene-4,8-dione (T4)

$^1\text{H NMR}$ / 400 MHz / CD_2Cl_2

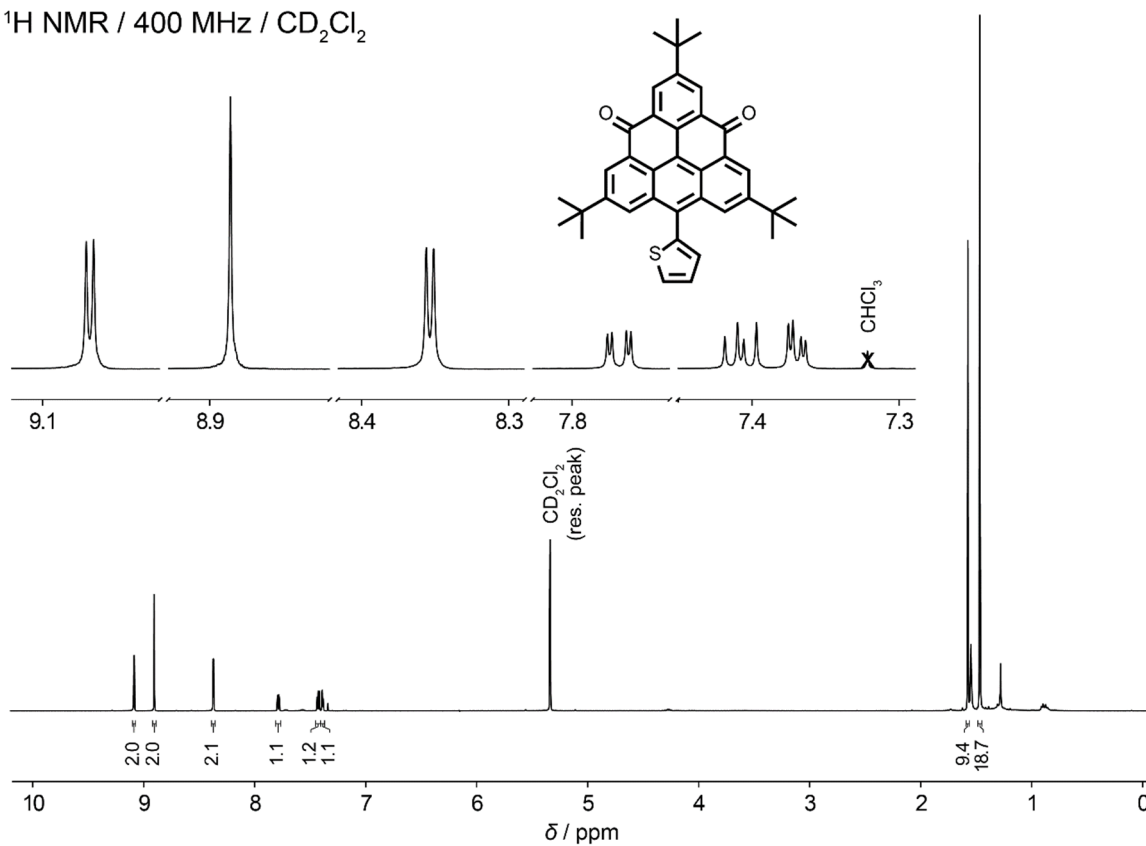


$^{13}\text{C NMR}$ / 150 MHz / CD_2Cl_2

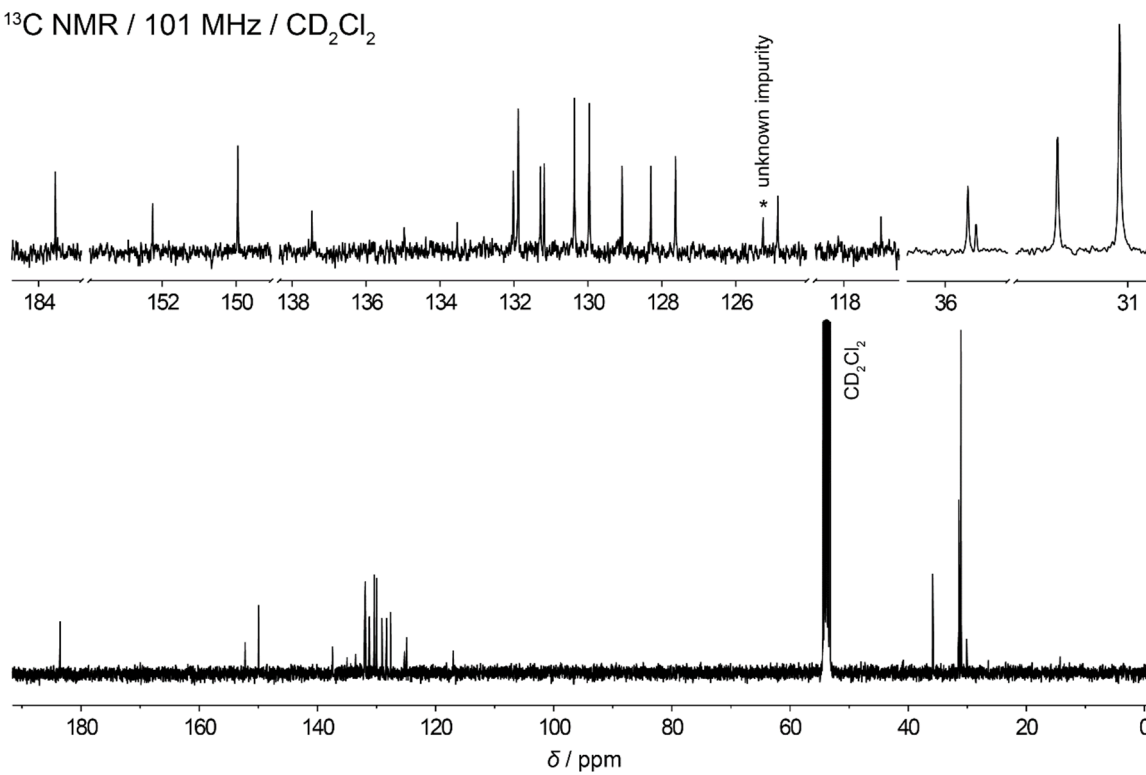


2,6,10-Tri-*tert*-butyl-12-(thiophen-2-yl)dibenzo[*cd,mn*]pyrene-4,8-dione (T5)

^1H NMR / 400 MHz / CD_2Cl_2



^{13}C NMR / 101 MHz / CD_2Cl_2



A7. Cartesian Coordinates

T1_H, $E = -1540.44332001$ Hartree

6	-6.186800	1.151292	-0.341519
6	-4.787652	1.163508	-0.344906
6	-4.064043	-0.003509	-0.005215
6	-4.786768	-1.171199	0.334096
6	-6.185920	-1.160287	0.329830
6	-6.888122	-0.004829	-0.006079
6	-4.082641	2.416045	-0.710629
6	-2.596699	2.368471	-0.704426
6	-1.899661	1.168445	-0.349086
6	-2.607445	-0.002822	-0.004768
6	-0.458031	1.171057	-0.353922
6	0.214414	2.372569	-0.736330
6	-0.483324	3.507969	-1.073775
6	-1.894591	3.505826	-1.053286
6	-1.898865	-1.173465	0.340121
6	-0.457369	-1.174633	0.346027
6	0.254302	-0.001483	-0.003592
6	-4.080842	-2.423056	0.700427
6	-2.594942	-2.374102	0.695176
6	-1.891907	-3.510720	1.044604
6	-0.480647	-3.511436	1.066067
6	0.216127	-2.375320	0.729008

8	-4.692461	-3.449601	0.995748
8	-4.695029	3.442063	-1.006214
6	1.750853	-0.002071	-0.004539
1	-2.458307	-4.398827	1.307308
1	0.053725	-4.412034	1.354402
1	1.299941	-2.376737	0.753026
1	-6.700176	2.069584	-0.608535
1	-7.974284	-0.005344	-0.006429
1	-6.698609	-2.079047	0.596559
1	1.298213	2.375393	-0.758911
1	0.050383	4.409167	-1.361448
1	-2.461724	4.393399	-1.316215
6	2.459115	0.608520	1.032114
6	3.864196	0.617323	1.051292
6	4.529367	-0.004677	-0.009167
6	3.852398	-0.629145	-1.073220
6	2.455662	-0.618711	-1.051569
1	1.899586	1.077823	1.836140
6	4.604831	1.297508	2.218860
1	5.612805	-0.009277	-0.017362
6	4.660814	-1.290015	-2.206475
1	1.886902	-1.084045	-1.848494
6	3.756030	-1.925550	-3.279232
6	5.547453	-0.225250	-2.895434
6	5.560611	-2.402340	-1.616887
1	4.375221	-2.382013	-4.059456

1	3.118177	-2.713203	-2.862328
1	3.111428	-1.182961	-3.762945
1	6.147331	-2.878111	-2.411996
1	6.263635	-2.010385	-0.874496
1	4.957789	-3.177642	-1.130178
1	6.133691	-0.682455	-3.701738
1	4.935061	0.572253	-3.331515
1	6.250226	0.237787	-2.194898
6	6.136225	1.213596	2.074797
6	4.209240	2.792374	2.277481
6	4.208762	0.610744	3.547810
1	6.613106	1.710666	2.926836
1	6.489596	0.176276	2.059224
1	6.489589	1.710514	1.164067
1	4.723206	1.087874	4.390725
1	3.132107	0.674715	3.736475
1	4.484425	-0.450006	3.538440
1	4.722661	3.289561	3.109326
1	4.486959	3.308197	1.351017
1	3.132469	2.925429	2.425204

T2_H, $E = -1340.45634450$ Hartree

6	5.221115	-1.155980	-0.098508
6	3.822635	-1.184657	-0.064352

A35

6	3.085376	0.022159	-0.032617
6	3.794486	1.246129	-0.036978
6	5.193222	1.250643	-0.072643
6	5.908751	0.055657	-0.103072
6	3.132694	-2.497276	-0.063897
6	1.646568	-2.466919	-0.038310
6	0.935220	-1.223994	0.001281
6	1.629251	0.004872	0.003633
6	-0.506094	-1.244668	0.028803
6	-1.163246	-2.512880	-0.014977
6	-0.452168	-3.688823	-0.054114
6	0.958695	-3.664631	-0.059931
6	0.907247	1.216854	0.041402
6	-0.533865	1.203343	0.084847
6	-1.233420	-0.029121	0.073354
6	3.074457	2.541984	-0.002170
6	1.590061	2.476337	0.046870
6	0.876037	3.657394	0.104816
6	-0.533512	3.648098	0.170001
6	-1.217680	2.455695	0.163709
8	3.673692	3.617163	-0.010966
8	3.756967	-3.557866	-0.087521
6	-2.726621	-0.047480	0.109135
1	1.432976	4.589236	0.107911
1	-1.076899	4.586516	0.232082
1	-2.299819	2.453231	0.225196

1	5.744900	-2.106356	-0.121691
1	6.994500	0.068525	-0.130082
1	5.694833	2.213182	-0.074956
1	-2.246886	-2.536495	-0.021803
1	-0.975632	-4.639937	-0.087122
1	1.536677	-4.583069	-0.090347
6	-3.419605	-0.462349	1.261707
6	-4.807210	-0.479165	1.299186
6	-5.549317	-0.083360	0.175659
6	-4.878601	0.330632	-0.981349
6	-3.481665	0.346563	-1.002057
1	-2.858321	-0.768002	2.140495
1	-5.342220	-0.792942	2.190022
8	-6.903561	-0.137663	0.312075
1	-5.425225	0.637318	-1.865680
1	-2.971610	0.666061	-1.906909
6	-7.708909	0.251089	-0.791127
1	-8.742580	0.130638	-0.462809
1	-7.535581	1.299493	-1.066858
1	-7.529315	-0.387343	-1.665973

T3_H, $E = -1359.90173496$ Hartree

6	-5.487533	1.228510	-0.030975
6	-4.088373	1.231730	-0.029357

A37

6	-3.372266	0.011765	-0.002646
6	-4.104096	-1.198890	0.021145
6	-5.503092	-1.177669	0.017280
6	-6.197318	0.029935	-0.008201
6	-3.374961	2.530991	-0.058726
6	-1.889875	2.473031	-0.072241
6	-1.199817	1.217931	-0.033079
6	-1.916360	0.002389	0.000278
6	0.241981	1.212376	-0.042119
6	0.918466	2.467405	-0.133929
6	0.227897	3.656003	-0.172813
6	-1.181923	3.657931	-0.133074
6	-1.215666	-1.222279	0.036383
6	0.226033	-1.235284	0.051390
6	0.951169	-0.016068	0.006404
6	-3.407570	-2.507251	0.053056
6	-1.921948	-2.468408	0.072417
6	-1.229481	-3.662314	0.135610
6	0.180087	-3.678548	0.180825
6	0.886048	-2.498924	0.145267
8	-4.026840	-3.571404	0.067569
8	-3.980370	3.603056	-0.075892
6	2.441358	-0.026085	0.010224
1	-1.804209	-4.582932	0.162235
1	0.707133	-4.625550	0.253369
1	1.968395	-2.516208	0.196413

1	-5.994004	2.188311	-0.051440
1	-7.283492	0.036914	-0.010317
1	-6.021938	-2.130881	0.035682
1	2.001136	2.470720	-0.180831
1	0.767332	4.596139	-0.243709
1	-1.744677	4.585839	-0.162225
6	3.175385	0.484210	1.092719
6	4.565320	0.476512	1.105951
6	5.303594	-0.049435	0.019576
6	4.564115	-0.549246	-1.078263
6	3.174121	-0.541270	-1.070785
1	2.645587	0.889888	1.950803
1	5.076017	0.880176	1.971895
7	6.687971	-0.079945	0.033379
1	5.073841	-0.943697	-1.949003
1	2.643389	-0.931187	-1.935588
6	7.410086	-0.473710	-1.164544
6	7.410866	0.597028	1.096732
1	8.481536	-0.458181	-0.957262
1	7.146524	-1.494587	-1.467469
1	7.215299	0.195192	-2.017574
1	8.482482	0.452523	0.948609
1	7.210553	1.679641	1.124006
1	7.153486	0.180084	2.078298

T4_H, $E = -1743.38226158$ Hartree

6	-1.298374	-0.663537	1.001598
6	-0.570602	-0.000003	0.000002
6	-1.298372	0.663533	-1.001594
6	-2.689418	0.657615	-1.012128
6	-3.411269	-0.000001	0.000001
6	-2.689419	-0.657618	1.012131
6	0.921249	-0.000002	0.000003
6	1.636117	1.197806	0.255976
6	3.077908	1.195669	0.245876
6	3.786357	0.000000	0.000001
6	3.077910	-1.195671	-0.245873
6	1.636119	-1.197811	-0.255971
6	5.242920	0.000001	-0.000001
6	5.966654	1.192041	0.237450
6	5.261591	2.470562	0.495256
6	3.775843	2.420822	0.500138
6	5.966656	-1.192038	-0.237453
6	7.365789	-1.180346	-0.234367
6	8.067718	0.000003	-0.000004
6	7.365787	1.180351	0.234361
6	3.775846	-2.420823	-0.500136
6	5.261594	-2.470560	-0.495257
6	0.967111	2.423776	0.558217
6	1.665391	3.583113	0.800247

6	3.075667	3.582073	0.763536
6	3.075671	-3.582075	-0.763533
6	1.665395	-3.583118	-0.800241
6	0.967114	-2.423781	-0.558211
8	5.873535	3.519096	0.698779
8	5.873539	-3.519093	-0.698781
1	3.644098	-4.487643	-0.951494
1	1.132132	-4.501490	-1.028246
1	-0.115773	-2.427727	-0.601245
1	7.878579	2.118629	0.420875
1	9.153880	0.000004	-0.000005
1	7.878581	-2.118623	-0.420882
1	-0.115775	2.427720	0.601253
1	1.132127	4.501484	1.028253
1	3.644093	4.487642	0.951497
1	-0.764671	1.172361	-1.799872
1	-3.224500	1.159861	-1.811119
7	-4.824561	0.000000	0.000001
1	-3.224503	-1.159863	1.811121
1	-0.764674	-1.172366	1.799876
6	-5.545819	-1.142691	0.452558
6	-5.545817	1.142693	-0.452559
6	-6.648666	-0.990764	1.306865
6	-7.363702	-2.107856	1.735162
6	-6.982815	-3.390409	1.335131
6	-5.881363	-3.544585	0.490531

6	-5.171723	-2.431853	0.042440
1	-6.939832	0.003988	1.629153
1	-8.215570	-1.973461	2.396481
1	-7.538228	-4.259247	1.676373
1	-5.579452	-4.536164	0.163712
1	-4.326494	-2.554118	-0.627683
6	-6.648661	0.990767	-1.306869
6	-7.363694	2.107860	-1.735169
6	-6.982806	3.390413	-1.335137
6	-5.881357	3.544587	-0.490533
6	-5.171720	2.431854	-0.042439
1	-6.939827	-0.003985	-1.629159
1	-8.215560	1.973466	-2.396491
1	-7.538217	4.259251	-1.676380
1	-5.579445	4.536166	-0.163713
1	-4.326494	2.554117	0.627686

T5_H, $E = -1546.68754812$ Hartree

6	-4.608727	1.203691	-0.085964
6	-3.210522	1.215587	-0.036075
6	-2.488361	-0.000001	-0.010891
6	-3.210519	-1.215592	-0.036073
6	-4.608725	-1.203699	-0.085962
6	-5.309796	-0.000005	-0.111274

6	-2.505436	2.520710	-0.009451
6	-1.020327	2.473313	0.043590
6	-0.324615	1.221379	0.066770
6	-1.031669	0.000000	0.040662
6	1.115224	1.225333	0.116909
6	1.789862	2.484053	0.145264
6	1.093357	3.668514	0.122183
6	-0.317712	3.661985	0.069996
6	-0.324612	-1.221377	0.066773
6	1.115227	-1.225327	0.116914
6	1.824446	0.000004	0.139259
6	-2.505430	-2.520713	-0.009445
6	-1.020322	-2.473313	0.043598
6	-0.317704	-3.661983	0.070012
6	1.093366	-3.668508	0.122206
6	1.789867	-2.484045	0.145282
8	-3.117399	-3.587906	-0.030119
8	-3.117408	3.587902	-0.030126
6	3.307803	0.000007	0.182307
1	-0.883069	-4.588496	0.050745
1	1.627356	-4.613983	0.144760
1	2.873209	-2.489499	0.191736
1	-5.121596	2.160074	-0.103946
1	-6.395220	-0.000006	-0.150231
1	-5.121591	-2.160083	-0.103942
1	2.873204	2.489509	0.191711

1	1.627346	4.613990	0.144727
1	-0.883080	4.588497	0.050725
6	4.131325	0.000050	1.280130
6	5.522048	0.000042	0.952250
6	5.746661	-0.000007	-0.395780
16	4.260969	-0.000044	-1.291364
1	6.693920	-0.000023	-0.918655
1	6.315575	0.000071	1.691647
1	3.748644	0.000085	2.295353

CURRICULUM VITAE

Peter Ribar

Date/place of birth January 8th 1990 in Galanta, Slovakia

Nationality Slovak

Education

02/2014 – 03/2019 University of Basel, Department of Chemistry, Basel, Switzerland

PhD in Chemistry

Thesis: “*Synthesis and study of molecules based on triangular graphene fragments*”.

Supervisor: Prof. Dr. Michal Juríček & Prof. Dr. Marcel Mayor

Date of Examination: 29th of March 2019

09/2011 – 08/2013 Comenius University in Bratislava, Slovakia

M.Sc. in Organic and Bioorganic Chemistry

Thesis: “*Synthesis of arylaminooxazoles with biological activity*”,

Supervisor: Professor Andrej Boháč

09/2008 – 08/2011 Comenius University in Bratislava, Slovakia

Bc. in Biochemistry

Thesis: “*Motion synthesis of antiangiogenic inhibitors based on arylaminooxazoles*”, Supervisor: Professor Andrej Boháč

Awards

Travel fund, University of Basel, 2017

Travel fund, University of Basel, 2016

2016 Chemistry Travel Award by SCNAT, SCS and SSFC

Publications

4. **P. Ribar**, T. Šolomek, M. Juríček, *Org. Lett.* **2019**, *21*, 7124.

3. **P. Ribar**, T. Šolomek, L. Le Pleux, D. Häussinger, A. Prescimone, M. Neuburger, M. Juríček *Synthesis* **2017**, *47*, 899.

2. P. Ravat, **P. Ribar**, M. Rickhaus, D. Häussinger, M. Neuburger, M. Juriček *J. Org. Chem.* **2016**, *81*, 12303.

1. P. Ravat, T. Šolomek, **P. Ribar**, M. Juriček *Synlett* **2016**, *27*, 1613.

Conferences

7. The 17th International Symposium on Novel Aromatic Compounds, 23-28 July 2017, Stony Brook, USA

6. Fall Meeting of the Swiss Chemical Society, 15 September 2016, Zürich, Switzerland

5. The 15th International Conference on Molecule-Based Magnets, 4–8 September 2016, Sendai, Japan

4. 35th Regio-Symposium on Organic and Bioorganic Chemistry, 14–16 September 2015, Falkau, Germany

3. Fall Meeting of the Swiss Chemical Society, 11 September 2014, Zürich, Switzerland

2. 34th Regio-Symposium on Organic and Bioorganic Chemistry, 8–10 September 2014, Sornetan, Switzerland

1. 7th International Conference on Molecular Electronics, 24–29 August 2014, Strasbourg, France

